The role of apoptosis in *in vitro* and *in vivo* models of amyotrophic lateral sclerosis

Thesis

THE ROLE OF APOPTOSIS IN *in vitro* AND *in vivo* MODELS OF AMYOTROPHIC LATERAL SCLEROSIS

Paolo Bigini

Thesis submitted for the degree of Doctor of Philosophy

The Open University

Laboratory of Receptor Pharmacology

Department of Biochemistry and Molecular Pharmacology

Mario Negri Institute for Pharmacological Research

Milano, Italy

September 30th, 2004

LIST OF CONTENTS

ACKNOWLEDGMENTS **Pag. 10**

COLLABORATIONS **Pag. 12**

ABSTRACT **Pag. 14**

LIST OF TABLES AND FIGURES **Pag. 16**

LIST OF ABBREVIATIONS **Pag. 23**

CHAPTER 1 HUMAN AMYOTROPHIC LATERAL SCLEROSIS

1.1 Clinical hallmarks: symptoms and diagnosis **Pag. 31**

1.1.1 Epidemiology (incidence, prevalence, onset) **Pag. 31**

1.1.2 Symptoms **Pag. 33**

1.1.3 Diagnosis **Pag. 35**

1.1.3.1 Clinical criteria **Pag. 35**

1.1.3.2 Neuropathological and hystopathologycal criteria **Pag. 36**

1.2 Neuropathological and hystopathological alterations **Pag. 37**

1.2.1 Upper motor neurons and corticospinal tract **Pag. 37**

1.2.2 Lower motor neurons **Pag. 37**

1.2.2.1 Neurofilament alterations **Pag. 38**

1.2.2.2 Intracellular inclusions **Pag. 39**

1.2.2.3 Mitochondrial alterations **Pag. 40**

1.2.2.4 Axonal alterations **Pag. 40**

1.3 Aetiopathological hypotheses **Pag. 41**

1.3.1 Genetic involvement **Pag. 41**

1.3.1.1 fALS1 (SOD1) **Pag. 41**

1.3.1.2 fALS2 (ALSIN) **Pag. 42**

1.3.2 Glutamate-induced excitotoxicity **Pag. 43**

1.3.3 Oxidative stress and mitochondrial abnormalities **Pag. 46**

1.3.4 Neurofilaments disorganization and axonal strangulation **Pag. 48**

1.3.5 Intracellular aggregates and/or failure of protein folding **Pag. 48**

1.3.6 Reactivegliosis-inducedneuroinflammation **Pag. 49**
1.4 Pharmacotherapy **Pag. 53**
1.4.1 ALS and clinical trials **Pag. 53**
1.4.2 Antiexcitotoxic drugs **Pag. 56**
1.4.2.1 Riluzole **Pag. 56**
1.4.2.2 Dextromethorphan and L-threonine **Pag. 57**
1.4.2.3 Ca^{++} channels blockers **Pag. 57**
1.4.3 Neurotrophic factors **Pag. 58**
1.4.3.1 BDNF **Pag. 59**
1.4.3.2 CNTF **Pag. 60**
1.4.3.3 TRH **Pag. 61**
1.4.3.4 IGF-1 **Pag. 62**

CHAPTER 2 APOPTOSIS IN NEURONS

2.1 Principles of neuronal death in embryonic and adult brain **Pag. 63**
2.1.1 Morphological changes in neuronal apoptosis **Pag. 64**
2.2 Molecular mechanisms of neuronal apoptosis **Pag. 67**
2.2.1 Extrinsic pathway **Pag. 70**
2.2.1.1 Death receptors **Pag. 70**
2.2.2 Intrinsic pathway **Pag. 72**
2.2.2.1 Neurotrophic factors withdrawal **Pag. 72**
2.2.2.2 Ca^{++} overloading **Pag. 73**
2.2.3 Antiapoptotic and proaptotic molecules **Pag. 75**
2.2.4 The role of mitochondria **Pag. 76**
2.2.4.1 Mitochondrial membrane potential **Pag. 76**
2.2.4.2 The permeability transition pore **Pag. 77**
2.2.4.3 Cytochrome-c release **Pag. 78**
2.2.4.4 Apoptosis-initiating factors **Pag. 78**
2.2.5 Caspases **Pag. 80**
2.2.6 Caspases substrates **Pag. 82**
2.2.6.1 Nuclear substrates **Pag. 82**
2.2.6.2 Cytoskeletal substrates **Pag. 83**
2.3 Apoptosis and neurodegenerative diseases **Pag. 85**
2.3.1 Positive evidence **Pag. 85**

2.3.2 Controversial evidence **Pag. 86**
2.3.3 ALS and apoptosis **Pag. 87**
2.4 Neuroprotective and anti-apoptotic effects of erythropoietin **Pag. 90**
2.4.1 EPO and erythropoyesis **Pag. 90**
2.4.2 EPO and neuroprotection **Pag. 91**

CHAPTER 3 *In vitro* AND *in vivo* models of ALS: ADVANTAGES AND PITFALLS
3.1 Cellular models **Pag. 93**
3.2 Animal models **Pag. 94**
3.2.1 *mnd* mouse **Pag. 95**
3.2.2 *pmn* mouse **Pag. 96**
3.2.3 Wasted mouse **Pag. 96**
3.2.4 SOD1 transgenic mouse **Pag. 97**
3.2.5 Wobbler mouse **Pag. 97**

CHAPTER 4 PRIMARY CULTURES OF MOTOR NEURONS
4.1 Purified and mixed cultures **Pag. 100**
4.1.1 Purified cultures of motor neurons **Pag. 100**
4.1.2 Mixed glia/neurons cultures **Pag. 101**
4.2 Primary cultures of motor neurons and ALS-associated toxicity **Pag. 101**
4.2.1 Cu/Zn SOD1 mutation and Fas-L activation **Pag. 101**
4.2.2 Glutamate-induced excitotoxicity **Pag. 103**
4.2.2.1 AMPA and Kainate overstimulation **Pag. 103**
4.2.2.2 Ca^{++} influx and the role of GluR 2 subunit **Pag. 104**
4.2.2.3 The role of astrocytes **Pag. 106**
4.2.3 Free radicals exposure **Pag. 108**
4.2.4 Mitochondrial inhibition **Pag. 109**
4.2.5 Proteasome inhibition **Pag. 109**
4.2.6 Neurotrophic factors withdrawal **Pag. 111**
4.2.6.1 BDNF **Pag. 111**
4.2.6.2 CNTF **Pag. 112**

CHAPTER 5 THE WOBBLER MOUSE

5.1 Genetic **Pag. 113**

5.2 Symptoms **Pag. 114**

5.3 Neuropathological and hystopathological alterations **Pag. 117**

5.3.1 Motor neurons **Pag. 117**

5.3.1.1 Hystometry and histology **Pag. 117**

5.3.1.2 Cytology **Pag. 119**

5.3.2 Axons **Pag. 120**

5.3.3 Muscles **Pag. 121**

5.4 Aetiopathological markers **Pag. 122**

5.4.1 Glutamate-induced excitotoxicity **Pag. 122**

5.4.2 Oxidative stress **Pag. 122**

5.4.3 Mitochondrial abnormalities **Pag. 124**

5.4.4 Neurofilaments accumulation **Pag. 124**

5.4.5 Intracellular aggregates and/or failure of protein folding **Pag. 125**

5.4.6 Reactive gliosis **Pag. 127**

5.5 Pharmacological trials **Pag. 130**

5.5.1 Growth factors **Pag. 130**

5.5.1.1 BDNF and CNTF **Pag. 130**

5.5.1.2 IGF-1 **Pag. 130**

5.5.1.3 T-588 and cardiotrophin 1 **Pag. 131**

5.5.1.4 LIF **Pag. 132**

5.5.1.5 IL-6 **Pag. 132**

5.5.2 Antiglutamatergic agents **Pag. 134**

5.5.3 Mitochondrial agents **Pag. 134**

5.5.4 Antioxidants **Pag. 135**

5.6 Wobbler and apoptosis **Pag. 136**

CHAPTER 6 AIM OF THE STUDY

CHAPTER 7 MATERIALS

CHAPTER 8 *In vitro* EXPERIMENTAL PROCEDURES

8.1 Primary cultures of motor neurons **Pag. 147**

8.1.1 Animals **Pag. 147**

8.1.2 Motor neurons cultures **Pag. 147**

8.1.3 Pharmacological treatments **Pag. 148**

8.2 Immunocytochemistry **Pag. 148**

8.2.1 SMI32 for non-phosphorylated neurofilaments **Pag. 149**

8.2.2 EPOr **Pag. 151**

8.2.3 GluR 1-4 **Pag. 151**

8.2.4 Active Caspase 3 and Caspase 9 **Pag. 153**

8.2.5 Cytochrome-c **Pag. 154**

8.3 Hoechst 33258 staining **Pag. 154**

8.4 Mito-Tracker staining **Pag. 154**

8.5 Propidium Iodide and SYTO 59 staining **Pag. 155**

8.6 Mitochondrial trans membrane potential measurement **Pag. 155**

8.7 Laser scanning confocal microscopy setting up **Pag. 156**

8.8 Statistics **Pag. 157**

CHAPTER 9 *In vivo* EXPERIMENTAL PROCEDURES

9.1 Genotyping **Pag. 158**

9.2 Pharmacological treatments **Pag. 159**

9.2.1 EPO treatment **Pag. 159**

9.2.2 RPR 119990 treatment **Pag. 160**

9.2.3 Riluzole treatment **Pag. 161**

9.3 Behavioural scores recording **Pag. 162**

9.3.1 Paw and walking abnormality **Pag. 162**

9.3.2 Running time **Pag. 163**

9.3.3 Grip strength **Pag. 163**

9.4 Haematocrit measurement **Pag. 163**

9.5 Spinal cord perfusion and slices preparation **Pag. 164**

9.6 Immunohystochemistry **Pag. 166**

9.6.1 ChAT **Pag. 166**

9.6.2 Cd11b **Pag. 166**

9.6.3 TNF-α and TNF receptors **Pag. 167**

9.6.4 Active caspases 3, 7, 8 and 9 **Pag. 168**
9.6.5 GluR 1-4 **Pag. 169**
9.6.6 BDNF **Pag. 170**
9.6.7 EPOr **Pag. 171**
9.6.8 Densitometric analysis **Pag. 171**
9.7 Hystological staining **Pag. 172**
9.7.1 NISSL staining **Pag. 172**
9.7.2 In Situ End Labelling (ISEL) colorimetric assay **Pag. 173**
9.7.3 Mitochondrial complex I staining **Pag. 174**
9.8 Immunoblotting **Pag. 175**
9.8.1 AMPA receptor subunits (GluR 1-4) **Pag. 175**
9.8.2 Glutamate transporters (GLAST and GLT1) **Pag. 176**
9.8.3 Densitometric measurement **Pag. 176**
9.9 Glutamate determination in plasma **Pag. 176**
9.10 [^{3}H] uptake experiments **Pag. 177**
9.11 Mitochondrial activity measurement **Pag. 178**
9.11.1 Oxygen consumption rate **Pag. 178**
9.11.2 Spectrophotometric assays **Pag. 178**
9.12 ChAT activity determination **Pag. 179**
9.13 Statistics **Pag. 180**

CHAPTER 10 *In vitro* RESULTS

10.1 BDNF/serum withdrawal induces apoptosis in primary cultures of motor neurons **Pag. 182**
10.1.1 Introduction **Pag. 182**
10.1.2 Experimental design **Pag. 183**
10.1.3 Results **Pag. 184**
10.1.4 Discussion **Pag. 190**
10.2 Chronic treatments with AMPA and Kainate induce cell death in primary cultures of motor neurons by different mechanisms **Pag. 192**
10.2.1 Introduction **Pag. 192**
10.2.2 Results **Pag. 193**
10.2.2.1 AMPAr subunits expression **Pag. 193**
10.2.2.2 AMPA and kainate toxicity: time-course **Pag. 198**

10.2.2.3 Nuclear fragmentation and membrane permeabilization **Pag. 200**
10.2.2.4 Caspases 3-9 activation **Pag. 203**
10.2.3 Discussion **Pag. 209**
10.3 EPO selectively protects primary cultures of motor neurons from apoptosis **Pag. 211**
10.3.1 Introduction **Pag. 211**
10.3.2 Results **Pag. 212**
10.3.2.1 EPO receptor is expressed in embryo rat spinal motor neurons **Pag. 212**
10.3.2.2 Serum/BDNF deprivation and EPO **Pag. 212**
10.3.2.3 EPO protects motor neurons exposed to kainate but not to AMPA **Pag. 217**
10.3.2.4 EPO reduces nuclear fragmentation in kainate treated motor neurons **Pag. 218**
10.3.2.5 EPO inhibits caspases 3 and 9 activation in kainate treated motor neurons **Pag. 219**
10.3.3 Discussion **Pag. 221**
10.4 EPO exerts its anti-apoptotic effect on primary cultures of motor neurons by inhibiting the mitochondrial depolarization produced by kainate treatment **Pag. 223**
10.4.1 Introduction **Pag. 223**
10.4.2 Results **Pag. 224**
10.4.2.1 Cytochrome-c release **Pag. 224**
10.4.2.2 Mitochondrial membrane potential **Pag. 226**
10.4.2.3 AMPA, kainate and the mitochondrial PTP **Pag. 229**
10.4.3 Discussion **Pag. 230**

CHAPTER 11 MECHANISMS OF MOTOR NEURON DEATH IN THE CERVICAL SPINAL CORD OF WOBBLER MICE
11.1 Motor neuron loss: time-course in wobbler mice **Pag. 233**
11.1.1 Introduction **Pag. 233**
11.1.2 Experimental design **Pag. 234**
11.1.3 Results **Pag. 235**
11.1.3.1 Genotyping **Pag. 235**
11.1.3.2 Motor neuron counting **Pag. 236**
11.1.4 Discussion **Pag. 244**
11.2 Neuroinflammation and apoptosis **Pag. 246**
11.2.1 Introduction **Pag. 246**

11.2.2 Experimental design **Pag. 246**
11.2.3 Results **Pag. 247**
11.2.3.1 Microglial staining **Pag. 247**
11.2.3.2 TNF-α immunostaining **Pag. 249**
11.2.3.3 TNF receptors immunohystochemistry **Pag. 251**
11.2.3.4 Active caspase 8 immunohystochemistry **Pag. 253**
11.2.4 Discussion **Pag. 255**
11.3 Excitotoxicity and wobbler mouse motor neuron disease **Pag. 257**
11.3.1 Introduction **Pag. 257**
11.3.2 Experimental design **Pag. 257**
11.3.3 Results **Pag. 258**
11.3.3.1 Glutamate determination in plasma **Pag. 258**
11.3.3.2 Glutamate transporters **Pag. 258**
11.3.3.3 AMPAr expression and localization **Pag. 261**
11.3.4 Discussion **Pag. 270**
11.4 Mitochondria and apoptosis **Pag. 271**
11.4.1 Introduction **Pag. 271**
11.4.2 Experimental design **Pag. 271**
11.4.3 Results **Pag. 272**
11.4.3.1 Mitochondrial activity **Pag. 272**
11.4.3.2 Active caspase 3, -7, -9 immunohystochemistry **Pag. 275**
11.4.3.3 ISEL staining **Pag. 279**
11.4.4 Discussion **Pag. 282**

CHAPTER 12 PHARMACOLOGICAL TREATMENTS

12.1 EPO fails to arrest neuromuscular impairment and motor neurons loss in wobbler mice **Pag. 285**
12.1.1 Introduction **Pag. 285**
12.1.2 Experimental design **Pag. 286**
12.1.3 Results **Pag. 287**
12.1.3.1 Behavioural scores **Pag. 287**
12.1.3.2 Neuropathological estimation **Pag. 291**
12.1.3.3 EPOr immunohystochemistry **Pag. 292**
12.1.3.4 Haematocrit measurement **Pag. 294**

12.1.4 Discussion **Pag. 295**

12.2 Riluzole, unlike the AMPA antagonist RPR119990, reduces motor impairment and partially prevents motor neurons death in wobbler mice **Pag. 296**

12.2.1 Introduction **Pag. 296**

12.2.2 Experimental design **Pag. 298**

12.2.3 Results **Pag. 299**

12.2.3.1 Behavioural scores **Pag. 299**

12.2.3.2 Neuropathological estimation **Pag. 307**

12.2.3.3 BDNF immunostaining **Pag. 309**

12.2.4 Discussion **Pag. 312**

CHAPTER 13 APOPTOSIS AND ALS: A LESSON FROM CELLULAR AND ANIMAL MODELS OF MOTOR NEURON DEGENERATION

13.1 Neurotrophic factors starvation and apoptosis **Pag. 319**

13.2 Glutamate-induced excitotoxicity and apoptosis **Pag. 323**

13.3 Glial-induced neuroinflammation and apoptosis **Pag. 326**

REFERENCES

ACKNOWLEDGEMENTS

- First, I would like to acknowledge my head of laboratory and director of studies, Tiziana Mennini, for always being a point of reference during the development of my thesis.

- I would like to thank my second supervisor, Vincenzo Crunelli, for critically reading the manuscript and for giving me advice in the structuring of this thesis.

- I wish to express my gratitude for the support of the Mario Negri Institute, in particular the director Silvio Garattini and my head of Department and director of academic activities, Mario Salmona, for giving me the opportunity to do this PhD.

- I also would like to acknowledge Daniela Curti, Ettore Beghi, Pietro Ghezzi and Antonio Migheli for their critical analyses and for their cultural contribution.

- I wish to thank all my colleagues, in particular Elena Fumagalli and Sara Barbera, for their indispensable collaboration, Ilario Mereghetti and Massimo Farina for their informatics support and Alfredo Cagnotto, an important point of reference for the lab activities. Moreover I would like to thank the "motor neurons' team" (Simona, Claudio, Francesca and Massimiliano). Many thanks to Rita Campi for statistical advices.

- I'm grateful to Felice De Ceglie and Alessandro Soave for the graphic assistance.

- I am very grateful to Noeleen De Angelis and Gary David Odd for

giving me precious advice in English writing.

- A special thanks to Massimo Tortarolo, a sparring partner, a source of help and calmness and, above all, a dear friend.

- Many many thanks, once again, to my parents and their powerful PC, which allowed me to see the sea and the beach through the window, while I was writing this thesis on summer holydays. Next time, I will advice them to buy a lap top!

- Last, but not least, I wish to express my total and unconditioned gratitude, and not only, to Antonella for putting with me over these last stressful months.

COLLABORATIONS

- The measurement of mitochondrial membrane potential in cultures of motor neurons, the evaluation of mitochondrial respiration and mitochondrial enzymes activity in mice were performed in collaboration with Prof. Daniela Curti, Dr. Giovanna Levandis and Dr. Barbara Santoro, Department of Cellular & Molecular Physiological & Pharmacological Sciences, University of Pavia, Italy.

- The measurement of protein levels of AMPA receptor subunits, GluR 1-4, in the mice cervical spinal cord homogenates were carried out in collaboration with Prof. Monica De Luca and Dr. Fabrizio Gardoni, Department of Pharmacological Sciences, University of Milan, Italy.

- In situ end labelling (INSEL) experiments in the mice cervical spinal cord of wobbler mice and in cerebellar sections of weaver mice were done in collaboration with Prof. Antonio Migheli and Dr. Cristiana Atzori, Department of Anatomy, Pharmacology and Forensic Medicine, University of Torino, Italy.

- The measurement of plasmatic aminoacids levels in mice were performed in collaboration with Mr. Antonio Bastone, Laboratory of Biochemistry and Protein Chemistry, Department of Biochemistry and Molecular Pharmacology, Mario Negri Institute of Milan, Italy.

- The experiments of [^{3}H]glutamate uptake in the mice cervical spinal cord homogenates were carried out in collaboration with Dr. Marco Gobbi, Dr. Marcella Funicello and Dr. Lorenza Pirona, Unit of Synaptic Transmission, Laboratory of Receptor Pharmacology, Department of Biochemistry and Molecular Pharmacology, Mario Negri Institute of Milan, Italy.

ABSTRACT

Amyotrophic lateral sclerosis (ALS) is a neurodegenerative disease leading to motor neurons death. Although many studies were performed, the aetiology and the features of cellular death occurring in ALS are poorly understood, and studies carried out from autoptic samples do not allow to clarify early events occurring in ALS. To understand the basic mechanisms leading to motor neuronal death in ALS and to detect the different steps involved in motor neuron degeneration, alternative models are required.

The wobbler mouse is one of the most reliable models of human motor neurodegenerative diseases. In the wobbler mouse neuromuscular deficits that are related to a selective vulnerability of cervical spinal cord motor neurons have an early onset and progress rapidly.

In my project of thesis I first characterized apoptosis in primary cultures of motor neurons exposed to detrimental stimuli, and then I evaluated the possible involvement of apoptosis in the cervical spinal cord neurons of early symptomatic wobbler mice.

In primary cultures of motor neurons I found that: I) BDNF deprivation produced apoptotic cell death, II) AMPA and kainate induced apoptotic or non apoptotic cell death depending on the experimental conditions utilized, III) EPO selectively protected motor neurons committed to dye apoptically.

In wobbler mice I found that: I) mitochondrial activity is reduced but caspase 9-mediated apoptosis does not seem involved, II) glutamate induced excitotoxicity does not seem involved in motor neuron degeneration, III) markers of neuroinflammation, such as activated microglia and TNF-α, appeared highly increased in the cervical region of early symptomatic wobbler mice but this process does not seem to induce the activation of caspase 8-mediated apoptosis.

Pharmacological treatments confirmed that an antiglutamatergic agent (RPR 119990) and an antiapoptotic agent (EPO) were ineffective, while riluzole showed protective effects.

Although alternative cell death pathways should be investigated, my study excludes apoptosis as the mechanism of death in cervical motor neurons of wobbler mice.

LIST OF TABLES AND FIGURES

Figure 1.1 Motor neurons and muscles selectively affected in ALS Pag. 30

Table 1.1 Clinical criteria included in El Elscorial diagnostic scale Pag. 34

Table 1.2 Neuropathological criteria included in El Escorial scale Pag. 35

Figure 1.2 Glutamate-induced excitotoxicity and motor neuron death Pag. 45

Figure 1.3 Glial-induced motor neuron toxicity Pag. 52

Table 1.3 Clinical trials in ALS Pag. 55

Figure 2.1 Extrinsic apoptotic pathway and death receptors Pag. 68

Figure 2.2 Intrinsic apoptotic pathway and neurotrophic factors withdrawal Pag. 69

Table 3.1Neuropathology of murine models of ALS Pag. 93

Figure 4.1 Cell death pathways in motor neurons transfected with human mutated SOD-1 dismutase gene Pag. 102

Figure 5.1 Neuropathological and biochemical alterations in wobbler mouse motor neuron disease Pag. 129

Figure 8.1 Avidin Biotin Complex (ABC) staining enhancement Pag. 151

Figure 9.1 Surgical devices for rodents perfusion Pag. 165

Table 10.1 Percentage of motor neurons viability in mixed glia/neurons cultures after chronic deprivation of serum and BDNF Pag. 184

Table 10.2 Percentage of motor neurons viability in purified cultures after chronic deprivation of serum and BDNF Pag. 184

Table 10.3 Percentage of fragmented nuclei in purified motor neurons after 18 hours of serum and BDNF deprivation Pag. 184

Figure 10.1 SMI32 staining in cultured on mixed cultures Pag. 186

Figure 10.2 Hoechst staining in cultures of purified motor neurons Serum/BDNF deprived Pag. 187

Table 10.4 Percentage of active caspase 3 positive motor neurons in

purified cultures after 6 hours of serum and BDNF deprivation Pag. 188

Figure 10.3 Active casapse-3 immunostaining in cultures of purified motor neurons six hours after serum/BDNF deprivation Pag. 189

Figure 10.4 GluR1 immunostaining in cultures of purified motor neurons Pag. 194

Figure 10.5 GluR2 immunostaining in cultures of purified motor neurons Pag. 195

Figure 10.6 GluR3 immunostaining in cultures of purified motor neurons Pag. 196

Figure 10.7 GluR4 immunostaining in cultures of purified motor neurons Pag. 197

Figure 10.8 Motor neurons death time-course following AMPA or kainate exposure Pag. 199

Table 10.5 Percentage of fragmented nuclei in motor neurons (mixed glia/neurons cultures) exposed to AMPA or kainate Pag. 200

Figure 10.9 Syto59 and PI staining in purified cultures of motor neurons following AMPA or kainate exposure Pag. 202

Figure 10.10 SMI32 and active caspase-3 immunostaining in mixed glia/neurons cultures exposed to AMPA and kainate Pag. 204

Table 10.6 Percentage of active caspase 3 positive cells in motor neurons (mixed glia/neurons cultures) exposed to AMPA or kainate Pag. 205

Figure 10.11 SMI32 and active caspase-9 immunostaining in mixed glia/neurons cultures exposed to AMPA and kainate Pag. 206

Table 10.7 Percentage of active caspase 9 positive cells in motor neurons (mixed glia/neurons cultures) exposed to AMPA or kainate Pag. 207

Figure 10.12 SMI32 and active caspase-3 and -9, cellular staining Pag. 208

Figure 10.13 EPOr staining in mixed and purified cultures of motor neurons Pag. 213

Table 10.8 Protective effect of EPO treatment on motor neurons survival after chronic deprivation of serum and BDNF Pag. 214

Table 10.9 Protective effect of EPO in reducing the percentage of

fragmented nuclei in purified motor neurons

(18 hours of serum/BDNF deprivation) Pag. 214

Table 10.10 Protective effect of EPO in reducing the percentage of active

caspase 3 motor neurons (6 hours after serum/BDNF deprivation) Pag. 214

Figure 10.14 Effect of EPO treatment at the basal condition Pag. 216

Table 10.11 Effect of EPO on motor neuron survival (mixed glia/neurons

cultures) after AMPA or kainate chronic exposure Pag. 217

Table 10.12 Effect of EPO on percentage of fragmented nuclei in motor

neurons 18 hours after to AMPA or kainate Pag. 218

Table 10.13 Effect of EPO on percentage of caspase 3 positive cells in motor

neurons 6 hours after to AMPA or kainate Pag. 219

Table 10.14 Effect of EPO on percentage of caspase 9 positive cells in motor

neurons after 6 hours after to AMPA or kainate exposure Pag. 220

Figure 10.15 Cytochrome-c and Mito Tracker immunostaining Pag. 225

Table 10.15 Levels of mitochondrial energisation in purified cultures

of motor neurons after 18 hours to AMPA or kainate exposure Pag. 226

Figure 10.16 JC-1 and Hoechst staining Pag. 228

Table 10.16 Effect of cyclosporin A_2 on motor neuron survival (mixed glia/neurons cultures) after 48 hours to AMPA or kainate exposure Pag. 229

Figure 10.17 Motor neuron death pathways (mixed glia/neurons cultures) exposed to AMPA 1μm or kainate 5 μm Pag. 232

Figure 11.1 Wobbler genotyping Pag. 236

Figure 11.2 Nissl staining, cervical spinal cord Pag. 238

Figure 11.3 ChAT staining, cervical spinal cord Pag. 239

Figure 11.4 Nissl staining, motor neurons Pag. 241

Figure 11.5 ChAT staining, motor neurons Pag. 242

Figure 11.6 Motor neurons death time-course during symptoms progression in wobbler mice Pag. 243

Figure 11.7 CD11b, microglial, staining Pag. 247

Figure 11.8 TNF-α immunostaining Pag. 249

Figure 11.9 TNFR1 immunostaining Pag. 251

Table 11.1 ChAT and caspase 8 positive cells in the cervical spinal cord of 4 week-old wobbler mice and healthy littermates Pag. 253

Figure 11.10 Active caspase 8 immunostaining Pag. 254

Table 11.2 Aminoacids concentrations in the plasma of wobbler mice and age matched healthy littermates Pag. 258

Figure 11.11 Western blots of glial glutamate transporters , GLT1 and GLAST, in cervical spinal cord homogenates Pag. 259

Table 11.3 GLT-1 and GLAST protein levels in the cervical spinal cord Pag. 260

Table 11.4 [^{3}H] glutamate uptake in P2, cervical spinal cord homogenates Pag. 260

Figure 11.12 GluR1 immunostaining in the cervical spinal cord Pag. 262

Figure 11.13 GluR2 immunostaining in the cervical spinal cord

Figure 11.14 GluR3 immunostaining in the cervical spinal cord Pag. 266

Figure 11.15 GluR4 immunostaining in the cervical spinal cord Pag. 267

Table 11.5 GluR 1-4 protein levels in cervical spinal cord homogenates

(post synaptic densities) Pag. 268

Figure 11.16 Western blots of GluR1-4 in cervical spinal cord homogenates Pag. 269

Figure 11.17 Representative trace/readout of QO_2 measurement Pag. 274

Figure 11.18 Mitochondrial complex I, hystochemical staining Pag. 275

Table 11.6 ChAT and caspase 9 positive cells in the cervical spinal cord

region of 4 week-old wobbler mice and healthy littermates Pag. 275

Table 11.7 ChAT and caspase 7 positive cells in the cervical spinal cord

region of 4 week-old wobbler mice and healthy littermates Pag. 276

Table 11.8 ChAT and caspase 3 positive cells in the cervical spinal cord region

of 4 week-old wobbler mice and healthy littermates Pag. 276

Figure 11.19 Active caspases-9-7-3 immunostaining, cervical spinal cord Pag. 278

Figure 11.20 Active caspases-9-7-3 immunostaining, motor neurons Pag. 279

Figure 11.21 Nissl and ISEL staining, cervical spinal cord (wobbler mouse)

and cerebellum (weaver mouse) Pag. 280

Figure 12.1 Body weight, paw abnormality, walking abnormality

in EPO treated wobbler mice Pag. 288

Figure 12.2 Running time and grip strength in EPO treated wobbler mice Pag. 290

Table 12.1 Nissl positive motor neurons in the cervical region of wobbler mice and healthy littermates after chronic treatment with EPO Pag. 291

Table 12.2 Biceps weight of wobbler mice and healthy littermates after chronic treatment with EPO Pag. 291

Table 12.3 ChAT activity in the cervical spinal cord homogenates, EPO and vehicle treated wobbler mice and healthy littermates Pag. 292

Figure 12.3 EPOr immunostaining after chronic treatment with EPO Pag. 293

Table 12.4 Haematocrit levels in wobbler and healthy littermates after chronic treatment with EPO Pag. 294

Figure 12.4 Body weight in RPR119990 and riluzole treated wobbler mice Pag. 300

Figure 12.5 Paw abnormality in RPR119990 and riluzole treated wobbler mice Pag. 302

Figure 12.6 Walking abnormality in RPR119990 and riluzole treated wobbler mice Pag. 303

Figure 12.7 Running time in RPR119990 and riluzole treated wobbler mice Pag. 305

Figure 12.8 Grip strength measurements in RPR119990 and riluzole treated wobbler mice Pag. 306

Table 12.5 Nissl positive motor neurons in the cervical region of wobbler mice and healthy littermates after chronic treatment with riluzole Pag. 307

Table 12.6 Nissl positive motor neurons in the cervical region, of wobbler mice and healthy littermates after chronic treatment with RPR119990 Pag. 307

Table 12.7 Biceps weight of wobbler mice and healthy littermates after chronic treatment with riluzole Pag. 308

Table 12.8 Biceps weight of wobbler mice and healthy littermates after chronic treatment with RPR119990 Pag. 308

Figure 12.9 BDNF immunostaining after chronic treatment with riluzole, cervical spinal cord Pag. 310

Table 12.9 Percentage of BDNF immunodensity in motor neurons of wobbler mice and healthy littermates after chronic treatment with riluzole Pag. 311

LIST OF ABBREVIATIONS

- ABC, (Avidin Biotin Complex)
- ADAM8, (a disintegrin-like and metalloproteinase 8)
- ADP, (Adenosine DiPhosphate)
- AIDS, (Acquired Immuno Deficiency Syndrome)
- AIFS, (Apoptotic-Initiating Factors)
- AIS, (Analyser Image Software)
- ALCAR, (Acetyl-L-CARinitine)
- AMPA,(α-Amino-3-hydroxy-5-Methyl-4-isoxazole Propionate receptor)
- AP-1, (Activator Protein 1)
- Apaf-1, (Apoptosis Protease Activating Factor-1)
- Ask-1, (Anti-Apoptosis Signal-Regulating Kinase)
- ALS, (Amyotrophic Later Sclerosis)
- ASL FRS, (ALS Functional Rating Scale)
- ATP, (Adenosine Triphosphate)
- BAD,(Bcl-2 Activating Death)
- BBB, (Blood Brain Barrier)
- BCL-2, (B-cell Lymphome 2)
- BDNF, (Brain-Derived Neutrophic Factor)
- BID, (Bcl-2 Interacting Domain)
- BIM, (Bcl-2 Interacting Mediator)
- BSA, (Bovine Serum Albumine)
- CAD, (Capsase-Activate DNAase)
- cAMP, (Adenosine Cyclic Monophosphate)
- CCM, (Complete Colture Medium)

- CdK, (Cyclin-dependent Kinase)
- CED, (Caernobitidis Elegans Death-Domain)
- CGC, (Cerebellar Granule Cells)
- ChAT, (Choline Acetyl Transferase)
- CNS, (Central Nervous System)
- CNTF, (Ciliary Neutrophic Factor)
- CNQX, (6-cyano-7-nitroquinoxaline-2,3-dione)
- CRE, (cAMP Responsive Element)
- CS, (Citrate Synthase)
- CT-1, (Cardiotrophin-1)
- DAB, (3,3'-Diaminobenzidine)
- DED, (Death Effector Domain)
- DFF, (DNA Fragmetation Factors)
- DISC, (Death-Inducing Signaling Complex)
- DIV-6, (6^{th} division)
- DMSO, (Dimethyl Sulfoxide)
- DNA, (Deoxy Ribonucleic Acid)
- DR4-DR5, (Death Receptors 4-5)
- DTNB, (5-5'-dithiobis 2-nitrobenzoic acid)
- E-14, (Embryonic day 14^{th})
- EAAT-1-2 , (Excitatory Amino Acid Transporter-1-2)
- EDTA, (Ethylendiamine)
- Egl-l, (Egg-Laying-1)
- EGTA, (Ethylene glycol-bis(2-amioethylether)-N,N,N',N'-tetraacetic acid)
- EPO, (Erythropoietine)

- ER, (Endoplasmic Reticulum)
- ERF, (Extracellular signal-Regulated Kinase Factor)
- ERK, (Extracellular signal-Regulated Kinase)
- ETC, (Electron Transport Chain)
- FADD, (Fas-Associated Death Domain)
- FasL, (Fas ligand)
- FCS, (Fetal Calf Serum)
- FDA, (Food and Drug Administration)
- GAGS, (Glycosaminoglycans)
- GDNF, (Glial Derived Neurotrophic Factors)
- GEFS, (Guanine-Nucleotide Exchange Factors)
- GFAP, (Glial FIbrillary Acidic Protein)
- GGA, (Geranylgeranylacetone)
- GIRK2, (G-protein-dependent Inward Rectifier K channels)
- GluR 1, 2, 3,4, (Glutamate receptors)
- GM-CSF, (Granulocyte Macrophages Colony Stimulating Factor)
- hBOT, (Hyperbaric Oxigen Therapy)
- HIF-1, (Hypoxia-Inducibile Trascription Factor)
- HIV-1, (Human Immunodeficiency Virus type 1)
- Hsp70, (Heat Shock Protein)
- IAPS, (Inhibitor of Apoptosis Proteases)
- ICAD, (Inhibitor Capsase-Activate DNAase)
- IGF-1, (Insuline- Like Growth Factor-1)
- IgG, (Immunoglogulin G)
- IL, (Interleukine)

- IP, (Intraperitonally)
- ISEL, (In Situ End-Labeling)
- JAK, (Janus Activated Kinase)
- JNK, (c-Jun N-terminal protein kinase)
- JPLS, (Juvenile Primary Lateral Sclerosis)
- LBHIS, (Lewis Body-Like Hyaline Inclusions)
- LIF, (Leukemia Inhibitory Factor)
- LMN, (Lowor Motor Neuron)
- L-NAME, (Nomega-nitro- l-arginine methyl ester)
- LPS, (Lipopolysaccharide)
- MAP, (Mitogen-Activated Protein)
- MK801,((+)-5-methyl-10,11-dihydro-5H-dibenzo(a,d)cyclopheten-5,10-imine maleate)
- MND, (Motor Neuron Degeneration)
- MPTP, (1-Methyl-1,4-Phenyl-1,2,3,6-tetrahydropyridine)
- mtDNA, (Mitochondrial DNA)
- NA, (Noradrenaline)
- NADH, (Nicotidamide Adenine Dinucleotide)
- NBT, (Nitro Blue Tetrazolium)
- N-CAM, (Neuronal-cell Adhesion molecule)
- NF, (Neurofilament)
- NF-kB, (Nuclear Factor-*kB*)
- NGF, (Nerve Growth Factor)
- NMDA, (N-methyl-D-aspartate)
- NO, (Nitric Oxide)

- NOND, (Naturally Occuring Neuronal Death)
- NOS, (Nitric Oxide Syntetase)
- NQBX, (2,3-dioxo-6-nitro-1,2,3,4,-tetrahydrobenzo[f]quinoxaline-7-sulfonamide)
- P, (Post Natal days)
- P2, (Sinaptosomal Preparation)
- P38, (Protein Stress Activated 38)
- PARP-1, (Poly(ADP-Ribose) Polymerase-1)
- PBS, (Phosphate Buffered Saline)
- PCD, (Programmed Cell Death)
- PI, (Propidium Iodine)
- PI_3K, (Phosphoinositide-3 Kinase)
- PkB or AKT, (Protein Kinase B)
- *Pmn*, (Paralysè Natural Mutant Mouse)
- PMT, (Photomoltiplicator)
- PSD, (Post Synaptic Density)
- PTP, (Permeability Transition Pore)
- QO2, (Quotient Oxygen Consum)
- RER, (Rough Endoplasmic Reticulum)
- RFLP, (Restriction Fragment Length Polymorphism)
- rHuEPO, (Recumbinant Human Erythropoietin)
- RNA, (Ribonucleic Acid)
- ROD, (Related Optical Density)
- ROS, (Radical Oxigen Free)
- RT-PCR, (Real Time Polymerase Chain Reaction)
- SD, (Standard Deviation)

- SDS, (Sodium Dodecyl Sulphtae)
- SE, (Standard Error)
- Slc1a4/ASCT1, (Alanine, Serine, Cysteine, Threonine Trasporter 1)
- SMA, (Spino Muscular Atrophy)
- SMI, (Stenberger Monoclonal Incorporated)
- SOD-1, (Superoxide Dismutase-1)
- STAT-5
- T-588,(R(-1)-1-(benzo(b)thiopen-5yl)-2-(2(N,n-diethylamino)ethoxy)ethanol hydrochloride)
- TBS, (Tris Buffered Saline)
- Tdt, (Terminal Deoxinucleotidyl Transferase)
- TGF-α, (Tumor Growth Factor- α)
- TMPD, (N,N,N'N'- Tetramethyl-p-Phenylendiamine)
- TNF, (Tumor Necrosis Factor)
- TRADD, (TNF-Related-Associated Death Domain)
- TRAF2/RIP 1, (Tumor Necrosis Associated Factor 2/ Receptor-Integrated Protein 1)
- TRAIL, (TNF-Related Apoptosis - Inducing Ligand)
- TRH, (Thyrotropin-Releasing Hormone)
- TrkB, (Tyrosine Kinase receptor B)
- TRPM, (Testosterone Repressed Prostate Message 2)
- TUNEL, (d-UTP Nick and Labelling)
- UMN, (Upper Motor Neuron)
- UV, (Ultra Violet)
- VEGF, (Vascular Endotelial Growth Factor)

- Wr, (Wobbler)

INTRODUCTION

CHAPTER 1

HUMAN AMYOTROPHIC LATERAL SCLEROSIS

1.1 Clinical hallmarks: symptoms and diagnosis

1.1.1 Epidemiology (incidence, prevalence, onset)

Amyotrophic lateral sclerosis (ALS) is a progressive neurodegenerative disorder involving primarily motor neurons in the spinal cord, brainstem and cerebral motor cortex and leading to denervation, muscular atrophy and paralysis (Fig 1.1 Rowland) [Brooks, 1994].

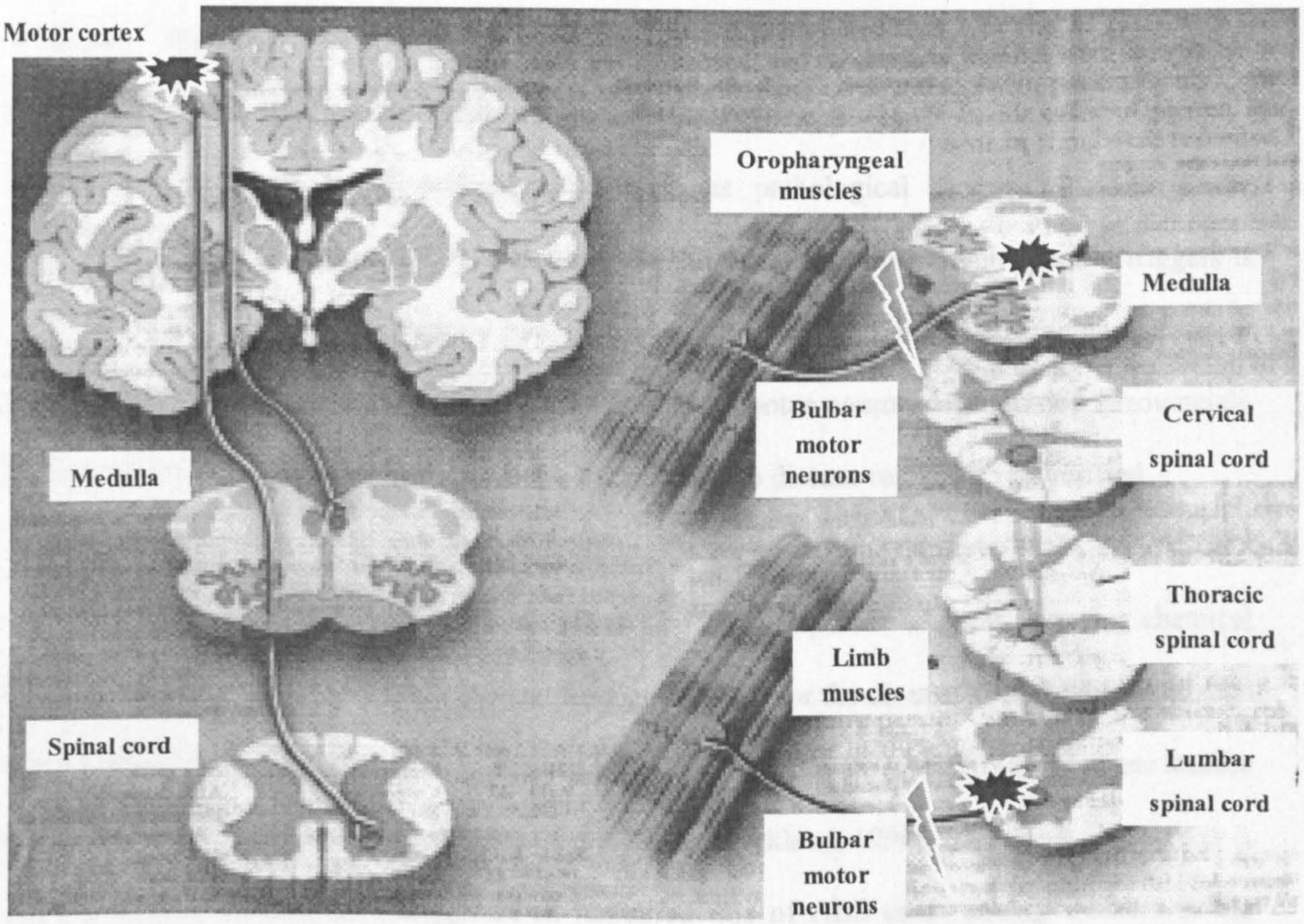

Figure 1.1 Pattern of cellular districts that are more affected in ALS. Upper and lower motor neurons loss produce a marked denervation and a consequent atrophy of skeletal muscles. Paralysis and respiratory failure are the main symptoms that lead to the death of ALS patients

ALS is a progressive disease and the prognosis is negative. The average of survival from

symptoms comparison is < 5 years. Worst prognoses are associated with a younger age at symptoms onset and a limb onset symptoms in contrast to early bulbar dysfunction [Eisen, 1993;Jablecki, 1989;Strong, 1991].

ALS affects between 1.2 and 1.8/ 100,000 individuals [Eisen, 1993;Jablecki, 1989 ;Strong, 1991]. This age-dependent disorder is increasing in incidence at a rate, which cannot be accounted for by population aging alone.

Three variants of ALS are generally considered: I) the Pacific type (often associated with dementia); II) the familial form (fALS) (the majority of which are autosomal dominant in their inheritance) [Rosen, 1993] and; the sporadic ALS. The disease is sporadic in approximately 90% of cases [Rowland, 1998]. Familial cases show a typical pattern of autosomal dominant inheritance, but only in a few percentage of familial cases (20%) the correlation between the pathology to a well known gene mutation is known [Cudkowicz, 1997].

Environmental factors are considered of interest as pathological factors of ALS [Chou, 1992;Arvidson, 1992;Kapaki, 1997]. Unfortunately the identification of such specific triggers is very difficult. Anecdotal case reports and retrospective views have indicated trauma, stress or environmental exposure as possible factors that lead to motor neuron degeneration [Provinciali, 1990]. However, a correlation between these factors and the disease remains to be verified.

A higher incidence of ALS was observed among factory workers, domestic staff, athletes and labourers involved in heavy manual work [Bracco, 1979]. Exposure to areas of major chemical industry has also been suggested to account for a greater risk for the disease. Chemical agents, such as lead, mercury and solvents, seem to increase the level of risk for ALS. However, these studies are limited in the number of patients [Abarbanel, 1985 ;Strickland, 1996].

Epidemiological studies have suggested an increased rate of ALS cases among workers in the plastics industry, people whose have had recent trauma or significant electrical injury [Strong, 1991] , and among professional Italian footballers [Beretta, 2003].

1.1.2 Symptoms

The clinical onset of ALS is characterized by asymmetrical spread of symptoms that involves multiple levels of the neuraxis [Brooks, 1994 ;Munsat, 1988]. Although there is a formal separation between sporadic and familial groups, both forms show similar clinical and pathological features and seem to share common pathophysiological mechanisms [Andersen, 1997].

The low frequency and the late onset of the disease suggests that sporadic ALS may have a preclinical phase. During the preclinical phase it is thought that a series of events create a state of susceptibility that leads to the development of symptoms. No clear evidence of neuropathological, neurophysiological or biochemical markers are as yet available to identify a patient as potentially susceptible for ALS before symptom onset [de Carvalho, 2003].

During the early symptomatic period there are neuropathological alterations (involving motor neuron size, corticospinal tract alteration and motor axonal conduction modification), that are sub-pathological changes in ALS. The onset of the clinical phase is revealed by functional changes in ALS patients and possible abnormalities in isokinetic muscle tests at time when isometric strength is not yet reduced in these patients [de Carvalho, 2003].

Symptomatic phase produces a rapid evolution at the same level of neuroaxis, in horizontal direction, prior to rostral or caudal spread throughout the neuraxis. In patients with a distinct anatomical onset of symptoms, usually the progression of the disease follows a different pattern of evolution [Rowland, 1991].

The early phase is followed by a symptomatic stage in which sub clinical alterations diffuse from focal to more symmetrical generalisation. At this point ALS patients show changes in isokinetic strength as well as early changes in isometric strength. During this phase, pathology is usually reported to be more severe in regions where ALS had initially started but progressively increases even in regions in which the symptoms had spread [Ince, 1998].

Nevertheless the clinical involvement of other systems is not considered in ALS diagnosis, recent studies have revealed the concomitant presence of unrelated symptoms, including sensory dysfunction, autonomic nervous system abnormalities mood alterations and cognitive abnormalities [Mulder, 1983; Daube, 2000].

Respiratory failure is the most common cause of death in ALS patients. Respiratory deficits are

due to the progressive atrophy of respiratory muscles. Very often, in ALS patients, the diaphragm appears to be particularly vulnerable to atrophy [Brooks, 1994]. Measurements of forced vital capacity are useful to identify early respiratory problems [Borasio, 1997]. Dyspnea at rest is the earlier hallmark of respiratory failure. As the respiratory difficulty increases, attacks of sleep apnea do not permit to patients to sleep supine. During the development of the disease, when respiratory forced activity is completely lost, patients need to use accessory ventilation. Respiratory failure finally leads to the death of most ALS patients [Gelanis, 2001].

1.1.3 Diagnosis

1.1.3.1 Clinical criteria

The early diagnosis of ALS is based on the recognition of a clinical pattern of symptoms, aided by electrophysiological determination [Swash, 2000]. The loss of muscular strength has been considered as a surrogate marker for the loss of motor neurons. However, the even more pressing requests for a universal and precise diagnostic criterion led to a classification in 1990. This determination was called "El Escorial" scale. "El Escorial" scale is based on different parameters, clinical features that allow distinguishing ALS from other motor neuron diseases.

The "El Escorial" scale classifies the probability of a patient having ALS, according to the degree of clinical certainty in relation to other pathologies, such as multiple sclerosis, cervical myelopathy and other similar neuromuscular disorders [Brooks, 1994].

The "El Escorial" scale includes four degrees of certainty for the diagnosis of ALS. They can range from "clinically definite" to "clinically suspected". The four different levels of certainty are reported below.

-Definite ALS: is defined by upper motor neuron (UMN) and lower motor neurons (LMN) signs in bulbar and in two spinal regions, or UMN and LMN signs in three spinal cord regions.
-Probable ALS: is defined by UMN and LMN signs in at least two regions and UMN signs in a region rostral to LMN signs.
-Possible ALS: is defined by UMN and LMN signs in one region or UMN signs in two or three regions.
-Suspected ALS: is define by UMN and LMN signs in two or three regions.

Table 1.1 Clinical criteria included in the El Escorial diagnostic scale.

Although the "El Escorial" scale represents a valid criterion to diagnoses ALS, this approach can not evaluate the progression of symptoms. To determine a more efficient protocol to score the progression of symptoms, an alternative series of tests (the Amyotrophic Functional Rating Scale (ALS FRS)) have been undertaken. The ALS FRS is a ten-item scale with five different scores for each item. The total score is obtained by the sum of scores for each single item and increases

proportionally to the symptomatological worsening. The evaluation of three bulbar functions (speech, salivation and swallowing), one respiratory function (breathing), three upper-extremity (handwriting, cutting food and dressing), one truncal function (turning in bed) and two lower-extremity (walking and climbing stairs) are included in ALS FRS (ALS CNTF Treatment Study group-no authors listed).

The aim of this scale is: I) to provide an unique, simple, reproducible, sensitive and specific protocol to test the possible efficiency of drugs during clinical trials; II) to better characterize and separate the evolution of symptoms among the different forms of ALS; III) to define the different stages of disease for a population of patients who might have all types of onset.

1.1.3.2 Neuropathological and hystopathological criteria

In 1994 neuropathological analyses were included in the "El Escorial" diagnostic criteria (World Federation of Neurology Research Group on Neuromuscular Disease Subcommittee on Motor Neuron Disease). The guidelines to make neuropathological diagnoses of ALS are listed below.

Features that support the diagnosis:
Selective atrophy of the motor cortex
Greyness and atrophy of anterior spinal nerve roots compared with normal roots
Grains of the lateral columns of the spinal cord
Atrophy of skeletal muscles
Features that rule out the diagnosis of ALS or suggest the presence of additional disease
• **Plaques of multiple sclerosis**
• **A focal cause of myelopathy**

Table 1.2 Neuropathological parameters of diagnosis included in the El Escorial scale

Because of the inadequacy to confirm a diagnosis of ALS exclusively by gross examination of the brain and spinal cord tissues, light and electron microscopy analyses are needed.

1.2 Neuropathological and hystopathological alterations in ALS patients

In the study of neurodegenerative diseases, knowledge of the descriptive neuropathology is essential to clarify the clinical pattern of the disease, to differentiate among distinct pathologies sharing similar symptoms and to understand if neuropathological observations found in animal models are similar to human condition. For this reason a short description of most important hysto/cyto-pathological alterations characterizing can be very useful to better understand clinical aspects of the disease.

1.2.1 Upper motor neurons and corticospinal tract

In the cerebral cortex a marked decrease of large pyramidal motor neurons has been predominantly observed in the motor area. However, neuronal abnormalities are not confined in the motor cortex; a lesser extent of damage is also reported in the premotor areas, sensory cortex and temporal cortex. Quantitative histological studies of cortical motor neurons revealed changes in size with shortened and fragmented dendrites. Accumulation of neurofilaments and ubiquinated proteins are common before motor neurons death [Kiernan, 1991].

Demyelination, due to axonal degeneration of descending large myelinated fibers of cortical motor neurons, is a common feature in the corticospinal tract of ALS patients. Moreover, corticospinal fibres show a marked axonal swelling and spheroids containing packed neurofilamentous material and other cellular debris are found [Chou, 1992].

1.2.2 Lower motor neurons

A marked loss of large anterior horn cells has been observed by Nissl stained cell counting, this pattern of lower motor neurons loss in the anterior horn of ALS patients is to be patchy and focal [Tsang, 2000]. Quantitative histological studies have shown that large motor neurons are selectively involved. In these cells neuronal shrinkage or atrophy precedes neuronal death and also involves alterations to axons and dendrites. Loss of Nissl substance (chromatolysis), vacuolization and lipofuscin deposits are sometimes detectable in the remaining anterior horn motor neurons [Kiernan, 1991].

Since spinal motor neurons represent the best- studied and characterized group of motor

neurons in ALS, a detailed description of ultrastrutural alterations found in spinal motor neurons is reported below.

1.2.2.1 Neurofilament alterations

The cytoskeleton plays a pivotal role in several processes of eukaryotic cells. Mitosis, cell motility, endocytosis, and the maintenance of cellular shape are allowed to cytoskeletal components. Moreover, in neurons, cytoskeletal organisation is fundamental to connecting the cellular body to the periphery, axons and dendrites, and to regulating the transport of a large amount of molecules by an extensive network of microtubules and filaments [Bloom, 1998]. Neurofilaments are the most abundant filamentous component in neurons. They are divided in three different classes, light neurofilaments (NF-L) medium neurofilaments (NF-M) and heavy neurofilaments (NF-H) depending on their molecular size [Al-Chalabi, 2003]. In healthy motor neurons neurofilaments are expressed in the perikarya and are then transported to the periphery in a not-phosphorylated form. When neurofilaments reach their targets they are phosphorylated, the phosphorylation is a crucial event to the assembly of singles neurofilaments. This mechanism of assembling is essential for the extension of axons and to maintain the integrity of neuronal morphology [Shea, 2003].

In the recent years a growing body of evidence suggests that various neurodegenerative diseases share a similar process in which neurofilaments are phosphorylated and accumulated in the cell body of dying neurons [Taylor, 2002;Zhao, 2001].

A common pathological feature, observed in autoptic samples of ALS patients, is the presence of a marked accumulations of intermediate filaments in the perikaryon of motor neurons and in their axons [Gambetti, 1983;Hirano, 1984]. Immunostaining experiments with monoclonal antibodies directed against the three different form of neurofilaments showed levels 5 to 10 times higher of immunopositivity in motor neurons from ALS patients compared to non ALS motor neurons [Rouleau, 1996]. Abnormal neurofilaments accumulation in the perikaryon occurs in two distinct patterns: homogeneously diffuse or focally accumulated in various shapes.

Neurofilaments are not the unique category of cytoskeletal components present in ALS inclusion bodies. Peripherin is another protein detected in the majority of inclusions in motor neurons of ALS patients [Sterneck, 1996;Migheli, 1993;Corbo, 1992]. Peripherin is normally expressed in

peripheral sensory neurons but is almost absent in the motor neurons [Escurat, 1990;Troy, 1990]. However, peripherin gene expression can be up regulated by nerve injury and inflammatory cytokines [Wong, 1990].

1.2.2.2 Intracellular inclusions

Several types of inclusion bodies that have been found in the perikarya of anterior horn motor neurons are immunoreactive to ubiquitin [Leigh, 1989].

Ubiquitin is a 76-amino-acid protein that is involved in an ATP-dependent nonlysosomal proteolysis of abnormal or short-lived proteins [Leigh, 1991]. Although ubiquitin inclusions in lower motor neuron are unique to ALS tissues, ubiquitin-immunoreactive intraneuronal inclusions are often observed in the upper motor neurons [Morris, 2001;Noda, 1997] and are not specific to this disease [Wilson, 2001]. By immunoelectron microscopy observation, it has been shown that these ubiquitin-reactive inclusions are composed of small 10-15 Å linear fragments whose the exact identity remains undiscovered [Okamoto, 1991].

Lewy-body-like hyalin inclusions were originally described as a characteristic feature of posterior columns and spinocerebellar tracts in ALS patients, but furthermore they have been also found in the soma and in the proximal axons of anterior horn motor neurons [Murakami, 1990]. These inclusions measure 7 to 20 µm in diameter and are surrounded by a lighter, slightly basophilic halo and contain a dense eosinophilic core of granules associated with a patchy shaped aggregate of filaments. These filaments are not immunoreactive to any cytoskeletal components such as neurofilaments, tubulin, microtubule-associated protein 2, and phosphorylated tau protein. These inclusions are similar to those described in the Lewy bodies in Parkinson's disease.

Bunina bodies are hystologically described as small, eosinophilic, irregularly shaped, 2 to 3 µm in diameter and exclusively found in the perikaryon. Ultrastructurally, they are electron dense amorphous structures surrounded by lysosomial vesicles, endoplasmic reticulum fragment, lipofuscin granules and other debris.

An intriguing relationship between bunina bodies and Golgi apparatus fragments has been hypothesised because of the presence in the bunina bodies of marked immunoreactivity for anti-cystatin C antibody, a protein highly expressed in Golgi apparatus [Okamoto, 1991].

1.2.2.3 Mitochondrial alterations

In recent years, observations of mitochondrial morphological alterations in the central nervous system (CNS) of ALS patients have accumulated. A fine ultrastructural examination of the synapses in ALS patients showed mitochondrial alterations in the anterior horn motor neurons (lumbar spinal cord) not only in degenerated neurons, but, to a lesser extent, in neurons that appear normal. Mitochondrial abnormalities include dense conglomerates of aggregated, dark mitochondria and presynaptic vesicles, and also bundles of neurofilaments, and a marked increase of presynaptic vesicles. These observations suggest that a substantial synaptic alteration, including mitochondrial changes, occurs in the early stages of anterior horn neuron death process in ALS patients [Swerdlow, 1998].

Hirano showed that, in dendrites and in the axon hillock of degenerating motor neurons, mitochondria are swollen and highly vacuolized, and it was also reported that abnormal mitochondrial morphology in the nerve terminal and in other peripheral tissues of ALS patients [Hirano, 1984]. Abnormal mitochondrial morphology is found in ALS patients may be related to a many factors, as oxidative injury, increased cytosolic calcium concentration and mtDNA mutations [Beal, 2003;Swerdlow, 2000].

1.2.2.4 Axonal alterations

As in other neurodegenerative diseases, axonal swelling represents a common event detectable in ALS. In ALS patients the axons are swollen and typically show well-defined structures that are identified as spheroids [Carpenter, 1968]. These structures are eosinophilic bodies and are usually greater than 20 μm in diameter. They contain packed 10-nm-thick neurofilaments. Like intraneuronal neurofilament accumulations, spheroids are phosphorylated. However, spheroids have not been found exclusively in ALS tissues and many other neurological diseases are characterized by the presence of phosphorylated neurofilaments and neurofilamentous conglomerates [Manetto, 1988;Chou, 1992].

Interestingly, axonal swellings are more frequent in younger than in older ALS patients and in the patients with shorter as opposed to longer clinical course [Kurosumi, 1979].

1.3 Aetiopathological hypotheses

1.3.1 Genetic involvement

Genetic risk factors for ALS have been studied extensively. Familial Amyotrophic Lateral Sclerosis (fALS) forms, are a clinically and genetically heterogeneous class of pathologies with multiple autosomal-dominant and recessive forms [Rosen, 1993]. Molecular genetic analysis of fALS has led to the discovery of several genes involved in ALS.

1.3.1.1 f ALS1 (SOD1)

In 1991 the first ALS gene (ALS1), for an autosomal-dominant form of fALS, was mapped to chromosome 21q [Siddique, 1991]. Two years later the cytosolic copper-zinc superoxide dismutase (*SOD1*) gene was shown to be the ALS1 gene [Rosen, 1993]. SOD1 is a 153-amino acid metalloenzyme with high expression in nervous tissue, liver and erythrocytes. The enzyme catalyzes the conversion of the superoxide radical anion (O_2^-) to molecular oxygen (O_2) and hydrogen peroxide (H_2O_2). Presently, more than 90 different mutations in all five exons of this gene have been identified [Cudkowicz, 1997].

The majority of mutations in *SOD1* are missense mutations and there is no clear correlation with the clinical expression of the disease (genotype-phenotype correlation) [Andersen, 1997]. This inter- and intrafamilial variability precludes precise predictions on the course of the disease. Clinical characteristics, age at onset, and survival vary greatly between and among specific mutations. The phenotypic variability extends from rapidly progressive disease with only lower motor neuron signs to a very slowly progressing disease with upper and lower motor neuron signs [Camu, 1999].

It is unclear how mutations in *SOD1* cause ALS. As the level of residual SOD1 enzyme activity does not correlate with disease expression in ALS patients, the loss of function of SOD1 is not a probable cause of motor neuron degeneration [Ratovitski, 1998]. Other toxic effects of *SOD1* mutations may involve increased vulnerability to excitotoxic mechanisms by selective inactivation of the glutamate transporter, EAAT2/GLT1 [Trotti, 1999], or by mitochondrial degeneration [Jaarsma, 2000].

Neurofibrillary depositions and Lewy body-like inclusions belong to the pathological spectrum

of ALS1 [Shaw, 1997]. Immunohystochemical co-localization of SOD1 in neuronal Lewy body-like hyaline inclusions (LBHIs) in the spinal cords of ALS1 patients indicates that SOD1 is a component of LBHI [Kato, 2000].

1.3.1.2 f ALS2 (ALSIN)

Autosomal-recessive fALS was first described in a large inbred family in Tunisia showing linkage to the chromosomal region 2q33-34. Symptoms occurred in the first or second decade of life, and included progressive spasticity of the limbs and the facial and pharyngeal muscles. Survival is relatively long (15 to 20 years) [Hentati, 1994].

Recently, the gene for ALS2 was identified in Tunisian and Kuwaiti families and named *alsin* or *als2* [Hadano, 2001]. Alternative splicing of this gene produces a short and a long transcript. Deletions affecting both transcripts result in the ALS2 phenotype, whereas homozygous deletions in exon 9 and affecting only the short form of the protein, cause juvenile primary lateral sclerosis (JPLS). JPLS is even rarer than ALS2, and its phenotypic presentation consists of slowly progressive spastic paraparesis and muscle weakness of the oro-facial and ocular muscles. Expression of the mouse ortholog of *alsin* was found in neuronal cells throughout the brain and the spinal cord. Because Alsin has protein domains with similarities to pleckstrin and guanine-nucleotide exchange factors (GEFs) known to activate GTPases, Alsin may act as a regulator/activator of GTPases, and modulate microtubuli assembly, membrane organization and trafficking in neurons [Kanekura, 2004].

1.3.2 Glutamate-induced excitotoxicity

Glutamate-induced excitotoxicity is the best-characterized factor in the ALS pathogenesis. Excitotoxicity is basically due to an overstimulation of postsynaptic glutamate receptors. This overstimulation can generate an excessive influx of Ca^{++} and Na^{+} into the neurons and the following activation of damaging pathways ultimately leading to cell death [Choi, 1987]. Both glial and neuronal glutamate transporters play a pivotal role in avoiding excitotoxicity stimuli by removing the excess of glutamate released into the synaptic cleft from presynaptic neurons and, consequently, by preventing the overstimulation of postsynaptic glutamate receptors. The evidence of an abnormal glutamate metabolism and an impaired expression of the glial glutamate transporter GLT-1, known as (EAAT2 in humans) in ALS patients suggests that glutamate-induced excitotoxicity plays a key role in generating ALS disease [Rothstein, 1993].

Different studies have reported a significant increase of glutamate levels in cerebrospinal fluid and serum of sporadic ALS and a selective local loss of EAAT2 in the anterior horn of affected spinal cord regions in ALS patients. In addition, a significant decrease of glutamate uptake from cerebral and spinal homogenates in about two-thirds of sporadic ALS patients has been measured [Rothstein, 1994].

Glutamate overstimulation produces its neurotoxic effect acting through both the N-methyl-D-aspartate (NMDA) receptors and the alpha-amino-3-hydroxy-5-methyl-4-isoxazole propionate (AMPA)/kainate ionotropic receptors. However, while NMDA receptors seem to mediate most acute neuronal injury, AMPA/kainate receptors seem to be associated to detrimental effects produced following a slower and prolonged overstimulation. This latter mechanism appears to be more related to chronic processes, such as neurodegenerative diseases and ALS [Weiss, 1991].

AMPAr are cation-conducting complexes, the receptors are composed of four subunits (GluR1-4) and are always constituted as an heteromeric protein. The alternative assembly of the different subunits produces important differences in the electrophysiological properties of AMPAr [Jonas, 1995].

A possible mechanism of excitotoxicity due to a post-transcriptional editing of the calcium impermeable subunit (GluR2) of AMPAr has been postulated [Takuma, 1999]. Ca^{++} permeability is largely determined by the GluR2 subunit, receptors incorporating edited GluR2 subunit

show a limited Ca^{++} permeability in comparison with GluR2-lacking channels or containing the unedited form of GluR2. This effect is attributable to the presence of an arginine in its pore-forming segment in GluR2, in a position occupied by a glutamine in the other AMPAr subunits [Hume, 1991;Burnashev, 1992].

This critical arginine residue is formed at the pre-mRNA stage by RNA editing [Sommer, 1991]. The relative Ca^{++} permeability of native AMPAr in neurons is inversely correlated with the rate of edited GluR2 and the divergence in relative Ca^{++} permeability of AMPAr between different neuronal cell types could be an important constituent of selective vulnerability [Pellegrini-Giampietro, 1997]. It has been widely demonstrated that different neuronal cell types can diverge in GluR2 expression, in the rate of GluR2 editing and in the desensitisation properties of their AMPAr [Raman, 1994] and such differences may be related to the selective vulnerability of motor neurons that occurs in ALS. In figure 1.2 are summarized the main events involved in glutamate-induced excitotoxicity.

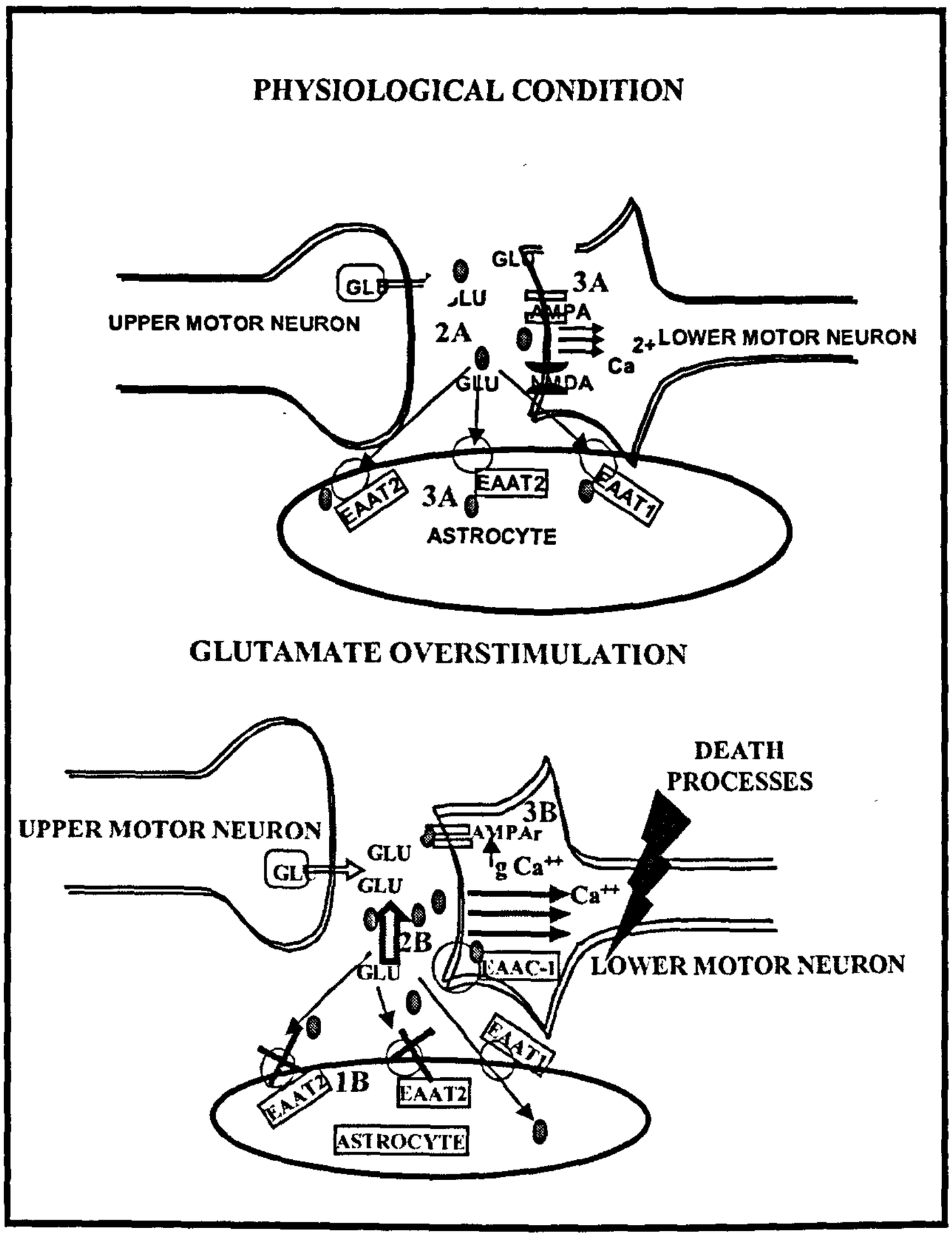

Figure 1.2 Important alterations of glutamate metabolism that are found in ALS patients can account for a glutamate-induced excitotoxicity in motor neurons. The possible concomitant effects produced by decreased amount and reduced functional expression of the main glial glutamate transporter (EAAT2) leading to increased liquoral levels of glutamic acid. An augmented Ca^{++} permeability, due to a reduced process of editing for GluR2 mRNA, could induce a Ca^{++} overloading thus activating a series of different cell death pathways in lower motor neurons (see Chapter 2).

1.3.3 Oxidative stress and mitochondrial abnormalities

The hypothesis that oxygen free radical-mediated neurotoxicity may contribute to pathogenesis of ALS originated from the discovery of the human Cu^{++}/Zn^{++} superoxide dismutase-1 (SOD1) mutation in a group of fALS patients and the demonstration of reduced enzyme activity in affected individuals [Rosen, 1993].

A major source of free radicals production can be due to a defective flux of electrons through the mitochondrial membrane, during the process of oxidative phosphorylation. Mitochondria produce ATP via the creation of an electrochemical gradient across the mitochondrial inner membrane. This gradient is obtained by the pumping of H^+ ions through protein complexes that form the electron transport chain (ETC). As electrons are transported through the ETC they undergo a series of redox reactions. These steps are required to produce the electrochemical gradient to transport H^+ ions across the membrane. This H^+ flux through the H^+–ATP pore is the driving force to transform ADP into ATP. The final electron acceptor is molecular oxygen that is transformed in $O_2^{\cdot}$. $O_2^{\cdot}$ usually reacts with H_2O thus producing H_2O_2. In physiological conditions the large amount of reactive oxygen species (ROS), principally superoxide anions (O_2^-) and hydroxyl radicals (OH^-), produced from reduction of O_2 by electrons, is readily converted to H_2O_2 from superoxide-dismutase and further convereted to H_2O and O_2 by catalase.

The ROS produced by mitochondria can react with a wide series of substrates, such as lipids and NO, thus generating catastrophic effects for the cell [Cassarino, 1999].

A large body of evidence indicates oxidative damage as one of the most probable aetiological factors to initiate ALS pathology. An increase of protein carbonyl content has been reported in frontal and motor cortex and in spinal cord of ALS patients [Oteiza, 1997]. Increased level of immunopositivity for 3-nitrotyrosine and neuronal nitric oxide synthase (nNOS) has been found in the spinal cord motor neurons of both sporadic and fALS patients [Abe, 1997]. On the other hand, further studies did not reveal nNOS alteration in motor neurons, but showed an increase of nNOS activity in astrocytes of spinal cord and sub cortical white matter in ALS patients [Sasaki, 2000].

As in other neurodegenerative diseases, a relevant source of risk in ALS disease is constituted by ageing and, consequently, with the processes have implicated in ageing. A classic feature of ageing is represented by ROS overproduction induced through a loss of function of mitochondria.

Several mitochondrial abnormalities have been found in ALS patients [Beal, 2000;Cassarino, 1999]. The first evidence of involvement of mitochondria in ALS arose from electron microscopy studies, in which an abnormal mitochondrial morphology in muscles of ALS patients was shown. Moreover, in the same study, a decrease in mitochondrial number was also reported in intramuscular nerves of ALS patients [Hirano, 1984].

Using a metabolic assay, a significant reduction in cytochrome oxidase activity and an increase of either complex I activity alone [Bowling, 1993] or both complex I and II was found in ALS patients [Browne, 1998]. This study also showed that others enzymatic activities of ETC (complexes II-III and IV) were not altered.

The increased activity of complex I in ALS patients may be due to a compensatory mechanism in response to the oxidative damage of the inner mitochondrial membrane components that may cause electron leakage and the uncoupling of oxidative phosphorylation.

A further study reported a decreased activity of complex IV. In this work mitochondrial activity was evaluated by staining spinal cord sections from post post-mortem tissues obtained from ALS and no neurological patients [Borthwick, 1999]. Complex IV deficiency has been also described in muscles of sporadic ALS patients, in which complex IV negative muscles fibres were found [Chung, 2002]. A detailed comparison of mitochondrial activity obtained from lymphocytes of fALS patients and healthy humans, clearly showed an impaired response of fALS mitochondria to uncouplers of oxidative phosphorylation, an altered mitochondrial ultrastructure and an abnormal electron transport chain functioning [Curti, 1996].

Finally, it is important to report as drugs, acting primarily on energy metabolism, were effective to delaying muscle atrophy and to reducing degeneration of spinal motor neurons in animal models of motor neuron diseases [Klivenyi, 1999;Ikeda, 2000].

The results obtained in the last few years suggest that, although there is no evidence that ALS is a mitochondrial cytopathy and the temporal and causal role of mitochondria in motor neuron degenerative process have not yet been clarified, mitochondrial alteration must be considered as a possible aetiological factor in ALS pathology.

1.3.4 Neurofilaments disorganization and axonal strangulation

Both in sporadic and in familial forms of ALS, neurofilament alterations seems to play an important role in the pathogenesis of the disease [Julien, 2000].

Since neurofilaments are heavily expressed in motor neurons it has been suggested that the level of neurofilaments may be an important factor in determining the selective vulnerability of motor neurons. The direct involvement of neurofilaments in the pathogenesis of ALS was suggested by the evidence of mutations, in a subset of ALS patients, in a gene that encodes for the heavy neurofilament subunit [Bomont, 2000]. However, how this aberrant expression of neurofilament can lead to a selective damage for motor neurons is still unclear.

About the role played by neurofilaments in ALS pathology it is important to note that the formation of intraneuronal aggregates, highly enriched in phosphorylated neurofilaments, is a peculiarity of motor neurons in ALS patients. This increase of highly phosphorylated neurofilaments could also suggest that the failure in the metabolism of neurofilaments may be the first step of a series of processes leading to neurofilament accumulation, axonal strangulation and neuronal cell death. However, it has been also suggested that upstream defects, such as, axonal transport deficit, glutamate induced excitotoxicity, SOD1 mutation, inflammatory response, might cause the disorganisation of neurofilaments in the cell body; in that case neurofilament alteration would represent more an effect than a cause of the disease [Ackerley, 2000;Asahara, 1999].

1.3.5 Intracellular aggregates and/or failure of protein folding

As reported for other neurodegenerative diseases, like Alzheimer's disease, prion disease, Kennedy and Hungtinton's disease, protein accumulation in motor neurons of ALS patients may be caused by the formation of aggregates due to an alteration of the process of misfolded proteins degradation [Ross, 2004]. The mutant SOD1 protein was reported to sequester chaperones that are required for promoting the correct folding of many proteins, whereas ubiquitin-mediated protein degradation might be inhibited by those aggregates. Aggregates intensely immunoreactive for SOD1 are found in the motor neurons of fALS patients carrying SOD1 mutations, and ubiquitin deposits have been reported in lower motor neurons in both sporadic ALS and fALS patients. The evidence of a large amount of ubiquitin positive aggregates in motor neurons of ALS patients strengthens the

hypotheses that a failure in ubiquitin-proteasome system can be responsible for protein accumulation [Valentine, 2003;Migheli, 1999;Valentine, 2003;Migheli, 1999].

1.3.6 Reactive gliosis-induced neuroinflammation

Although the CNS has been considered for many years as an immune privileged organ, a well-characterized repertoire of inflammatory responses are observed in different types of brain injury. Many different types of neurodegenerative diseases share a common pattern of events in which, not only the dying neurons undergo cellular changes, but also the morphological and functional properties of neighbouring cells are affected. These cellular changes are common in different species and likely reflect an evolutionarily conserved program which plays an important role in the protection against infectious pathogens and the repair of the injured nervous system. The group of cells that more actively participate to this response are microglial cells and astrocytes, for this reason this response is often indicated as reactive gliosis [Raivich, 1999].

Although a marked reactive gliosis in anterior horn and motor cortex from ALS patients was already described several years ago, the interest of microglial activation as pathogenetic factor in ALS is recent and reflects previous experimental evidence showing that microglial activation plays a relevant role in motor neuron degeneration [Turner, 2004].

Microglial cells are functionally related to peripheral tissue macrophages and, like macrophages in other tissues, resting microglia appears to participate in the immune surveillance of the nervous system [Eglitis, 1987]. Resting microglia are characterized by a stellate morphology composed by thin and ramified processes. Resting microglial cells are unable to migrate and are characterized by low level of metabolic activity [Compston, 1997]. In response to injury, microglial cells modify their physiology and rapidly produce a transformation from a resting into an activated state. Activated microglial cells markedly increase their size; cell bodies swell and acquire a round shape, together with a decrease in the ramification of distal branches. During this phase of morphological changes, microglial activation proceeds through a series of steps characterized by a conspicuous expression of molecules for cell adhesion, cytoskeletal organization, antigen presentation and cell membrane receptors [Streit, 1989].

Once activated microglial cells migrate to the injured side, this step is identified as homing

process. The homing of activated microglia permits the adhesion to damaged structures like lesioned neurons or degenerating neurite terminals [Angelov, 1996].

The presence or absence of cell death and phagocytosis determines the further development of the microglial response after the process of homing. When neuronal damage declines without a massive neuronal death, microglial number is progressively reduced and activated cells switch off their metabolic machinery reducing the expression of many proteins and reverting to a resting state. Interestingly, during this latter phase microglial cells return to their original state characterized by a territorial distribution, highly ramified morphology and moderate levels of complement receptors, Fc-receptors and IgG immunoreactivity [Raivich, 1999].

On the other hand, neuronal cell death produces an additional modification of microglial cells toward a phagocytotic phenotype. This transformation guarantees the clearance of tissue by removing neural debris from injured area. Phagocytotosis is not only important to remove neuronal fragments but it is often required for the removal of disconnected neurites in both natural occurring axonopathy and in experimental axotomy [Bauer, 1995]. Removal of large cellular structures like dead pyramidal cells or degenerating motor neurons frequently leads to the formation of microglial nodules consisting of microglial phagocytes [Streit, 1988].

Another important component of the neuroinflammatory response is represented by astrocytes. Astrocytes represent about 75-80% of glial cells in the CNS. Astrocytes can be divided in two main groups: stellar-fibrillary astrocytes and protoplasmatic astrocytes. Fibrillary astrocytes are generally found in the white matter whereas protoplasmatic astrocytes are located in the grey matter and exhibit numerous short and thicker highly ramified processes with many membranous extensions [Bignami, 1972].

The cellular modifications occurring in reactive astrocytes play an important role in neuroglial response. As for microglia, the astrocyte response to injury can be divided into different serial steps. A rapid increase of GFAP synthesis, related to a glial hypertrophy, is evident in the early phase of neuroinflammatory response [Tetzlaff, 1988]. This early morphological transformation from protoplasmic to fibrillary astrocytes in the neural parenchyma can be tightly controlled by several factors, including cytokines, which regulate different steps in this activation response [Lucas, 1995].

The release of these cytokines, often accompanied by an increase of their receptors on motor neurons surface [Mennini, 2004], can activate cellular pathways that lead to the death of motor neurons. In addition diffusible factors released from dying neurons can activate protoplasmatic astrocytes and increase both the GFAP levels and the expression of a series of distinct molecules [Viviani, 2000].

A schematic representation of the complex processes between activated microglia/astrocytes and motor neurons is reported in figure 1.3

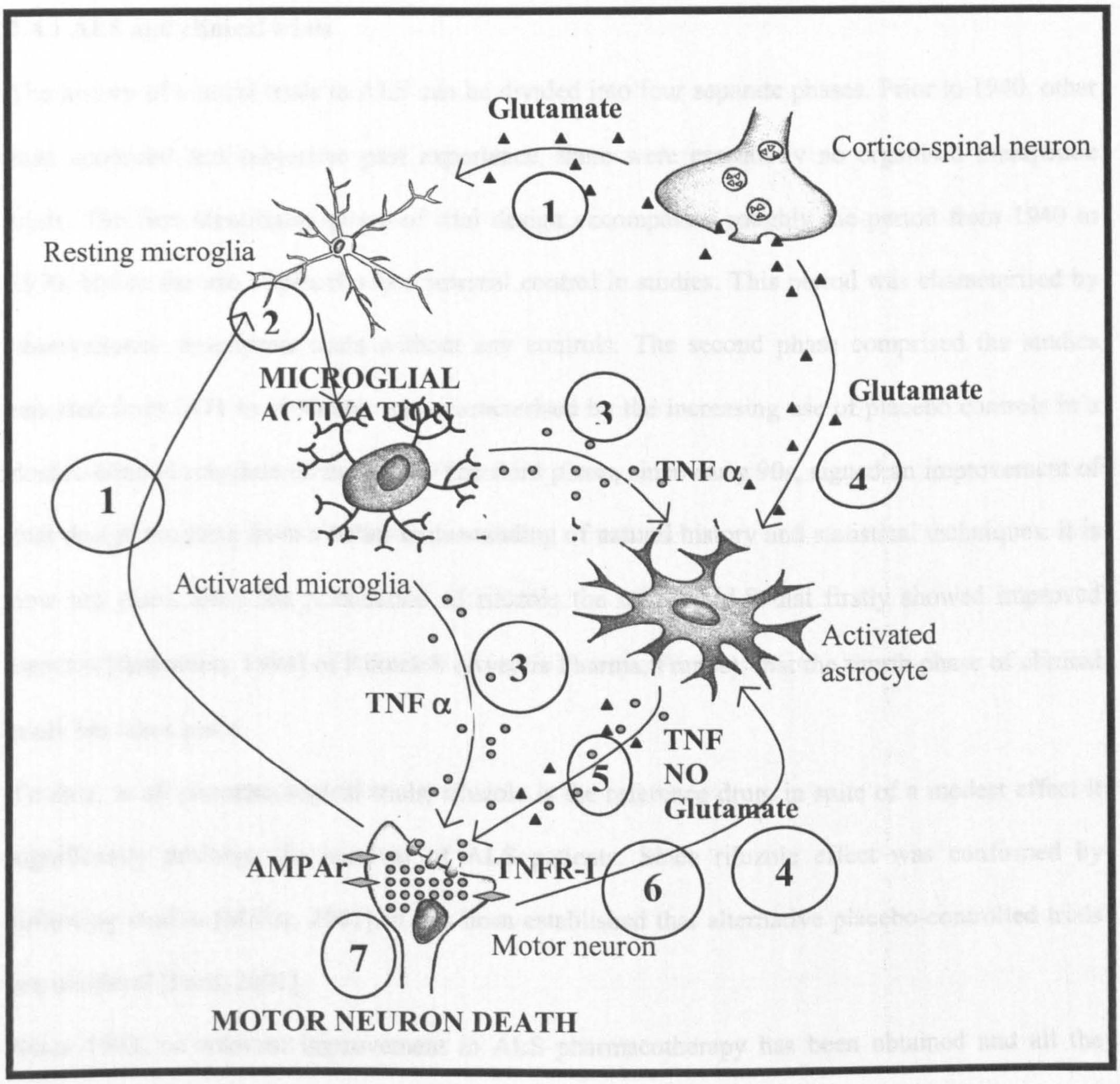

Figure 1.3 The main processes likely involved in the glial-dependent motor neuron toxicity are shown in this drawing. 1-Diseased motor neurons release some factors that stimulate resting microglia, 2-microglial cells are activated, 3-activated microglia releases factors interacting with other cells, 4- release of soluble molecules from upper and lower motor neurons activate astrocytes, 5-astrocytes release further molecules able to interact to motor neurons, 6-the factors released from glial cells stimulate intracellular pathways in motor neurons that, 7-induce motor neuron death.

1.4 Pharmacotherapy of ALS

1.4.1 ALS and clinical trials

The history of clinical trials in ALS can be divided into four separate phases. Prior to 1940, other than anedoctal and subjective past experience, there were essentially no organised therapeutic trials. The first identifiable phase of trial design encompasses roughly the period from 1940 to 1970, before the use of placebo as a internal control in studies. This period was characterised by observational, descriptive trials without any controls. The second phase comprised the studies reported from 1971 to 1990 and was characterised by the increasing use of placebo controls in a double-blinded schedule of treatment. The third phase, since early 90s, signed an improvement of trial design resulting from a better understanding of natural history and statistical techniques. It is now ten years, since the publication of riluzole the trial in ALS that firstly showed improved survival [Bensimon, 1994] of Rilutek® (Aventis Pharma, France), that the fourth phase of clinical trials has taken place.

To date, in all pharmacological trials, riluzole is the reference drug, in spite of a modest effect it significantly prolongs the survival of ALS patients. Since riluzole effect was confirmed by following studies [Miller, 2001], it has been established that alternative placebo-controlled trials are unethical [Ford, 2001].

Since 1993, no relevant improvement in ALS pharmacotherapy has been obtained and all the clinical trials performed so far have been ineffective. It has been postulated that the efficacy of riluzole is due to its antiglutamatergic effect and that the reduction of excitotoxic glutamate-mediated stimulus could partially counteracts the progressive motor neuron degenerative process. However, further clinical trials, by treating the patients with others glutamate antagonists, completely failed both in prolonging survival and in decreasing the slope of clinical worsening [Miller, 1999]. The actual therapeutical effect of riluzole in ALS disease is not yet fully understood and several studies to elucidate alternative mechanisms of action played by this drug are still under investigation.

As reported in section 1.3, several aetiological hypotheses to account for ALS disease have been postulated and different pharmacological strategies to arrest or, at least, to slow the progression of

symptoms have been proposed.

In the last decade the rationale to define a therapy for ALS was to plan clinical trials by agents that: I) have been shown to be effective in *in vitro* or in *in vivo* models of motor neuron degeneration, such as neurotrophic agents, compounds that support mitochondrial activity, or anti-apoptotic agents; II) have been reported to counteract the detrimental effect caused by stimuli that have been postulated to be involved in ALS, such as antiglutamatergic agents, anti-inflammatory agents, calcium regulators, antiviral drugs.

To provide a clear description about the most relevant clinical trials in ALS, it is possible to include the different drugs tested in accordance with their specific pharmacological activities (see table 1.3).

AGENT	EFFICACY +	EFFICACY -
Antiglutamatergic		
Riluzole	o	
L-Threonine		o
Branched amino acids		o
Gababpentin		o
Lamotrigine		o
Dextromethorphan		o
Ca-channel blockers		
Verapamil		o
Nimodipine		o
Antioxidants		
Acetylcysteine		o
Vitamin E		o
rhSOD1 (intrathecal)		o
Neurotrophic factors		
CNTF		o
TRH		o
rhIGF-1		o
BDNF		o
Immunomodulatory		
Cyclophosphamide		o
Plasmapheresis		o
Cyclosporine		o
α-interferon		o
Dopaminergic pathway		
L-Dopa		o
Deprenyl		o
Cholinergic pathway		
Physostigmine		o
Neostigmine		o
3,4-Diaminopyridine		o
Tetrathyroaminoacridine		o
Antiviral		
Tilorone		o
Modified snake venom		o
Miscellanous		
Gangliosides		o
Amantadine		o
Guanidine		o

Table 1.3 CLINICAL TRIALS IN ALS

1.4.2 Antiexcitotoxic drugs

1.4.2.1 Riluzole

Riluzole is, at present, the only drug approved from the Food and Drug Administration (FDA) for the treatment of ALS. Riluzole is considered to exert its protective effect in ALS patients by acting as an antiexcitotoxic agent [Lacomblez, 1996]. Riluzole treatment can block different processes inducing the release of glutamate from presynaptic neurons and therefore can inhibit the glutamate-mediated overstimulation of postsynaptic glutamate receptor [Pratt, 1992;Zona, 1998]. In the last fifteen years several findings have confirmed the well-known antiglutamatergic properties of riluzole. It has been reported that riluzole inhibits the release of glutamate in the rat caudate nucleus [Cheramy, 1992], blocks sodium channels in their inactivated state in myelinated fibers [Benoit, 1991], modulates Na^+ currents and the late component of outward K^+ currents in cultured cortical neurons [Zona, 1998], activates a G-protein-dependent process that inhibits glutamate release [Doble, 1996] and modulates the kainate-induced Na^+ currents in rat cortical neurons [Zona, 2002].

In two distinct therapeutic trials, riluzole prolonged the survival by three to six months [Bensimon, 1994;Lacomblez, 1996]. In one of these trials the treatment slightly slowed the decline in the strength of limb muscle but failed to reduce others considered clinical parameters. In one retrospective analysis [Riviere, 1998] patients who received riluzole remained in a milder state of the disease longer than placebo-treated ALS patients. More recent evidence, by utilizing proton density magnetic resonance spetroscopy, has demonstrated that patients, treated with riluzole, had a less marked progression of neuronal loss compared to placebo treated group [Kalra, 1999]. The effect of riluzole reinforced the hypothesis that glutamate-induced excitotoxicity was related to ALS and prompted the scientific community to plan several clinical trials using more specific antiglutamatergic agents. The most relevant treatments including antiexcitotoxic agents are reported below.

1.4.2.2 Dextromethorphan and L-threonine

Dextromethorphan is a NMDA antagonist utilized in experimental models of ischemia [Steinberg, 1991]. Dextromethorphan was tested in ALS patients for 12 weeks in a double-blind crossover trial. Thereafter surviving patients protracted the treatment for 6 months but clinical and neurophysiological tests did not show any positive effect in the treated group [Askmark, 1993].

Glycine is an inhibitory neurotrasmitter in the mammalian CNS. In 1980 it was shown that L-threonine administration increases glycine concentration in the rat CNS [Maher, 1980]. Based on this finding, L-threonine was administered in ALS patients to reduce the excess of excitatory neurotrasmission.

Several studies were performed using different doses of L-threonine [Blin, 1992;Hugon, 1996]. Although a functional improvement was recorded at the initial phase of the treatment, modulation of the glicinergic transmission does not seem to alter the clinical evolution of ALS. However, it is important to note that the glycine not only works as an inhibitory neurotransmitter in the spinal cord but also acts as an allosteric agonist of the NMDA glutamate receptor and greatly facilitates its activation [Johnson, 1987]. This dual role in neurotransmission may in part account for an explanation of the failure of L-threonine treatment in ALS patients.

1.4.2.3 Ca^{++} channels blockers

Two different aetiologycal hypotheses of ALS disease (the toxicity produced by Ca^{++} overload following postsynaptic glutamate receptor overstimulation, and the over expression of IgG antibodies against L-type calcium channels) may be blocked by a common strategy of treatment passing through calcium-channel blockage. In light of this suggestion two classical drugs classified as calcium antagonist, verapamil and nimodipine, were tested in two distinct clinical trials.

The slopes of declining respiratory function and the limb weakness were not significantly different in the verapamil treated group compared to placebo treated patients. Verapamil was ineffective in slowing the clinical progression in ALS patients[Miller, 1996].

The effect of another Ca^{++} channels blocker, nimodipine, was studied in ALS patients. The scores of isometric muscle strength and respiratory function were used to compare the nimodipine treated and the placebo treated group. No difference in adverse events occurred in placebo vs. drug-

treated patients, but diarrhoea and nausea were more common with nimodipine. Moreover, there was no significant difference in the rate of decline of pulmonary function or limb strength during treatment with drug or placebo. Nimodipine was ineffective in slowing the progress of ALS [Miller, 1996].

In summary, all antiglutamatergic agents tested until now did not produce significant clinical improvement. This evidence suggests that the mechanism of action of riluzole is not exclusively related to the reduction of the glutamate-induced toxicity and that additional mechanisms may contribute to the actual effectiveness of this drug in ALS care.

1.4.3 Neurotrophic factors

Because of the landmark discovery that the nerve growth factor (NGF) rescued sympathetic chicken neurons after axotomy and that its withdrawal markedly reduces the neuron survival [Levi-Montalcini, 1987] in the 80s and 90s, the use of neurotrophins as potential therapeutical factors in neurodegeneartive diseases had a massive and sometimes uncontrolled development.

In ALS studies, these investigations included trials with the brain-derived neurotrophic factor (BDNF), the ciliary neurotrophic factor (CNTF), the thyrotropin-releasing hormone (TRH) and the insulin-like growth factor 1(IGF-1).

1.4.3.1 BDNF

BDNF has been shown to have a protective role in preventing cell death in several experimental models of neurodegenerative diseases. In embryonic rat spinal cord motor neurons [Henderson, 1993] and in neonatal rat facial motor neurons following axotomy [Yan, 1992] BDNF was highly protective in reducing the percentage of mortality. In addition, BDNF has been found to reduce motor impairment and the motor neuron loss in a murine model of motor neuron degeneration, the wobbler mouse [Ikeda, 1995]. In a first series of treatments BDNF was effective on increasing survival and on delaying the loss of pulmonary function in ALS patients. In contrast, in a phase III study, the survival in patients treated with BDNF was identical to placebo. Although the treatment failed, post hoc analyses showed that those ALS patients with early respiratory impairment and those developing altered bowel functions showed statistically significant benefit. In further clinical trials, performed by intrathecal delivery of a recombinant methionyl human BDNF (met-BDNF) the majority of patients reported mild sensory symptoms. They included paraesthesias or a sense of warmth, which were usually confined to the lower limbs and were frequently exacerbated by neck flexion. In most instances these symptoms decreased or even disappeared over several weeks. However, both small number of patients and the design of the study did not permitted conclusions about the efficacy of the treatment.

Immunohystochemical studies, in neuronal somata and proximal processes of large-sized anterior horn cells of non-ALS patients, revealed a punctate staining for BDNF, the same immunostaining pattern was found in the spared anterior horn cells detected in ALS patients. These findings suggest that BDNF expression in ALS patients is unchanged, and that motor neurons would be sufficiently supplied with endogenous BDNF from other neuronal subpopulations in the spinal cord. Interestingly, immunochemical experiments revealed that the tyrosine kinase receptor-B (TrkB), the high affinity functional receptors for BDNF, is less phosphorylated on tyrosine residues in ALS patients spinal cord samples than in controls and therefore less active [Mutoh, 2000]. These findings would suggest an abnormality in TrkB-mediated intracellular signalling in ALS spinal cord and open the possibility of an alternative therapeutic intervention with agents that have the possibility to increase this intracellular signalling (i.e. Acetyl-L-carnitine).

1.4.3.2 CNTF

CNTF is a neuroactive cytokine having a potent survival effect in spinal motor neurons of embryonic chicken and rat, and demonstrating to be active in decreasing the clinical worsening in wobbler mice. Moreover, mice lacking the CNTF gene develop mild but progressive motor neuron loss, and CNTF contents in the lateral corticospinal tract were markedly lower in ALS patients than in controls [Albrecht, 2002;Gatzinsky, 2003;Ikeda, 1995;Ono, 1999]. These results suggest that: I) motor neuron survival requires high levels of CNTF and; II) the under-threshold level of CNTF, which was measured in ALS patients, could generate motor neuron toxicity.

Based on these hypotheses, clinical trials with CNTF were designed. First clinical trials, in which CNTF was systemically administered, were highly toxic and all treatments were interrupted. More recently the "ALS CNTF Treatment Study Group" has reported that the administration of recombinant human CNTF subcutaneously, markedly decreased the appearance of side effects but did not produce any significant improvement in slowing disease progression [ALS CNTF Treatment Study Group, 1996]. Later on, a phase I trial of CNTF delivered intrathecally was designed to determine the safety of this new route of administration as well as the pharmacokinetics and the drug distribution. With intrathecal administration no clinical signs of meningeal irritation, no asthenia, fever, nausea, weight loss, were seen, and it was also reported that the CNTF was well distributed along the spinal canal. Although CNTF was well tolerated and well distributed into the spinal cord region, this treatment did not reduce the gradual decline in motor strength and performance of standard skills [Penn, 1997]. Further studies are thus required to well establish the pharmacological prospective of CNTF treatment.

1.4.3.3 TRH

TRH receptors are localized in different anatomical regions of CNS, including the ventral horn of the spinal cord and several data seem to support the idea of this hormone in ALS care. In fact TRH has been reported to increase extracellular levels of acetylcholine and accelerate acetylcholine turnover in brain [Giovannini, 1991], to have a neurotrophic effect on cultures rat embryonic ventral spinal cord cells of rat embryo [Iwasaki, 1989] and to protect against spinal cord motor neuron degeneration in a murine model of ALS (the wobbler mouse) [Kozachuk, 1987].

However, no positive effect was recorded from different clinical trials previously performed and semi quantitative and quantitative neurological functions were similar in TRH-treated and in placebo-treated group [Brooke, 1989;Munsat, 1992;Brooks, 1987].

In ALS patients a temporary increase in the strength of some muscles following the administration of TRH has been reported, but no change in functional performance was noted and the course of the illness was not altered [Kozachuk, 1987].

1.4.3.4 IGF-1

IGF-1 receptors are highly expressed in muscular surface, in brain and in spinal cord [Daughaday, 1972;Lund, 1986]. By *in vitro* studies it was demonstrated that supplementation of IGF-1 in the culture media promotes neurite formation and increases survival of peripheral and central neurons [Bothwell, 1982;Recio-Pinto, 1986;Bothwell, 1982;Recio-Pinto, 1986]. The beneficial effect of IGF-1 was also observed after *in vivo* administration. IGF-1 stimulated neurogenesis after nerve sciatic axotomy [Vergani, 1999]. In addition, it prolonged the lifespan by slowering the disease progression in two murine models of ALS, the SOD1 transgenic mouse and the wobbler mouse [Kaspar, 2003;Gorio, 2002].

Three distinct clinical trials were carried out. The first produced convincing results, by slowing the progression of the disease [Vaught, 1996]. However this outcome was not confirmed in two further clinical trials performed by treating ALS patients with recombinant human IGF-1. These studies did not show clinical improvement and the therapeutic evidence provided from this compound was not considered sufficiently reliable to obtain the FDA approval for IGF-1 in ALS care [Borasio, 1998;Lai, 1997].

Many other clinical trials were conducted using antioxidant compounds [Desnuelle, 2001; Louwerse, 1995], immunomodulants agents [Brown, 1986; Gourie-Devi, 1997; Haverkamp, 1994; Beghi, 2000; Meucci, 1996; Mora, 1986], agents modulating the dopaminergic [Lange, 1998; Mendell, 1971] and the cholinergic activity [Norris, 1993; Aquilonius, 1992], antiviral agents [Olson, 1978; Rivera, 1980; Bradley, 1984; Lacomblez, 1989] and gangliosides [Olson, 1978; Rivera, 1980; Bradley, 1984; Lacomblez, 1989].

Unfortunately all the clinical trials performed in ALS patients, produced negative results. New strategies as antiapoptotic agents, stem cell implantation, and VEGF administration are now under investigation and preclinical studies in animal models of motor neuron degeneration are still in progress.

The striking dichotomy between the efficacy of many agents in animal models of motor neuron degeneration (see Chapter 5) and their ineffectiveness in the care of ALS patients induces a crucial reflection. What is the relevance of pharmacological treatments, both in *in vitro* and in *in vivo* models of ALS, without a clear comprehension about the basic cell death mechanisms occurring in these models of study?

For the development of disease-specific therapies, both in *in vitro* and in *in vivo* studies, better information that clarifies the specific cell death mechanism(s) leading to motor neuron death is needed.

CHAPTER 2

APOPTOSIS IN NEURONS

2.1 Principles of neuronal death in embryonic and adult brain

In contrast to other cells, neurons are permanent cellular population and they do not undergo turnover and self-renewal. For this reason, neurons have to be preserved against detrimental stimuli produced by environmental injuries and external perturbations. In order to maintain the rate of neuronal death as low as possible, during the evolution, several protective mechanisms have enforced.

It is possible to distinguish two main events characterizing neuronal death an early physiological and a pathological cell death.

The first is identified as the programmed cell death (PCD). PCD is characterized by the loss of a high percentage of neurons that are generated from neural precursors during the early phase of CNS formation. This type of death is indicated as "naturally occurring neuronal death" (NOND). It is generally believed that a correct balance between cell proliferation and NOND during development is fundamental to determine the ultimate structure, architecture, size, and shape of tissues in the CNS. The existence of naturally occurring cell death was first described more than 50 years ago in the neuroepithelial tissue at the beginning of neurulation [Glucksmann, 1951].

PCD is a highly phylogenetically conserved mechanism by which eukaryotic cells die following a stereotyped series of molecular events [Glucksmann, 1951;Clarke, 1976;Saunders, 1966]. The most important process of death in PCD, is universally identified as apoptosis. During brain development apoptosis is responsible for the control of the final numbers of neurons in the central and peripheral nervous system [Glucksmann, 1951].

Although neuronal apoptosis is a typical feature of development, several toxic stimuli, associated with pathological conditions, have been shown to be able in inducing apoptosis [Sastry, 2000]. Among these agents it is worthwhile to mention oxidative stress, nitric oxide (NO), excitatory aminoacids neurotransmitters and related agonists (glutamate, NMDA, AMPA, kainic and

quisqualic acids), neurotoxic drugs, peptides and proteins (β-amyloid, HIV-1 gp120), and lipids (ceramide, retinoic acid, phosphatidylinositol-3-phosphate).

Although physiological and pathological apoptosis are two completely distinct events, both processes are characterized by similar morphological and biochemical features [Sloviter, 2002].

2.1.1 Morphological changes in neuronal apoptosis

In an ultrastructural study performed in several embryonic tissues Schweichel and Merker proposed three main types of cell death occurring during the development, on the basis of the role of lysosomes in cell disruption [Schweichel, 1973]. In the first type, cell death occurs without any detectable activation of endogenous lysosomes, but phagocytosis and secondary lysosome activation induced by macrophages destroy the cells. This process was identified as heterophagocytosis. In the second type of cell death (autophagocytosis) cells are eliminated after activation of their own lysosomal enzymes. In the third type there is no obvious lysosome intervention.

Although this original view was then revised and improved, it is possible to recognize ultrastructural features of type 1 cell death in the current definition of apoptosis, while at least a variant of type 3 shares several features with necrosis. An exhaustive description and classification of morphological alterations that diversify the different types of cell death, was described by Clarke in 1990 [Clarke, 1990]. In this study Clarke described in detail the morphological diversity and the multiple mechanism involved in developmental cell death of neurons and proposed its well-known threefold classification. This classification was published in "Anatomy and Embriology: number 181, year 1990". In the following pages it will be exactly reported the explanation of morphological alterations during apoptosis.

"Morphological types of dying cells...

...Type 1: Apoptosis

(condensation, fragmentation,phagocytosis)

Schweikel and Merker's (1973) first type begins with condensation of both the nucleus and the cytoplasm. In the nucleus, dense chromatin masses appear and increase in number until the nucleus has become frankly pyknotic (i.e., condensed). Under high magnification, the DNA fragments can be seen to be packed together more closely in the regions of dense chromatin. Outside the nucleus, the most striking change is that cell membrane becomes convoluted, being drawn deep to the cytoplasm, which may give the cell a starlike appearance. Subsequently, the processes of the star constrict proximally and detach from the cell. They are then phagocytosed and their contents degraded in heterolysosomes. Most of the cytoplasmatic organelles are initially normal, although they become abnormally closely packed, reflecting a loss of cytosol (Bellairs 1961). However, there is a loss of ribosomes from polysomes and rough endoplasmic reticulum, and the polysomes may even disappear (Schweichel and Merker 1973; O'Connor and Wyttenbach 1974; Pilar and Landmesser 1976)[Schweichel, 1973;O'Connor, 1974;Pilar, 1976].

Scweichel and Merker found that this type of cell death occurred in almost all isolated dying cells, but never in region of wholesale destruction. They observed it in many different regions including the apical ectodermal ridge (Schweichel 1972)[Schweichel, 1972(1);Schweichel, 1972(2)] *and parts of the nervous system. However, the identification of the dying cells in the apical ectodermal ridge as type 1 does not agree with an earlier report (Jurand 196)* [Jurand, 1975] *in which they had many of the properties of type 2 (autophagic) dying cells (see below). In some cases free ribosomes crystallize (Bellairs 1961; Mottet and Hammar 1972; O'Connor and Wyttenbach 1974)* [Bellairs, 1961;Mottet, 1972 #;O'Connor, 1974], *which probably reflects a cessation of their protein synthetizing capacity.*

Many workers have described this kind of cell death sequence of condensation followed by fragmentation and phagocytosis occurs not only in development (Wyllie et al. 1973; Kerr et al. 1974) [Wyllie, 1973;Kerr, 1974], *but in physiological tissue turnover in adults, in various tissues exposed to cytotoxic agents or immunological attack, in tumours, and in hormone-induced*

atrophy(for reviews, see Kerr et al. 1972, 1987; Wyllie 1981; Wyllie et al. 1984 a) [Kerr, 1972;Kerr, 1987;Wyllie, 1981;Wyllie, 1984].

Following an initial designation as "shrinkage necrosis"(Kerr 1965,1971) [Kerr, 1971;Kerr, 1965], *Kerr et al(1972). coined the term "apoptosis", which in Greek denotes the dropping of petals from flowers or leaves from trees, and recalled to these authors the role of this kind of cell death in tissue kinetics, which they wished to emphasize. The term has caught on, particularly in the pathological literature (see below), and I shall therefore use it, although its connotation of cell death in tissue kinetics is inappropriate in our present context of development. This type of cell death has also been described as "primary or precoucious pycnosis"* [Beaulaton, 1982]*(Beauloton and Lockshin 1982), but I would be reluctant to use this terminology because the autophagic kind of cell death (type 2; see below) sometimes also involves early pyknosis.*

The "nuclear" (as opposed to "cytoplasmatic"- see below) type of neuronal death described by Pilar and Landmesser (1976) [Pilar, 1976] *is clearly of type 1, since according to these authors the nucleus become electron-opaque and its chromatin becomes clumped, followed by cytoplasm changes, notably the freeing of ribosomes from polysomes and RER.".*

2.2 Molecular mechanisms of neuronal apoptosis

Our current knowledge on the gene regulation involved in apoptosis is mainly achieved from studies on the nematode worm *Caernobitidis elegans* [Yuan, 1995;Meier, 1998;Liu, 1999;Hengartner, 2001]. In *C. elegans*, in which 131 out of 1090 somatic cells undergo developmental apoptosis, four genes named *ced-3*, *ced-4*, *ced-9* and *egl-1* form the "death machinery" which is responsible for the execution of the cells undergoing PCD [Hengartner, 1997]. In mammals, apoptosis is mainly regulated by two group of molecules: I) the classes of molecules belonging to "BCL2 family" and apoptosis protease activating factor-1 (Apaf-1), that corresponds to CED-3/4 and that act as adapter, and; II) the caspases, a family of aspartyl-specific cysteine proteases possessing a cleavage property, that correspond to CED-9 associated proteins and that act as executor of apoptosis [Putcha, 2004].

Apoptotic processes can be roughly confined in two main pathways termed "extrinsic" and "intrinsic". Although they show profound differences both pathways are able to activate caspases and both require the formation of large multi-protein complexes [Bratton, 2000].

The extrinsic pathway utilises a specific class of receptors identified as “death receptors". Death receptors are members of the tumor necrosis factor (TNF) receptor superfamily. They, once coupled to their cognate TNF family ligand, rapidly activate a series of processes leading the cleavage of different caspases typical of apoptosis [Ashkenazi, 1998]. A schematic representation of the mechanism involved in death receptor activation is shown in figure 2.1.

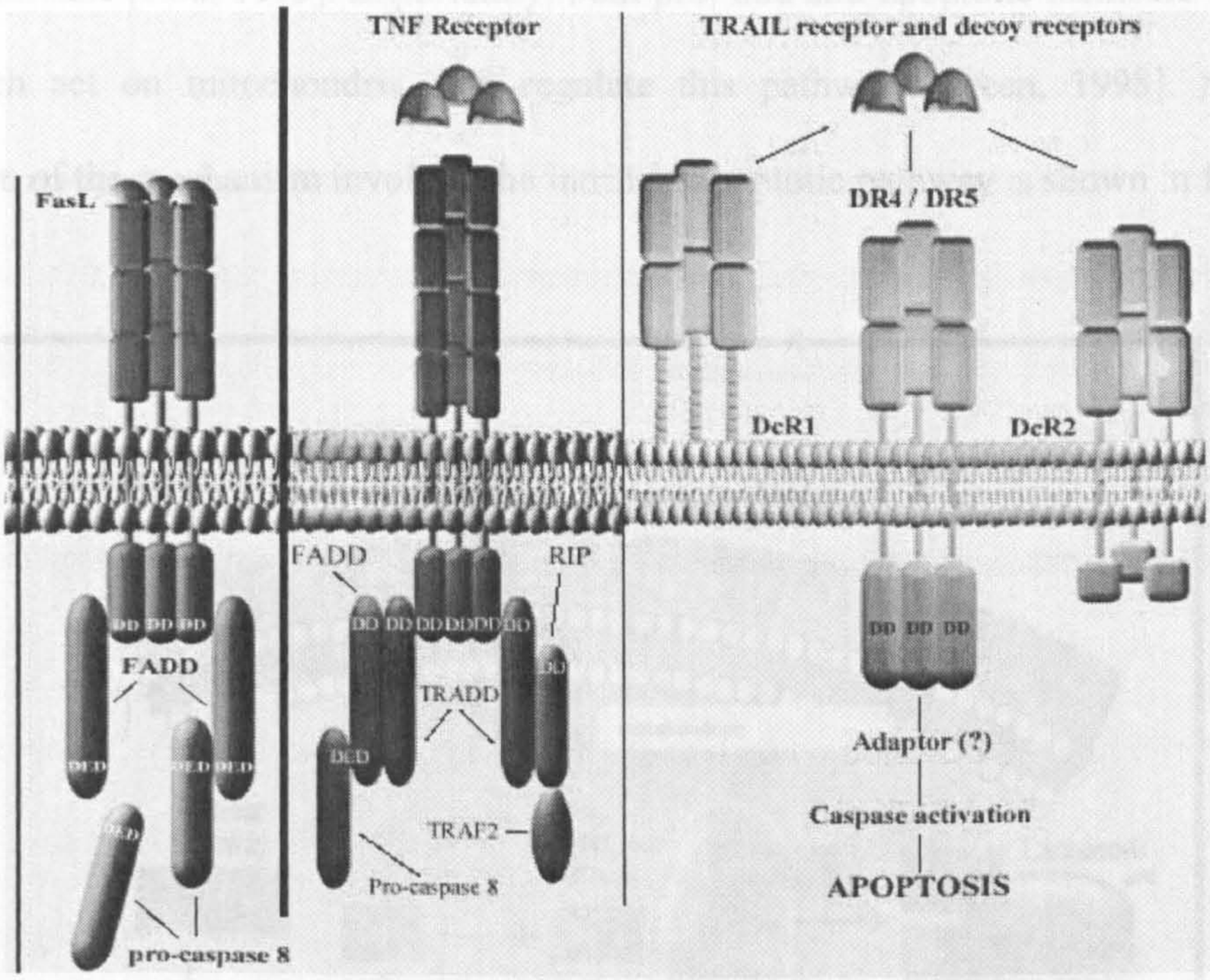

Figure 2.1 Death receptors and extrinsic apoptotic pathway

By contrast, the intrinsic pathway is triggered in response to a variety of stress conditions, such as cytotoxic drugs or growth factor withdrawal. The cascade of events produced by the intrinsic pathway selectively induces a mitochondrial perturbation and the release of cytochrome-c. In the cytoplasm cytochrome-c interacts with Apaf-1 and procaspase-9 to form a 700 kDa complex known as the `apoptosome' which results in autocatalytic processing of caspase-9 and initiation of the caspase cascade [Zou, 1999]. Importantly, both pro- and anti-apoptotic members of the BCL2 family, which act on mitochondria, can regulate this pathway [Green, 1998]. A schematic representation of the mechanism involved the intrinsic apoptotic pathway is shown in figure 2.2.

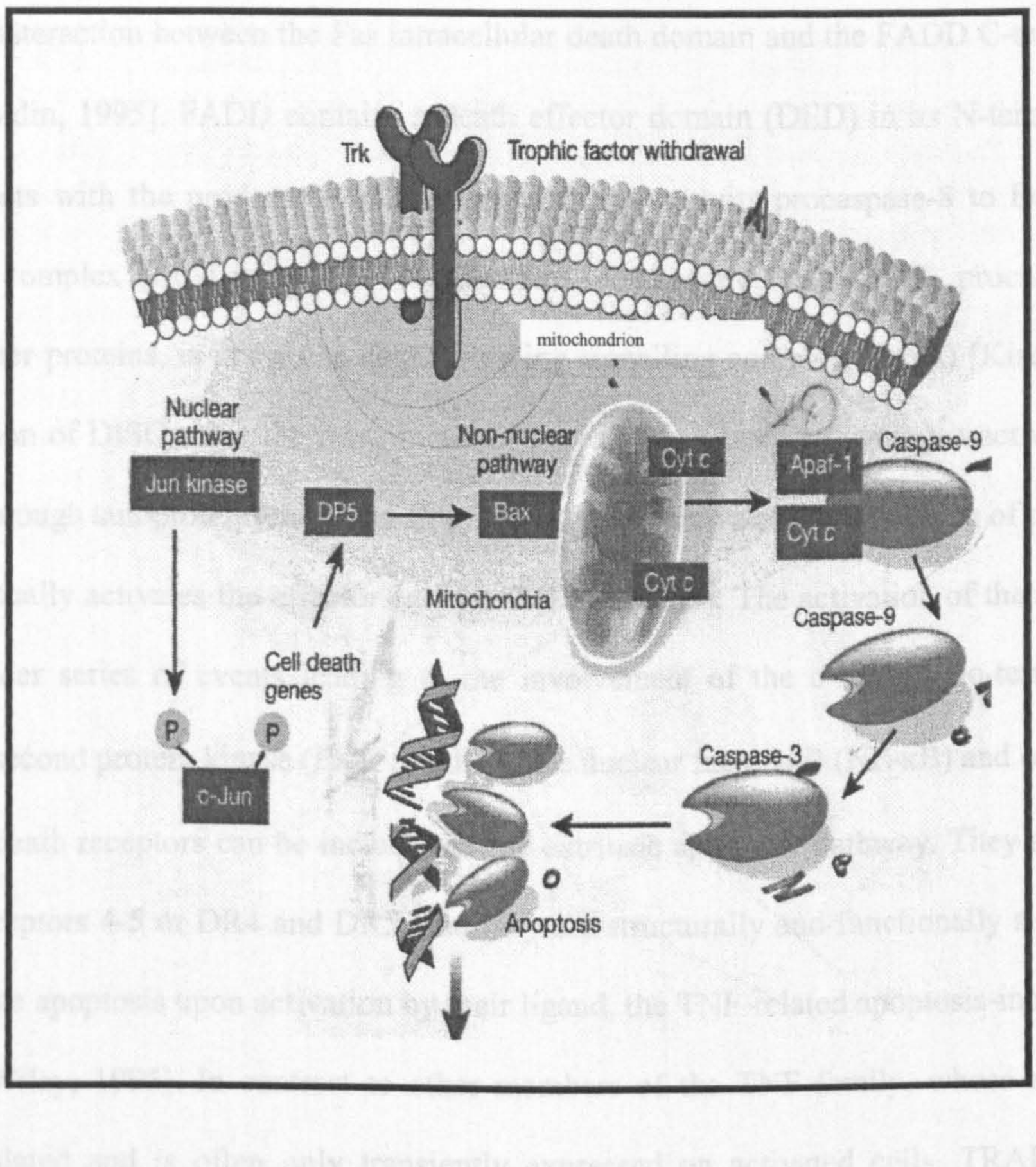

Figure 2.2 Intrinsic apoptotic pathway activated by trophic factor withdrawal

2.2.1 Extrinsic pathway

2.2.1.1 Death receptors

Death receptors are cell surface receptors that are able to trigger apoptosis. Among the members of the TNF receptor (TNFR) Fas (CD95/Apo-1) and the p75 neurotrophin receptor ($p75^{NTR}$) family are recently demonstrated to be involved in neuronal death [Raoul, 2002].

The Fas apoptotic pathway has been extensively investigated as a model system for mammalian apoptosis. Fas molecules preassemble into homotrimers via the preligand-binding assembly domain in the extracellular regions [Chan, 2000;Siegel, 2000]. Upon binding to the trimeric Fas ligand (Fas-L), Fas recruits a cytosolic adapter protein, Fas-associated death domain (FADD), through an interaction between the Fas intracellular death domain and the FADD C-terminal death domain [Boldin, 1995]. FADD contains a death effector domain (DED) in its N-terminal region. DED interacts with the prodomain of procaspase-8 and recruits procaspase-8 to Fas forming a multimeric complex [Boldin, 1996]. This complex, formed by Fas, FADD, procaspase-8, and possibly other proteins, is known as death-inducing signalling complex (DISC) [Kischkel, 1995]. The formation of DISC, after the recruitment of procaspase-8 leads to zymogen activation, likely occurring through autoproteolytic processing. This process activates the signalling of procaspase 8, which eventually activates the effector caspase 3 [Blatt, 2001]. The activation of these complexes elicits a wider series of events leading to the involvement of the c-Jun amino-terminal kinase (JNK), the second protein kinase (PKB or AKT), the nuclear factor-κB (NF-κB) and other targets.

Two other death receptors can be included in the extrinsic apoptotic pathway. They are classified as death receptors 4-5 or DR4 and DR5, and they are structurally and functionally similar to Fas. They mediate apoptosis upon activation by their ligand, the TNF-related apoptosis-inducing ligand (TRAIL) [Wiley, 1995]. In contrast to other members of the TNF family, whose expression is tightly regulated and is often only transiently expressed on activated cells, TRAIL mRNA is expressed constitutively in a wide range of non neural tissues. Similarly, DR4 and DR5 transcripts are expressed in many normal tissues [Wiley, 1995]. In neurons, the activation of TRAIL receptors induces the cleavage of procaspase-8 [Griffith, 1998]. Caspases-8 activation can be detected within minutes after the addition of TRAIL to target cells, suggesting that caspase-8 is one of the proximal

components of TRAIL signalling. Studies using co-transfection/co-immunoprecipitation experiments have also shown that the TNF-receptor-associated death domain (TRADD) may be recruited by both TRAIL-R1 and -R2 [Chaudhary, 1997]. In addition it was found that both TRAIL-R1 and -R2 can induce NF-κB activation, but are also capable of inducing JNK kinase activity [Hu, 1999]. TRAIL induces NF-κB activation by a caspase-sensitive event and cannot produce apoptosis by inhibiting NF-κB activation. This process implicates the presence of a protein, whose cleavage by caspases precedes NF-κB activation [MacFarlane, 2000].

TNFR1, together with TNFR2, mediates the pleiotropic effects of TNF-α, a primary inflammatory cytokine whose activation is thought to be involved in different diseases associated to neuronal injury or an inflammatory response. TNFR1 is expressed ubiquitously, while TNF-α is produced mainly by activated macrophages, T cells and microglial cells. Upon binding to TNF-α, TNFR1 associates with an adapter protein, TRADD [Hu, 1999], which then recruits FADD to activate caspase-8 and tumor necrosis-associated factor 2 and receptor-integrated protein 1 (TRAF2/RIP1) to activate JNK and NF-κB, respectively [Stanger, 1995;Ting, 1996].

2.2.2 Intrinsic Pathway

While the extrinsic pathway seems to be activated by a relatively small number of structurally related ligands, intrinsic, or mitochondrial-apoptosome associated apoptosis, can be triggered by a wide variety of structurally unrelated agents. This implies that intrinsic apoptosis can be induced by more than one single mechanism [Sastry, 2000].

2.2.2.1 Neurotrophic factors withdrawal

During development the neurons that fail to establish proper connections with their respective postsynaptic targets die to the lack of a sufficient trophic support. Intrinsic apoptosis caused by trophic factors withdrawal, represents the primary source of neuronal apoptosis in embryo CNS. This is an active process that involves the release of cytochrome-c and requires synthesis of proteins.

It was initially proposed that trophic factors exert a tonic inhibition by inactivating apoptotic pathway and consequently their removal activated the cascade of events inducing cytochrome-c release and caspases activation. To date, an alternative hypothesis has been proposed [Sanchez, 2001] and the current picture of sympathetic neuronal death pathway is as follows.

Consequently to the lack of NGF, neurons express and activate proteins that may play critical roles in apoptotic signal transduction, including two transcription factors of the activator protein-1 (AP-1) family, c-jun and c-fos. c-jun and other factors may act together to regulate the expression of different proapoptotic molecules. The phosphorylation of c-Jun by JNK and the consequent activation of a molecule belonging to the proapoptotic adapter proteins, the "BCL2 interacting mediator" of cell death (BIM) [Yuan, 1995], are considered as the critical step for development of competence-to-die in sympathetic neurons deprived of NGF [Whitfield, 2001]. Following its phosphorylation c-jun promotes BIM activation and the consequent translocation of BAX, from cytosol to mitochondrial outer membrane close to mitochondrial megapore known as the permeability transition pore (PTP). Translocation of Bax to mitochondria lead to mitochondrial depolarization and cytochrome-c release finally activating the caspases cascade cell signalling [Sartorius, 2001].

The possible contribution of trophic factor (serum and BDNF) withdrawal in inducing

apoptotic cell death in primary cultures of motor neurons will be widely investigated as object of this thesis (see chapter 10).

2.2.2.2 Ca^{++} overloading

Ca^{++} overloading can be important factor, principally in excitable cells, to activate intrinsic apoptotic pathways. The induction of apoptosis by Ca^{++}overloading depends on the intensity of Ca^{++} influx [Orrenius, 1994].

Although excitotoxicity and the resulting imbalance of neuronal Ca^{++} homeostasis have been extensively studied, the downstream mechanisms generated from increased $[Ca^{++}]_i$ are still poorly understood. Potential targets of Ca^{++} include kinases, phosphatases, proteases, phospholipases, NOS and mitochondrial deficits [Choi, 1995;Nicotera, 1997;Leist, 1997].

In *in vitro* experiments, by using rodent cerebellar granule cells (CGC), it has been demonstrated that high doses of glutamate produce a typical necrosis identified by the disruption of membrane integrity, the collapse of mitochondria, the membrane potential decay and the swelling of nuclei. In contrast, by maintaining a milder excitotoxic stimulation, by lower but longer lasting exposure to glutamate or glutamate agonists, a great percentage of neurons did not die by necrosis but following an apoptotic pattern [Ankarcrona, 1995]. These results suggested that, depending on the selective alteration in the different targets, due to the intensity of Ca^{++} entry, neurons can shift from apoptotic to necrotyc/lytic cell death [Ankarcrona, 1995;Nicotera, 1997].

In agreement with previous results, in different experiments carried out in CGC cultures exposed to low doses of excitotoxins, Leist confirmed the typical pattern of apoptosis in which the nuclear fragmentation, proteolysis of α-fodrin and the translocation of phosphatidylserine to the outer layer of plasmatic membrane, were seen prior to any loss of cell integrity and membrane impermeability. All these events were prevented both by glutamate receptor antagonists and by caspase inhibitors. In contrast, in CGC exposed to higher concentration of glutamate, caspase inhibitors resulted weakly protective [Leist, 1997].

This evidence suggested a possible coexistence of two different processes of death. The authors proposed that the two distinct pathways are differentially activated depending on the intensity of

cell death signal.

When Ca^{++} influx is slow and relatively moderate the pathway involving protease activation is activated. This pathway is likely related to a delayed loss in Ca^{++} homeostasis and its effect is almost completely prevented by agents that inhibit the cleavage of caspases. On the other hand, stronger glutamatergic stimulation can produce a massive Ca^{++} influx. In this latter condition In order to maintain the physiological ratio $[Ca^{++}]_{out}/[Ca^{++}]_{cytosol} \approx 10^4$, free Ca^{++} is first readily inactivated by calcium binding proteins, (i.e. calbindin, calretinin, parvalbumin). If calcium binding protein activity is insufficient to restore physiological levels of free Ca^{++}, the excess is removed from the cytoplasm and stored in different sub cellular components, such as mitochondria and ER, by a process of uptake. This rapid accumulation of Ca^{++} reduces the functionality of these organelles thus provoking a so fast decay in cellular activity that the cells, that are triggered to undergo to apoptosis, are instead forced to die by necrosis [Volbracht, 1999].

2.2.3 Antiapoptotic and proaptotic molecules

Mammalian B-cell lymphoma-2 (BCL2) proteins [Hengartner, 1994], are constituted of at least 15 proteins structurally related to CED-9 and grouped in the so-called BCL2 protein family [Adams, 1998 ;Chao, 1998 ;Newton, 1998]. All members of the family posses at least one of the four conserved BCL-homology (BH) domains (BH1, BH2, BH3, and BH4). Besides to BCL2, some of these proteins (such as BCL-X_L and BCL-W) act as survival factors, whereas others (such as BAX, BAK, BAD, and BID) are pro-apoptotic agents. BCL2 and BCL-X_L can prevent the release of cytochrome-c from mitochondria, avoiding assembling of the apoptosome, and thereby protecting cells from being killed [Li, 1998 ;Luo, 1998]. In addition, BCL-X_L in mammals interacts with Apaf1. This interaction results in inhibition of the association of Apaf1 with procaspase 9 and with consequent blockage of apoptosome formation and caspase 9 activation [Adams, 1998].

Some of the BCL2 family members can interact with each other by forming homo- or heterodimers. Although the subcellular location of each component of the BCL2 family differs slightly, most of them are found in the outer mitochondrial and in nuclear membranes. In normal conditions, BCL2 is concentrated in the outer mitochondrial membrane, while BAX is largely confined to the cytosol and translocate to the mitochondrial outer membrane once apoptotic pathway is activated [Hsu, 1997].

BID is normally cytoplasmic and apparently inactive; following proteolytic activation, BID translocates to the mitochondria and triggers the mitochondrial death pathway, as evidenced by the release of cytochrome-c.

On the other hand, BAD has been shown to be regulated by protein phosphorylation, which allows its sequestration by chaperone protein 14-3-3 and inhibition of its proapoptotic activity [Zha, 1996].

While BCL2 is placed in the intermembrane space the pro-apoptotic family members (BAD, BAX, BID) may be either cytosolic or present on the cytoplasmic surface of the outer mitochondrial membrane [Zimmermann, 2001].

2.2.4 The role of mitochondria

2.2.4.1 Mitochondrial membrane potential

The importance of mitochondria in the initiation of apoptosis is illustrated by the finding that mitochondrial factors can induce chromatin condensation and nuclear fragmentation typical of apoptosis in cell free Xenopus egg extracts [Newmeyer, 1994]. In many cases mitochondrial apoptosis is associated with a sequence of events that includes the PTP opening, the decrease of mitochondrial membrane potential ($\Delta\Psi_M$) and the release in the cytoplasm of small mitochondrial proteins responsible for the initiation of caspase mediated apoptosis, the apoptotic-initiating factors (AIFs). Depending on different physiological effectors, the PTP complex can adopt an open or a closed conformation but physiologically, most if not all PTPs are closed [Zoratti, 1995;Bernardi, 1996].

The $\Delta\Psi_M$ is dependent on the capacity of mitochondrial complexes I, III, and IV to use electron energy in the carrier molecules nicotinamide adenine dinucleotide (NADH), ubiquinone, and cytochrome-c to pump protons out of the mitochondrial matrix by transporting them across the inner mitochondrial membrane. The $\Delta\Psi_M$ and the ΔpH contribute to a proton electromotive force (δp). Since $\Delta\Psi_M$ is the greatest contributor to δp, it can be assumed that $\Delta\Psi_M$ varies almost linearly with the ATP/ADP ratio and provides an estimate of the ATP/ADP ratio within individual mitochondria [Tager, 1983].

In most experimental conditions in which apoptosis is induced, $\Delta\Psi_M$ decay is one of the earliest, if not the earlier, detectable event to discriminate this type of cell death [Wadia, 1998]. In neuronal apoptosis induced by NGF withdrawal $\Delta\Psi_M$ was found significantly reduced 3-6 h prior to nuclear DNA fragmentation and chromatin condensation [Sasaki, 2000].

2.2.4.2 The permeability transition pore

Opening of the PTP dissipates any remaining proton gradient across the mitochondrial membrane and further reduces the $\Delta\Psi_M$. In addition, PTP opening allows to free exchange between the mitochondrial matrix and the extramitochondrial cytosol of solutes and proteins smaller than 1500 Da. This exchange of soluble factors can produce mitochondrial swelling, the rupture of the outer mitochondrial membrane and the consequent release of AIFs components, in particular cytochrome-c, from the intermembrane space of the mitochondria into the cytoplasm [Goldstein, 2000].

Several factors are known to influence opening or closure of the PTP, one of the elements that favours pore closing and acts as anti-apoptotic agent is Cyclosporin A. Cyclosporin A binds to the PTP and maintains it in a closed position. Moreover it also promotes pore closure by binding cyclophilins that otherwise induce PTP opening in the presence of Ca^{++} [Bernardi, 1996].

The anti-apoptotic protein BCL2 maintains closure of the PTP in a manner similar to cyclosporin A. In fact BCL2 resides on the mitochondrial outer membrane close to the peripheral benzodiazepine receptor (PBR) and form a blockage for the ion flux between the outer and the inner membrane. On the other hand, the anti-apoptotic proteins BCL2 and BCL-X_L work to prevent cytochrome-c release from mitochondria, and thereby protect cells from death [Kluck, 1997]. BCL-X_L similarly regulates $\Delta\Psi_M$ and matrix volume within mitochondria. Thus, opening of the PTP is a critical step in many forms of apoptosis and is proposed to constitute an irreversible step in the process [Mignotte, 1998].

2.2.4.3 Cytochrome-c release

Because in physiological condition, cytochrome-c does not move through the PTP, it can be released into the cytoplasm through fractures in the mitochondrial membrane.

Cytochrome-c normally resides in the space between the outer and the inner membrane of mitochondria. During apoptosis the pro-apoptotic molecules are activated and translocate to the mitochondria where they induce the release of cytochrome-c (and other proteins) from the intermembrane space. It has been previously mentioned (see section 2.2.2) that a key event in the intrinsic pathway is constituted by the release of cytochrome-c into the cytosol [Neame, 1998].

At high and medium levels of $\Delta\Psi_M$ cytochrome-c content in mitochondria varies randomly with $\Delta\Psi_M$ thus maintaining its level over a physiological threshold. At low $\Delta\Psi_M$ levels, intramitochondrial cytochrome-c levels fall dramatically and nearby cytoplasmic cytochrome-c levels increase reciprocally [Gorman, 2000]. Once diffused into the cytosol cytochrome-c is able to initiate the processing of multiple caspases activation. In different experiments performed on cell-free extracts, depletion of caspase 9 rendered all the other caspases unresponsive to cytochrome-c, suggesting that all of these caspase activation events lie on the same pathway, with caspase-9 at the apex of the cascade [Garrido, 1999;Garrido, 1999].

2.2.4.4 Apoptosis-initiating factors

AIFs represent an important class of cytosolic proteins which are normally located in the intermembrane space of mitochondria and which promote the propagation of apoptotic cascade once cytochrome-c is released from mitochondria in response to a fall in $\Delta\Psi_M$ and of PTP opening [Newmeyer, 1994].

Apaf1 is a part of a large protein complex, the apoptosome [Adams, 1998]. Upon binding to cytochrome-c (also indicated to as Apaf2), which is released from mitochondria at the onset of apoptosis, a series of conformational changes lead to Apaf1 multimerization and association with procaspase-9 (or Apaf3) with the generation of the about 1 MDa molecular weight, the apoptosome [Adams, 1998].

In addition to cytochrome-c, another protein, with the dual name Smac/DIABLO is released

together with cytochrome-c during early phase of apoptosis. Smac/DIABLO has been identified as adapter molecule from mitochondria and caspases activation [Verhagen, 2000]. It promotes caspases activation both by associating with the apoptosome and inhibiting a family of proteins that function as inhibitors of apoptosis (IAPs).

2.2.5 Caspases

Caspases are known to cleave a number of structural targets as well as RNA splicing and DNA repair-associated proteins but can also process other caspases [Casciola-Rosen, 1994;Tewari, 1995]. Caspases can serve both as transducers and executioners of cell death [Reed, 2000].

To date the 14 members of the caspase family can be divided into three subfamilies on the basis of the peptide-sequence preferences of their substrates: I) the ICE-protease subfamily (caspases 1, 4, 5, 13 and 14, and murine caspases 11 and 12); II) the CED-3 subfamily (caspases 3, 6, 7, 8, 9 and 10) and; III) the caspase 2 subfamily. Each of the 14 different mammalian caspases may be responsible for cleavage of several different molecules, reflecting the more complex structural morphology of apoptosis. Each caspase is initially synthesized as a zymogen and requires processing at specific cleavage sites to generate the active enzyme. Different subsets of caspases are activated depending on the different pro-apoptotic stimuli [Li, 1997].

In the intrinsic apoptotic pathway caspase 9 seems to be the first caspase to become activated, almost certainly due to clustering of this protease via Apaf-1. Apaf-1 and procaspase 9 form a complex at a 1:1 ratio (Zou H 1999). Thus, procaspase 9 molecules are brought into close proximity by Apaf-1 and activated by autocleavage. Active procaspase 9 then cleaves and activates procaspase 3 [Li, 1997]. There may be a positive feedback loop between these two caspases, as active caspase 3 cleaves partially processed caspase-9 to generate the final form of the mature caspase 9 [Roth, 2001]. Cytochrome-c is able to initiate the process of activation for several caspases (-2, -8, -9 and -10) but all these events were blocked by removal of caspase 9 from extracts, confirming that this protease is indispensable for cytochrome-c-initiated program of death and occupies an apical point in the caspase cascade [Garrido, 1999].

Caspase 3 and -7 were activated downstream of caspase 9 and these caspases propagate the caspase cascade by activating caspase 2, -6, -8, and -10 alternatively.

The pattern of caspase 3 breakdown suggests that caspase 9 attacks this molecule between the large and small subunits and that caspase 3 subsequently removes its own prodomain by autocatalysis. The pattern of immunostaining for cleaved caspase 3 indicated that caspase 3 is cleaved in the cytosol and then rapidly translocated into the nucleus. It is well known that activated caspase 3 is responsible for proteolytic cleavage of several proteins in apoptosis [Tsutsumi, 2001].

Activated caspase 3 in turn activates caspase 2 and -6 [Chang, 2000].

An independent activation of apoptotic pathway in which caspase 9 seems preferentially interact with procaspase 7 is observed in different apoptotic pathways in neurons. Although the contribution of caspase 7 activation in apoptosis is controversial, in neurons exposed to staurosporine, a different timing and a distinct subcellular over expression of caspase 7 with respect to the classical profile of caspase 9/caspase 3 cleaved substrates was found. This evidence suggests that some differences could exist between caspase 3 and caspase 7-mediated cell signalling [Deas, 1998]. Interestingly immunohystochemical studies carried out to characterize the type of motor neuron death occurring in SOD 1 transgenic mice (see section 3.2.4) revealed a marked and selective immunoreactivity for caspase 9 and caspase 7 was observed in degenerating motor neurons following BAX translocation and cytochrome-c release [Guegan, 2001].

In contrast, activation of caspases 1, -4 and -5 was not observed in response to cytochrome-c release. This evidence suggests that these caspases participate at the upstream level of the release of cytochrome-c into the cytosol [Liu, 1996;Pan, 1998]. On the other hand, caspases 3, 6, and 8 are preferentially activated by the Fas/TNF-mediated death pathway [Zimmermann, 2001].

Caspases often function in cascades; an upstream caspase (initiator caspase) is activated by its interaction with a caspase adapter(s). Once activated, the initiator caspase processes and activates one or more downstream caspases (effector or executioner caspases). The activated effector caspases then cleave various cellular proteins, leading to apoptotic cell death.

2.2.6 Caspases substrates

To date, more than 60 proteins have been shown to be substrates of one or more caspases in mammalian cells, and the list is still growing. These substrate proteins contain one or more caspase cleavage sites in interdomain linker sequences [Stroh, 1998].

2.2.6.1 Nuclear substrates

Well-documented targets for the activated caspases are nuclear elements.

During apoptosis, nuclear DNA is condensed and degraded into large bodies (50 to 300 kb) and subsequently into small oligonucleosomal fragments of several hundred base pairs, for this reason a standardised assay to determine apoptosis is the typical observation of DNA laddering following electrophoresis in agarose gel.

Historically, one of the first proteins identified as being cleaved during apoptosis by diverse stimuli was the poly (ADP-ribose) polymerase-1 (PARP-1). PARP-1 cleavage activity was in fact used to identify and purify caspase3 as an effector caspase [Nicholson, 1995;Tewari, 1995]. PARP is a nuclear enzyme that senses DNA nicks and catalyzes the ADP-ribosylation of hystones and other nuclear proteins in order to facilitate DNA repair. PARP is cleaved at a single site by caspase-3, which separates the N-terminal DNA-binding domain from the catalytic domain and inactivates the enzymatic activity [Lazebnik, 1994].

Biochemical purifications have led to the discovery of a caspase-regulated DNAase complex termed DFF (DNA fragmentation factor) that is composed of a DNase termed CAD (caspase-activated Dnase) and its inhibitor ICAD [Liu, 1997]. In healthy cells, CAD is complexed with ICAD and functionally inactive. In apoptotic cells, ICAD is cleaved by caspase 3 and -7. The cleavage provokes the release of CAD and the degradation of nuclear DNA [Sakahira, 1998]. DFF induces both chromatin condensation and DNA fragmentation *in vitro* [Liu, 1997], and cells from mice deficient for DFF activity exhibit neither of these classic apoptotic features when induced to die [Zhang, 1998].

Interestingly, another caspase 3-activated factor, named acinus, induces chromatin condensation without affecting DNA fragmentation [Sahara, 1999].

Although there are multiple sensors that record and transduce DNA damage within mammalian

cells, one of the most important is the p53 tumor suppressor protein. p53 plays a critical role as a transducer of damage to genomic integrity into growth arrest and/or apoptosis. DNA damage triggers stabilization and accumulation of p53, which then initiates either a G_1 cell cycle arrest or apoptosis [Fraser, 1996]. It seems that, in response to appropriate stimuli, p53 translocates to the nucleus and plays a regulatory role in directing primary neurons toward differentiation or apoptosis [Caelles, 1994 ;Wagner, 1994]. p53 can induce apoptosis even after treatment with translational or transcription blockers, indicating that p53 can induce apoptosis through pathways that do not require *de novo* protein synthesis [Haupt, 1996].

Several lines of evidence converge to indicate that neurons undergo to apoptosis by p53-dependent or -independent pathways, depending on the stimulus responsible for the death.

2.2.6.2 Cytoskeletal substrates

The cytoskeleton is another important target for active caspases Apoptotic cells do not exclusively undergo to nuclear fragmentation, but also show shrinkage, and, in non neuronal tissues, cells become detached from surrounding cells and from the basal membrane. The molecular logic behind these changes appears more evident after the biochemical identification of many cytoskeletal proteins that are cleaved by caspases [Cotter, 1992].

Caspases attack multiple targets in the cortical actin architecture, α-fodrin and focal adhesion kinase, two components of the focal adhesion complex, which links cortical actin filaments, plasma membrane, and transmembrane proteins to the extracellular matrix, are cleaved by caspases and this process can lead to cell body shrinkage [Martin, 1996]. Actin itself is cleaved by effector caspases and the caspase-generated fragments may contribute directly to apoptotic changes of cell shape [Stroh, 1998].

Given some morphological similarities between apoptosis and mitotic catastrophe it is important to note that, in presence of active caspase 3 the cyclin-dependent kinase (Cdk) activity increases, and that the inhibition of Cdk activity attenuates apoptosis in several experimental systems [Shi, 1994]. A number of proteases, including cysteine proteases and calpains have been shown to contribute to apoptosis. Specific calpains have been shown to contribute to the cleavage of the cytoskeletal

protein actin that occurs during apoptosis and calpain inhibitors have shown to block actin cleavage in apoptosis. Interestingly, it has been also reported that calpains, once activated by caspases, can cut and inactivate the active form of caspase 3, thus producing a negative feedback [Jordan, 1997;Nath, 1996;Jordan, 1997;Nath, 1996].

Many other proteins found to be caspase substrates are cleaved by effector caspases in the late phases of apoptosis. The kinetic data imply that this group of proteins may not have primary roles in regulating the decision to undergo cell death but they are activated to produce subsequent events of apoptosis, such as phagocytosis of apoptotic bodies or recycling of the cellular constituents. For instance, phosphatidylserine externalization at the plasma membrane facilitates phagocytosis of apoptotic bodies. Its externalization requires caspase activity. In this view, the activation of signalling cascades by caspases can be considered a "message from the dead".

2.3 Apoptosis and neurodegenerative diseases

2.3.1 Positive evidence

In adult neurons, apoptosis can be caused by exposure to excitatory amino acids [Mitchell, 1994;Bonfoco, 1995], 1-methyl-4-phenyl-1, 2,3,6-tetrahydropyridine (MPTP) [Tatton, 1997] and its metabolite MPP^+ [Dipasquale, 1991;Mochizuki, 1994], 6-hydroxydopamine, the 25-35 fragment of β-amyloid protein and prion protein [Chiesa, 2000;Forloni, 1996;Chiesa, 2000;Forloni, 1996], mutated presenilin 2 [Wolozin, 1996], mitochondrial complex I inhibitors [Hartley, 1994], high levels of dopamine [Ziv, 1994] or levodopa [Walkinshaw, 1995], the AIDS protein gp120 [Muller, 1992] and overexpression of the mutant superoxide dismutase (SOD-1) gene [Rabizadeh, 1995].

In recent years, apoptosis has been described in a variety of human neurodegenerative diseases, primarily based on the use of *in situ* end labelling (ISEL) or dUTP nick and-labelling (TUNEL) techniques to detect neuronal nuclei with apparent DNA cleavage. ISEL-positive nuclei have been found in the brain of patients with Parkinson's disease [Mochizuki, 1996 ;Cotman, 1994], Alzheimer's disease [Dragunow, 1995], Huntington's disease [Thomas, 1995] and TUNEL positive cells were found in spinal motor neurons of ALS patients [Tews, 1997].

In different inherited neurodegenerative diseases, including Huntington's disease and spinocerebellar ataxia, a marked involvement of apoptosis was observed in distinct regions of the brain, and, interestingly, several polyQ proteins have been found to be substrates for caspase 3 [Martin, 1999].

BCL2, was found to be decreased in neurons of Alzheimer's patients with neurofibrillary tangles, still resulting unchanged or increased in nearby unaffected neurons [Vyas, 1997].

In Alzheimer's disease post-mortem brains, an increase of c-Jun immunostaining has been reported. c-Jun positive immunostaining was observed in cells without ISEL-positive nuclei. This evidence suggested that these neurons may have entered the early stages of the apoptotic process but had not yet progressed to the point of nuclear DNA cleavage [Anderson, 1996;MacGibbon, 1997].

Increased levels of BAX and c-Jun were further found in cortical neurons from Alzheimer's patients, but without evidence of nuclear DNA cleavage. This apparent controversy could also suggest an activation of these molecules thus lacking the progression of apoptotic cell death

program [Roth, 2001;Su, 2001].

At present, it is not possible to determine a direct correlation between the decrease in $\Delta\Psi_M$ and its contribution in human neurodegenerative diseases. Evidence of mitochondrial impairment was reported in Parkinson's, Alzheimer's, and Huntington diseases [Bertoni-Freddari, 2004;Beal, 2003]. This reduction of mitochondrial activity may be responsible for apoptosis through a relative failure of proton pumping and a consequent decrease of $\Delta\Psi_M$. However, as yet, these hypotheses are still too weak and more direct correlation between $\Delta\Psi_M$ decay and the following steps of apoptosis (i.e. caspase9 and capspase-3 activation) must be produced to account for apoptosis in neurodegenerative diseases.

2.3.2 Controversial evidence

During the last decade apoptosis has become an appealing aim of study about cell death mechanisms in neuropatholgy. Therefore, the concept of apoptotic involvement in neuronal cell death has been widely used and abused in these general terms in relation to neurological diseases but its experimental demonstration is very problematic.

Although positive staining of individual neurons with ISEL or (TUNEL) technique has been proposed to unambiguously establish the presence of apoptosis [Tatton, 1997], these techniques, if not coupled to an accurate ultrastructural study, are not necessarily unequivocal markers for detecting of apoptosis. Moreover, several reports have demonstrated that TUNEL positivity is not exclusively specific for apoptotic neurons and does not even necessarily label cells that are committed to die [Stadelman, 2001].

For instance, the high percentage of ISEL positive neurons that were reported in distinct studies [Mochizuki, 1996;Cotman, 1994] did not account for the rate of neuronal death that can occurs in Parkinson's and Alzheimer's disease, where neurons die asynchronously and over many years. This artefact may be due to changes in tissue perfusion and oxygen levels occurring in the period prior to death that accelerate the entry of these cells into the final stages of apoptosis.

There are numerous claims that a postulated apoptotic cell death pathway plays an etiological role in Alzheimer's disease. However, although at least 7 different caspases have been implicated in

regulating neuronal death in response to β-amyloid exposure, the direct involvement of caspase-dependent neuronal apoptosis in neurons of Alzheimer's patients remains uncertain [Roth, 2001].

In the case of Parkinson's disease, distinct groups have consistently failed to confirm previous report describing the occurrence of apoptosis in the substantia nigra [Hoglinger, 2004].

In addition it has been also reported the presence of caspase 3 positive neurons in the substantia nigra of patients with Parkinson's disease, but the correlation between the degree of dopaminergic cell loss in Parkinson's disease and the high number of caspase 3 positive neurons in post-mortem samples obtained from no neurological patients, utilized as control in this study, these subjects is far from convincing [Hartmann, 2001].

2.3.3 ALS and apoptosis

Recent studies have suggested that apoptosis may be responsible for motor neuron degeneration in ALS.

Although there are several observations of chromatin condensation in motor neurons of ALS patients, the effective involvement of apoptosis in neuronal cell death still remains to be demonstrated. The main source of doubt about apoptotic motor neuron death in ALS arises from the absence of DNA fragmentation, reported by Martin in the most cited study in which apoptosis is claimed in ALS [Martin, 1999].

In order to detect DNA fragmentation in motor neurons from ALS patients many other studies were performed.

In two distinct investigations, TUNEL positivity was reported in the motor cortex, brainstem, cervical, thoracic and lumbar spinal cord of ALS patients [Ekegren, 1999]. However, in these two studies, TUNEL positive neurons were also found in control patients, thus suggesting a possible bias due to changes in tissue perfusion and oxygen levels in the period prior to death. In addition, an other group failed to provide evidence of DNA cleavage using in situ nick translation, a technique that involves the use of DNA polymerase I, and TUNEL staining both in motor cortex and lumbar cord segments [Migheli, 1994].

These controversial results suggest that, to ensure proper discrimination between apoptotic and

non-apoptotic motor neuronal death, TUNEL/ISEL studies should be supplemented with morphological and ultrastructural analyses.

Although histochemical studies did not provide a clear indication of DNA fragmentation such results are supported by the presence of different apoptosis-related markers observed in ALS patients tissues.

In a study conducted at the lumbar spinal cord level, the mRNA content of the antiapoptotic molecule BCL2 was found significantly decreased in ALS patients compared to patients that did not present neurological disorders. In the same study no significant differences were found, among the two experimental groups, by comparing the BCL-2 mRNA in unaffected regions of the lumbar spinal cord, dorsal horns and sensory nuclei [Mu, 1996].

In a similar study, no difference was found in BCL2 mRNA levels in the thoracic region but an increase in BAX was found in ALS patients [Ekegren, 1999].

A direct consequence of antiapoptotic/proapoptotic molecules imbalance and mitochondrial depolarization is represented by the release of cytochrome-c from the mitochondria to the cytosol.

In addition to observations indicating a prevalence of the proapoptotic component and an alteration in PTP pore in motor neurons from ALS patients [Ekegren, 1999], cytochrome-c positive immunostaining was found in the cytosol of spinal motor neurons in sporadic ALS patients [Guegan, 2001]. In this study a weak and punctuate cytochrome-c immunostaining was observed in controls motor neurons, by contrast, in ALS patients, the remaining motor neurons exhibited a homogeneous and intense immunostaining possibly due to cytochrome-c release. However neither a double staining (indicating the integrity of mitochondria) nor further confirmations by the following steps (APAF1 or active-caspase9) were investigated in this work. Thus, it is possible that the different pattern of staining of cytochrome-c in motor neurons of ALS patients may be due to a mitochondrial collapse and loss of integrity occurring in dying neurons, rather than an actual process of active release of cytochrome-c from mitochondria to the cytosol.

Further evidence implicating caspases activation in the motor neuron death occurring in ALS derives from two distinct studies. A significant increase in caspase 3 activity in the spinal cord anterior horn and motor cortex of ALS patients was described by Martin [Martin, 1996] and a

massive increase, more than 80%, of caspase-1 activity was reported in the spinal cord from ALS patients [Li, 2000].

Although different results suggesting an apoptotic involvement in ALS motor neuron death are reported, these data resulted often weak and controversial. For this reason it is important to remind that, in a chronic disease like ALS, conclusive evidence of apoptosis are difficult to obtain given the rapidity of the apoptotic cell death process in relation to the relatively long lasting time-course of the disease.

In acute models of neuronal death generated by excitotoxic exposure [Portera-Cailliau, 1996], trophic factors deprivation [Al-Abdulla, 1998] and axotomy [Heimer, 1978], evident signs of apoptotic involvement are observed from few to a maximum of 24 hours after injury. This short range of time to detect apoptosis suggests that, in a chronic disease like ALS, very few cells from several thousand motor neurons might be expected to show signs of ongoing apoptosis at any one time in temporally static post-mortem sample. Thus, a very large number of sections should be examined to obtain a true picture of the involvement of apoptosis in ALS patients: nevertheless caution should still be used in interpreting these data because of the late stage of motor neurons obtained from autopsy samples.

2.4 Neuroprotective and antiapoptotic effects of erythropoietin in different models of neurodegeneration

2.4.1 EPO and erythropoyesis

Erythropoietin (EPO) is a 30,400-dalton glycoprotein that regulates red cell production [Fisher, 1971]. In humans, EPO is produced by peritubular cells in the kidney [Jacobson, 1957;Fisher, 1971], and small amounts of extra-renal EPO are produced by the liver [Zanjani, 1977]. EPO binds to an erythroid progenitor cell surface receptor that, when activated, becomes dimerized [Declercq, 1995].

EPO acts primarily to rescue erythroid cells from PCD in an anti-apoptotic manner. Using the EPO-dependent human erythroid progenitor cell line HCD-57, Silva [Silva, 1996] showed that EPO maintained erythrocytes precursors viability via repressing apoptosis by up regulating Bcl-xL, an anti-apoptotic gene of the Bcl-2 family. By culturing erythrocytes in the absence of EPO, Bcl-2 and Bcl-xL are rapidly down regulated and the cells die apoptically. In support of this link between EPO and anti-apoptotic factors it has been reported that knockout mice for Bcl-xL exhibited foetal liver haematopoietic defects and had a severe anaemia during embryogenesis [Silva, 1996].

EPO acts synergistically with several growth factors (SCF, GM-CSF, IL-3, and IGF-1) to increase the survival and to augment the rate of maturation and proliferation of erythroid progenitor cells (primarily colony-forming unit-E) [Wu, 1995;Lin, 2004]. Oxygen-dependent regulation of EPO gene expression is controlled by a hypoxia-inducible transcription factor (HIF-1) [Semenza, 1991]. Other effects of EPO include a haematocrit-independent vasoconstriction-dependent hypertension, increased endothelin production, up regulation of tissue renin, change in vascular tissue prostaglandins production, stimulation of angiogenesis, and stimulation of endothelial and vascular smooth muscle cell proliferation [Smith, 2003;Vaziri, 1997;Nowicki, 1995].

Recombinant human EPO (rHuEPO) is currently being used to treat patients with anaemia associated with chronic renal failure, nonmyeloid malignancies in patients treated with chemotherapeutic agents, perioperative surgical patients, and autologous blood donation [Langston, 2003].

2.4.2 EPO and neuroprotection

Over the last ten years, a prominent role for EPO has been defined in the CNS and there is a growing interest on the potential therapeutic use of EPO for neuroprotection. It is now widely known that EPO does not only affect the haematopoietic system, but it can be considered a multifunctional trophic factor with an effect on the general homeostasis of the entire organism [Konishi, 1993;.

Brines et al. [Brines, 2000] reported that rHuEPO crosses the BBB and this passage is increased in conditions of neural injury. Although the BBB is considered impermeable to large molecules, recent studies clearly demonstrate that some high-molecular-mass molecules can be specifically transported into the brain across the capillary endothelium [Chong, 2002;Martinez-Estrada, 2003]. Several studies have been directed to evaluate the neurotrophic and neuroprotective function of EPO in different conditions of neuronal damage, such as hypoxia, cerebral ischemia and brain trauma [Brines, 2000;Agnello, 2002;Siren, 2001;Villa, 2003].

In a *in vitro* model of cerebral ischemia, comprising hypoxia and glucose deprivation, EPO (30pM) was shown to protect cultures of neurons from death and, in mixed astrocytes/cortical neurons cultures, in which a nonlethal ischemic event was induced, EPO demonstrated to exert its neuroprotective/anti-apoptotic action by inhibiting neuronal death via a cascade of phosphorylation starting from the dimerization of Jak-2 [Digicaylioglu, 2001].

In *in vivo* studies Sadamoto et al demonstrated that EPO reduces degeneration in rats with permanent middle cerebral artery occlusion. Using *in situ* hybridization technique, they also found that EPOr mRNA is up-regulated in the periphery of the cerebrocortical infarction, the so-called ischemic penumbra [Sadamoto, 1998]. In 1999, Bernaudin et al. reported the potential role of EPO in focal permanent cerebral ischemia induced in mice by permanent occlusion of the left middle cerebral artery. Mice treated with intraventricular injection of recombinant mouse EPO produced a significant reduction of the infarction volume at the periphery.

Because of EPO acts by increasing the neuronal survival only in the penumbra but not in the necrotic core, it has been postulated that EPO only protects the penumbra in relation to the different type of neuronal death occurring in the ischemic core and in the penumbra area, respectively. It would be possible to argue that EPO does not protect against the first type of death because the temporal window between the ischemic induction and the cellular death in the core is too short to avoid the therapeutical effect of EPO. However, even if EPO is administrated several hours before the ischemic injury, this compound results ineffective in reducing the rate of death at the ischemic core. This evidence further supports the hypothesis of a selective anti-apoptototic effect of EPO [Bernaudin, 1999].

Sirèn et al. showed that rHuEPO administration, in rats with middle cerebral artery occlusion, dramatically reduces the infarction area 24h after ischemic induction [Siren, 2001].

In addition, EPO not only protects neurons from cell death induced following ischemia, but also from a variety of other detrimental stimuli, including excitotoxins exposure and glucose deprivation.

Morishida at al showed that, in cultures of neurons, EPO pre-treatment prevented glutamate-induced neurons death in a dose-dependent manner [Kawakami, 2001]. The anti-excitotoxic effect of EPO has been further confirmed in cultures of cortical neurons exposed to glutamate or glutamate-receptor agonists [Sinor, 2000]. Although a short incubation with EPO (5 min or less) has already capable to induce a partial neuroprotection against glutamate toxicity, a relatively long incubation period (8h) is required to obtain a consistent neuroprotection.

Finally, it is important to note that rHuEPO treatment improved brain function, as shown by findings from neuropsychological tests and electrophysiological measurements [Nissenson, 1992].

Although the discovery of the production of EPO by neuronal cells it is quite recent, treatments with rHuEPO have definitively highlighted its neurotrophic and protective effect of the hormone, thus opening new frontiers in the treatment of diseases of the CNS, mainly in pathologies where apoptosis is involved.

CHAPTER 3

in vitro AND *in vivo* models of ALS: ADVANTAGES AND PITFALLS

Several aetiopathological hypotheses have been proposed to explain the death of motor neurons that occurs in ALS. These hypotheses are generated from different experimental data, clinical and biochemical estimations, post-mortem analyses in the spinal cord and brain tissues and by the evidence provided from different neurodegenerative processes that leads to neuronal death in other types of acute or chronic disorders. However, these approaches lack a well-established pathological mechanism occurring in ALS because of their incapability to obtain experimental evidence concerning the early events of motor neuron degeneration. In ALS patients the condition of motor neurons in post-mortem tissues represents the main limit in studying the early events involved motor neuron death. Consequently, alternative models are required in order to bypass the limit of investigation deriving from post-mortem samples.

For this reason, *in vivo* and *in vitro* models of motor neuron disorders represent a useful tool to obtain more detailed information about the main detrimental processes leading to motor neuron death.

3.1 Cellular models

Although embryonic spinal cord motor neurons obtained from primary cultures are the best characterized model of study in the field of *in vitro* research, different approaches are available. Several tissue culture studies using human CNS tissue have been carried out, but they gave insufficient information about spinal cord neurons in culture [Gilden, 1975]. Since the main limitations to obtaining human primary cultures motor neurons are represented by the source of the tissue (the embryo), cultures of adult human spinal cord have been reported as explants or dissociated cultures [Peterson, 1977;Erkman, 1989;Kim, 1990;Peterson, 1977]. Unfortunately, these cultures are extremely fragile and their low percentage of viability (even in basal conditions and in

presence of serum and trophic factors) did not produce useful results.

Because of the difficulties in studying human spinal cord cultures, the use of non-human spinal cord cultures is considered a reliable alternative of research. Organotypic cultures and cell-lines derived from tumours, or from cells that are dedifferentiated and transformed *in vitro*, such as the fusion product of mouse neuroblastoma with primary mouse embryonic spinal cord neurons [Cashman, 1992] are widely used in ALS research.

The use of organotypic cultures, while maintaining reciprocal cell interaction and the presence of well-differentiated motor neurons, has two main limitations: the impossibility to perform analyses at the single cell level, and the detrimental effects of "experimental axotomy" on motor neurons. This form of axotomy is due to the fact that, in early postnatal age, the axons are already connected to their specific peripheral targets, and therefore, during the preparation of organotypic slices, the proximal stump of axon remains connected to the motor neurons whereas the distal part is lost.

The possibility to perform a single cell study and to avoid the problems arising from "experimental axotomy" is derived from immortalized cell lines. However the use of cell lines as a model of motor neuron degeneration has not been entirely successful. This is due mainly to the fact that these cells often appear and behave like motor neurons but they are not motor neurons. Moreover, it is important to note that, they are frequently obtained by differentiation programs or from tumour cells which possess relevant differences both in term of cell biology and in their response to different external stimuli.

For this reason, although such approaches can provide information to the basic mechanisms of cytotoxicity, primary cultures of motor neurons (obtained from embryonic rats mice and chickens) are the most reliable and direct model to perform more accurate and rapid measurements on different cell death pathways and to evaluate the effectiveness of future therapeutic strategies.

3.2 Animal models

The development of animal models for human diseases is an important scientific goal since they can provide valuable insights into the disease process itself. An ideal animal model of a human disease should satisfy a number of criteria, including the recapitulation of the pathogenic process, the presentation of the clinical and pathological features of human disease, and the

responsiveness to disease-modifying events, such as treatments.

Several animal models of ALS have been proposed but yet none are thought to be completely satisfactory [Pioro, 1995;Price, 1994;Strong, 2000;Gurney, 1994]. The absence of a faithfull animal model of ALS is due largely to the paucity of knowledge about the aetiology and the pathogenesis of human ALS.

This reflects the inevitable limitation of accurability reproducing human diseases in species with a different physiology and anatomy. Anyway, it is important to remember that all models of motor neurodegenerative diseases contribute to the understanding of common detrimental processes that lead to motor neuron death.

The animal models for motor neuron disorders can be classified in three main categories: pharmacotoxicological models, animals showing spontaneous motor neuron degeneration and transgenic mouse models.

Below a short description of the most common animal models of ALS is summarized, whereas a more detailed characterization of our model of study, the wobbler mouse, will be reported in Chapter 5.

3.2.1 *mnd* mouse

The *mnd* mutation is a spontaneous, dominant mutation localised to chromosome 8 [Messer, 1992]. The *mnd* disease, characterized as a model of neuronal ceroid lipofuscinosis [Bronson, 1993;Pardo, 1994], was initially proposed as a model of motor neuron disease, like ALS [Martin, 1999;Messer, 1994]. In fact, *mnd* mouse exhibits adult-onset, progressive spastic paralysis moving from caudal to cranial spinal cord levels. The onset of the disease is recognisable at 6 months of age, the motor impairment progresses rapidly and lead to premature death at 10-12 months [Messer, 1993]. In spite of this rapid symptoms evolution the number of choline acetyltransferase (ChAT) immunopositive motor neurons and the ChAT activity in the spinal cord and hind leg muscles of symptomatic *mnd* mice is similar to control mice [Mennini, 2002]. The neuropathological hallmarks of *mnd* are inclusion bodies containing immunoreactive ubiquitin [Mazurkiewicz, 1991], degenerating mitochondria [Vance, 1997;Bertamini, 2002], lipofuscin and ATP synthase subunit-c accumulation [Pardo, 1994;Faust, 1994], the loss of Nissl substance, displaced neurofilaments [Callahan,

1991], and the loss of photoreceptors with degeneration of retinal cells [Messer, 1992;Messer, 1993].

This series of clinical features render the *mnd* mouse a more appropriate model of human Batten's disease than of classical ALS [Battaglioli, 1993].

3.2.2 *pmn* mouse

The "paralysé natural mutant" (*pmn*) mouse carries a recessive mutation on the chromosome 13 [Brunialti, 1995]. Neuropathological and clinical signs have an early onset (2 weeks) and a rapid progression of symptoms [Schmalbruch, 1991]. Symptomatic phase begins at two weeks of age and evolves rapidly to death at around 40 days. Distal axonopathy is the most relevant sign of this pathology. In motor neurons, cell bodies and proximal axons are relatively preserved. Neurogenic muscle atrophy and subsequent paralysis are prominent [Kennel, 1996]. In the *pmn* mouse both growth factors and pharmacological agents, including riluzole have been shown to reduce symptoms progression [Haase, 1998;Sagot, 1995]. Nonetheless in *pmn* the mechanism of motor neuron death is not yet characterized, the evidence that Bcl2 overexpression failed to slow clinical progression and to prolong the survival, account for a non-apoptotic cell death process [Blondet, 2002].

3.2.3 Wasted mouse

The wasted mouse carries a recessive mutation that has been identified as a deletion of a sequence of DNA on chromosome 2 that prevents the expression of the gene coding for the translation elongation factor EG1α2 [Chambers, 1998]. It is still unclear why the disruption of this protein involved in protein synthesis should produce such a specific neurological syndrome.

In the wasted mouse, neuropathological and clinical signs have an early onset, before the second week of age, and a very fast progression that leads to death within a month. Pronounced vacuolization is observed throughout the anterior horn region and in the brainstem of motor nuclei [Lutsep, 1989]. Spinal motor neurons degenerate and are lost, whilst upper motor neurons appear to be unaffected. Wasted mice also show lymphoid hypoplasia and other immunological anomalies [Kaiserlian, 1986;Libertin, 1994].

Although many neuropathological hallmarks observed in the wasted mouse share with human disease, the early onset of symptoms and the short time of survival render extremely difficult to determinate the possible effectiveness of pharmacological treatments.

3.2.4 SOD1 transgenic mouse

The most characterized transgenic model for studying familial ALS is the transgenic mice for the mutation Cu^{++}/Zn^{++} superoxide dismutase (SOD1). Since 1993, when Rosen *et al.* reported the correlation between this mutation and a 20% of familial cases of ALS [Rosen, 1993], several lines of transgenic mice, and rats,, carrying different point mutations associated to human mutations, were produced [Gurney, 1994;Wong, 1995;Bruijn, 1997].

The onset of symptoms differs among the different type of mutation; however, all these mutations are able to produce a selective process of motor neuron degeneration. On the other hand, transgenic mice expressing the wild type form of human SOD1 ($hSOD1^{wt}$), thus showing mild neuropathological alterations in lumbar motor neurons, do not show neurological disorders, appear phenotypically comparable to healthy mice and do not present a "shortened life-span" [Jaarsma, 2000].

The spinal cord motor neurons are mostly affected to the disease, the motor degenerative process follows a lumbar/cervical gradient, at the late stage of the disease almost all spinal motor neurons are disappeared and the death commonly occurs by respiratory failure. Cytological studies have demonstrated that degenerating motor neurons appeared highly vacuolized. At the end stage, the cytoplasm of motor neurons is almost empty; Nissl staining is very weak and not homogeneously distributed. Moreover, filamentous inclusions immunopositive for ubiquitin and neurofilaments are present in some of the surviving neurons [Gurney, 1994].

3.2.5 Wobbler mouse

The wobbler mouse was originally characterized and described by Falconer in 1956. This mutation was first observed in some animals belonging to a C57BL/Fa strain and was associated with a wobbly gait characteristic of the mice. Mutant mice show a rapid and selective vulnerability of cervical spinal cord motor neurons. From the 3^{rd} to the 12^{th} week of age the number of cervical

motor neurons is reduced by about 65%. The onset of symptoms and their progression coincide with the rate motor neuron loss. Wobbler mice show a progressive atrophy of forelegs muscles accompanied to a marked decrease in muscular strength and motor ability. Although the wobbler disease was classified for a long time in the group of the spino muscular atrophy (SMA) because no neuronal alterations were been detected in the cortex, a result obtained using an *in vivo* approach by proton magnetic resonance spectroscopy confuted this idea. In this study Pioro observed that the cell bodies and the neurites of neurons of the neocortex had a strong immunoreactivity for ubiquitin and an accumulation of NF-H was observed in neuronal-cell bodies of the cerebral cortex [Pioro, 1998]. Although the actual loss of neurons has not yet been demonstrated in the cortex, this result suggests that neuronal target in wobbler mice is not restricted to lower motor neurons but may involve the brain areas. This finding renders this model more similar to ALS than to SMA [Pioro, 1998].

The wobbler mouse is a reliable model to investigate about the symptomatological, neuropathological and biochemical alterations leading to motor neuron degeneration. The main aetiopathological hypotheses that have been considered responsible for motor neuron death in humans, such as excitotoxicity, oxidative stress, deficit of trophic factors and accumulation of toxic proteins and aggregates, have been tested in wobbler mice. The results obtained have pointed out several defects that are common of human's diseases.

A summary of the main neuropathological features characterizing the different animal models of ALS is summarized in table 3.1.

NEUROPATHOLGICAL HALLMARKS	mnd	pmn	WASTED	SOD1^{G93A}	WOBBLER
Anterior horn cell changes	Lysosomial accumulation	Chromatolysis	Vacuolization	Vacuolization	Vacuolization
Anterior horn cell loss	None	Limited	Extensive	Extensive	Cerv. sp cord
Brainstem motor neuron loss	Some	Limited	Extensive	Extensive	Present
Axonopathy	Absent	Extensive	Present	Present	Present
Denervation	Unknown	Present	Present	Present	Present
Upper motor neurons	Minimal	Absent	Present	Some loss	Limited
Other neuronal groups	Absent	Brainstem	Absent	Absent	Brainstem

Table 3.1 Neuropathological alterations in murine models of ALS (modified from Doble 2000).

CHAPTER 4

PRIMARY CULTURES OF MOTOR NEURONS

4.1 Purified and mixed cultures

4.1.1 Purified cultures of motor neurons

In 1981 Schnaar and Schaffner first described the procedure to obtain purified motor neuron cultures. In that study, motor neurons were separated from the other cells by centrifugation and, using a correct density of neutral substance (metrizamide) a highest percentage of motor neurons was obtained [Schnaar, 1981].

This technique was then modified and adapted from several researchers and in 1993, Henderson and colleagues [Henderson, 1993] published a protocol to better purify motor neurons. Their method allows to obtain purified cultures of embryonic motor neurons (E14-15) by using antibodies specifically directed against the low affinity receptor NGFr, p75, which is highly expressed in rat embryo (E 14) motor neuron cell surface. This procedure of purification is commonly identified as immunopanning.

The immunopanning markedly increased the percentage of purified motor neurons and also their resistance on plating.

Unfortunately, although immunopanning increased the survival of purified cultures of motor neurons, these cultures are still highly vulnerable and their life span is influenced by several external parameters. Because of long term survival is a basic requirement to study a chronic disease or evaluate the effect produced by exposure to toxic and/or protective agents, the use of alternative condition, such as mixed co cultures, is often more indicated to study motor neuron behaviour.

4.1.2Mixed glia/neurons cultures

An alternative source of investigation is represented by mixed glia/neurons cultures. Mixed cultures, obtained from anterior horn of embryonic spinal cord without cells purification, allow to prolong motor neuron survival and, moreover, to reproduce the physiological condition.

A further application of mixed glia/neurons cultures involve the purification of a controlled layer of glial cells over which purified motor neurons are plated.

In mixed glia/neurons cultures, glial cells surround motor neurons and maintain a physiological supply of trophic factors. This interaction produces an extensive neurites outgrowth, a higher ramification of branched dendritic trees, and a more sustained formation of synapses and, above all, a longer life span compared to purified motor neurons that are laid to a simple laminine-polyornithine growing substratum on coated plastic.

Cultures of motor neurons represent a reliable tool to evaluate, at the single cell level, the action of different stimuli that have been postulated to be involved in ALS aetiopathogenesis.

4.2 Primary cultures of motor neurons and ALS-associated toxicity

4.2.1 Cu/Zn SOD1 mutation and Fas-L activation

The cell signalling induced by coupling of Fas-L to their receptors was deeply studied in control motor neurons and in motor neurons transfected with different missense mutation of human SOD-1 gene [Raoul, 2002].

In this study soluble oligomerised Fas-L or an agonistic anti-Fas antibody were administered, both in normal and in hSOD-1 transfected cultures. This study was carried to detect whether and how the intracellular death domain associated to Fas-L, was able to engage the upstream cascade leading to apoptotic activation either in the absence of an additive excitotoxic exposure or trophic deprivation. Interestingly, it has been shown that lethal Fas-L associated signalling pathway required transcriptional upregulation of neuronal nitric oxide synthase (nNOS) as well as the interaction of several proteins (Daxx, ASK1 and p38). The authors also elucidated that the mechanisms inducing nNOS transcription is finely tuned by p38 activity and that p38 (a kinase that is recently reported to be overexpressed in the ventral horns of h SOD-1 G93A

transgenic mice [Tortarolo, 2003]) plays a crucial role in enhancing the production of nitric oxide. Moreover the authors measured the toxicity produced by Fas-L administration in motor neurons overexpressing SOD-1 mutated gene compared to that in motor neurons overexpressing the wild-type form of SOD-1 human gene. They found that the rate of survival in "SOD-1 mutated motor neurons" was significantly lower compared "wild-type SOD-1 motor neurons". This result confirmed that mutant SOD-1 gene expression significantly enhanced the Fas-mediated motor neuron vulnerability. Moreover, they first produced direct evidence about the role of hSOD-1 mutated protein in the extrinsic apoptotic pathway involving TNF receptor family. A scheme showing the intracellular cascade of events produced by Fas-L in "SOD-1 mutated motor neurons" is reported in figure 4.1.

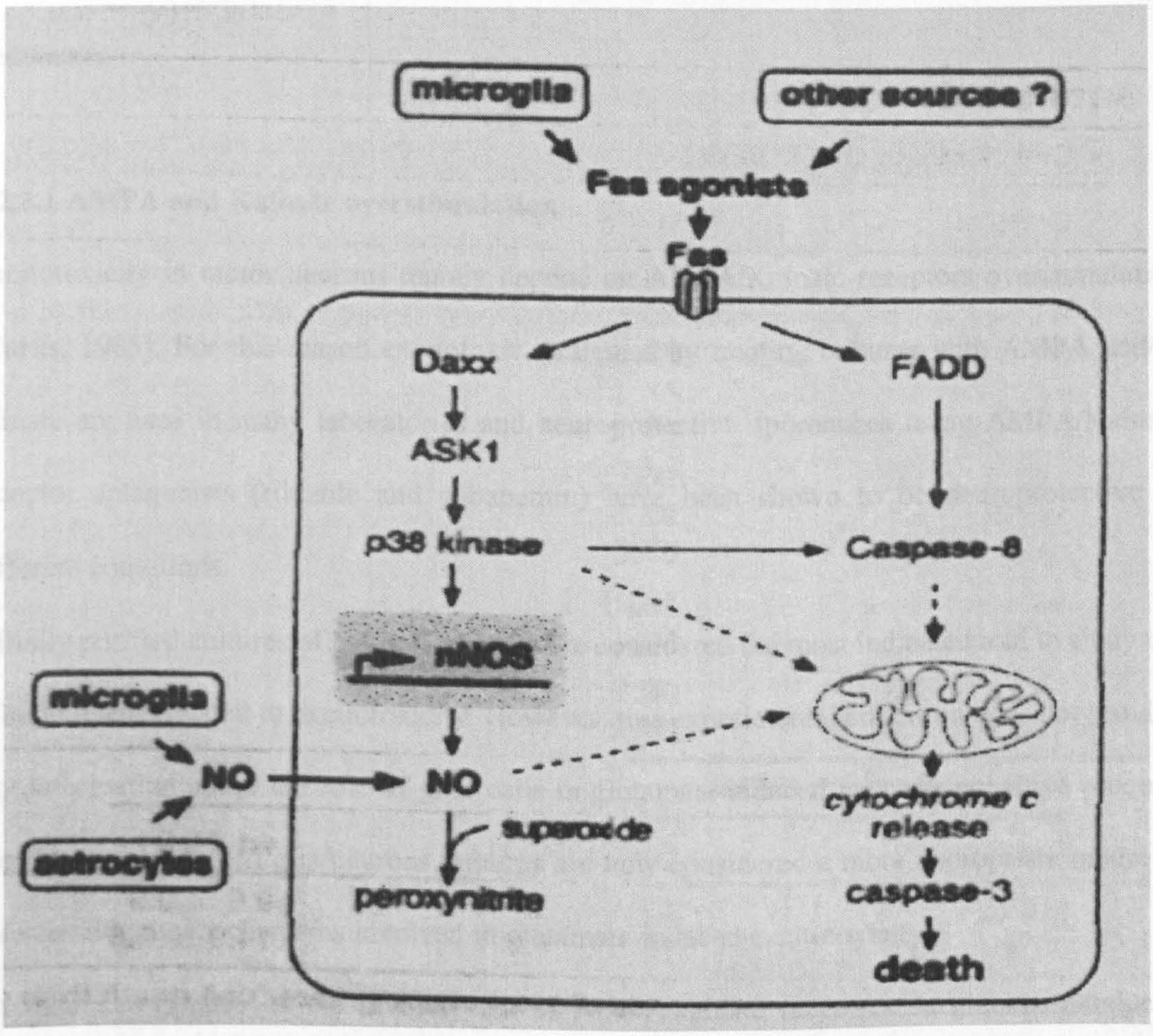

Figure 4.1 A non cell-autonomous death pathway can be triggered by different detrimental stimuli. The overexpression in motor neurons of mutant SOD1 enhances the toxicity of NO and FAS ligand exposure. Moreover, upon this stimulation, astrocytes and microglial cells represent a further source of damage for motor neurons (From Raoul, C., et al., *Motoneuron death*

triggered by a specific pathway downstream of Fas. potentiation by ALS-linked SOD1 mutations. Neuron, 2002. 35(6): p. 1067-83.)

4.2.2 Glutamate-induced excitotoxicity

The role played by different components of glutamate-induced excitotoxicity, such as glutamate receptors, glial glutamate transporters, alteration in glutamate metabolism, has been extensively investigated both in ALS patients and in different animal models of ALS. However, to better understand the cellular and molecular mechanisms involved in glutamate-induced motor neuronal vulnerability, *in vitro* studies are required.

Cultures of neurons greatly contribute in understanding the role of glutamatergic neurotoxicity and represent a reliable approach to evaluating the effectiveness of several pharmacological treatments.

4.2.2.1 AMPA and Kainate overstimulation

Excitotoxicity in motor neurons mainly depend on AMPA/Kainate receptors overstimulation [Curtis, 1985]. For this reason excitotoxic strategies by treating cultures with AMPA and/or kainate are used in many laboratories and neuroprotective approaches using AMPA/Kainate receptor antagonists (riluzole and gabapentin) have been shown to be neuroprotective in different conditions.

Initially purified cultures of motor neurons were considered the most indicated tool to study the cellular events related to excitotoxicity. However, this experimental condition does not provide any information about the role of glial cells in glutamate-induced neurodegenerative process. For this reason, mixed glia/neurons cultures are now considered a more appropriate model to investigating the mechanisms involved in glutamate-induced excitotoxicity.

An indirect evidence of the involvement of AMPA/kainate receptors in glutamate-induced neuronal death was reported in the rat neurons cultures exposed to ALS patients cerebrospinal fluid [Couratier, 1993]. In this study it was observed that the neuronal toxicity produced by cerebrospinal fluid of ALS patients was prevented by treating the cells with 6-cyano-7-

nitroquinoxaline-2,3-dione (CNQX), a selective antagonist to AMPA/kainate. Contrary to NMDA receptor antagonists, CNQX produced a neuroprotective effect by significantly reducing the percentage of death.

Carriedo [Carriedo, 1995;Carriedo, 1996] first reported that: I) embryo cultures of motor neurons are selectively vulnerable to AMPA/kainate receptor-mediated injury and; II) the *in vitro* kainate injury is dependent on the influx of Ca^{++}. Motor neurons were preferentially injured by brief (40 min) kainate exposure, but not by NMDA exposure and; III) Ca^{++} removal from the media, during a brief kainate exposure, reduced the toxic effect by maintaining a high percentage of motor neurons with large cellular body and a marked SMI-32 immunopositivity. On the contrary, at the same doses of kainate, the raising of extracellular Ca^{++} caused higher motor neurons susceptibility.

By hystochemical techniques, based on kainate-stimulated uptake of Co^{++} [Pruss, 1991], it was observed that a high percentage of these neurons (about 80%) posses Ca^{++} permeable AMPA/kainate receptors. This evidence suggests that a rapid Ca^{++} entry through Ca^{++}-permeable AMPA/kainate channels makes motor neurons more vulnerable than other types of spinal neurons to excitotoxicity.

4.2.2.2 Ca^{++} influx and GluR 2 subunit

Several experiments were performed to evaluate the vulnerability of motor neurons exposed to AMPA/kainate compared to other spinal cord neurons. In these studies the role of AMPA/kainate receptors in motor neurons and in dorsal horn neurons was widely investigated. It was found that 20 minutes of kainate administration produces a dose dependent reduction of motor neurons survival but did not decrease dorsal horn neuron survival. Moreover it was also reported that this selective toxicity is dependent on $[Ca^{++}]_{out}$ and is completely inhibited by the specific AMPA antagonist LY300164 and by Joro spider toxin, a selective blocker of AMPAr lacking of the edited GluR2 subunit.

It has been widely demonstrated that different neuronal cell types can diverge in GluR2 expression, in the rate of GluR2 editing and in the desensitisation properties of their AMPAr.

These differences may be related to the selective vulnerability of motor neurons that occurs in ALS [Van Den Bosch, 2000;Vandenberghe, 2000].

Although GluR2 immunopositivity was observed in almost all motor neurons, double-staining experiments demonstrated that GluR2 positive motor neurons were also positive to Co^{++} uptake and sensitive to kainate stimulation. This result indicated that, despite the abundant expression of GluR2, a subset of AMPAr lack of the GluR2 subunit and they are therefore Ca^{++} permeable. The relative Ca^{++} permeability of AMPAr and the amount in GluR2 was measured by combining whole-cell patch-clamp electrophysiology and single cell RT-PCR and compared between motor neurons and dorsal horn neurons. GluR2 resulted almost completely edited in both group of neurons. In addition, electrophysiological measurements did not reveal differences from motor neurons and dorsal horn neurons in terms of Ca^{++} conductance, kinetics of AMPAr desensitisation, receptor deactivation, and open channel probability. However, when the density of functional AMPAr in the whole membrane was measured, the amplitude of AMPAr current density (AMPAr current/cell capacitance) was 2.5 higher in motor neurons than in dorsal neurons. Finally the authors also demonstrated that AMPAr are responsible for the kainate induced inward Ca^{++} currents.

These results suggested that the high Ca^{++} current density passing through AMPAr might be responsible for the selective kainate-induced excitotoxicity observed in motor neurons.

To better understand the link between the glutamate dependent Ca^{++} influx and the excitotoxic mechanism proposed in ALS, a series of experiments with a more prolonged time of kainate exposure were performed. By treating motor neurons for 24 hours with low doses of kainate (5 to 20 times lower than in acute treatment) a selective loss of SMI32 positive motor neurons with a little or no damage in the other spinal neuronal populations was observed [Carriedo, 1996]. Consistently with previous studies in spinal cord slices [Rothstein, 1993], the toxicity seemed to be mediated primarily through activation of AMPA/Kainate receptors, rather than NMDAr, as demonstrated by the evidence that the 2,3-dioxo-6-nitro-1,2,3,4,-tetrahydrobenzo[f]quinoxaline-7-sulfonamide (NBQX), a selective AMPAr antagonist, was

fully protective whereas (+)-5-methyl-10,11-dihydro-5H-dibenzo(a,d)cyclopheten-5, 10-imine maleate (MK801), a compound that inhibits the NMDAr activity, was ineffective.

4.2.2.3 The role of astrocytes

Glial cells can extend the damage produced by glutamate agonists by increasing the stimulation of postsynaptic receptors and the consequent Ca^{++} wave. This assumption was confirmed by the evidence that neuronal vulnerability to kainate was two- to three-fold higher in co-cultures than in monoculture, and that this value increased by prolonging the time in co-culture. The increase in neuronal kainate vulnerability with time in co-culture was associated to a marked rise in the proportion of co cultured neurons expressing Ca^{++}-permeable AMPA/kainate receptors, as determined by kainate-activated Co^{++}-uptake. Neurons in monoculture had no kainate-activated Co^{++}-uptake. Neurons were immunoreactive to specific antibodies against the AMPAr subunits GluR1 and GluR2 both in monoculture and co-culture. This study indicated that motor neuron differentiation in glia/neurons cultures is associated with an increased vulnerability to kainate and increased expression of Ca^{++}-permeable AMPA/kainate receptors. In this paradigm glial cells support basal survival and differentiation of neurons, but potentiate kainate-induced neuronal death [Comoletti, 2001].

In addition, astrocytes express a large number of receptors for neurotransmitter, including functional AMPA/kainate receptors and metabotropic GluRs. Accumulating evidence indicates that such receptors may be a target for the glutamate released from the presynaptic terminals [Porter, 1992]. This evidence strongly supports the view that glutamate not only stimulates postsynaptic receptors but can also activate receptors located on the nearby astrocyte membranes. In two studies performed in mixed glia/neuron cultures the authors independently observed that $[Ca^{++}]_i$ elevations induced in astrocytes were followed by $[Ca^{++}]_i$ elevations in the neighbouring neurons [Parpura, 1994]. Moreover, excitation of neurons following the passage of calcium waves in neighbouring astrocytes was observed to be reduced by administration of glutamate receptor antagonists [Hassinger, 1995].

These studies indicate that: I) glutamate-stimulated activity can trigger $[Ca^{++}]_i$ increase in astrocytes and; II) $[Ca^{++}]_i$ elevations in astrocytes can start signalling to neurons. Thus, the neuronal calcium response comprised an indirect component mediated by glutamate, most likely released from the astrocytes [Pasti, 1997]. The possible role of astrocytes in enhancing motor neurons toxicity exposed to excitotoxins can be further reinforced by the direct demonstration that astrocytes release glutamate in response to stimulation of mGluRs and, more efficiently, in response to coincident stimulation of mGluRs and AMPA/kainate glutamate receptors [Bezzi, 1998].

4.2.3 Free radical exposure

Oxidative stress has been frequently associated to motor neuron degeneration. The experiments performed in purified cultures of motor neurons have shown that these cells are vulnerable to physiological oxidants. Treatments with radical-generating systems showed that motor neurons chronically exposed to low levels of oxidative stress die by apoptosis. By increasing the doses of oxidants, apoptogenic factors are still able to induce the upstream events of apoptosis but often, during the propagation of apoptotic pathway, the cells undergo a sudden decay of ATP levels, and die before apoptotic pathway is ended. Depending on the rate of oxidation it is possible to observe a mixed condition in which the characteristic of both apoptosis (shrunken nucleus, cleavage of caspases) and necrosis (membrane disintegration, leaky cells) are combined. When cells are depleted of energy, they die necrotically and when their energy supply is normal and mitochondrial function is undisturbed, they can finish the time- and energy- consuming process of apoptosis.

The exposure of motor neurons to a substance that slowly releases nitric oxide (NO) is a more subtle way to expose motor neurons to free radicals [Kaal, 1997]. Under oxidative stress NO, that in physiological condition acts as neurotransmitter and neuromodulator agent, can react with superoxide to form an aggressive oxidant, the peroxinitrite [Beckman, 1996]. NO, possibly through peroxinitrite, is thought to play a role in ALS pathology [Beckman, 1993].

The role of oxidative stress on motor neuron degeneration is under investigation in mixed glia/neurons cultures, also because many authors have postulated that the detrimental action of oxidative stress in ALS patients may be amplified by glial activation. To better understand the link between astrogliosis and oxidative stress, a series of experiments were carried out. Cassina [Cassina, 2002] reported that the exposure of spinal cord astrocyte monolayers to peroxynitrite causes a sustained process of reactive gliosis and that furthermore promotes apoptosis of embryonic motor neurons subsequently plated on that monolayer. Interestingly, motor neuron death was largely prevented by NOS inhibitors and peroxynitrite scavengers but not by trophic factors that otherwise support motor neuron survival in the absence of astrocytes.

The role of glial cells in exacerbating the effects of NO was also reported by Comoletti et al. [Comoletti, 2001]. They observed that nitric oxide produced from glial cells increased the glutamate-induced toxicity and that the application of a nitric oxide synthase inhibitor, the nomega-nitro- l-arginine methyl ester (L-NAME), significantly reduced the percentage of motor neurons death in mixed glia/neurons cultures.

4.2.4 Mitochondrial inhibition

Evidence is increasing that mitochondrial dysfunction is involved in ALS pathogensis (see section 1.2.2.3).

Since mitochondria represent a preferential target for a plethora of toxic stimuli is quite impossible, by performing *in vivo* studies, to establish whether mitochondrial alterations represented a cause or an effect of an earlier defect. For this reason *in vitro* studies are a reliable strategy to evaluate the effects produced by direct alterations of mitochondria in motor neurons activity and viability.

To study the role of mitochondrial dysfunction an *in vitro* model of chronic motor neuron toxicity, based on malonate-induced inhibition of complex II in the mitochondrial ETC chain, was developed. Mitochondrial inhibition has been shown to be highly toxic both for motor neurons and for dorsal horn neurons. Mitochondrial inhibition was further reproduced inhibiting the complex IV by sodium azide. The results, obtained by inhibiting complex IV were similar to those obtained by inhibiting the complex II: in both conditions motor neuronal death occurred by apoptosis. In this model of mitochondrial dysfunction, several molecules were tested. It has been reported that the free radical scavenger alpha-phenyl-N-tert-butylnitrone, the AMPA/kainate receptor antagonist CNQX significantly reduced motor neuron death induced by malonate [Kaal, 1999].

4.2.5 Protcasome inhibition

Recently, proteasome inhibition has been suggested to be a possible contributor in ALS aetiopathogenesis and the effect of two proteasome inhibitors, lactacystin and epoxomicin, was

investigated on cultured spinal cord neurons [Kikuchi, 2002]. The incubation of proteasome inhibitors in cultures of spinal cord neurons induced neurotoxicity in a dose-dependent manner and that motor neurons were more vulnerable than the other spinal neurons. Morphological studies revealed that motor neurons treated with proteasome inhibitors showed cell bodies with the cytoplasm markedly altered and presenting a characteristic granular pattern. Moreover, proteasome-induced neurotoxicity has been accompanied with apoptotic nuclear changes, post-translational modification of cellular proteins, generation of intracellular free radicals, reduction in the amount of reduced glutathione, and mitochondrial dysfunction. Interestingly, the neurotoxic effect was reduced by the administration of low concentration of geranylgeranylacetone (GGA), which is widely used as an antiulcer drug. GGA was found to induce the expression of heat shock protein 70 as well as thioredoxin, which may partly contribute to the protective effect of GGA. These data suggest that the inhibition of proteasome may play a role in the mechanism of neurodegenerative processes leading to the motor neuron loss.

4.2.6 Neurotrophic factors withdrawal

Purified cultures of motor neurons represent a valid target to evaluate the effectiveness of many pharmaceutical strategies and to understand molecular alterations elicited in response to a perturbation of the environmental conditions such as a decrease in neurotrophic factors concentration. Extensive studies were performed on purified cultures of motor neurons in order to better clarify the mechanism of action played by endogenous neurotrophic factors, such as NGF, BDNF, NT-4, CNTF, and also to test different drugs reported to have a protective and neurotrophic effect in *in vivo* models.

4.2.6.1 BDNF

Henderson et al. [Henderson, 1993] reported that isolated motor neurons are very sensitive to BDNF and NT-4, and their withdrawal induces apoptosis [Kaal, 1997]. Further experiments indicated that motor neurons in mixed glia/neurons cultures are less vulnerable to BDNF deprivation [Comoletti, 2001], likely because of the neurotrophic supply provided by astrocytes, which express and release the glial derived neurotrophic factor (GDNF).

Neurotrophins, such as BDNF and NT-4, cannot replace muscle extract but in the presence of muscle extract they have a significant effect on survival preventing apoptotic cell death.

Although the survival promoting action of BDNF and other neurotrophins has been adequately demonstrated (see section 2.2.2.1), the molecular mechanisms that are involved in their anti-apoptotic action are not yet completely elucidated.

In a recent study in chick embryo spinal cord motor neurons, in which BDNF promotes cell survival, the intracellular pathways that may be involved in the BDNF-induced motor neurons survival was accurately analyzed [Dolcet, 1999]. The authors reported that, downstream the binding to its receptors, BDNF activated the extracellular-regulated kinase (ERK), mitogen-activated protein (MAP) kinase and the PI_3K pathways. To examine the contribution of these pathways on the survival they treated cultures of motor neurons in presence of BDNF with PD 98059, a specific inhibitor of MAP kinase, and LY 294002, a selective inhibitor of PI_3K. PD 98059, at doses that significantly reduced the phosphorylation of ERKs, did not show any

prominent effect on neuronal survival. However, LY 294002 at the dose that inhibited the phosphorylation of Akt, a down-stream element of the PI_3K, completely abolished the motor neuron survival effects of BDNF. This result confirmed that the PI_3K associated pathway plays an important role on the cell survival and that the tonic stimulation provided by BDNF is required to avoiding the activation of specific apoptotic pathways.

4.2.6.2 CNTF

In addition to the role played by BDNF, GDNF and NT3-4, in the last few years the link between CNTF and motor neurons survival has been exploited by different authors both *in vitro* and *in vivo* studies [Magal, 1991;Ikeda, 1995].

CNTF treatment in astrocytes increases their ability to increase the number of ChAT positive neurons in ventral spinal cord more than twofold compared to untreated astrocytes [Albrecht, 2002]. The correlation between neurotrophic factors and ChAT expression in cultures of motor neurons was then confirmed by the results obtained in our laboratory by acetyl-L-carnitine (ALCAR) treatment [Bigini, 2002]. In mixed glia/neurons cultures we observed that ALCAR markedly increased both ChAT and Trk-B immunostaining. We hypothesized that the increase in ChAT immunoreactivity observed after ALCAR treatment, was not due to maintenance of physiological levels of ChAT, but was likely related to a neurotrophic-like response. It has been in fact reported that the stimulation of tyrosine kinase receptors and activation of the microtubular associated protein kinase (MAPK) cascade causes extensive phosphorylation and activation of the cAMP response element (CRE), in a region involved in the activation of ChAT gene transcription (cholinergic locus in rats) [Ginty, 1994].

CHAPTER 5

THE WOBBLER MOUSE

5.1 Genetic

Although many efforts have being done for several years to elucidate the symptomatological and neuropathological hallmarks of wobbler motor neuron degenerative process, the genetic component associated to this disease is still unknown and since 1992, the year of the mapping of locus wr, few progresses have been done in this field of research [Kaupmann, 1992].

Falconer provided the first important genetic evidence. Based on statistical analysis of the wobbler strain progeny, he showed that the mutated gene responsible for the disease is autosomal, recessive and apparently unique. Moreover, it was been reported that the wobbler karyotype did not reveal any visible sign of chromosomal deletion or translocation [Andrews, 1974]. Twelve years ago Kaupman first individuated that the mutation linked to wobbler mouse disease is localized on a proximal region of chromosome 11; this region was identified as "wr locus". Later on, it has been also reported that the region of interest, identified by recombination, covers 4 MB and presents a conversed synteny on human chromosome 2p13-14 [Kaupmann, 1992;Resch, 1998]. The genes localized in the wr locus correspond to *Ugp2* which in humans encodes a muscle isoform of UDP-glucose phosphorylase, *peli1* that is believed to be an adaptor protein in different cellular pathways, *Otx1* a homeobox gene involved in the control of brain development, *Hcc8* identified as hepatocellular carcinoma antigen, *Mor2* which encodes cytoplasmic malate dehydrogenase and three others genes, *Homoloc13*, *Kiaa0903* and *Homoloc2*, which functions are still unknown [Wedemeyer, 1996;Fuchs, 2002].

The level of the transcripts of these genes was measured and no differences were reported from wobbler mice and healthy littermates [Korthaus, 1996]. In addition a knockout mouse for Otx1 expressed an epileptic phenotype likely unrelated to the wobbler motor neuron disease.

In order to investigate a potential candidate mutation in a gene located to proximal region of "wr locus" on chromosome 11, we have recently collaborated with a group of genetists from Edinbourgh University. The gene investigated is a gene corresponding to the Slc1a4 / ASCT1 (Alanine, Serine, Cysteine, Threonine transporter 1) and it is another member of the glutamate transporter family. In humans it is positioned in a region which maps to 2p14, and this is a region of conserved synteny with the wr locus on mouse chromosome 11. We have successfully extracted DNA and RNA from the wobbler and control tissues, and we have measured their expression using RT-PCR analysis. We found that Slc1a4 / ASCT1 is expressed at similar levels (at the RNA level at least) in both wobbler and age matched healthy mice. Then we sequenced the coding region, in case there was a more subtle mutation, but we did not find any difference between wobbler and healthy mice (Newberry and Bigini 2002 unpublished).

These results raised the possibility that the wobbler mutation involves a noncoding sequence that could be localized up-stream the wr locus.

Although the genetic alteration responsible for the wobbler mouse disease has not yet been identified, it is possible to individuate homozygous wobbler mice. In fact, by exploiting previous observations reporting an inner strain polymorphism between mouse strains new Zeeland black NZB mice and C57BL/6 at the *Gln-ps1* locus [Augustin, 1997], pre-symptomatic diagnosis can be easily performed by genotyping assay [Rathke-Hartlieb, 1999].

5.2 Symptoms

A detailed and still convincing description of the neurological symptoms characterizing the wobbler mouse disease was done by Duchen and Strich over thirty years ago [Duchen, 1968]. In that study they observed that clinical symptoms are mainly related to the loss of cervical spinal cord and, to a lesser extent, of brainstem motor neurons. In spite of the early onset and the rapid symptoms progression it is possible to divide the clinical evolution of the wobbler neurological syndrome into three phases.

The presymptomatic phase comprises the first three weeks of postnatal life. Around that period the animals that carry the mutation do not show any difference on phenotype compared to

healthy littermates, and no clinical signs were recorded. This phase is then followed by a rapid worsening, this evolutionary stage lasts from third/fourth to twelfth week of age and produces a relevant deficit in motor activity accompanied by a marked muscular atrophy and a loss of weight of forelimb muscles [Duchen, 1968].

The third phase is characterized by a stabilization of symptoms and is identified as plateau stage. During this phase a sustained loss of motor neurons is not observed, also because the sub-population of motor neurons selectively involved in this degenerative process, such as the cervical spinal motor neurons, are already almost completely disappeared. At the beginning of the plateau stage the volume of the spinal cord in affected mice is halved compared to healthy littermates. This reduction involves both the dorsal and the ventral horns and appears more a result of cell loss, than a side effect of the impaired growth. Indeed, 3 week-old wobbler mice are often already smaller than their healthy littermates, although the volume of their spinal cord is not yet changed [Boillee, 2001;Bose, 1999].

Despite its denomination, the presymptomatic phase may correspond to a subtle alteration of motor functions. For example in the strain used in my thesis, the NFR/wr line, an abnormality in the righting reflex at three to seven postnatal days of age and an impaired performance during grid walking are reported [Bose, 1999;Bose, 1998]. Although neuropathological alterations are widely described at the presymptomatic stage, no clinical signs are observed prior to the 3rd week of age.

From 3rd week of age, wobbler mice begin to growth slower than healthy littermates and, only a week later, they are 40-50% (also depending on the strain) smaller that their age-matched control mice. At the 3rd/4th week wobbler mice already show an altered position of fingers, wrists and paws. This alteration derives from muscular atrophy and produces unsteady gait with a discrete tremor. Afterwards, instability and wobbling of the gait develop progressively thus producing alteration in walking that is a typical feature of motor impairment occurring in the wobbler mice. As previously proposed by Kozachuk and colleagues, these two parameters of abnormalities can be useful to determine the degree of clinical worsening during this phase of the disease [Kozachuk, 1987].

Although the tension in the forelimbs of wobbler mice, recorded by electromyography, becomes lower at the 3rd week, muscular strength is unchanged compared to healthy mice until 4th week of age [Rathke-Hartlieb, 1999;Smith, 1995]. Later on muscular strength rapidly decreases in the following weeks instead of increasing as in control mice [Ikeda, 1995]. In the NFR strain, at around the 11th/12th week of age, wobbler mice have reduced their grip strength scores by about 90% passing from ~20 grams to ~2,0 grams. A progressive decay in the muscular strength of the neck and the head was also reported, on the contrary, the hind legs' muscles remain spared over this period. At the end of this phase, in three month-old wobbler mice, the electromyography recordings of the forelimbs muscles displays characteristics of muscular denervation. In contrast the hind limb muscles are eletromyographically unaffected [Andrews, 1974]. In the late stage of the disease no remarkable alterations in hind legs muscles, diaphragm muscle, muscles deputed to deglutition and mastication are reported. This evidence suggests that, in contrast to human condition, the decease in wobbler mice does not seem strictly related to a primary motor neuronal involvement.

Almost all affected animals follow the pattern of symptoms evolution reported above; however, few animals exhibit a sudden dramatic worsening of symptoms leading to the death within the fourth-fifth week of life.

Although the wobbler mice are first known for their neurological symptoms, the males also suffer from infertility [Heimann, 1991]. Wobbler males are unable to reproduce, despite the normal morphology of their genital apparatus and normal levels of gonadal testosterone due to altered spermatozoa functional motility. In females pregnancy was never reported; however direct evidence explaining the origin of this infertility has not yet been described. The wobbler mutation may affect the female gametogenesis, but it is also possible that the mind retardation and the muscular weakness of mutants are the cause of a deficiency in mating.

5.3 Neuropathological and hystopathological alterations

5.3.1 Motor neurons

5.3.1.1 Hystometry and hystology

As mentioned before, the polymorphic marker close to the *wr* locus offers the opportunity of a preclinical diagnosis and consequently allows to investigating about the possible morphological alterations before the onset of the disease in the wobbler mice. To date few studies have been reported by exploiting genotyping assay. A morphometric analysis of cervical spinal cord motor neurons (C5-T3) in wobbler and healthy littermates from P10 to P40 showed that: I) vacuolar degeneration is present in wobbler mice at just before clinical symptoms in about 10% of motor neurons, moreover some interneurons also present vacuolar degeneration; II) no difference in motor neuron size is detectable till 2^{nd} week of age while a significant increase in dimension appears from 2^{nd} to 3^{rd} week age (interestingly, in the following weeks, the motor neurons of healthy mice increased their size while the motor neurons of wobbler mice reduces their cell body); III) over the 3^{rd} week of age the size distribution of neurons in healthy mice presents a major peak at around 160 μm^2 and a second one around 350 μm^2, corresponding to the appearance of large motor neurons. Motor neurons size distribution in age matched wobbler mice has a major peak at around 100μm^2. In contrast, a minor peak at around 300 μm^2 (that can be observed in two weeks old wobbler mice) has disappeared after the 2^{nd} week of life.

The authors concluded that the loss or absence of differentiation of this particular sub-population of large motor neurons, could represent a key event in the course of the disease and could have important consequences for the clinical progression observed in the wobbler mouse. However, since in wobbler mice spinal cord the cervical region is selectively interested by the pathology while thoracic and lumbar motor neurons are spared [Duchen, 1968;Bradley, 1982], the choice to evaluate a such a caudal tract (C5-T3) in this study is somewhat questionable.

Although the preclinical diagnosis by genotyping is a recent discovery, many hystological and molecular studies in presymptomatic wobbler mice, particularly in the cervical spinal cord region, have been already reported since the early 80s [Mitsumoto, 1982].

Cytoplasmatic vacuolization is the more relevant marker in degenerating motor neurons of wobbler mice. However, this typical feature is rare in the spinal motor neurons prior the evolutionary phase of the disease [Duchen, 1968;Andrews, 1974]. During the presymptomatic stage, morphological alterations of neurons are less evident. An enlarged soma and a weak positivity for Nissl staining primarily characterizes affected motor neurons. Stereological measurements have confirmed the enlargement of perikaryon in the cervical spinal cord of P18-to P 22-old wobbler mice [Dockery, 1997]. At this stage, cells with diverse anomalies have also been reported in the brainstem, in the ventral reticular magnocellular nucleus, and in the motor nuclei of the cranial nerve V and VII. In contrast, abnormal neurons were rarely found in the red nucleus, substantia nigra, anterior posterior colliculi, and deep nuclei of the cerebellum. Sporadic degenerating neurons characterized by a reduced Nissl staining or chromatolysis have been also described in thalamic nuclei that belong to the extrapyramidal system and in brainstem at two week of age [Rathke-Hartlieb, 1999]. No abnormalities were reported at this stage in the cerebral cortex [Duchen, 1968].

Despite these morphological changes, the number of motor neurons in the cervical spinal cord of three week-old wobbler did not result significantly lower compared to healthy littermates [Blondet, 2002].

The progressive loss of motor neurons starts during at around the 4^{th} week of life in concomitance with the appearance of symptoms, and characterizes the evolution of the disease. In the cervical region of affected mice, a massive loss of motor neurons (about 50%) is reported from the 3^{rd} to the $6/7^{th}$ week of age [Duchen, 1968;Haenggeli, 2002;Mitsumoto, 1982]. Within the cervical spinal cord, the number of degenerating motor neurons varies according to the segment, the rostral (C1-C3) region is the most severely affected, but at all times, cervical motor neurons displayed the same trend of neurodegeneration [Junier, 1994].

Using a retrograde labeling of the median nerve motor neurons it has been observed that about 50% of the motor neurons area disappeared in six weeks old mice [Pollin, 1990] and a measurement performed in the abducens nucleus revealed a 31% of motor neuron loss in wobbler mice at 4-5 weeks of age compared to healthy littermates.

Although the loss of cervical motor neuron is the most striking marker of neurodgeneration in the wobbler mouse, other subpopulations of motor neurons are affected. In the abducens nucleus, degenerating motor neurons displayed a loss of Nissl staining in cell bodies but were rarely vacuolated [LaVail, 1987]. In the motor nuclei of the brainstem the extent of motor neuron loss is much less important than in the cervical spinal cord. In the facial motor nucleus, only 15% of motor neurons have disappeared in 5 week-old wobbler mice [Coulpier, 1996].

The measurement of motor neurons was performed in cranial nuclei of wobbler mice at two stages of the disease, at the presymptomatic phase (P21), and an intermediate phase of the disease (6 weeks of age). A significant decrease of hypoglossal motor neurons was reported both in early symptomatic (25%) and in 6 week-old wobbler mice (28%) compared to age-matched control mice. A decrease of trigeminal motor neurons number (13 %) was observed in the symptomatic phase [Haenggeli, 2002].

During the progression of symptoms, features of degeneration, other than vacuoles, were observed both in spinal and in cortical motor neurons.

5.3.1.2 Cytology

The characteristics of affected motor neurons in the wobbler mice are atypical. Vacuoles earliest appear in the cell body and become increasingly large and numerous until they completely pervade the soma [Duchen, 1968]. Their composition is not yet determined; they are not electron-dense but result empty. Moreover other ultrastuctural alterations like the presence of tubular structures and an increased number of lysosomes are detectable in affected motor neurons [Andrews, 1974;Biscoe, 1982].

Some vacuolated motor neurons can be still found in aged wobbler mice, but the frequency is very low [Duchen, 1968;Junier, 1994].

Large and medium-sized motor neurons in "stabilized" wobbler mice (4 to 6 months of age) showed a modified neurite arborization, characterized by shorter and thinner dendrites and a reduction in the density of the dendritic spines.

5.3.2 Axons

Two weeks after the birth, cervical ventral-roots nerves and the mean axons number in the median and ulnar nerves, the nerves that are later most severely interested to denervation, are similar in wobbler mice and in control littermates [Mitsumoto, 1982]. At the 3rd week of age some intramuscular nerve trunks contain fragmented axons, and many pre-terminal axons present a fine sprouting and innervate more than one muscle fiber but first degenerating myelinated fibers appear only at the end of third week of age. The absence of an early axonal alteration indicates that the wobbler motor neuron degeneration primarily affects the perikaryon of motor neurons (primary neuropathy) and that the axonal alteration is delayed compared to the cell body degeneration (secondary axonopathy) [Mitsumoto, 1982].

At the beginning of the symptomatic stage, when alterations of perykaria are evident, morphological alteration of axons, described at the presymptomatic stage, become amplified. The thin, beaded axons sprout and the number of motor nerve terminals are lowered [Mitsumoto, 1990;Duchen, 1968]. The number of large-diameter fibers is greatly reduced and this process of axonal alteration is maintained over the entire period of symptoms progression [Lewkowicz, 1979]. Signs of axonal degeneration are also reported to be associated with a reduced diameter of the myelin sheaths and even a loss of myelin leading to the presence of non-myelinated fibers of large diameter.

In contrast, by experiments of quantitative hystomorphometry, we have observed that in median nerve of twelve week-old wobbler mice, corresponding to the end of the clinical progression, no significant reduction in the thickness of myelin sheaths fiber was found. Although a significant decrease in the total number of myelinated fibers (49%), a higher percentage of altered myelinated fibers and a marked reduction of the myelinated fiber area (65%), were seen. This result suggests that, in spite of a relevant process of axonal degeneration, demyelinaton does not seem a feature of wobbler motor neuron disease (Bigini and De Angelis 2000 unpublished).

The morphological abnormalities observed in the axons originating from cervical spinal cord motor neurons are always accompanied by an alteration of axonal transport system, likely

related to the accumulation of abnormal neurofilaments already observed in the presymptomatic period. At the symptomatic phase the amount of proteins transported by slow axonal transport, fast anterograde transport and slows retrograde transport is notably reduced [Mitsumoto, 1990]. In spite of these apparent abnormalities, the axons maintain their regenerative properties in response to a crush or a cut, thus showing a slower and less effective process than in healthy mice [Mitsumoto, 1985]. Axonal collateral sprouting is often observed and could partially compensate for the functional consequences of the neuronal loss [Blondet, 1992;Duchen, 1968].

5.3.3 Muscles

Changes in the muscle structure are not detectable in the presymptomatic. The atrophy occurs in the same progressive manner as motor neuron degeneration. Atrophy is particularly relevant in muscles of the head, neck, shoulders and forelimbs. The muscles of the proximal portion of the forelimb, particularly biceps muscles, are more severely affected than those located in the distal position. On the other hand, the trunk and hind legs muscles are not affected [Blondet, 1992;Duchen, 1968].

In symptomatic wobbler mice the weight of the injured muscles is decreased, as well as the total number of muscle fibers [LaVail, 1987]. Atrophied muscle are first located at the periphery of the muscle fascicles, and gradually form clusters of abnormal fibers. These abnormalities of muscle fibers are characterized by a reduction in their diameter, an enlargement of sarcolemmal nuclei with prominent nucleoli often located in the central position and a reduction in the length of the post-junctional membrane [Mitsumoto, 1982].

The muscles of symptomatic wobbler mice display a mixture of normal and affected areas, the size of the muscle fibers and end plates are significantly decreased and this reduction cannot be exclusively related to the reduced rate of growth that occurs during the evolutionary phase [Mitsumoto, 1996;Lewkowicz, 1979]. Alterations of neuromuscular synapses have been detected during both the evolutionary phase and the phase of plateau, after the 12^{th} week of age. At the end of the progression of symptoms, about 90% of the neuromuscular junctions

proximally connected to cervical motor neurons are deprived of the neuronal-cell adhesion molecule (N-CAM) and have a reduced acetylcholine esterase activity [Yung, 1994].

5.4 Pathological events and aetiology

5.4.1 Glutamate-induced excitotoxicity

As previously discussed, astrocytes play a fundamental role for the maintenance of glutamate extracellular levels under a toxic threshold in many areas of CNS [Danbolt, 2001 #469], and an excitotoxic effect due to a defective activity of the main glial glutamate transporters has been repeatedly considered as one of the most relevant components of various degenerative processes both in human and in animas [Rothstein, 1994;Cleveland, 2001].

In cultures of astrocytes obtained from the cervical spinal cord of 4 week-old wobbler mice higher levels of glutamate and glutamine were found in the extracellular medium. These abnormalities were accompanied by decreased intracellular levels of glutamate. Since this imbalance was demonstrated to be reversed by manipulation of glutamine concentration in the medium, the authors concluded that a deficit in the system of conversion glutamate/glutamine might play an important role in glial glutamate transporters activity and therefore in the glutamate-induced excitotoxity [Ait-Ikhlef, 2000].

Although astrocytosis in the cervical spinal cord of wobbler mice has been reported to involve selectively a population of astrocytes which is glutamine synthetase-negative, this abnormality in astroglial metabolism has not yet been confirmed by other *in vivo* studies. In addition, in the cervical spinal cord of symptomatic wobbler mice, the density of glutamate-binding sites, measured by experiments of autoradiography, was unaltered [Krieger, 1991].

To date, this body of evidence neither confirm nor confute the possible implication of glutamate-induced excitotoxicity in motor neuron degeneration that occurs in the wobbler mouse. For this reason a more detailed investigation about the role of glutamate, and above all AMPA-kainate-induced excitotoxicity will be developed in this thesis.

5.4.2 Oxidative stress

Evidence of oxidative damage has been reported in the cervical spinal cord of symptomatic wobbler mice. Histochemically, positive staining for nNOS, an enzyme which catalyzes the

formation of NO, is reported to be exclusively in pathologic conditions, such as axotomy, ventral root avulsion or during apoptosis.

In the wobbler mouse motor neurons NOS induction was revealed by the nicotinamide adenine dinucleotide phosphate diaphorase (NADPH-diaphorase) diaphorase hystochemistry and nNOS immunoreactivity [Clowry, 1993;Clowry, 1996;Gonzalez Deniselle, 1999;Tsuzaka, 2001]. NADPH-diaphorase was found particularly increased in morphologically altered motor neurons and this trend increases during the clinical progression.

Nonetheless this technique is currently used in different laboratories as a specific marker for nNOS induction, I did not find differences in NADPH levels in cervical motor neurons between wobbler and healthy littermates at different stages of the disease (Bigini and Barbera 2004 unpublished).

By immunohystochemical experiments, we detected an overexpression of 4-hydroxynonenal-modified proteins, an indicator of lipid peroxidation, exclusively in the anterior horn of cervical spinal cord of symptomatic wobbler mice. This result further suggests a possible correlation between oxidative stress and motor neuron degeneration occurring in wobbler mice [Corvino, 2003].

Another indirect evidence, suggesting the implication of oxygen radicals in the wobbler motor neuron progression derives from the beneficial effects produced by chronic treatments with different scavengers [Ikeda, 1995;Abe, 1997].

5.4.3 Mitochondrial abnormalities

As in ALS patients, mitochondria have been reported as preferential target in different models of motor neurodegeneration. Morphological alterations of mitochondria and reduced activity of complexes I and IV of the mitochondrial respiratory enzymes were described in the presymptomatic phase in the murine model of fALS associated to the mutation of $SOD1^{G93A}$ transgenic mice [Browne, 1998;Bendotti, 2001].

In the cervical spinal motor neurons obtained from wobbler mice both light and electron microscopy observations have shown altered mitochondria with damaged cristae and a swelled shape [Gonzalez Deniselle, 2002].

By stimulating isolated mitochondria using pyruvate and malate as substrates consumption, it was observed that in mitochondria obtained from the brain of symptomatic wobbler mice, the oxygen consumption was lowered by 33% compared to healthy littermates. Moreover, incubating isolated mitochondria by using ascorbate and N,N,N',N'-tetramethyl-p-phenylenediamine the difference between wobbler and healthy littermates further increased by approximately reaching the 80%. According to these results the authors suggested that dysfunctional mitochondrial respiration occurring in the wobbler mouse brain and that this deficit could be mainly due to an impaired function of complex IV [Xu, 2001].

A following study was carried out to compare the mitochondrial activity in the motor cortex and in the spinal cord. A significant decrease in mitochondrial complex III and IV and in respiration rates was found in the whole spinal cord of early symptomatic wobbler mice and a marked decrease in oxidative phosphorylation was seen both in spinal cord and in motor cortex of affected mice [Dave, 2003].

Although these results agree with the hypothesis of a decay of mitochondrial activity in symptomatic wobbler mice, both studies lack to selectively evaluate these parameters in the cervical spinal cord and do not provide an accurate analysis of each single mitochondrial complex.

5.4.4 Neurofilament accumulation

Presymptomatic wobbler mice showed altered levels of mRNA for three neurofilament subunits NF-L, NF-M and NF-H [Pernas-Alonso, 1996]. As previously reported in section 1.2.2.1, excessive accumulation of proteins is a common of neurodegenerative diseases, and abnormal accumulation frequently occurs in motor neurons in patients with sporadic ALS [Carpenter, 1968;Hirano, 1984]. In wobbler mice a significant increase of mRNA for neurofilaments was already reported in embryonic (E15) stage and remained higher compared to the healthy mice till 21 days old mice, the oldest time-point examined. Although in wobbler mice a marked increase in neurofilaments transcripts has been reported in embryonic stage no changes in proteins levels were observed by immunohystochemistry prior the 2nd week of age [Pernas-Alonso, 1996]. No alteration in neurofilament expression was detected in any other CNS area at this stage. Interestingly, as in other genetically unrelated pathologies leading to motor neuron death in animal models, the overexpression of neurofilaments and their consequent accumulation into the perikarya, represent a common event in the pathological evolution [Xu, 1993;Cote, 1993]. This common feature further confirms the high sensitivity of neurofilament metabolism to a broad range of genetic insults occurring in motor neurons. An increase of mRNA levels of NF-H and NF-M has been reported in the stage between the onset of disease and the early symptomatic phase in the ventral horn of cervical spinal cord. By using an antibody (SMI31) directed against the NF-H/NF-H forms, I recently observed the presence of intra cytoplasmatic accumulation of neurofilaments in motor neurons of 4 week-old wobbler mice (Bigini 2003 unpublished).

5.4.5 Intracellular aggregates and/or failure of protein folding

Neurofilaments are not the unique proteins accumulate in the cell body of motor neurons during the progression of the disease. The presence of the protein inclusions, often conjugated with ubiquitin, is an usual phenomenon in different pathologies including ALS, Alzheimer's disease, Parkinson's disease and several neurological syndromes caused by an expansion of poly-glutamine tract [Braak, 2000;Lansbury, 2000]. These observations have led to the suggestion that altered chaperone activity may contribute to increase in misfolded proteins and accumulation of ubiquinated conglomerates in the cell body, thus producing a dramatic

blockade of metabolic activities. In fact, chaperone activity guarantees the prevention of proteins misfolding and the correct maintenance of protein conformation and also promotes the ubiquitination and the consequent degradation of abnormal proteins by the proteasome complex. The possible link between the activity of chaperone proteins and the process of neuronal death is further supported by the evidence that experimental upregulation of the heat shock protein 70 (HSP70) and/or of members of the DNAJ/HSP40 co-chaperone family lowers the intracellular inclusions of altered proteins, and protects cellular models of the polyglutamine diseases and of ALS linked to SOD1 mutation [Stenoien, 1999]. HSP70 and DNAJ/HSP40 proteins act in a co-operative manner to prevent the accumulation of improperly folded proteins [Hayes, 1996]. In wobbler mice the accumulation of abnormal proteins, other than neurofilaments, has been reported in the cytoplasm of cervical motor neurons, and ubiquitin-immunopositive deposits have been observed at the end of the presymptomatic phase during the development of the disease [Andrews, 1974;Mitsumoto, 1982].

5.4.6 Reactive gliosis

As for other neurodegenerative diseases, reactive gliosis accompanies motor neuron degeneration progression in wobbler mice. The characteristic hallmarks of reactive gliosis, an increased expression of GFAP coupled with hypertrophied morphology are observed in the cervical spinal cord and in the brainstem obtained from symptomatic wobbler mice [Hantaz-Ambroise, 1994;Laage, 1988;Rathke-Hartlieb, 1999]. In the original strain (C57BL/Fa), reactive gliosis occurs as early as the onset of symptoms and progresses during the symptomatic phase also invading the whole gray matter and the anterior part of the anterior white matter. The age of maximal astogliosis was found to coincide with the peak of motor neuron loss and then is maintained after the evolutionary phase of the disease, thus persisting until the death of animals.

According to the results obtained in C57BL/Fa, I observed a mild but significant increase of GFAP levels in the cervical homogenate obtained from 4th week-old wobbler mice compared to healthy littermates, with a further increase in 12th week-old mutants, while no difference in the amount of GFAP was measured in the lumbar homogenates at both phases of clinical progression. No difference in GFAP levels were found by comparing the lumbar spinal cord homogenates obtained from the same animals [Bigini, 2001].

No signs of gliosis were observed in the brain areas that display occasional degenerating neurons, and our unpublished immunohystochemical observations have confirmed this biochemical result. By staining frontal cortex sections with GFAP, we have observed a very weak immunopositivity, both in the early and in the late symptomatic wobbler mice. Moreover the pattern of staining we observed in the frontal cortex of wobbler mice did not differ compared to the occipital cortex obtained from the same animals and from the frontal cortex of healthy littermates (Bigini and Barbera 2003 unpublished).

Activated microglial cells were shown in the spinal region of wobbler mice from the 3rd week of age [Rathke-Hartlieb, 1999;Boillee, 2001]. At the end of the presymptomatic phase microglial cells are localized around affected motor neurons with their arborization disposed and organized to wrap ill motor neurons. Interestingly, in this phase of disease, an increase in

the number of microglial cells is not yet observed [Laage, 1988;Boillee, 2001]. During the symptomatic phase, in the cervical region, it is possible to note a marked microglial proliferation, mainly in the ventral region. The evidence that astrogliosis is not confined to the area of neurodegeneration, but rather extends to the dorsal part of the spinal cord, has suggested that astrocytes could themselves be a primary target of the disease and different *in vivo* experiments seem to support this hypothesis [Hantaz-Ambroise, 1994;Ait-Ikhlef, 2000;Gonzalez Deniselle, 1999].

Like astrocytes, microglial response increases during the progression of motor neuron degeneration reaching a plateau at 10/12 weeks of age. Following the evolutionary phase a weak but progressive reduction was observed in the cervical spinal cord of wobbler mice. This decrease was first associated to a reduction of phagocytosis from microglial cells that are committed to remove motor neurons debris. However, despite the relevant process of microgliosis during the peak of motor neuronal loss, microglial cells scarcely display the typical rounded shape attributed to microglial cells engaged in phagocytosis [Boillee, 2001;Streit, 1989;Raivich, 1999].

Gliosis is often accompanied by enhanced protease activities, possibly due to remodeling of tissue following brain injury [Lukes, 1999]. In the wobbler cervical spinal cord the expression of two metalloproteinases, MT1-MPP and disintegrin-like and metalloproteinase (ADAM8), is enhanced. These proteins are expressed both in activated astrocytes and in microglial cells [Schlomann, 2000;Rathke-Hartlieb, 2000]. The ability of TNFα to enhance the expression of ADAM8 in cultures of astrocytes from symptomatic animals indicates that glia may indeed be a target of this cytokine.

A recruitment of lymphocytes is also observed in the cervical spinal cord region of symptomatic wobbler mice even if the BBB appears intact, these lymphocytes are scattered in the ventral horn and seem anatomically unrelated to motor neurons [Boillee, 2001].

A schematic representation of behavioural, hystological and biochemical abnormalities occurring during the symptoms progression in wobbler mice is shown in figure 5.1.

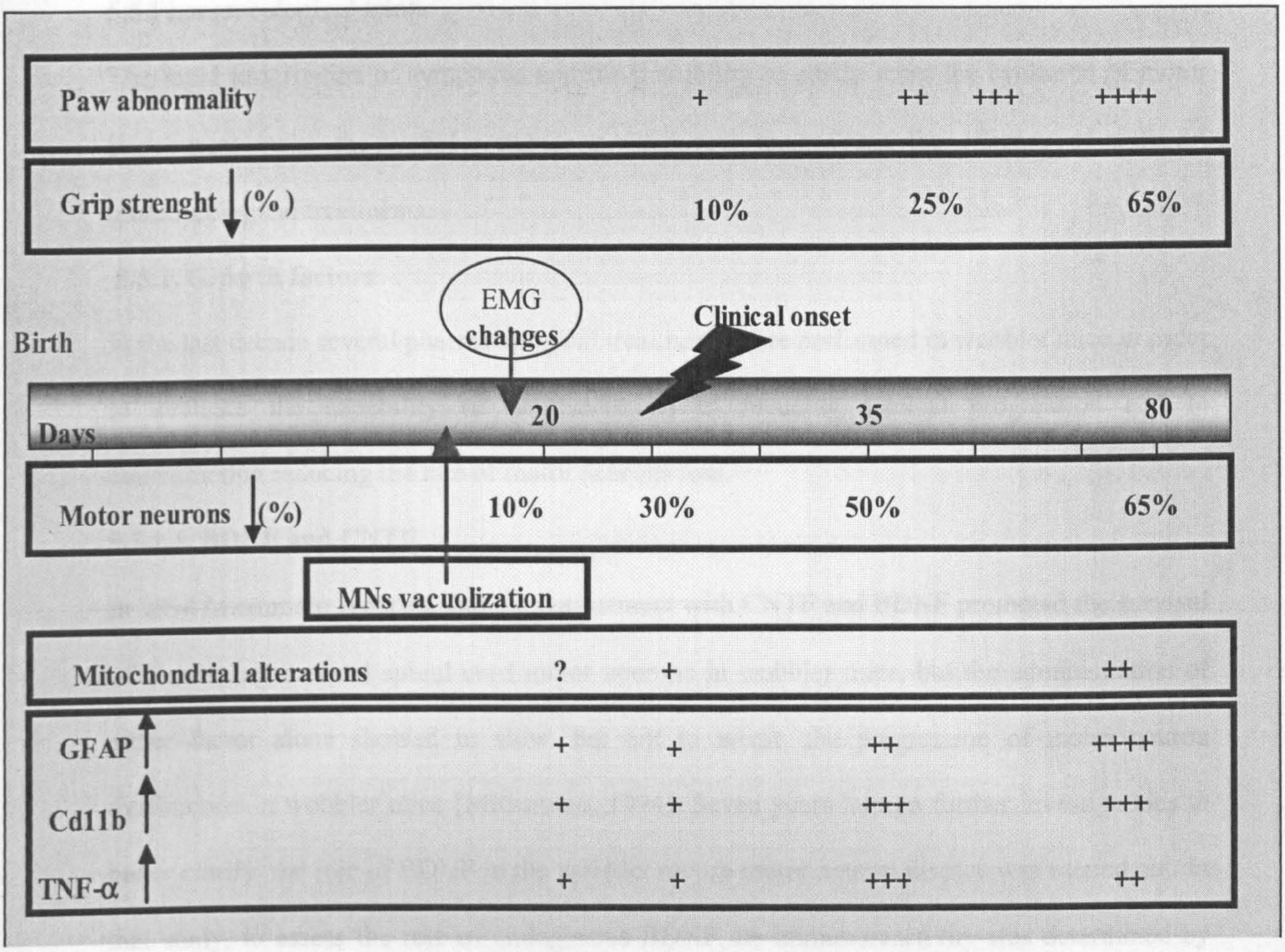

Figure 5.1 Symptomatological, neuropathological and biochemical alterations occurring in wobbler mice during the evolution of the disease

5.5 Pharmacological trials

The rapid progression of symptoms and the possibility to easily score the evolution of motor impairment make the wobbler mouse a valid tool to evaluate the efficacy of different pharmacological treatments.

5.5.1. Growth factors

In the last decade several pharmacological treatments were performed in wobbler mice in order to evaluate the capability of neurotrophins, to reducing clinical progression and to counteracting reducing the rate of motor neurons loss.

5.5.1.1. BDNF and CNTF

In 1994 Mitsumoto reported that the cotreatment with CNTF and BDNF promoted the survival of developing cervical spinal cord motor neurons in wobbler mice, but the administration of either factor alone showed to slow, but not to arrest, the progression of motor neuron dysfunction in wobbler mice [Mitsumoto, 1994]. Seven years later, a further investigations to better clarify the role of BDNF in the wobbler mouse motor neuron disease was carried out. In that study, to assess the role of endogenous BDNF, its immunoreactivity was determined by semi quantitative analysis. The cervical spinal cord of affected wobbler mice showed a significantly greater BDNF immunoreactivity compared to that of healthy littermates and the treatment further increased immunoreactivity in the affected cervical spinal cord motor neurons. In addition it was reported reported that exogenous BDNF treatment partially inhibited the increased NOS activity, measured by NADPH-diaphorase hystochemistry. They suggested that BDNF may be an important factor in halting nitric oxide (NO)-mediated motor neuron degeneration [Tsuzaka, 2001].

As in humans, the clinical and pharmacodynamic effects met-BDNF and met-free BDNF were compared by a clinical trial performed in early symptomatic wobbler mice. Both Met- and met-free BDNF improved grip strength and running time compared to vehicle. The plasmatic levels of BDNF did not differ between the two different BDNF groups. met-free BDNF exerted similar effects compared to met-BDNF in wobbler mice [Ishiyama, 2002].

5.5.1.2 IGF-1

Since recombinant human insulin-like growth factor-I (IGF-I) is considered to be a possible therapeutic agent for the ALS treatment (see section 1.4.3.4), a series of clinical trials were carried out in wobbler mice to determine the possible beneficial effect of IGF-I administration. The first study reported that IGF-I treated wobbler mice underwent a marked weight increase from 3 to 6 weeks of treatment compared to placebo treated wobbler mice. At the end of the treatment, grip strength was 40% higher in IGF-I treated versus placebo treated group. Mean muscle fiber diameter was increased in IGF-I treated mutants. However, in this study the muscle ChAT activity measured in the forelegs muscles and the number of spinal cord motor neurons were similar in both groups [Ikeda, 1995].

The role of IGF-I in decreasing the clinical progression in wobbler mice was further confirmed by treating early symptomatic mice with IGF-I and glycosaminoglycans (GAGs). GAGs are constituents of proteoglycans, and the supplementation of GAGs promotes *in vitro* neuritogenesis and stimulates nerve regrowth and muscle reinnervation, mainly in correlation with an increase in trophic factor mRNA expression.

Although each single treatment produced a significant protection compared to the vehicle-treated group, the effect of the combination treatment was significantly higher than that of the single drug. The treatment halted motor neuron loss and markedly reduced the decay of forelimb muscle morphometry and function [Gorio, 1998;Vergani, 1999]. Another positive effect, deriving from this pharmacological cocktail, was that the arrest of the progression of motor neuron disease was observed at low doses of IGF-I thus increasing the safety of possible treatment with a neurotorophic factor [Gorio, 2002].

5.5.1.3 T-588 and cardiotrophin 1

R(-)-1-(benzo(b)thiophen-5yl)-2-[2(N,N-diethylamino)ethoxy]ethanol hydrochloride (T-588) is a compound which has been shown to exhibit a wide range of neurotrophic effects both *in vivo* and *in vitro* [Iwasaki, 1989]. The chronic treatment with T-588 in symptomatic wobbler mice potentiated the grip strength, attenuated forelimb contracture and increased the weight of the biceps muscles. T-588-treated wobbler mice showed a delayed denervation, a lower degree

of muscle atrophy and higher activities of ChAT and lactate dehydrogenase in the biceps muscles [Ikeda, 2000].

Another neurotrophic agent, the cardiotrophin-1 (CT-1), was proposed for the treatment of wobbler mice. CT-1 treatment has been found to be effective in preventing deterioration in paw and walking position. Grip strength declined steadily in the vehicle group, whereas in the CT-1 group it declined at week 1 but increased thereafter to exceed baseline strength by 5% at week 4. Running time was significantly improved in CT-1 treated wobbler micefaster with CT-1. Biceps muscle twitch tension, muscle weight, mean muscle fiber diameter, and intramuscular axonal sprouting were significantly greater with CT-1 treatment. Histochemistry revealed a trend to a modest increase in the number of immunoreactive motor neurons, as determined by both ChAT and c-Ret antibodies in CT-1-treated wobbler mice.

The number of large myelinated motor axons significantly increased with treatment. The authors concluded that CT-1 exerts myotrophic effects as well as neurotrophic effects in this mouse model [Mitsumoto, 2001].

5.5.1.4 LIF

Leukaemia inhibitory factor (LIF) is a cytokine that belongs to the group including CNTF, IL-6, CT-1, OM and IL-11 [Kurek, 1998] that has been shown to produce positive *in vitro* stimulating myoblast proliferation. For this reason the role of LIF as a possible neuroprotective agent was also investigated in the wobbler mouse. Subcutaneous injection of LIF significantly slowed progression of forelimb atrophy from the 2nd week up to the end of treatment. Although grip strength both in saline- and in LIF-treated animals decreased rapidly after 7 days, the LIF-treated group had a significant delay in reduction of strength after 4 weeks. Moreover, a significant reduction of biceps muscle weight loss was reported, and the mean diameter of muscle fibres and the percentage of denervated was significantly increased in LIF-treated compared to vehicles [Ikeda, 1995].

5.5.1.5 IL-6

Interleukin-6 (IL-6) is a multipotential cytokine that shares signal transduction pathways with CNTF and LIF. IL-6 triggers homodimerization of gp130, whereas CNTF and LIF induce heterodimerization of gp130 and LIF receptor. The cotreatment with IL-6 and soluble IL-6 receptor (sIL-6R) improved symptomatic and neuropathological progression in wobbler mice. On the contrary IL-6 or sIL-6R alone did not delay the progression of symptoms. These results indicated that the neuroprotective mechanism for IL-6/sIL-6R on wobbler mouse differs from that of CNTF or LIF alone thus suggesting that IL-6/sIL-6R complex may function on motor neurons through activation and homodimerization of gp130 [Ikeda, 1995].

5.5.2 Antiglutamatergic agents

The role of glutamate receptors mediated excitotoxicity has been evidenced in different animal models of motor neuron degeneration. In $SOD1^{G93A}$ mice and in *mnd* mice *in vivo* treatments with glutamate receptors antagonists are active both in improving motor efficiency and muscular strength and in prolonging the survival [Canton, 2001;Mennini, 1999;Van Damme, 2003].

To test whether motor neuronal death in wobbler mouse syndrome was associated to the overstimulation of NMDAr, a treatment with the NMDAr antagonist (MK801), was carried out in wobbler mice just after birth or in early symptomatic phase.

In the group of animals in which the treatment started four days after birth, MK801 (in doses of 0.5/mg/kg/day) resulted highly toxic, whereas the group that initiated the treatment at 3/4 weeks of age well tolerated a dose of 1g/kg/day. In this latter group the treatment lasted for 8 weeks. During that time both clinical progression and possible side effects, such as lethargy or ataxia, were monitored. Although the group treated from 4^{th} to 12^{th} week of age did no show side-effects, no significant difference in the body weight and in the progression of symptoms was reported by comparing in MK801-treated and saline-treated wobbler mice [Krieger, 1992].

5.5.3 Mitochondrial agents

The implication of mitochondrial deficits in the evolution of wobbler mouse motor neuron syndrome was further confirmed by two distinct treatments in which energetic substrates were active in reducing clinical progression in wobbler mice.

As previously described in $SOD1^{G93A}$ transgenic mice [Klivenyi, 1999], the chronic treatment with creatine monohydrate potentiated grip strength, attenuated forelimb contracture and increased the weight of biceps muscles in early symptomatic wobbler mice.

Mice treated with higher doses of creatine monohydrate showed delayed denervation atrophy of the biceps muscles and reduced degeneration of the spinal motor neurons. Creatine levels in biceps muscles were increased by approximately 20% following administration of higher-dose

creatine monohydrate. In comparison with vehicle, treatment with higher doses of creatine monohydrate improved behavioural performances and reduced atrophy and motor neuron loss. Thus, oral administration of creatine monohydrate delayed the progression of disease in wobbler mice [Ikeda, 2000].

More recently, an original approach, by treating early symptomatic wobbler mice with a hyperbaric oxygen therapy (HBOT), has been shown to produce positive effects. The rate of respiration for complex IV in mitochondria isolated from motor cortex was improved by 40% after HBOT and the onset and clinical progression resulted significantly delayed in HBOT treated wobbler mice. Neither hystopathological estimation nor measurement of mitochondrial activity in the cervical spinal cord was performed following this treatment [Dave, 2003].

5.5.4 Antioxidants

In the wobbler mouse motor neuron disease few convincing clinical outcomes are, as yet, achieved by treating affected mice with molecules possessing antioxidant properties.

A possible protective effect of a novel free radical scavenger, OPC-14117, on the progressive motor neuron death in wobbler mice was examined. The treatment with OPC-14117, improved the clinical parameters such as mortality, motor activity, and forelimb weakness in a dose-dependent manner. The treatment of wobbler mice with the drug reduced age-dependent increase of lipid peroxides in the spinal cord, and a supplement of the drug in the homogenate of spinal cord reduced the formation of lipid peroxides generated by an exogenous addition of ascorbate or xanthine/xanthine oxidase. These results suggest that OPC-14117 has a protective effect on the motor neuron death probably as a free radical scavenger, resulting in an improvement of clinical symptoms in wobbler mice [Abe, 1997].

The effects produced by a treatment with an antioxidant therapy in neuromuscular dysfunction were also evaluated by treating wobbler mice with lecithinized superoxide dismutase. In this study [Ikeda, 1995] the treatment improved the motor impairment by reducing muscle weakness and contracture of the forelimbs in this animal. Lecithinized superoxide dismutase

treatment also prevented denervation, muscle atrophy and delayed degeneration of spinal motor neurons in wobbler mice.

A further study was conducted in early symptomatic wobbler mice with a non-selective NOS inhibitor, L-NAME, was carried out. The treatment with L-NAME potentiated grip strength and attenuated deformities in the forelimbs and arrested the loss of motor neurons. To a lesser extent, L-NAME-treated mice displayed slowed progression of disease. This study indicated that nNOS inhibitor may be a candidate for promising therapy in lower motor neuron disease or motor neuropathy [Ikeda, 1998].

Many others clinical trials with different types of pharmacological agents, such as steroid hormones, gangliosides, plasminogen activators, were reported to be active in reducing clinical progression and neuropathological alterations observed in the wobbler mouse motor neuron disease [Gonzalez Deniselle, 1997;Gonzalez Deniselle, 1999;Gonzalez Deniselle, 2002;Gonzalez Deniselle, 2004;Blondet, 1992;Bose, 1999;Lisovoski, 1997]. However, despite these encouraging results in the wobbler mice, the clinical trials of some of these molecules in ALS patients had no significant effect (see chapter 1).

5.6 Wobbler and apoptosis

Although the animal models of human ALS allow to accurately characterize cell death processes by investigating the early events occurring in dying motor neurons, an unambiguous characterisation of cellular death occurring in cervical spinal cord motor neurons has not yet been documented both hystologically and ultrastucturally.

The finding of motor neurons death in SOD1 transgenic provided inconclusive results. Although some authors reported the activation of apoptotic markers (caspase1 and caspase3) in the motor neurons of lumbar spinal cord, and a therapeutic effect after treatment with the antiapoptotic molecule zVAD-Fmk was also reported [Liu, 1996;Pasinelli, 2004] . Migheli et al. reported the absence of TUNEL staining in the same anatomical region, thus excluding apoptotic death [Migheli, 1999].

In the wobbler mouse the nature of motor neurons death has not been fully elucidated. An autolytic type of death has been described by Popper et al. In 4 week-old wobbler mice they

reported: I) no evidence of inflammation and monocyte infiltration in the spinal cord, II) no DNA fragmentation (no motor neurons were labeled using TUNEL staining), III) vacuolisation of cell bodies and dense basophilic nuclei in the motor neurons and; IV) increase of mRNA levels of testosterone repressed prostate message 2 (TRPM-2) in cervical spinal cord. However, the absence of TUNEL staining in the wobbler spinal cord may be due to a non-appropriate time point studied in this slowly progressing degenerative disease. Moreover the authors did not give details on the effective number of spinal cord sections analyzed and the region examined (cervical Vs lumbar) [Popper, 1997].

The protease-activated receptor 1 (PAR-1), a G-protein-coupled member of seven-transmembrane domain superfamily, when coupled with thrombin, elicits a signaling pathway that leads to neural cell death. Salcedo et al. reported a fivefold greater level of PAR-1 mRNA in the spinal cord of wobbler mouse. This increase was greater in the cervical compared with the lumbar segment; it was also found that PAR-1 was already increased in wobbler cords at E12. However these data do not supply clear evidence that the increase in PAR1 generates a mechanism leading to apoptosis of cervical motor neurons. Since thrombin elevates the Ca^{++} after PAR-1 activation, up-regulation of PAR-1 may contribute both to apoptotic as well as to non-apoptotic neural death in wobbler mouse [Salcedo, 1998].

As previously reported, the most significant abnormality found in wobbler mice is the vacuolar neuronal degeneration accompanied by a loss in the number of motor neuron, starting from the third week of age. Blondet and co-workers observed, using TUNEL staining in spinal cord section, a massive DNA fragmentation in different cell types, including glial cell as well as motor neurons, before the appearance of clinical symptoms. After examination of spinal cord sections (C7-T3), 60% of motor neurons in the anterior horns exhibited TUNEL positivity, specifically between P18-P21. The DNA fragmentation was clearly transient since the authors never observed similar features at later stages (P22, P26, P30 and P60). The same pattern of TUNEL positivity is reported in glial cells, astrocytes were individuated by double labelling using GFAP coupled to rhodamine. No chromatin condensation or apoptotic bodies were observed in TUNEL positive cells, including motor neurons and astrocytes. The authors do not

explain clearly the choice of the spinal cord region under studies and do not report the number of sections analyzed for each sample. Furthermore a so close time window of TUNEL positivity seems too short in this slowly degenerative disease. Although the authors report a astroglial TUNEL staining positivity closely in the P18-P22 wobbler spinal cord, it is difficult to explain as neuron and glia show this specific feature of cell death exclusively around this time.

They argued that, in the narrow time window in which the positive TUNEL staining is seen in wobbler spinal cord, detrimental stimuli trigger an initial mechanism of DNA fragmentation without generating apoptosis. The failure of apoptotic pathway could be related to an efficient DNA repair mechanism, in fact a great percentage of these motor neurons survive this moment and are still present in old animals [Blondet, 2002].

The limitations to characterize correctly the type of cellular death in motor neuron diseases are linked both to the small number of cell and to the slow rate of neuronal death. In fact only a few cells out of many die at any given time making it difficult to determine whether the hallmarks of apoptosis are present.

To better clarify the mechanism of motor neuronal death that occurs in the cervical motor neurons of wobbler mice, I have focused my attention on the evaluation of the possible role of apoptosis in the process of cell death, by exploiting both hystological and pharmacological approaches.

AIMS OF THE STUDY

CHAPTER 6

AIMS OF THE STUDY

This study aims to verify, in *in vitro* and *in vivo* models of ALS, the role of apoptosis in motor neuron death. In addition, I tested a possible link between apoptosis and the occurrence of three different aetiopathological factors postulated to be involved in motor neuron degeneration in ALS patients: I) neurotrophic factors deficiency, II) glutamate-induced excitotoxicity and III) glial-induced neuroinflammation.

To better characterize, at the single cell level, the possible interaction between these detrimental stimuli and apoptosis, *in vitro* studies, using primary cultures of rat embryo motor neurons were performed.

In vitro studies

In primary cultures of motor neurons I investigated:

- The toxic effect produced by chronic deprivation of trophic factors or chronic exposure to two glutamate agonists (AMPA and kainate) at the concentrations required to produce 50% of cell death (EC50) after 48 hours of treatment.

- The possible apoptotic involvement after excitotoxicity or serum/BDNF deprivation, by evaluating the intrinsic apoptotic pathway at different steps (from mitochondrial PTP opening to DNA fragmentation).

- The possible protective and anti-apoptotic effect of EPO, a molecule that has been already reported to have anti-apoptotic and neuroprotective action in *in vitro* and *in vivo* models of neuronal death.

In vivo studies:

After *in vitro* characterization I focused my attention on evaluating whether: I) these mechanisms were present in the affected region (cervical spinal cord) of early symptomatic wobbler mice and; II) they can produce a mechanism of death associated to apoptosis.

This part of my study was mainly aimed to characterize:

- The possible involvement of neuroinflammation and apoptosis in cervical motor neuron degeneration, by evaluating microglial activation and overexpression of the extrinsic apoptotic pathway passing through TNF-α and TNFR 1 and caspase 8 activation.

- The potential role of glutamate-induced excitotoxicity, by verifying the expression and the activity of glutamate transporters and the expression and distribution of AMPAr subunits (GluR 1-4) in the cervical spinal cord samples early symptomatic wobbler mice and healthy littermates.

- The effects of chronic treatments with a selective AMPA antagonist (RPR 199900) and with riluzole in reducing the progression of symptoms and the neuropathological worsening occurring in wobbler mice.

- The possible involvement of mitochondria-dependent apoptosis in cervical motor neurons of wobbler mice by evaluating both mitochondrial activity and the main markers of apoptosis (caspase 9, -7 and -3, DNA fragmentation) and by performing a chronic treatment with EPO, a selective neuroprotective and antiapoptotic molecule that has been already shown, by *in vitro* experiments, to block neuronal apoptosis acting through mitochondria.

EXPERIMENTAL

PROCEDURES

CHAPTER 7

MATERIALS

Reagents and materials that were utilized during this thesis are listed in the following pages:

- (14 C) acetil-CoA, Amersham, Buckinghamshire, UK
- (3H)-L-Glutamate, Amersham, US
- 2-mercaptoetanole, SIGMA, Italy
- ABC complex, Vector Laboratories, UK
- Acetil CoA, SIGMA, Italy
- Acetonitrile, SIGMA, Italy
- Alexa 488 goat anti-rabbit secondary antibody, Molecular Probes, US
- Alexa 546 goat anti-mouse secondary antibody, Molecular Probes, US
- Alu I, Genecraft, Germany
- AMPA, Tocris, Italy
- Analyser AIS software, Imagin Research St.Catherine's, Ontario, Canada
- Anti alpha-tubulin, SIGMA, Italy
- Anti-Epo antibody, Santa Cruz Biotechnology, CA, US
- Antimicin A, SIGMA, Italy
- Anti-mouse as secondary antibody, Amersham,US
- Ascorbate, SIGMA, Italy
- B27, Life Technologies, GIBCO, Italy
- BDNF, Amgen, US
- Biotinylated anti-mouse antibody, Vector Laboratories Inc.,UK
- BSA, SIGMA, Italy
- Anti-Active capase 3 antibody, Promega, Italy
- Anti-Active caspase 7 antibody, Alexis Biochemical, UK
- Anti-Active caspase 8 antibody, Cell Signaling Technology, UK

- Anti-Active caspase 9 antibody, Alexis Biochemical, UK
- Anti-CD 11 antibody, Serotech, UK
- Anti-ChAT antibody, Chemicon, US
- Choline Chloride, SIGMA, Italy
- Cyclosporin A, SIGMA, Italy
- Anti-Cytochrome C antibody, BP Biosciences, Italy
- Diaminobenzidine, SIGMA, Italy
- DMSO, SIGMA, Italy
- DTNB, Wako Pure Chemical Industries, Tokyo, Japan
- EDTA, Fluka Biochemical, Germany
- EGTA, Acros, New Jersey, US
- FCS, Life Technologies, US
- Anti-GLAST antibody, Chemicon, US
- Anti-GLT-1 antibody, Santa Cruz Biotechnology, US
- Anti-GluR1 antibody, Chemicon, US
- Anti-GluR2 antibody, Chemicon, US
- Anti-GluR3 antibody, Santa Cruz Biotechnology, US
- Anti-GluR4 antibody, Chemicon International, US
- GraphPad Prism version 3.0a for Macintosh, GraphPad Software, US
- Grip-Strength transducer, Ugo Basile, Italy
- HEPES, Eurobio, Italy
- Hoechst 33258, SIGMA, Italy
- Image Tool Software (UTHSCASA), US
- Iodonitrotetrazolium Chloride, SIGMA, Italy
- JC-1, Molecular Probes, Eugene, OR, US
- Kainate, SIGMA, Milan, Italy
- KCN, SIGMA, Italy

- Laminin, SIGMA, Milan, Italy
- L-glutamic acid, SIGMA, Italy
- L-Glutamine, Biochrom AG
- Malate, SIGMA, Italy
- Malonate, SIGMA, Italy
- Mannitol, SIGMA, Italy
- Monoclonal antibody IgG192 (kindly gift from Bruno Hivert.Marseille)
- NADPH, SIGMA, Italy
- NBT, SIGMA, Italy
- N-dodecyl-D-maltoside, Calbiochem, Italy
- Neurobasal Medium, Life Techonologies, GIBCO, Italy
- NGS, Vector Laboratories, Germany
- N-N-N'-N'-tetramethyl-P-phenylenediamide, SIGMA, Italy
- OCT, Sakura Nihombashi, Tokio, Japan
- Olympus Fluoview Laser scanning, Japan
- Orange Mitotracker, Molecolar Probes, US
- Oxaloacetate, SIGMA, Italy
- Oxigraph, Hansatech, Denmark
- Paraformaldehyde, Merck, Darmstadt, Germany
- PBS, Life Technologies, GIBCO, Italy
- Penicillin, Seromed, Italy
- Poly-DL-ornitine, SIGMA Italy
- Propidium iodide, Molecular Probes, Eugene, OR, US
- Restriction enzymes, GIBCO, Italy
- Rotenone, SIGMA, Italy
- Riluzole, Aventis-Pharma, France
- RPR119990, Aventis-Pharma, France

- Scintillation mixture, toluene scintillator, Packard, US
- SMI-32, Sternberger Monoclonals Inc., US
- Streptomicin, Seromed, Italy
- Succinate, SIGMA, Italy
- Sulphosalicylic acid, SIGMA, Italy
- SYTO 59, Molecular Probes, US
- Tetraphenylboron, SIGMA, Italy
- TMPD, SIGMA, Italy
- Anti-TNFR1 antibody, Hycult Biotechnology, The Netherlands
- Anti-TNFR2 antibody, Hycult Biotechnology, The Netherlands
- Anti-TNF-α antibody, Hycult Biotechnology, The Netherland

CHAPTER 8

in vitro METHODS

8.1 Primary cultures of motor neurons

8.1.1 Animals

Procedures involving animals were conducted in conformity with the institutional guidelines that comply with national (D.L. n. 116, G.U., suppl. 40, Feb. 18, 1992) and international laws and policies (EEC Council Directive 86/609, OJL 358, 1, Dec. 12, 1987; NIH Guide for the Care and Use of Laboratory Animals, U.S. National Research Council, 1996).

8.1.2 Motor neuron cultures

Spinal cords were obtained from 15-day Sprague Dawley rat embryos. Meninges and other tissues (dorsal horn) were removed. The ventral horn was trypsinized and centrifuged through a 4% BSA cushion for 10 min at 300 × *g*. Cells (representing mixed neuron/glia culture) were seeded at a density of 20,000 cells/cm^2 into 24 mm well plates precoated with poly-DL-ornithine and laminin, and containing complete culture medium (CCM) as follows: Neurobasal medium, B27 (2%), L-glutamine 0.5 mM, horse serum 2%, 2-mercaptoethanol 25 µM, glutamate 25 µM, penicillin and streptomycin 1%, BDNF 1 ng/ml. The same medium (without glutamate) was added to the cultures on fourth and sixth day *in vitro*.

When indicated, motor neurons were further purified by immunopanning. The cells were added into a Petri dish coated with a monoclonal antibody IgG192 that recognizes the low affinity neurotrophin receptor (NGFR^{p75}). Motor neurons were recovered by using an excess of monoclonal antibody and then collected by centrifugation through a BSA cushion as described above. The counted motor neurons were added at low density (2000 cells/cm^2) into 24-mm or 35-mm well plates precoated with poly-DL-ornithine and laminin and containing CCM. For

immunofluorescence experiments cells were grown at similar densities on glass coverslips, precoated with poly-DL-ornithine and laminin.

Neurobasal medium contains physiological concentrations of Ca^{++} (1.8 mM) and Mg^{++} (0.8 mM).

8.1.3 Pharmacological treatments

Cultures were treated on the sixth day *in vitro* (DIV 6) for 48 hrs. Aliquots ranging from 20 to 50 µl of glutamate agonist solutions were added to each well, containing 1 ml of CCM without glutamate. Cell death was induced on sixth day in culture by incubation for 48 h with kainate (5 µM for mixed neuron/glia cultures and 50 µM for purified cultures), AMPA (1 µM for mixed glia/neurons cultures and 10 µM for purified cultures), as previously described [Comoletti, 2001].

EPO (2.5 pmol/ml) or vehicle was added to the cultures in concomitance to, or 72 hours before the induction cell death (by addition of excitotoxins or serum/BDNF deprivation) or preincubated 72 h before.

Cyclosporin A_2 2 µM was added simultaneously with glutamate agonists and kept for 48 hours.

8.2 Immunocytochemistry

In the immunocytochemical experiments, for each type of antibody tested, the following procedure was adopted: at the end of each treatment the medium was discarded and the cells were fixed with paraformaldehyde 4% (w/vol) in PBS for 40 min. Following this common step, the various protocols of immunostaining differed depending on the type of antibody used.

Immunocytochemical experiments were done by using two different methods of visualisation: I) fluorescent dyes coupled to a secondary antibody (immunofluorescence) or II) biotinylated secondary antibody that reacts with a third molecule in which both a molecule of avidin-biotin and molecules of horse-radish peroxidase are linked. The horseradish peroxidase (linked to the ABC complex) allows, in the presence of H_2O_2, diaminobenzidine oxidation with chromogenic reaction and a resulting brown staining product. More detailed descriptions of

immunocytochemical procedures are reported in the following sections.

8.2.1 SMI 32 for non-phosphorylated neurofilaments

For SMI 32 all the passages were conducted at room temperature.

After fixation the cells were rinsed in 0.1 M PBS (pH 7.4) three times for 5 minutes and then permeabilized in a solution of PBS containing Triton X-100 (0.2%) and a blocking agent, FCS 10% (vol/vol), to reduce non-specific reactions for 30 min. After permeabilization the cells were immediately incubated overnight with the anti-mouse monoclonal antibody SMI 32 (1:4000) in a solution of PBS and FCS (10%). Cells were then rinsed three times (5 minutes) and incubated with an anti-mouse secondary antibody.

For immunofluorescence staining the secondary antibody was the Alexa-546 goat anti-mouse (the fluorophore used was a dye conjugated to rhodamine and having a λ of absorption at 556 nm and a λ of emission at 573 nm -red fluorescence-). Cells were incubated for two hours in a solution of PBS containing the secondary antibody (1:200), and FBS (3%).

To avoid a decay of fluorescence, starting from the incubation of the secondary antibody, all steps were done in dark plates.

After incubation with the secondary antibody the cells were rinsed three times in PBS and then the coverslips, where the cells are grown, were placed and mounted on glass slides. To preserve the fluorescence and allow a brighter signal in epifluorescence microscopy, or laser confocal scanning, few drops of fluor save agent were put between the side of the coverslip containing the cells and the glass slide. This procedure was used in all experiments in which fluorescent dyes were used.

For avidin-biotin (ABC staining), after the incubation of SMI32 and the three rinses in PBS, cells were incubated for 1 hour with a biotinylated anti-mouse antibody (1:1000) in a solution of PBS containing FCS (5%).

After incubation with the secondary antibody the cells were rinsed three times (5 min) and then incubated for 1 hour in a solution containing reagent A (avidin) and reagent B (biotinylated

horseradish peroxidase) with PBS 0.1 M pH 7.4 at final 1% concentration (Triton X-100 was not used in this step). To increase the efficiency of staining, the A+B solution were prepared 30 minutes before the incubation and maintained at 4 °C just until the incubation.

After one rinse in PBS and two rinses in TBS 0.1 M pH 7.8-8.3, the cells were incubated for few minutes in TBS containing 0.5% DAB (w/V) and H_2O_2 (0.6 µl for 1 ml of solution, H_2O_2 was added just before application). As DAB is a photosensitive molecule, the DAB was dissolved and stored in a dark vial until incubation. The steps involved in the process of staining enhancement by the ABC method are shown in figure 8.1.

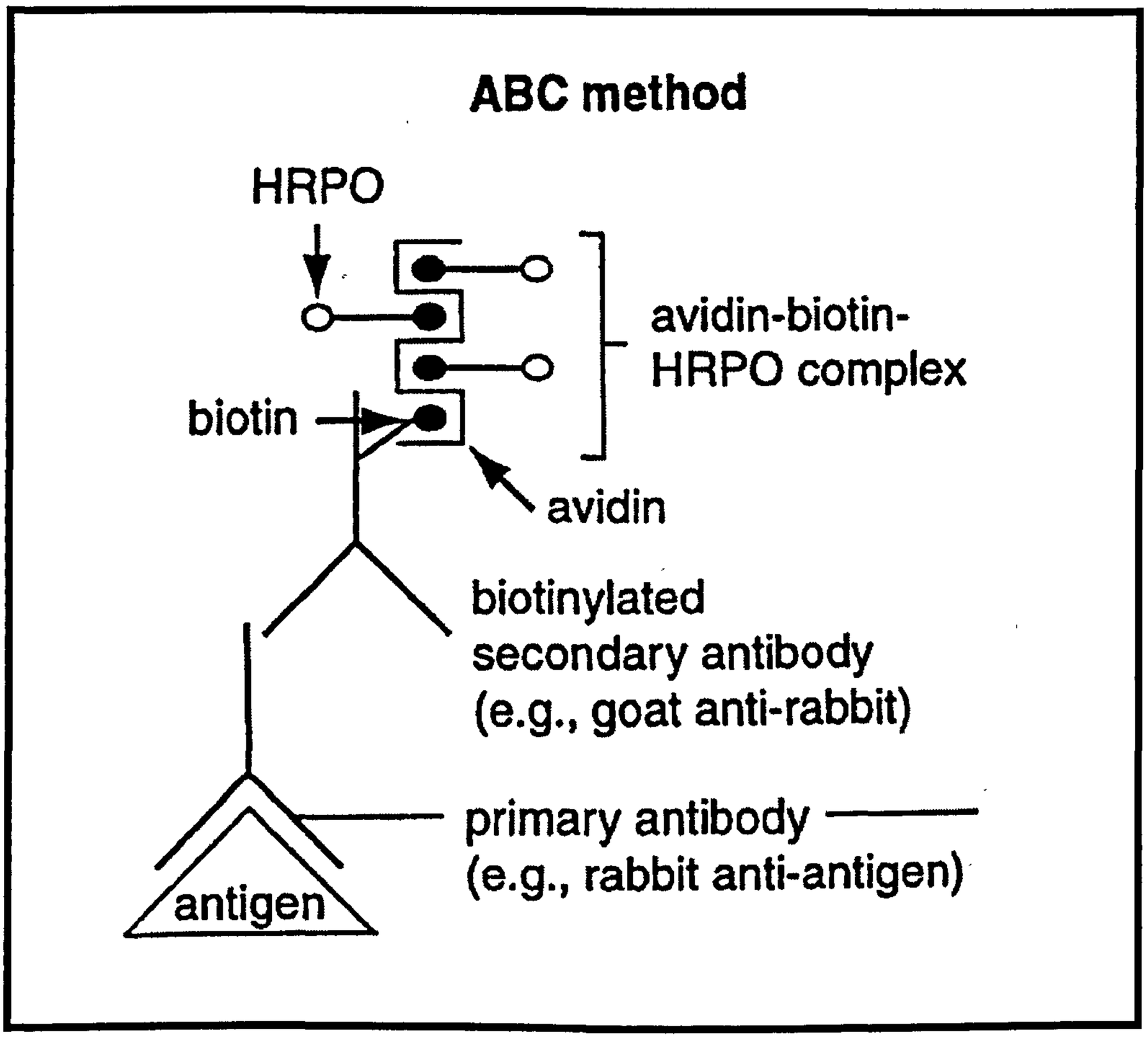

Figure 8.1 Schematic representation of events characterizing the immunoperoxidase process of immunohystochemistry with ABC method. Abbreviations: ABC, avidin-biotin conjugate complex; HRPO horseradish peroxidase.

8.2.2 EPO receptor

After fixation and three rinses in 0.1 M PBS pH 7.4, the purified cultures were permeabilized with Triton X-100 (0.2%) for 30 minutes and blocked with FCS (10%) in PBS. Cells were incubated overnight at 4 °C with the rabbit polyclonal primary antibody, raised against anti-Epo receptor (1:500), in absence or presence of an excess of blocking peptide (1:50). Next steps were carried out at room temperature. Cells were washed three times and then incubated for two hours in a solution of PBS containing biotinylated anti-rabbit (1:200) and FCS (1%). The following steps were identical to the SMI32 protocol (ABC kit method).

8.2.3 GluR 1-4

Before the incubation with the specific antibody directed against the four different subunits of the AMPAr, the same experimental procedure was used.

After fixation, purified cultures were washed three times in 0.1 M PBS pH 7.4 and then incubated in a solution of PBS containing Triton X-100 (0.4%) for 30 minutes at 4 °C. A further incubation in PBS and Triton X-100 (0.1%) and FBS (3%) for 15 minutes at 4 °C was then performed.

GluR1

The cells were incubated overnight at 4 °C in a solution of PBS containing an anti-rabbit polyclonal antibody raised against GluR-1 (1:500), Triton X-100 (0.1%) and FBS 3%. After incubation with the primary antibody, and two rinses in PBS at room temperature, cells were incubated for 2 hours at room temperature in a solution of PBS containing FBS (2%) and an Alexa-488 goat anti-rabbit secondary antibody (1:1000) (the fluorophore used was a dye conjugated to fluorescein (mistakenly abbreviated by its commonly-used reactive isothiocyanate form (FITC)) having a λ of absorption at 495 nm and a λ of emission at 519 nm -green fluorescence-).

GluR2

The cells were incubated overnight at 4 °C in a solution of PBS containing an anti-mouse monoclonal antibody raised against GluR-2 (1:1000), Triton X-100 (0.1%) and FBS 3%. After incubation with the primary antibody and the following three rinses in PBS at room temperature, the cells were incubated 1 hour at room temperature in a solution of PBS containing an Alexa-488 goat anti-mouse secondary antibody (1:2000) and FBS (4%).

GluR3

The cells were incubated overnight at room temperature in a solution of PBS containing an anti-goat polyclonal antibody raised against GluR-3 (1:1000), Triton X-100 (0.1%) and FBS 5%. After incubation with the primary antibody, and the following three rinses in PBS at room temperature, the cells were incubated 2 hours at room temperature in a solution of PBS containing an Alexa-488 mouse anti-goat secondary antibody (1:1000) and FBS (3%).

GluR4

The cells were incubated overnight, the first two hours at room temperature and then at 4 °C, in a solution of PBS containing an anti-rabbit polyclonal antibody raised against GluR-4 (1:200), Triton X-100 (0.1%) and FBS 1%. After incubation with the primary antibody, and three rinses in PBS at room temperature, the cells were incubated 2 hours at room temperature in a solution of PBS containing an Alexa-488 goat anti-rabbit secondary antibody (1:500) and FBS (2%).

8.2.5 Active Caspase 3 and Caspase 9

After fixation the cells were rinsed three times in 0.1 M PBS pH 7.4 and then permeabilized with Triton X-100 (0.1%) for 30 minutes and blocked with FCS (5%) in PBS. The incubation with the primary antibody against activated caspase 3 and 9 is described in the following paragraphs.

Active caspase 3

The cells were incubated for 36 hours, the first two hours at room temperature and then at 4 °C, in a solution of PBS containing an anti-rabbit polyclonal antibody raised against the cleaved form of capase 3 (1:100), Triton X-100 (0.05%) and FBS 1%. After incubation with the primary antibody, and three rinses in PBS at room temperature, the cells were incubated for 2 hours at room temperature in a solution of PBS containing an Alexa-488 goat anti-rabbit secondary antibody (1:500) and FBS (2%).

Active caspase 9

The cells were incubated overnight at 4 °C, in a solution of PBS containing an anti-rabbit polyclonal antibody raised against the cleaved form of capase 9 (1:100), Triton X-100 (0.05%) and FBS 2%. After incubation with the primary antibody, and three rinses in PBS at room temperature, cells were incubated for 2 hours at room temperature, in a solution of PBS containing an Alexa-488 goat anti-rabbit secondary antibody (1:1000) and FBS (4%).

8.2.5 Cytochrome-c

For cytochrome-c immunostaining fixed cells were rinsed for three times in 0.1 M PBS pH 7.4 and then preincubated for 15 minutes at room temperature in a solution of PBS containing FBS (10%). After three rinses in PBS the cells were permeabilized in a solution of PBS containing saponin (0.1%) for 15 minutes at room temperature and then incubated overnight at room temperature in a solution of PBS containing an anti-mouse monoclonal antibody raised against cytochrome-c (1:100) and FBS (5%) according to the method previously described by Sanchez-Alcazar and colleagues [Sanchez-Alcazar, 2001].

8.3 Hoechst 33258 staining

The cells were fixed overnight in Carnoy solution (3:1 methanol/acetic acid) and stained with Hoechst 33258 (0.1 µg/ml in PBS) at room temperature for 1h, then washed 10 times, 5 min each, with distilled water, air-dried overnight and covered with a glass coverslip.

Cells were observed with an epifluorescence microscope (Zeiss, Germany) using a filter with an excitation wavelength of 365 nm (UV).

8.4 Mito Tracker staining

The cell-permanent Mito Tracker probe contains a mild thiolreactive chloromethyl moiety that appears to be responsible for keeping the dye associated to mitochondria penetration. To stain mitochondria, non-fixed cells were incubated with a submicromolar concentration of Mito Tracker (100 to 500 nM, depending on the intensity of the staining). Mito Tracker was previously dissolved in dimethyl sulfoxide (DMSO), to obtain a starting concentration 1 mM, and further diluted (1:2 to 1:10) and added at a ratio of 1:1000 in the culture medium, maintained at 37 °C, to reach the nanomolar dilution required.

The culture medium was removed and substituted, for about 30 minutes, with the medium containing the Mito Tracker at 37 °C. After incubation the cells were immediately fixed, following the procedure of fixation reported above (see paragraph 8.2). This rapid fixation is required to avoid that the Mito tracker probes, which passively diffuse across the plasma

membrane and accumulate into the mitochondria, diffuse after incubation. Because the Mito Tracker probes are retained into the mitochondria after permeabilization with detergents or organic solvents, they maintain their fluorescent staining even following the immunocytochemical experiments.

For these experiments, an Orange-Mito Tracker probe was used. This probe has a λ of absorption at 554 nm and a λ of emission at 576 nm, and for this reason the same confocal microscope setting previously used for Alexa-546 fluorescent dyes, was adopted.

8.5 Propidium Iodide and SYTO 59 staining

The following experiments (sections 8.5, 8.6 and 8.7) were performed in collaboration with Prof. Daniela Curti at the Department of Cellular & Molecular Physiological & Pharmacological Sciences, University of Pavia, Italy.

Cells grown on glass coverslips were double stained with SYTO 59 (0.5 μM) and propidium iodide (PI, 10 μg/ml). SYTO 59 is a red fluorescent dye excited with the 633 line of a He/Neon laser and propidium iodide is excited at 488 nm with an Argon laser. The pseudocolour blue was chosen for SYTO 59 to distinguish between the fluorescence emission of this dye and that of PI (red). The cells were incubated at 37 °C for 20 min with the fluorescent probes as previously described [225]. At the end of the incubation, the cells were washed and resuspended in fresh buffer. Laser scanning confocal images were acquired with a DMS IRBE SP2 (Leach) inverted microscope.

8.6 Mitochondria transmembrane potential ($\Delta\Psi_M$)

The mitochondrial transmembrane potential was measured with the fluorescent probe 5,5',6,6'-tetracloro-1,1',3,3'-tetraetilbenzimidazol carbocianine (JC-1). Cells were incubated at 37 °C for 20 min with the fluorescent probe (3 μM). At the end of the incubation they were washed and resuspended in fresh buffer, then perfused with the same buffer in a 300 μl chamber whose bottom is the coverslip where the cells were grown. JC-1 is excited at 488 nm with an Argon

laser and emits at 527 nm (green fluorescence, in monomeric form) and at 590 nm (red fluorescence, JC-1 aggregates representing energized mitochondria). A "shift" from red to green fluorescence is observed upon depolarisation of the mitochondria. To minimise any photobleaching, laser scanning confocal images were acquired at 0.8-1 µm interval on the z axis for each field with a DMS IRBE SP2 (Leica) inverted microscope and a 63x oil objective (NA 1.3). Calibration and quantification were performed with Image Tool software (UTHSCSA). Fluoresce intensity was expressed as the ratio of the fluorescence emission at 590 nm and the total fluorescence emission at 590 and 527 nm (F_{red}/ F_{red}+F_{green}).

In some cases the cells were doubled stained with Hoechst 332588 (1 µM) and images were acquired with a sequential scanning program and an UV laser.

8.7 Laser scanning confocal microscopy setting up

For the double staining experiments (caspases/SMI 32 and Mito Tracker/cytochrome-c) the following setting of the laser scanning microscope (*Olympus Fluoview* microscope BX61 with confocal system FV500) was adopted. Dual excitation has been used, 488nm (LASER Ar) and 543 (LASER He-Ne green). To select the appropriate emission wavelength from the fluorophore, an emission filter designed to allow only a well-defined spectrum of emitted light to reach the detector was used, thus rejecting any remaining stray excitation or scattered light rejected. The filter used was a 510-550 BP for Alexa 488 and 560-600 BP for Alexa 546 and orange-Mito Tracker -see section 8.4- (filter allows band of selected wavelengths to pass through, while rejecting all shorter and longer wavelength). The image acquisition was done with different setting of photomultiplier (PMT), voltage (increasing this value improves the sensitivity), offset (darkens the image at the ratio set during image acquisition) and gain (brightness the image at the ratio set during image acquisition).

8.8 Statistics

Data are reported as mean values±S.D. and compared using ANOVA with Tukey's test. Dose-response curves were fitted accordingly to the four-parameter logistic equation:

$$y=\text{Bottom}+\frac{(\text{Top-Bottom})}{1+10^{(\log EC50X)\text{Hill slope}}}$$

which also gives an "asymptotic" standard error for each best-fit value.

Calculations were performed using Prism version 3.0a for Macintosh, Software, San Diego (CA, USA).

CHAPTER 9

In vivo METHODS

9.1 Genotyping

In order to identify wr/wr homozigous mice in presymptomatic stage (2^{nd} -3^{rd} week of age) a genotyping analysis was performed. An Alu I restriction polymorphism of a Cct 4 amplification product was used for testing the allelic status at the wr locus.

A small portion (0.5 cm) of the end segment of the tail was cut and digested overnight at 56 °C in 500 µl of lysis buffer (Puregene Genomic DNA Purification Kit for Mouse Tail Tissue, Gentra System) and 50 µg of Proteinase K (Gibco BRL). The following day, 500 µl of a mix 1:1 phenol-TRIS saturated: chloroform was added to each sample, shaking gently to obtain a homogeneous emulsion. The samples were centrifuged (12,000 rpm for 5 minutes) to obtain two separated phases: the supernatant contains the DNA, while the proteins form a layer between the phases.

The supernatant was carefully transferred in 500 µl of isopropanol to precipitate the DNA. After precipitation DNA was withdrawn and dispensed in 100 µl of Tris-EDTA solution (0.1 mM pH 7.5) and incubated for 4 hours at 56 °C. The DNA amplification of the small portion of DNA containing the Alu1 restriction polymorphism was carried out by PCR. Cct4 diagnostic primers were purchased from Gibco BRL. The PCR reactions were performed as follows: initial denaturation step 4 min at 94 °C followed by 35 cycles of 30s 90 °C denaturation, 30s Tann, 64 °C, and 30s 72 °C polymerisation. Restriction enzymes were obtained from Gibco BRL. PCR products (4 µl) were digested in a total volume of 10 µl with 10 U AluI for 1 hour at 37 °C, separated by 2% agarose gel electrophoresis and stained with ethidium bromide. In this way it is possible to screen the wobbler and healthy littermates (both homozygotes and etherozygotes mice). One single band is associated to the amplified product from homozygous +/+ healthy mice, which show no polymorphism. Two lower band are associated the amplified

product from wr/wr mice, which present polymorphism in both alleles. Three bands are associated to the amplified product from wr/+ healthy mice (one from the wild type allele and two from the mutated alleles.

9.2 Pharmacological treatments

9.2.1 EPO treatment

After the diagnosis of the disease at three weeks of age, 16 homozygous wobbler mice and 20 healthy littermates were randomly assigned to one of four experimental groups:

group 1: wobbler mice treated with EPO (10 animals);

group 2: wobbler mice treated with vehicle (10 animals);

group 3: control littermates treated with EPO (10 animals);

group 4: control littermates treated with vehicle (10 animals).

Animals were treated intraperitoneally, three times a week, with human recombinant erythropoietin (RhUEPO) at the dose of 4Units/g body weight (1U of EPO ≈ 10 ng of protein) or with the same volume of saline solution (10 ml/kg body weight).

All experimental groups included a similar number of male and female mice, since no sex-related differences in the evolution of the wobbler disease has been reported [Mitsumoto, 1994].

Epo was a gift from Dragon Pharmaceuticals (Vancouver, BC, Canada).

Animals were sacrificed at 12th weeks of age. Five animals for each group were sacrificed by decapitation; blood was drowned for haematocrit determination. The cervical spinal cord and the biceps muscles were rapidly dissected, frozen in n-pentane at –45 °C and stored at -80 °C until analysis. The other animals belonging to the four experimental groups were transcardially perfused with 4% paraformaldehyde in PBS.

Spinal cord and biceps muscles were removed, postfixed and cryopreserved by serial steps in sucrose solution. Samples were rapidly frozen in n-pentane at -45°C and stored at –80 °C until analysis.

9.2.2 RPR119990 treatment

For RPR119990 treatment, after the diagnosis of the disease at three weeks of age, 20 wobbler mice and 20 healthy littermates were randomly assigned to one of four experimental groups:

group 1: wobbler mice treated with RPR119990 (10 animals);

group 2: wobbler mice treated with vehicle (10 animals);

group 3: control littermates treated with RPR119990 (10 animals);

group 4: control littermates treated with vehicle (10 animals).

Mice were treated daily sub-cutaneously with 3 mg/kg of RPR119990 diluted in saline solution or with the same volume (10 ml/kg) of saline. Food (standard pellets) and water were supplied ad libitum.

All experimental groups included a similar number of male and female mice, since no sex-related differences in the evolution of the wobbler disease has reported [Mitsumoto, 1994].

RPR119990 was kindly provided by Aventis-Pharma (Aventis Pharma Centre de Récherche de Paris, Vitry Sur Seine, Cedex, France).

All mice receiving RPR119990 treatment were sacrificed at 12 weeks of age by transcardiac perfusion with 4% paraformaldehyde in PBS. Biceps muscles and spinal cord were rapidly dissected, post-fixed and cryoprotected. Samples were frozen in n-pentane at –45 °Cand stored at –80 °C until analysis.

9.2.3 Riluzole treatment

For riluzole treatment, after the diagnosis of the disease at three weeks of age, 20 wobbler mice and 20 healthy littermates were randomly assigned to one of four experimental groups:

group 1: wobbler mice treated with riluzole (10 animals);

group 2: wobbler mice treated with vehicle (10 animals);

group 3: control littermates treated with riluzole (10 animals);

group 4: control littermates treated with vehicle (10 animals).

Riluzole was administered in drinking water (final concentration: 150 μg/ml); the calculated dose for the treatment was 40 mg/kg/day. Vehicle-treated mice received tap water. Water consumption was calculated as 4 ml/animal/day and the volume needed was supplied by operators every two days, with addition of riluzole previously diluted in ethanol (0.05% of the final volume) for treated mice. Food (standard pellets) was supplied ad libitum.

All experimental groups included a similar number of male and female mice, since no sex-related differences in the evolution of the wobbler disease has been reported [456].

Riluzole was kindly provided by Aventis-Pharma (Aventis Pharma Centre de Récherche de Paris, Vitry Sur Seine, Cedex, France).

For each experimental group, five mice receiving riluzole treatment were sacrificed at 12 weeks of age by transcardiac perfusion with 4% paraformaldehyde in PBS. Immediately after perfusion, biceps muscles and spinal cord were rapidly dissected, post-fixed and cryoprotected. After freezing in n-pentane at –45 °C, biceps muscles and spinal cords were stored at –80 °C until analysis.

9.3 Behavioural scores recording

Behavioural trials for wobbler mice were carried out twice a week, by the same operator blinded to treatments. The clinical progression of the disease was monitored using both quantitative measurements (running time and grip strength tests) and semi-quantitative score (paw abnormality and walking abnormality tests), according to previously described protocols [Kozachuk, 1987] .

9.3.1 Paw and walking abnormality

Description of the test: the massive loss of cervical spinal cord motor neurons that occurs in wobbler mice lead to progressive atrophy of the innervated muscles, in particular biceps muscles of the forelegs are severely affected. Symptoms become evident starting from the $3^{rd}/4^{th}$ week of age and worsen rapidly until the wobbler mice show severe motor impairment that impede to walk correctly. At the same time, the front paws show progressive retraction of digits and the adduction of the paws to the body. Both the paw abnormality and the walking abnormality tests are observational; the operator assigns a score to these parameters, scaled from 0 to 4, on the basis of the severity of abnormalities.

The paw position is graded as follows:

score 0: normal

score 1: retracted digits

score 2: curled digits

score 3: curled wrists

score 4: forelimb flexed to body

The walking pattern is graded as follows:

score 0: normal

score 1: trembling (tremor without gait disturbance)

score 2: wobbling (gait disturbance)

score 3: curled paw walking

score 4: jaw walking (no use of front paw).

9.3.2 Running time

Description of the test: mice run over an inclined platform (75 cm long ramp inclined at one end to a height of 13 cm) stimulated with a gentle pressure on the tail (adverse stimulus). The running time is defined as the shorter time to reach the top of the platform from the bottom. Healthy mice rapidly improve their performances on the test until they reach the top of the platform in few seconds (1 to 3 sec.). On the contrary, wobbler mice need longer time to reach the top of the platform. Moreover these animals show a marked worsening of their performances, due to the progressive muscular atrophy in the forelegs..

9.3.3 Grip strength.

Description of the test: the mice are lifted by the tail and allowed to grasp with both forelegs to a horizontal bar, which is connected to a mechanoelectric transducer. The grip strength of the front paws is measured at the point when the mouse releases the horizontal bar as a result of a gentle traction applied by the operator. Healthy mice can record values higher than 100 grams, while values recorded by wobbler mice are very low (< 20 grams) and drastically reduced during symptoms progression. When animals are no longer able to grip the bar, grip strength is recorded as 0 grams. Values of grip strength were normalized dividing each value by body weight, in order to control for weight differences between wobbler and healthy mice.

9.4 Haematocrit measurement

Immediately after decapitation, few drops of blood were collected in heparinated capillary tubes (soda lime glass Micro Haematocrit Tubes, ALC International) and centrifuged at 3500 rpm for 20 min. at 20C°. Total and erythrocytes lengths were measured; the haematocrit value was calculated by dividing the particulate by total length and multiplying it by 100. For each sample, the mean of triplicate values was recorded.

9.5 Spinal cord perfusion and slice preparation

To ensure an optimal quality of spinal cord tissues for hystochemical determinations, tissues were fixed following the transcardial perfusion method described below:

- Before anaesthesia a peristaltic pump, including two boxes (the first one containing 0.1 M PBS, pH 7.4 at room temperature, and the other containing a solution of parformaldhheyde 4% dissolved in PBS at a pH ranging from 7.2-7.4) was prepared. This pump was connected to a 25-gage needle.
- A deep surgical anaesthesia was induced in mice by injecting intraperitoneally (IP) a solution of 0.6 g/Kg of chloral hydrate in saline (approx 150 µl for 20-g mouse).
- The pupil closure was checked before starting the perfusion to ensure that the animals were completely anaesthetized by gently touching the eye with a plastic pipette.
- When the animals were completely anaesthetized, the thorax was surgically opened, the diaphragm was cut and removed and the lateral part of thoracic cage was opened and directed to the back, by using a small clamp, in order to better penetrate into the beating hart (see figure 9.1).
- The 25-gage needle was then inserted in the left ventricle, closer to the aortic valves. This operation must be extremely accurate but, at the same time, fast. In fact, the absence of the diaphragm muscle activity and the consequent loss of respiration, may rapidly lead to an ischemic damage of the heart and a loss of blood circulation.
- When the 25-gage needle was inserted into the left ventricle, the flux of PBS solution was opened and the auricle of the right atrium was cut.
- The phase of washing tissues, to remove the blood cells was done by using about 15 ml of PBS for 20-g mouse and the phase of fixation was performed by using about 45 ml of fixative for a 20-g mouse
- After perfusion, the vertebral column was removed and postfixed, three hours at 4 °C, in the same solution used to perfuse the mouse.
- After fixation, samples were cryoprotected by three serial incubation at 4 °C, 2 hours each,

in a solution 0.1 M PBS, pH 7.4 containing increasing concentration of sucrose (10%, 20% and 30%). This process removes water from tissues and prevents freezing artefacts.

- After cryopreservation, samples were briefly dried and dipped in cooled isopentane (-35 °C to –45 °C). The time of immersion varies according to the type of tissue, its size and its shape. However it must be long enough to result in complete freezing but not so long to cause shrinkage or cracking of tissue.
- Micrometric slices from 20 to 40 µm of thickness were obtained by sectioning the tissues using a microtone housed in a freezing chamber placed at a temperature of –20 °C. In order to avoid breaking of tissues during sectioning spinal cord samples must be previously embedded in a small cylinder of OCT

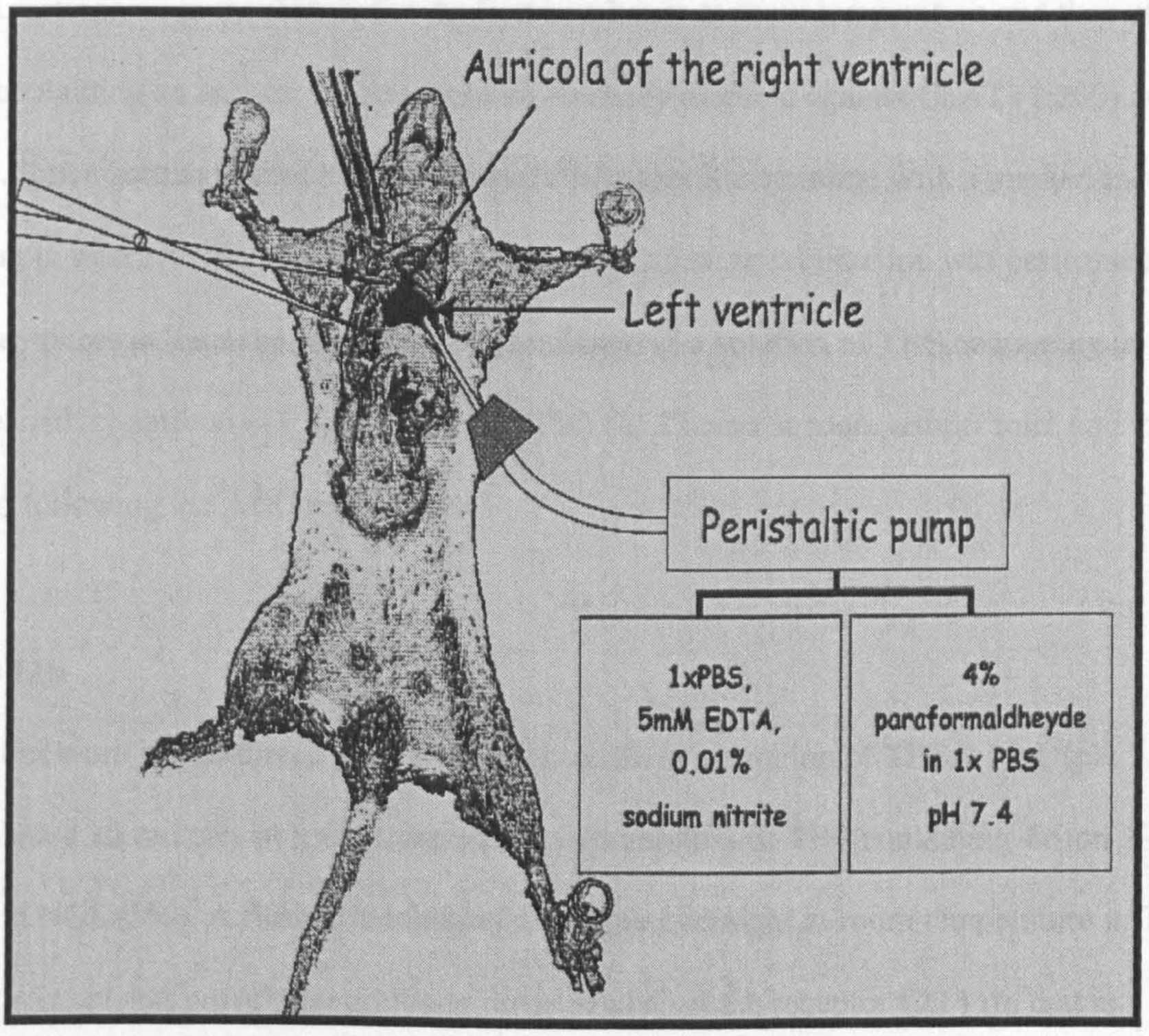

Figure 9.1 Schematic representation of surgical procedures utilized to perfuse the animal

9.6 Immunohystochemistry

For free floating immunohystochemistry, micrometric sections were placed in wells containing a buffered saline solution (PBS or TBS) and then rinsed three rinses (10 minutes each) to remove the OCT in solution.

For this immunohystochemistry, the ABC method, already described in the chapter 8 (see section 8.2.1), was utilized to visualize the immunoreactivity.

9.6.1 ChAT

After three rinses in TBS 0.1 M (pH 7.4) the sections were incubated for 1 hour at room temperature in TBS containing normal goat serum (10%), to avoid non-specific reactions. Then the sections were incubated, for the first two hours at room temperature and then at 4 °C, in TBS containing an anti-mouse monoclonal antibody directed against ChAT (1:200) and NGS 3%. Since permeabilized tissues showed a non-specific staining, with a marked increase of staining in interneurons and in fibers, in this study no permeabilization was performed. After three rinses in TBS the sections were incubated in a solution of TBS containing an anti-mouse secondary antibody (1:200) and NGS (1%) for 2 hours at room temperature and then processed following the ABC method.

9.6.2 CD 11b

The sections were rinsed three times, 5 minutes each, in a solution of TBS 0.1 M (pH 7.4) and then incubated 30 minutes at room temperature in a solution of TBS containing Triton X-100 (0.4%) and NGS (3%). A further incubation was done overnight at room temperature in TBS containing an anti-rat polyclonal antibody directed against the receptor CD 11b, that is selectively expressed in activated microglial cells (1:100), Triton X-100 (0.2%) and NGS (2%). After three rinses in TBS the sections were incubated in a solution of TBS containing an anti-rat secondary antibody (1:200) and NGS (2%) for 2 hours at room temperature and then processed following the ABC method.

9.6.3 TNF-α and TNF receptors

The sections were incubated 1 hour at room temperature in a solution 0.1 M TBS pH 7.4 containing NGS (10%) to reduce the non-specific staining, mainly due to cross-reaction of secondary antibodies.

For TNF-α immunostaining the section were incubated overnight at room temperature in the following solution: TBS 0.1 M (pH 7.4) containing NGS (1%), Triton X-100 (0.1 %) and primary antibody mouse monoclonal anti-human TNF-α (1:50). After three rinses in a solution of TBS the sections were incubated for two hours at room temperature in TBS containing an anti-mouse biotinylated antibody (1:100) and NGS (2%).

For TNFR1 and TNFR2 immunostaining the section were incubated overnight at room temperature in the following solution: TBS 0.1 M (pH 7.4) containing NGS (1%), Triton X-100 (0.2 %) and anti-rat polyclonal antibody for TNFR1 (1:100) or anti-rat polyclonal antibody TNFR2 (1:25). After three rinses in TBS the sections were incubated two hours at room temperature in TBS containing an anti-rat biotinylated antibody (1:100) and NGS (2%).

9.6.4 Active caspases 3, 7, 8 and 9

Active caspase 3

The sections were incubated in a solution containing PBS 0.1 M (pH 7.4) and FCS (10%) for 24 hours at 4 °C, and, the following day, rinsed three times and further incubated in PBS and Triton X-100 (0.5 %) for 45 minutes at room temperature.

These serial steps where then followed by an overnight incubation, at 4°C, in a solution containing PBS, an anti-rabbit polyclonal antibody raised against the cleaved form of capase 3 (1:100) and FCS (5%). After three rinses in PBS the sections were incubated with the secondary antibody in a solution of PBS containing a biotinylated anti-rabbit antibody (1:100) and NGS (4%) for 2 hours at room temperature.

Active caspase 7

The sections were rinsed for three times in solutions of PBS 0.1 M (pH 7.4) containing increasing amounts of NGS (1%, 5%, and 10%). After a 30 minute incubation at room temperature in PBS containing Triton X-100 (0.5 %), the sections were incubated for 48 hours, at 4 °C, in PBS containing an anti-goat polyclonal antibody raised against the active form of caspase 7 (1:50), Triton X-100 0.3% and NGS (5%). After three rinses in PBS the sections were incubated with the secondary antibody in a solution of PBS containing a biotinylated anti-goat antibody (1:100) and NGS (4%) for 2 hours at room temperature.

Active caspase 8

The sections were rinsed three times in PBS pH (0.1 M) 7.4 and then preincubated in a solution of PBS and H_2O_2 (0.1%) for 15 minutes at room temperature. After three rinses in PBS and NGS (1%) the cells were incubated overnight at 4 °C in a solution containing anti-mouse monoclonal antibody directed against the activated form of caspase 8 (1:50), Triton X-100 (0.3%) and NGS (5%). After this incubation the cells were rinsed three times in PBS and then incubated for 1 hour at room temperature in a solution of PBS containing a biotinylated anti-mouse antibody (1:200), Triton X-100 (0.2%) and NGS (3%).

Active caspase 9

Following a preincubation for 2 hours at room temperature in a solution 0.1 M PBS (pH 7.4) containing NGS (5%) the sections were incubated overnight at 4 °C in PBS containing an anti-rabbit polyclonal antibody raised against the cleaved form of capase 9 (1:100), Triton X-100 (0.05%) and FBS (2%). After incubation with the primary antibody, and three subsequent rinses in PBS at room temperature, the sections were incubated 2 hours at room temperature in PBS containing an anti-rabbit secondary antibody (1:200) and FBS (2%).

9.6.5 GluR 1-4

Before incubation with the specific antibodies directed against the GluR-1, 2, 4 subunits of AMPA receptor, the same experimental procedure was used. After three rinses in 0.1 M PBS (pH 7.4) containing FBS (5%) the sections were preincubated in PBS and then incubated in a solution of PBS containing Triton X-100 (0.5%) for 1 hour at room temperature.

In addition, for GluR3 immunostaining, a preincubation in a solution of PBS and albumin (0.5%) for 24 hours at 4 °C, in order to reduce the non-specific staining, was required.

GluR1

The sections were incubated overnight at 4 °C in a solution of PBS containing an anti-rabbit polyclonal antibody raised against GluR-1 (1:200), Triton X-100 (0.1%) and FBS 3%. After incubation with the primary antibody and three subsequent rinses in PBS at room temperature, the sections were incubated for 2 hours at room temperature in PBS containing an anti-rabbit secondary antibody (1:200) and FBS (3%).

GluR2

The sections were incubated overnight, at 4 °C in 0.1 M PBS containing an anti-mouse monoclonal antibody raised against GluR-2 (1:1000), Triton X-100 (0.1%) and FBS 3%. After incubation with the primary antibody and three rinses in PBS at room temperature the cells were incubated for 1 hour at room temperature in PBS containing a biotinylated anti-mouse

secondary antibody (1:2000) and FBS (4%).

GluR3

After three rinses in a solution 0.1 M PBS (pH 7.4) the sections were incubated overnight at 4 °C in a solution of PBS containing an anti-goat polyclonal antibody raised against GluR-3 (1:400), Triton X-100 (0.1%) and FBS (5%). After incubation with the primary antibody, and the following three rinses in PBS at room temperature, the cells were incubated for 2 hours at room temperature in a solution of PBS containing a biotinylated anti-goat secondary antibody (1:200) and FBS (3%).

GluR4

The sections were incubated overnight, the first two hours at room temperature and the following time at 4 °C, in PBS containing an anti-rabbit polyclonal antibody raised against GluR-4 (1:50), Triton X-100 (0.2%) and FBS 1%. After incubation to primary antibody and three rinses in PBS at room temperature, the cells were incubated for 2 hours at room temperature in PBS containing an anti-rabbit secondary antibody (1:100) and FBS (1%).

9.6.6 BDNF

For BDNF immunohystochemistry sections were pre-incubated 5 minutes at 4 °C in a solution 0.1M TBS (pH 7.4) containing TritonX-100 (0.4%) and then 90 minutes in a solution containing TBS TritonX-100 (0.4%), C_2H_5OH (20%) and H_2O_2 (0.6%). The sections where then incubated for 45 minutes at room temperature in a solution of TBS containing TritonX-100 (0.4%) and FBS (10%). The sections were then incubated overnight at 4 °C in a solution of TBS containing a biotinylated anti-rabbit polyclonal antibody directed against BDNF (1:1000), Triton-X100 (0.4%) and FBS (10%). After three rinses with TBS, sections were incubated for 1 hour at room temperature with a secondary anti-rabbit antibody (1:200) and FBS (10%).

9.6.7 EPOr

The sections were rinsed three times in 0.1 M PBS (pH 7.4) at 4 °C and then incubated for 40 minutes at 4 °C in a solution of PBS containing FBS (4%). The sections were then incubated overnight at 4 °C in PBS containing a rabbit polyclonal antibody directed against the c-terminal portion of receptor (1:200) and FBS (10%). After incubation with the primary antibody the sections were rinsed with PBS, three times for 5 minutes, and then incubated for two hours at room temperature in PBS containing biotinylated anti-rabbit antibody (1:200) and FCS (1%). In all immunohystochemical experiments the antibody visualization was carried out by reaction with 3-3'-diaminobenzidine (20 mg/ml in TBS 0.1 M (pH 7.8-8.3) in presence of 30% H_2O_2 (6 µl/1 ml)), the time of incubation ranged from few seconds to 5 minutes, depending on the strength of chromogen action produced for each single type of antibody. After this step the sections were washed twice with 0.1M TBS pH 7.4, maintained in a solution of NaCl 0.9% and then air-dried and coverslipped with DPX mountant (BDH Laboratory) for light microscopy analysis.

9.6.8 Densitometric analyses

Complex I staining, GLUR1-4 subunits and BDNF immunostaining were evaluated by densitometric analysis of single motor neurons of the ventral horns. This study was carried out in sections of cervical spinal cord (C2-C6) of wobbler mice and healthy littermates. For each animal, 5 slides with 4 sections each were digitally acquired and analysed using the image analyser AIS software (Imaging Research, St. Catharine's, Ontario, Canada) after software calibration with appropriate grey scale.

9.7 Histological staining

9.7.1 Nissl staining

Nissl staining is a well-characterized method to stain neurons. This procedure of staining is particularly specific for neurons in spite of their abundant content of cytosoplasmatic ribonucleic acids, which are intensively stained with cresyl violet.

Nissl staining was performed in sections of 30 μm of thick. The sections were obtained from perfused tissues of cervical spinal cord region. Nissl staining was done in wobbler mice at the presymptomatic, early symptomatic and late symptomatic stage and in healthy littermates. Serial sections, minimum 100, were processed to count the total number of motor neurons for each animal. At least 5 animals for each experimental group were utilized to compare the number of motor neuron in wobbler and healthy littermates.

The sections were placed in gelatinated glasses slides and, to obtain a good adherence of sections to slide's surface, the slides were hold for 12 hours in a drier at 4 °C.

The sections were then processed according to the protocol reported below:

- Incubation of slides in H_2O 1 minute
- Incubation of slides in C_2H_5OH 70% 5 minutes
- Incubation of slides in C_2H_5OH 96% 5 minutes
- Incubation of slides in C_2H_5OH 100% 5 minutes
- Incubation of slides in xylene 5 minutes
- Incubation of slides in C_2H_5OH 100% 5 minutes
- Incubation of slides in C_2H_5OH 96% 5 minutes
- Incubation of slides in C_2H_5OH 70% 5 minutes
- Incubation of slides in H_2O 1 minute
- Incubation of slides in cresyl violet 0.5% 6 minutes (cresyl violet is diluted in H_2O+ C_2H_5OH 20%, the best condition of staining were obtained by keeping the sections in this solution for 3 minutes.
- 10 rinses in H_2O

- 10 rinses in C_2H_5OH 70%
- Incubation of slides in C_2H_5OH 96% 3 minutes
- Incubation of slides in C_2H_5OH 96% e acetic acid 3% 20-30 seconds (the acetic acid rapidly reduced the staining intensity cautions have to be used to avoid the complete loss of cresyl violet staining in neurons). Usually the time of immersion in this solution ranged from 20" to 60". However the time of immersion was maintained constant when two different experimental groups were compared in the same experiment.
- Incubation of slides in C_2H_5OH 100% 2 minutes (check that C_2H_5OH 100% does not strongly reduced the staining)
- Incubation of slides in xylene 5 minutes

9.7.2 IN Situ End Labelling (ISEL) colorimetric assay

The in situ end-labelling (ISEL) method demonstrates DNA fragmentation, commonly regarded as a marker of apoptosis. This study was done in collaboration to Prof. A Migheli, Department of Anatomy, Pharmacology and Forensic Medicine, University of Torino, Italy. Deparaffinized sections, 5-10 µm of thickness, were digested in a mixture containing 0-2.5 µg/ml proteinase K for 15 min at room temperature. Alternative pre-treatment procedures were based on microwave oven heating (three 5-min cycles at 750 W). After quenching of endogenous peroxidase activity, sections were incubated in terminal deoxynucleotidyl transferase (TdT) buffer (25 mmol/liter Tris-HCl, 200 mmol/liter sodium cacodylate, 5 mmol/liter cobalt chloride) for 5 minutes and then in TdT solution (20 U of TdT enzyme and 1 nmol of fluorescein-11-dUTP, in 100 µl of TdT buffer) for 2 hr at 37C. After washing in a solution containing 1 x TBS, 0.3% Triton, and 2% BSA, the reaction was revealed incubating with anti-fluorescein sheep peroxidase-conjugated antibody (Boehringer–Mannheim) for 30 minutes at 37 °C and then in diaminobenzidine solution. Sections were serially mounted on Superfrost slides for ISEL staining. Before ISEL staining the sections were stained by using the Nissl method. In this way it was possible to observe both the motor neuron morphology and possible

alterations in DNA morphology.

9.7.3 Mitochondrial complex I staining

Quantitative hystochemical determination of mitochondrial complex I activity in the spinal cord was performed according to Jung et al. [Kozachuk, 1987]. Briefly, sections (18 μm thickness) of spinal cord were incubated in 0.1 M Tris-HCl (pH 7.4), 0.14 mM NADH, 1.0 mg/ml nitro blue tetrazolium (NBT), antimycin A (2μg/ml), 84 mM malonate and 2mM KCN. Hystochemical reactions were performed by incubating the slides for 40 min at room temperature. Rotenone (60 μM), a specific inhibitor of complex I, was added in a group of sections as negative control. After incubation, the sections were repeatedly rinsed and then laid on gelatinised slides. The activity of complex I in individual motor neurons was quantified as optical intensity of fixed regions of interest. The high degree of vacuolisation that occurs in the motor neurons of 12 week-old wobbler mice may introduce a possible source of error in the quantification. For this reason only motor neurons presenting a good morphology were chosen and the level of optical density was reported as the mean value obtained from several adjacent sections. At least 10 motor neurons for each slice of the spinal cord ventral horn were examined for each animal.

9.8 Imunoblotting

9.8.1 AMPA receptor subunits (GluR 1-4)

The study of immunoblotting for the AMPA receptor subunits GluR1-4 was done in collaboration with Dr. Fabrizio Gardoni, Department of Pharmacological Sciences, University of Milan, Italy. This study was performed by utilizing exclusively cervical spinal cord homogenates containing the fraction highly concentrated in pre and postsynaptic membranes and identified as postsynaptic density (PSD). To obtain PSD, the whole cervical spinal cord tissue was homogenized in ice-cold 0.32 M sucrose containing 1 mM Hepes, 1mM $MgCl_2$,1 mM $NaHCO_3$, 0.1mM phenylmethylsulfonyl fluoride, and a mixture of protease inhibitors (Complete, Roche Diagnostic, Milano) at pH 7.4 and centrifuged at 1,000 x *g* for 10 minutes. The supernatant was centrifuged at 3,000 x *g* for 15 minutes. The resulting pellet (containing mitochondria and synaptosomes) was resuspended in ice-cold 0.32 M sucrose containing 1 mM Hepes, 1 mM $NaHCO_3$, and 0.1 mM phenylmethylsulfonyl fluoride (buffer B); overlaid on sucrose gradient (0.85 to 1.0 to 1.2 M); and centrifuged at 82,500 x *g* for 2 h. The fraction between 1.0 and 1.2 M was diluted with buffer B containing 1% Triton X-100, stirred at 4 °C for 15 minutes, and centrifuged at 82,500 x *g* for 30 minutes. The resulting pellet was resuspended, layered on a sucrose gradient (1.0 to 1.5 to 2.1 M), and centrifuged at 100,000 x *g* for 2 h at 4 °C. The fraction between 1.5 and 2.1 M was removed and diluted with 150 mM KCl containing 1% Triton X-100. PSD were collected by centrifugation at 100,000 x *g* for 30 minutes at 4 °C.

Ten micrograms of PSD were then incubated overnight at 4 °C with the same antibodies utilized for immunocyto- and immunohystochemistry at the following concentrations, GluR1 (1:800), GluR2 (1:2000), GluR3 (1:3000) and GluR4 (1:500) in a solution of 0.1 M PBS containing 200 mM NaCl, 10 mM EDTA, 10 mM Na_2HPO_4 and 0.1% SDS.

The resulting proteins were resolved by SDS-PAGE, transferred onto polyvinylidene difluoride membranes, and blotted for 1 hour at room temperature in TBS containing 0.1% Tween 20 and 5% low fat dry milk. Detection was performed by chemiluminescence (ECL) with horseradish peroxidase-conjugated secondary antibodies (1:1500 dilution).

9.8.2 Glutamate transporters (GLAST and GLT1)

The antibodies were tested in homogenates obtained from the cervical spinal cord of wobbler mice and healthy littermates. The concentrations of the primary antibodies were for GLT-1-Ab (1:5000) and GLAST-Ab (1:4000).

The homogenates (about 5 micrograms for GLT-1, 10 micrograms for GLAST) were subjected to SDS-polyacrylamide gel electrophoresis (8% polyacrylamide gel), transferred to nitrocellulose membrane, and reacted with polyclonal antibodies.

The immunoreactive proteins were visualized with enhanced chemiluminescence (ECL, Amersham, US) using horseradish peroxidase-conjugated donkey antirabbit IgG (1: 2000).

Blots were incubated concomitantly with anti ß-tubulin (1:2000) using horseradish peroxidase-conjugated goat antimouse as secondary antibody (1:2000).

9.8.3 Densitometric measurement

The expression levels of the analyzed markers were evaluated by densitometric analysis using the image analyser AIS software (Imaging Research, St. Catharine's, Ontario, Canada), after digital acquisition of films and software calibration with appropriate grey scale. Values of density for each marker were normalized for the density values of actin (data not shown) in the same blot.

For quantitative evaluation of immunoreactivity, the optical densities were normalized to the optical density of ß tubulin in each animal.

9.9 Glutamate determination in plasma

These experiments were done in collaboration with Antonio Bastone at the Mario Negri Institute. Mice were killed by decapitation after overnight fasting, and blood samples were collected in heparinized tubes and diluted with 0.5% (w/v) sulphosalicylic acid solution (1:125 w/v). Samples were vigorously mixed and centrifuged. Aminoacid analysis was done on 50 µL supernatant fractions using a high performance aminoacid analyzer (AA Model 6300, Beckman Instrument Inc. Palo, CA), as previously described (Bastone A 1995).

9.10 [^{3}H]glutamate uptake

These experiments were performed in collaboration with Dr. Marco Gobbi at the Mario Negri Institute. Animals were sacrificed by decapitation and the spinal cord were rapidly removed, pooled and homogenized with a Teflon/glass homogenizer, in 10 vols of ice-cold 0.32 M sucrose, containing 1 mM EDTA, pH 7.4. The homogenate was centrifuged at 1,000xg for 10 minutes at 4 °C; the pellet was discarded and the supernatant (S_1) used to obtain the classical crude synaptosomal preparation (P_2) by centrifugation at 15,000xg for 30 minutes.

For the determination of glutamate uptake, pellets from P_2 were appropriately diluted in 0.32M sucrose, containing 1 mM EDTA, pH 7.4. (50 vols for P_2). 100 µL of homogenates from these preparations were added to tubes containing 800 µL of Krebs-HEPES buffer (5 mM Tris, 10 mM HEPES, 140 mM NaCl, 2.5 mM KCl, 1.2 mM K_2HPO_4, 10 mM glucose, pH 7.3); NaCl was substituted with equimolar choline chloride for non-specific uptake evaluation. Tubes were mixed and bath-warmed at 37 °C for 5 minutes. The uptake assay was started by the addition of 50 µL of 25nM [^{3}H] glutamate (Amersham, specific activity: 56 Ci/mmol) after dilution with cold L-glutamate at a final total concentration of 5µM. Tubes were incubated at 37 °C for 5 min and the uptake reaction was stopped by filtration with ice-cold choline buffer (3x2 ml) on nitrocellulose filters (Millipore, pore diameter: 0.65 µm). Filters were collected and the remaining radioactivity was counted with a LKB 1214 Rack Beta liquid scintillation counter (counting efficiency is about 60%). L-glutamic acid was obtained from Sigma. [^{3}H] glutamate uptake values were expressed as pmol/min/mg protein.

9.11 Mitochondrial activity

The following experiments (sections 9.11.1 and 9.11.2) were performed in collaboration with Prof. Daniela Curti, Department of Cellular & Molecular Physiological & Pharmacological Sciences, University of Pavia, Italy.

9.11.1 Oxygen consumption rate

QO_2 of somatic mitochondria in the tissue homogenate was measured by polarography with an oxygraph equipped with two thermostatic chambers set at 0.8 ml volume and 30° C and in a buffer of the following composition (in mM): KCl 110, mannitol 100, MOPS 20, glutamate 10, malate 1, EGTA 1, albumin 1.3 mg/ml, pH 7.0-7.2 (with HCl 1N). After the measurement of QO_2 in resting condition (basal QO_2), to stimulate ATP production and oxygen consumption ADP (200 µM) was added. The oxygen consumption rate through complexes I (NADH-ubiquinone reductase), II+ III and IV, was measured by using glutamate (10 mM) +malate (2.5mM), succinate (5mM) or artificial substrates (ascorbate 1.9 mM and N, N, N', N'-tetramethyl-p-phenylendiamine, TMPD, 1.5 mM) and inhibitors of the electron transfer chain (rotenone 4 µM; antimycin A 0.25 µM; KCN 5mM). Different substrates, cofactors and inhibitors were used to identify which step in the oxidative phosphorylation process was eventually impaired in the wobbler spinal cord. QO_2 was expressed in nmoles O_2/min/mg protein.

9.11.2 Spectrophotometric assays

Complex I was measured at 30 °C after two cycles of 20 s sonication (Misonix 2007) of the homogenate. The reaction mixture in a final volume of 1 ml was: 20 mM phosphate buffered solution (pH 7.5), 100 µM NADH, 1 mM KCN. The reaction was started by the addition of 50 µM ubiquinone-1 and read at 340 nm against a blank containing all the components except the starter. After 2 minutes rotenone 10 µM was added and the inhibited rate observed for a further 5 min. Complex I activity was calculated by subtracting from the overall rate, the rotenone non-

inhibited rate. Succinate dehydrogenase activity was evaluated at 500 nm and 30° C. The reaction mixture contained: 100 mM triethanolamine (HCl), pH 8.3, 0.5 mM EDTA, 2 mM KCN, 2 mM iodonitrotetrazolium chloride, 12 g/L Cremophor EL and 20 mM succinate, in a final volume of 1 ml.

Cytochrome-c oxidase activity (complex IV) was assayed at 550 nm (30° C) incubating the sample with 0.2 M TRIS-HCl buffer, pH 7.00; 0.1% n-dodecyl-D-maltoside and 25 mM reduced cytochrome-c. Cytochrome-c (50 mg) was reduced with ascorbate (15 mg) and eluted from PD-10 columns. The activity of citrate synthase (CS) was measured by the formation of 5-thio-2 nitrobenzoate from acetylcoA (100 µM), oxaloacetate (0.5 mM), 5,5'-dithiobis(2-nitrobenzoic acid) (0.2 mM DTNB) and Triton X-100 (0.5%) at 412 nm.

9.12 ChAT activity

ChAT was assayed using the method of Fonnum [477]. Spinal cords and muscles were dissected and homogenized in 0.1 w/v medium containing 0.3% Triton X-100. One µL of tissue suspension was added to 10 µL of incubation mixture containing 0.2 mM labelled acetyl donor ([^{14}C] Specific Activity 47 mCi/mL), 0. 25 M sodium phosphate buffer, 300 mM NaCl, 40 mM $MgSO_4$, 0.1 mM eserine phosphate, 8 mM choline chloride, 2% bovine serum albumin. Samples were vortexed and incubated for 10 min at 38 °C. After incubation, 9 µL of each sample was dispensed into vials containing 1250 µL of 0.25 M sodium phosphate buffer to stop the reaction, with 750 µL of kalignost (5 g of tetraphenylboron in 1000 mL of acetonitrile). Finally, the scintillation mixture (3 mL of toluene scintillator, Packard) was added. The vials were shaken slightly for 15 minutes and the radioactivity was counted using a liquid scintillation spectrometer LKB 1214 RACKBETA.

The protein content was determined using the Peterson's modification of Lowry's method.

ChAT activity was expressed as cpm/mg of tissue protein [337].

9.13 Statistics.

Data are shown as means ± S.D. Tukey's test analyses were used to compare biochemical and immunohystochemical values that are reported in chapter 11and 12. Behavioural tests results were compared using the two-way Anova analysis, with the Bonferroni's post-test. Statistical analysis for biceps weight and number of motor neurons was done with the one-way Anova with Bonferroni's post-test. All statistical analyses were carried out using the GraphPad Prism version 4.00 for Windows.

RESULTS

CHAPTER 10

In vitro RESULTS

10.1 BDNF/serum withdrawal induces apoptosis in primary cultures motor neurons

10.1.1 Introduction

During development of CNS the correct cytological architecture of tissues is guaranteed by a mechanism in which the redundant number of neurons, generated in the early phases of neurogenesis, is drastically reduced. The massive death occurring in embryonic life is regulated by the presence of different trophic factors, and neurons that fail to establish proper connections with their respective postsynaptic targets activates an apoptotic program of death. This process of selection is well known as neurotrophic factor competition [Clarke, 1976;Bennet, 2002;Levi-Montalcini, 1987;Oppenheim, 1975].

Although neurotrophic factor competition is a typical phenomenon related to the development, a correlation between neurotrophic factors and neuronal death is also detectable in adult brain. A link between the decrease of neurotrophic support and neurodegenerative diseases has been found in different *in vitro* and *in vivo* models of Alzheimer's disease, Parkinson's disease, Hungtington's disease and ALS [Canu, 2003;Cattaneo, 2001;Collier, 2003;De Yebenes, 2003].

Since BDNF has been reported to be the neurotrophic factor responsible for motor neuron survival in different models of ALS [Ikeda, 1995;Mitsumoto, 1994;Mitsumoto, 1994;Mitsumoto, 1999], in this study the vulnerability of embryonic rat spinal cord motor neurons chronically deprived (48 hours) of serum/BDNF was evaluated.

10.1.2 Experimental design

The effects produced by serum/BDNF deprivation were estimated both by measuring the rate of mortality, by SMI32 positive cells counting, and by investigating the presence of two distinct markers of apoptosis, DNA fragmentation, by Hoechst 33258 nuclear staining, and caspase-3 activation, by immunocytochemical staining using specific antibody directed against the cleaved form of caspase 3.

The viability of motor neurons the number of fragmented nuclei and the number of activated caspases were counted across four sides of the cover slip. For each slide four different fields were counted and the mean used for statistical analysis.

Other experiments were done following the procedures described in the chapter 8.

10.1.3 Results

Cultures of motor neurons, chronically deprived of serum/BDNF, showed a significant decrease of cell viability compared to motor neurons growing in basal conditions (control cells). The counting of SMI32 positive cells indicates that in mixed cultures the cell viability is reduced by 40% after serum/BDNF deprivation, and this difference was significantly higher in purified cultures, see figure 10.1. The values of the mean of motor neurons survival after serum/BDNF deprivation, expressed as percentage compared to their respective controls normalized to 100, are reported in tables 10.1 and 10.2.

	CTR	CTR- serum/BDNF
Motor neurons % SMI32 positive cells	**100±18.9**	**60±8.9****

Table 10.1 Percentage of motor neurons viability in mixed glia/neurons cultures after 48 hours of serum and BDNF deprivation. ** $p < 0.05$

	CTR	CTR- serum/BDNF
Motor neurons % SMI32 positive cells	**100±20**	**40±10*****

Table 10.2 Percentage of motor neurons viability in purified cultures after 48 hours deprivation of serum and BDNF deprivation. *** $p < 0.001$

Eighteen hours after serum/BDNF deprivation the percentage of apoptotic nuclei in purified motor neurons is significantly increased compared to control as revealed by DNA staining with Hoechst 33258 (see table 10.3).

	CTR	CTR- serum/BDNF
Fragmented nuclei % (Hoechst)	**100±9.2**	**312±21.3*****

Table 10.3 Percentage of fragmented nuclei in purified motor neurons after 18 hours of serum/BDNF deprivation; normalized to controls. *** $p < 0.001$

Representative nuclear staining is shown in figure 10.2. A marked increase of fragmented nuclei and the alteration of nuclear shape is evident in purified motor neurons following serum/BDNF deprivation, figure 10.2 (C, D) compared to control cells (Fig 10.2 A, B). Microphotographs at higher magnification clearly show as the nuclear integrity observed in control motor neurons (Fig 10.2 I) is lost after prolonged BDNF withdrawal (Fig 10.2 L).

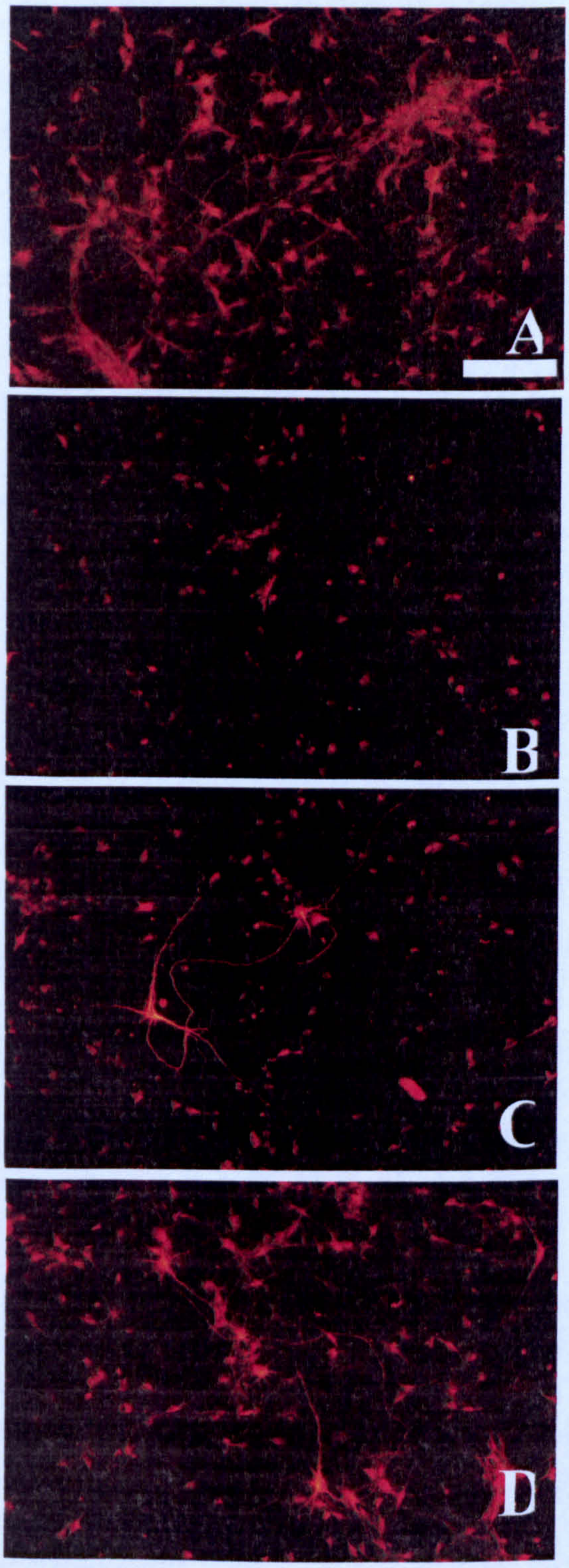

Figure 10.1 SMI32 staining in mixed cultures of motor neurons. Scale bar 200 μm. In basal condition it is possible to observe a high percentage of cells with a good morphology (A). Serum and BDNF withdrawal drastically reduced the total number of SMI32 positive cells (B), EPO alone produced a detectable growth of axons and dendrites (C) and significantly increased the total number of SMI32 positive cells after serum and BDNF deprivation (D).

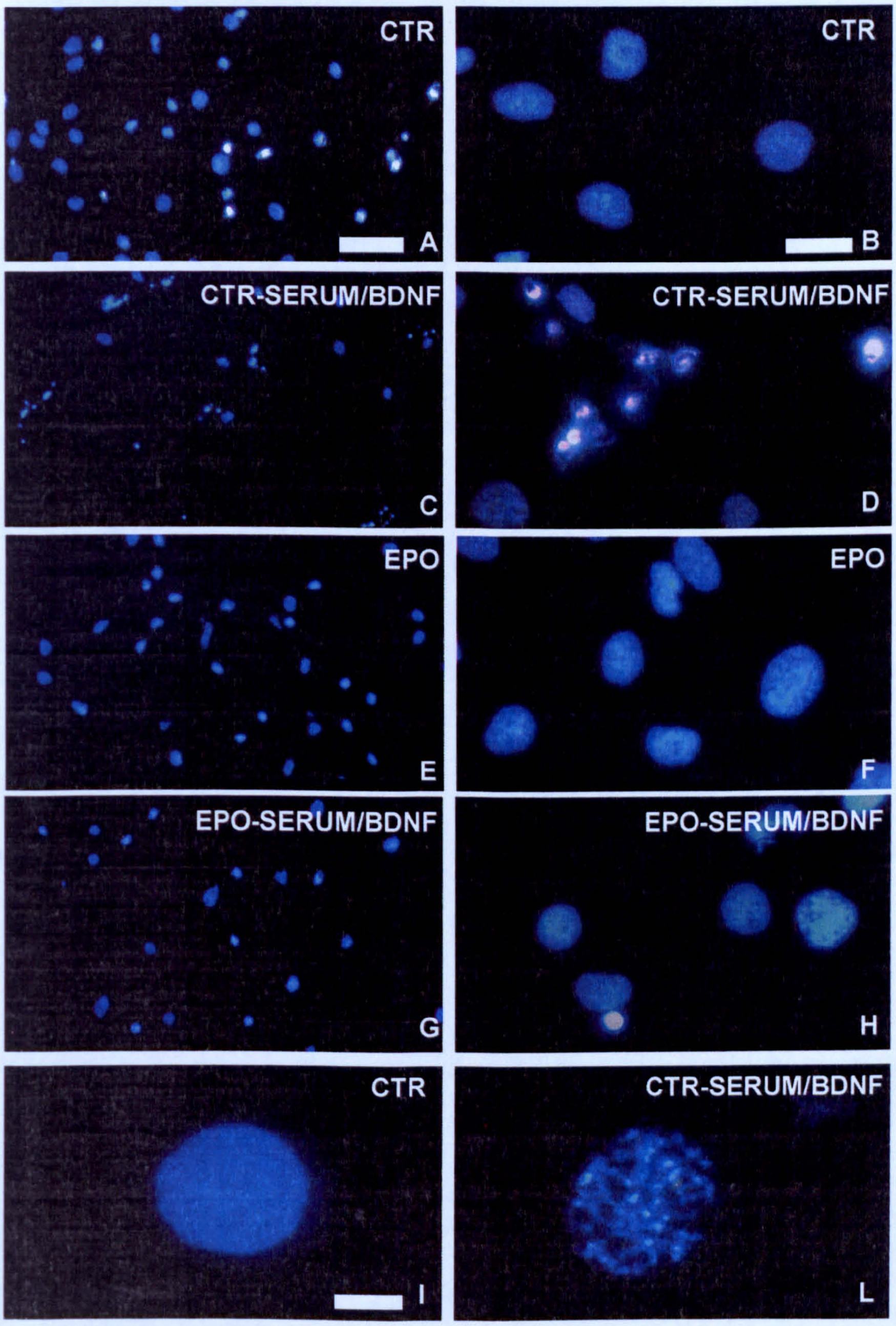

Figure 10.2 Hoechst staining in purified cultures of motor neurons. Scale bar, A, C, E, G 200 μm; B, D, F, H 40 μm: I, L 20 μm.In basal condition it is possibile to observe a high percentage of nuclei with a good morphology (A) and with a staining homogeneusly diffused in the whole surface (B and I). Serum and BDNF withdrawal drastically both reduced the total number (C) and the percentage of intact nuclei (D and L). EPO alone did not show marked differences

The apoptogenic role played by serum/BDNF withdrawal in purified cultures of motor neurons was further confirmed by the marked increase of active caspase 3 positive motor neurons number. Six hours after serum/BDNF deprivation, the number of caspase 3 positive motor neurons increased more than twofold compared to untreated cultures (se table

	CTR	**CTR- serum/BDNF**
Caspase 3 positive motor neurons (%)	**100±10.5**	**210±12.1*** **

Table 10.4 Percentage of active caspase 3 positive motor neurons in purified cultures after six hours of serum and BDNF deprivation; normalized to controls. *** $p < 0.005$.

A representative microphotograph of motor neurons stained for activated caspase 3 in purified cultures in basal conditions is shown in figure 10.3 A. Few cells were positive and the staining was moderate and bordered on the cell body. On the contrary, an increased number of caspase 3 positive motor neurons staining, and a more intense and distributed immunostaining was found in serum/BDNF deprived purified motor neurons (Fig 10.3 B). EPO treatment did not significantly reduced the number of caspase 3 positive cells compared to control (Fig 10.3 C) but greatly reduced the amount of caspase 3 motor neurons after 6 hours of serum and BDNF deprivation (Fig 10.3 D).

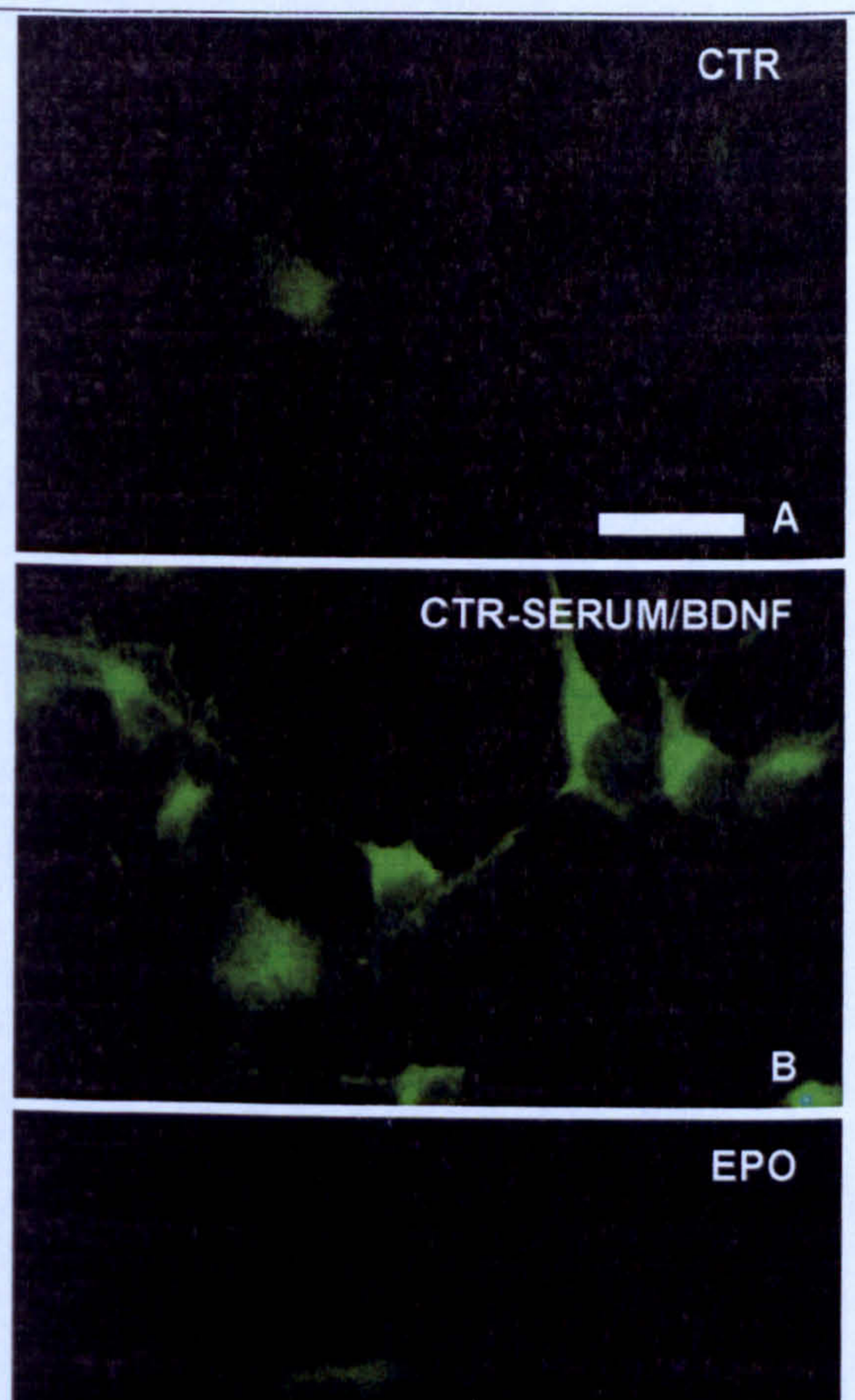

Figure 10.3 Active caspase 3 immunostaining in purified cultures of motor neurons. Scale bar 50 μm. In basal condition very few cells were positive against anti-active caspase 3 antibody (A). A marked increase of anti-active caspase 3 immunostaining was seen in purified motorneurons after 6 hours of serum and BDNF deprivation, in these cells it is easily detectable as the immunoreactivity is not only confined to the cytoplasm but it is also expanded at the arborizations and into the nucleus (B). EPO treatment produced a marked reduction in active caspase 3 motorneurons in purified cultures after six hours of serum and BDNF deprivation (C).

10.1.4 Discussion

As previously reported in other primary cultures of neurons deprived of NGF, GDNF and other neurotrophins [Kaal, 1997;Ikeda, 1995], the results obtained in primary cultures of motor neurons clearly demonstrates that the deprivation of trophic factors produces toxic effects [Bennet, 2002]. The significant decrease of survival in primary cultures of motor neurons that are reported both in *in vivo* and in *in vitro* studies, have confirmed the role of BDNF in preventing cell death [Henderson, 1993;Yan, 1992].

In this study I found that embryo rat primary cultures of motor neurons are killed by chronic deprivation, 48 hours, of serum and BDNF, and that, in purified cultures, they are more vulnerable than in mixed glia/neurons cultures. This small, but notable increase of cell resistance, observed in mixed glia/neuron cultures, could be in part due to the fact that astrocytes express and release important survival factor,as GDNF and CNTF. Regarding the role of GDNF in motor neuron survival, is important to note that, in the earliest phase of neuronal development of mammalian and avian species, GDNF withdrawal produced an almost complete loss of developing motor neurons. For this reason, to better understand the role of neurotrophic factors withdrawal in inducing apoptosis in motor neurons, purified cultures were exclusively investigated.

In addition, since the appearance of apoptotic markers is detectable earlier than motor neuron loss, and is not synchronous for each point of cell death pathway, the measurement of nuclear fragmentation was done 18 hours following serum/BDNF deprivation and the rate of caspase-3 activation was performed only after 6 hours from trophic factors starvation.

The correlation between BDNF and motor neuron death in ALS patients has been widely investigated from the early 90s. The possible aetiopathological role of neurotrophic factors withdrawal in ALS and, especially, the possible contribution of BDNF supply to counteract motor neuron loss in patients, was tested both in *in vivo* models of motor neurodegeneration and by different clinical trials (see sections 1.4.3.1 and 5.5.1.1). The results obtained were controversial and inconclusive: in wobbler mice BDNF was active, whereas in ALS patients all treatments failed.

The different outcomes produced by BDNF treatments in wobbler mice and in ALS patients could not be related to difference in BDNF crossing the BBB, since evidence of a BBB disruption in the wobbler mouse is not reported. More relevant might be the fact in animals, the treatment started at the early stage of the disease. Moreover, no relevant evidence about the mechanisms of motor neuron protection of BDNF was reported.

The results obtained from this study clearly demonstrates that in purified cultures of motor neurons, the deprivation of serum/BDNF leads to apoptosis.

10.2 Chronic treatments with AMPA and Kainate induce cell death in primary cultures of motor neurons by different mechanisms

10.2.1 Introduction

It has been previously reported that a chronic treatment for 48 hours with the three major glutamate agonists, AMPA Kainate and NMDA, produces a significant reduction of motor neuron viability in mixed glia/neuron cultures and that purified cultures of motor neurons are less vulnerable to glutamate agonists compared to motor neurons derived from mixed cultures [Comoletti, 2001]. In addition, both in purified and in mixed cultures a dose-response experiment for AMPA, kainate and NMDA were performed in order to obtain the concentration required to produce the 50% of cell death (EC50) after 48 hours of prolonged exposure for each excitotoxin [Comoletti, 2001].

In this study a more detailed characterization on the cell death mechanism(s) occurring in primary cultures of motor neurons exposed to excitotoxic stimuli was performed.

In a previous study, I demonstrated that both AMPA and kainate toxicity was almost completely reversed by the co administration of a selective AMPA receptor antagonist, NBQX [Comoletti, 2001]. This result suggested that AMPA and kainate share the same receptor to activate embryo motor neuron death after excitotoxic exposure. For this reason a detailed study of the cell death pathway(s) elicited by AMPA and kainate, at the concentrations needed to produce their EC50 after 48 hours, was performed. Moreover immunocytochemical experiments with antibodies directed against GLUR1-4 subunits in purified cultures of motor neurons was carried out to correlate the excitotoxic effects with the expression of AMPAR subunits. Since mixed glia/neuron cultures are closer to the physiological condition compared to purified motorneurons cultures, I decided to investigate these mechanisms in mixed glia/neurons cultures.

All the experiments were done following the procedures described in the chapter 8.

10.2.2 Results

10.2.2.1 AMPA receptor subunits expression

A marked immunopositivity for GluR1 was observed on cell bodies (fig 10.4A) with a more intense staining at the nuclear level (Fig 10.4 B). A low immunoreactivity for GluR1 was found along dendrites and axons, whereas stronger immunostaining was observed on the distal tract of axons and mainly at the synaptic endplate (Fig 10.4 C).

Immunofluorescence for GluR2 was found both in cell bodies and in their processes (Fig 10.5 A, B). Marked GluR 2 immunoreactivity was found in the distal part of axonal prolongation, which may correspond to the synaptic endplate (Fig 10.5 C). In contrast to GluR1 immunostaining, the nuclear area was unstained for GluR2 (Fig 10.5 D).

In purified cultures an intense immunoreactivity for GluR3 was seen (Fig 10.6 A). Similarly to GluR2, no nuclear staining was found but, interestingly, the nucleolus was stained using this antibody directed against GluR3 subunit (Fig 10.6 B). Dendrites and axons were positive for GluR3 immunostaining and a stronger immunopositivity was revealed at the branching points (Fig 10.6 C, D).

In purified cultures of motor neurons the intensity of the GluR4 immunostaining was markedly weaker compared to others subunits (Fig 10.7 A). GluR4 immunostaining was mainly detectable on cell bodies and in correspondence to the axon hillock (Fig 10.7 B). In the colours-scaled microphotograph of figure 10.7 C, where red staining represents the highest signal intensity and blue the lowest intensity (background), it is possible note that GluR4 positivity is more relevant in proximity to nuclear/cytoplasmic

area than in the cell surface. Neurites and dendrites were almost completely unstained with the exception of the zone close to dendritic branches, where a modest but detectable staining was observed (Fig 10.7 D).

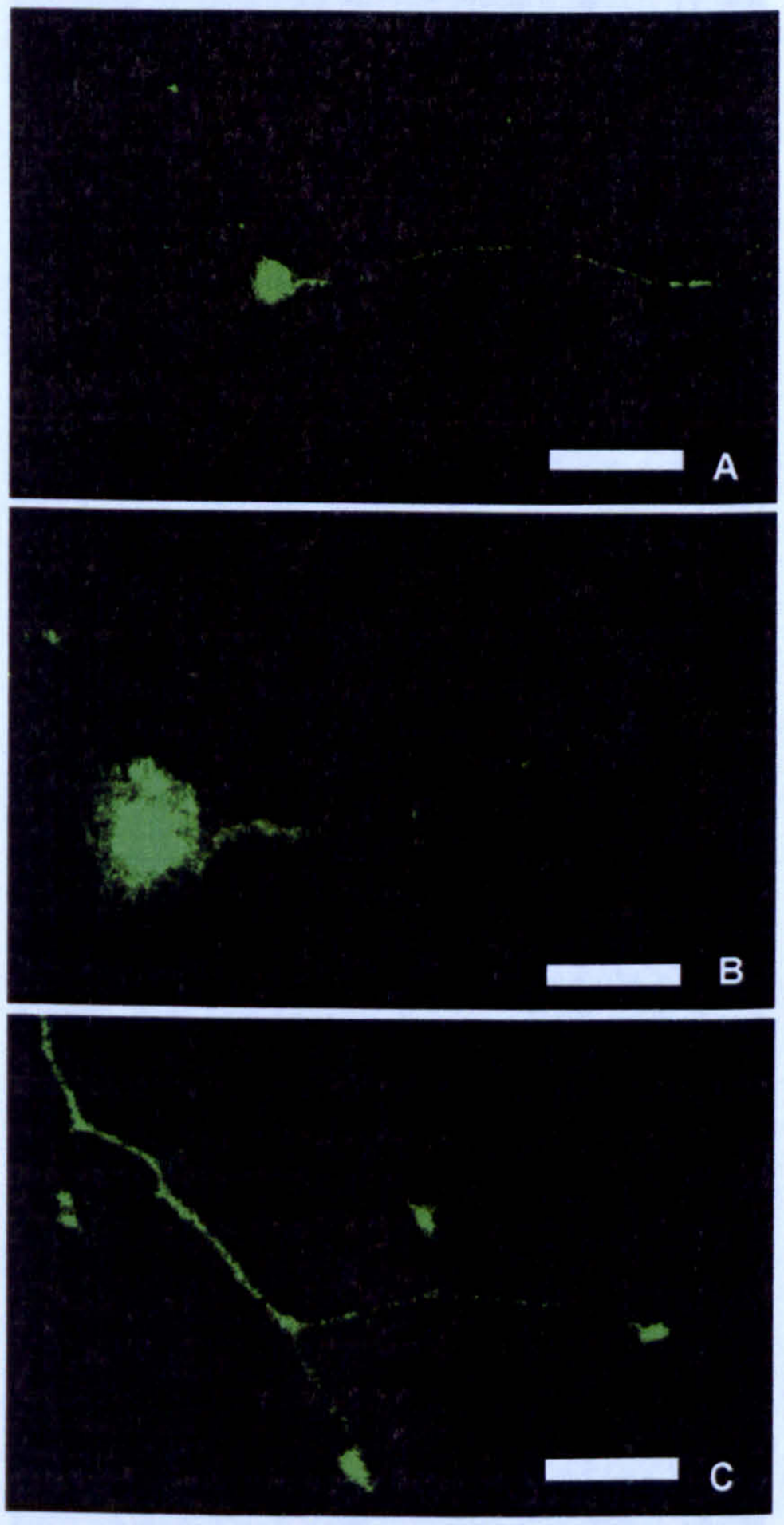

Figure 10.4 GluR1 immunostaining in purified cultures of motor neurons. Scale bar A, 100 μm; B 40 μm; C 25 μm. The pattern of GluR1 staining is detectable both in the cell body and, in lesser extent, at the periphery (A). In the cell body GluR1 it seems to be expressed in the membrane surface and in the cytoplasm (B), whereas in the ramifications of dendrites it results more concentrated in the growth cones (C).

Figure 10.5 GluR2 immunostaining in purified cultures of motor neurons. Scale bar, A-B 50 μm; C-D 25 μm. In lower magnification pictures (A and B) it is possible to note as GluR2 immunoreactivity covers the whole network of neuronal connections, perikarya, axons and dendrites. Moreover, as for GluR1, its expression resulted stronger in the distal zones, maybe in correspondence to growth cones (B). A particular of sell body clearly shows as nuclear surface is completely unstained for GluR2 (C).

Figure 10.6 GluR3 immunostaining in purified cultures of motor neurons. Scale bar, A100 μm; B 40 mm; C 50 μm; D 15 μm. In these cells GluR3 immunostaining is present both in cell bodies and in their arborizations (A). However, nuclear area is unstained with the exception of nucleolar zone (B). Neural network showed a milder but still evident immoreactivity for GluR3 (C) and , at higher magnification, it is possible to observe a synaptic zone highly positive for GluR3 immunostaining (D).

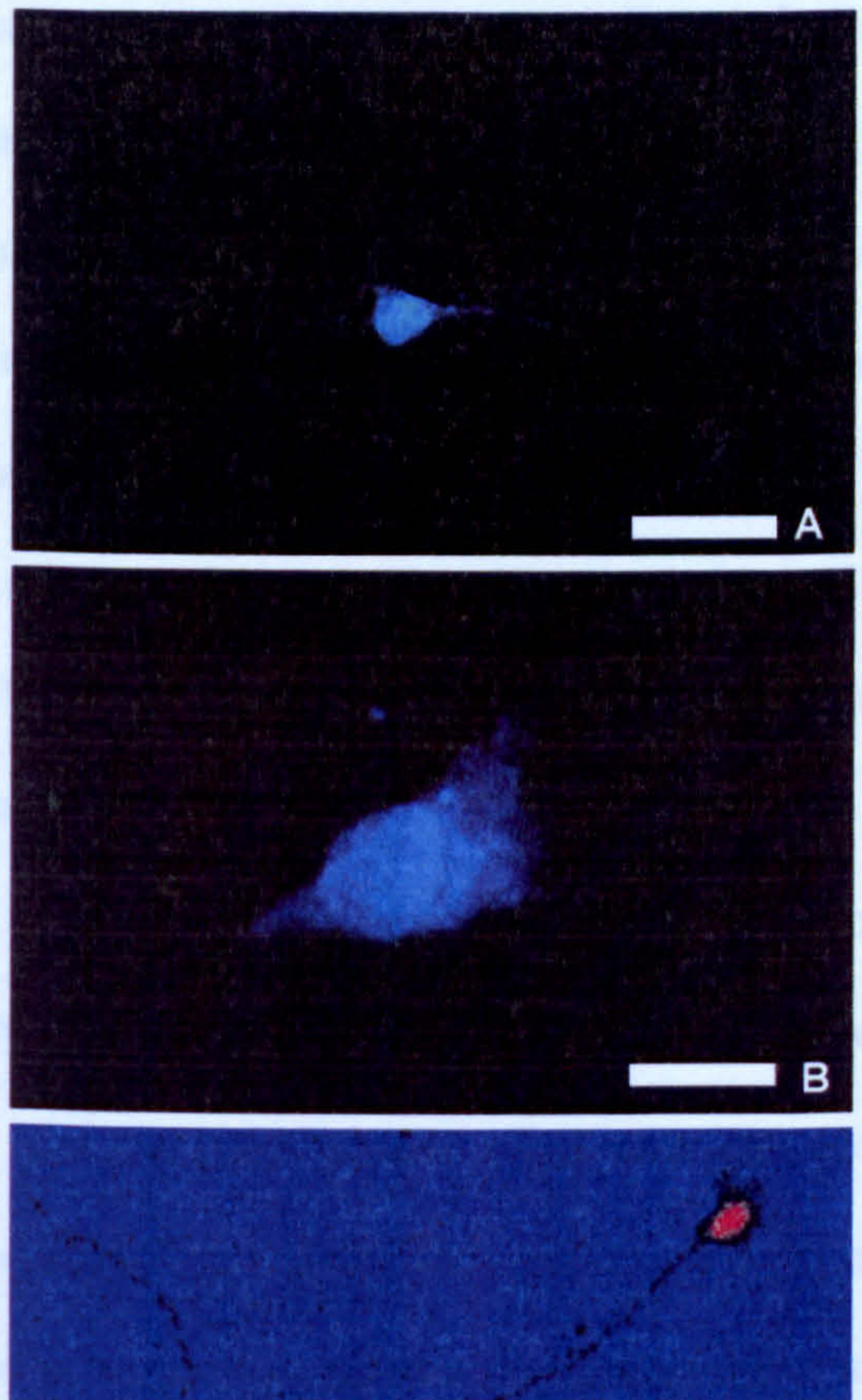

Figure 10.7 GluR4 immunostaining in purified cultures of motor neurons. Scale bar, A 50 μm; B, 40 μm; C 100 μm; D 20 μm. GluR4 immunoreactivity was greatly less intense compared to the other GluR subunits tested. GluR4 showed a low and circumscribing staining in the body cell and axon hillock exclusively (A and B). In the colours-scaled microphotograph it is possible note that GluR4 positivity is more relevant in proximity to nuclear/cytoplasmic area than in the cell surface (C). Neurites and dendrites were almost completely unstained with the exception of the zone close to dendritic branches, where a modest but detectable staining was observed (D).

10.2.2.2 AMPA and kainate toxicity: time-course

In order to select the appropriate time points to verify apoptotic markers, the time-course of AMPA- and kainate-induced motor neuron death was studied. After 6 hours of AMPA (1 μM) exposure a marked decrease of SMI32 positive motor neurons (35 ± 4% $p<0.01$) was found. After 6 hours, kainate (5 μM) lowered the percentage of SMI 32 positive cell only by 23 ±3%, $p<0.01$. A clear difference ($p<0.01$) between AMPA and kainate toxicity was observed 18 h after treatment: AMPA produced about maximal effect (64 ± 5%, $p<0.005$) while kainate-induced motor neuron death was only 34 ± 3% ($p<0.01$). After 48 hours of incubation the toxicity induced by AMPA was not different from that obtained after 18 h, while kainate produced 58 ± 5% motor neuron death.

These data clearly shown that, a short treatment with AMPA 1 μM produces a stronger effect on motor neuron cell death compared to kainate 5 μM. However, while AMPA induces a severe motor neuron death in the first few hours of incubation, reaching a maximal cell death at about 18 hours that is maintained until 48 hours, kainate produces a more modest and slower degree of motor neuron death, but progressively reduces the percentage of motor neurons even in the second half of treatment, from 18 to 48 hours, thus reaching similar levels of toxicity at the end of treatment (Fig 10.8).

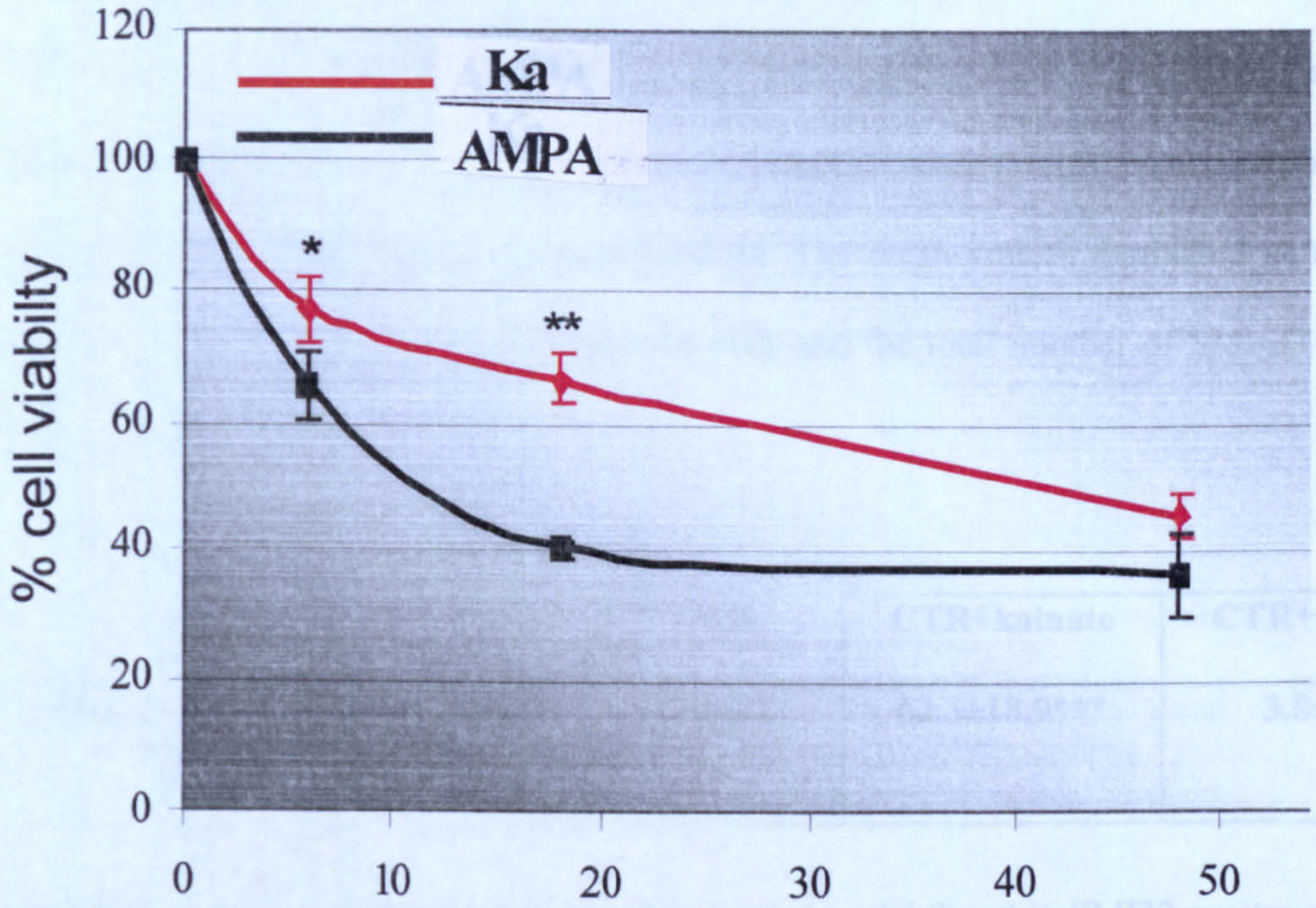

Figure 10.8 Cell viability of motor neurons in mixed glia/neurons cultures 6, 18, 48 hours after incubation with AMPA 1 μM or kainate 5 μM. The mean number of viable motor neurons measured in control conditions are normalized to 100 %.The rate of viability is expressed as percentage compared to controls.*$p<0.05$ **$p<0.001$ (Student's t-test).

10.2.2.3 Nuclear fragmentation and membrane permeabilization

Time course experiments allowed me to determine the appropriate times to verify apoptotic markers. To detect the possible involvement of apoptosis it was decided to stop the treatment after 6 hours to perform the immunocytochemical experiments for activated caspases 3 and -9, whereas 18 hours time point was used for DNA staining and mitochondrial transmembrane potential experiments.

While kainate highly increased the percentage of fragmented nuclei, AMPA treatment, although drastically reducing the total number of SMI32 positive cells, did not modify the percentage of fragmented nuclei in motor neurons. The mean values, expressed as the ratio between fragmented nuclei in SMI 32 positive cells and the total number of SMI 32 positive cells are reported in table 10.5.

	CTR	**CTR+kainate**	**CTR+AMPA**
% (fragm. nuclei in SMI32 + cells/ SMI32 + cells)	**4.1±0.6**	**62.3±18.9*** **	**3.8±0.9**

Table 10.5 Percentage of the ratio between fragmented nuclei found in SMI32 positve cells and the total number of SMI32 positive cells (SMI32 with fragmented nucleus/SMI32) in mixed glia/neurons cultures exposed to AMPA or kainate. ***$p<0.001$.

In order to detect if the kainate-induced motor neurons death was actually related to an apoptotic mechanism, double staining experiments using propidium iodide (PI) and SYTO 59, were performed (Fig 10.9 A-F). PI cannot penetrate the membrane of intact cells whereas SYTO 59 is a membrane permeable dye and stains nuclei. Necrotic cells exhibit cytoplasmic PI positivity (red) and nuclei that were both stained with PI and SYTO 59 positive (red+blue), whereas apoptotic cells were not PI positive and have condensed or fragmented nuclei stained with SYTO 59. Cells with regular sized nuclei stained with SYTO 59 represent healthy living cells.

In control cells the absence of PI positive cells is evident (fig 10.9 A). After 18 h of kainate exposure, several nuclei appeared condensed and fragmented; PI staining is absent or bordered the nuclear area (fig 10.9 C). In contrast, AMPA treatment produced massive PI staining in the whole cell and the nuclei resulted swollen and nucleic acids were scattered into the extracellular space (fig 10.9 E).

Representative microphotographs showing a higher magnification of nuclear area in motor neurons (controls (B), kainate-treated (D), AMPA-treated (G)) stained for Syto 59 and PI, are shown in figure 10.9.

These results evidenced that AMPA and kainate treated motor neurons undergo to a cell death process following two distinct morphologic patterns. Nuclear fragmentation, that was also quantitatively evaluated, and PI impermeability are the common features observed in kainate-treated motor neurons and suggest a process of death shared with apoptosis. On the other hand, the absence of nuclear fragmentation together with PI permeability and membrane disruption seems more likely to characterize a necrotic death or, at least, to exclude an apoptotic involvement in AMPA treated motor neurons.

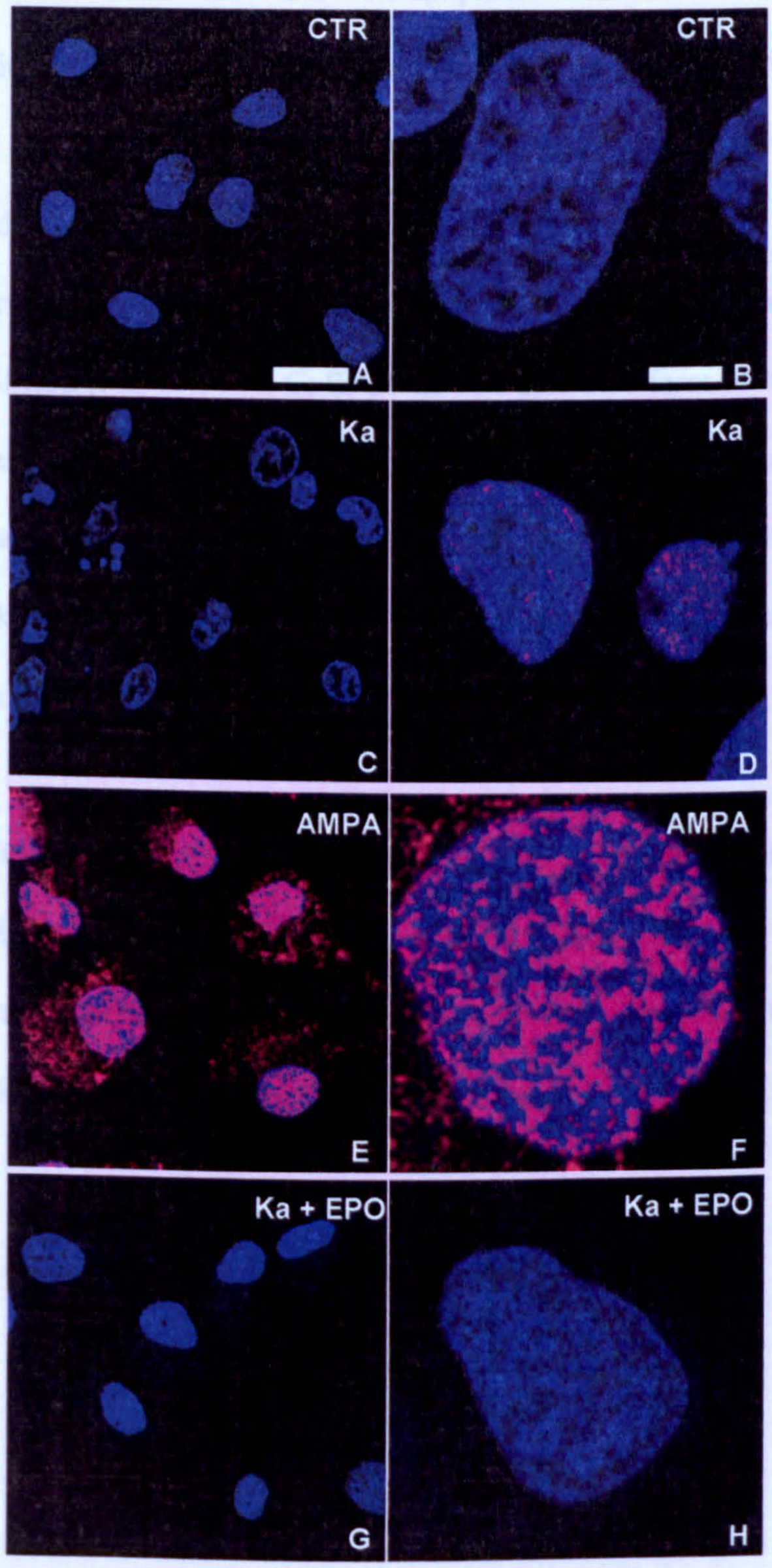

Figure 10.9 Syto59 (blue) and PI (red) double staining in purified cultures of motor neurons. Scale bar, A, C, E, G 40 μm. B, D, F, H 12.5 μm. Control cells exhibited a typical nuclear staining without either PI entry and DNA fragmentation (A and B). Kainate treated cells underwent to a massive DNA fragmentation and nuclear shrinkage thus remaining impermeable to PI (C and D). AMPA treated motorneurons showed a massive PI penetration accompanied by a nuclear enlargement (E and F). EPO completely counteracted the effect produced by kainate treatment (G and H).

10.2.2.4 Capase 3 and caspase 9 activation

To further confirm the selective involvement of apoptosis in motor neurons treated with 5μM kainate, but not with 1μM AMPA, immucytochemical experiments were performed using antibodies directed against the active form of caspase 3 and -9, the two caspases mainly involved in the cell death-signaling cascade active during apoptosis.

Mixed glia/neuron cultures, exposed to different conditions, were double-stained using specific antibodies against SMI32 (Fig 10.10 A, C, E, G) and the activated form of caspase 3 (Fig 10.10 B,D,F,H). Under basal conditions SMI 32 positive motor neurons showed a regular shape and size and very few activated caspase 3 positive cells were present (Fig 10.10 A,B). After 6 hours of treatment kainate significantly reduced the number of SMI 32 positive motor neurons and increased the number of cells expressing active caspase 3 cells (Fig 10.10 E,F), (Table 10.6).

Six hours after AMPA treatment the number of SMI 32 positive cells was reduced to a greater extent than after kainate treatment, and the remaining cells showed marked swelling. However, the amount of activated caspase 3 positive cells was very low, suggesting that a non-apoptotic mechanism of cell death is involved (Fig. 10.10 C, D), (Table 10.7).

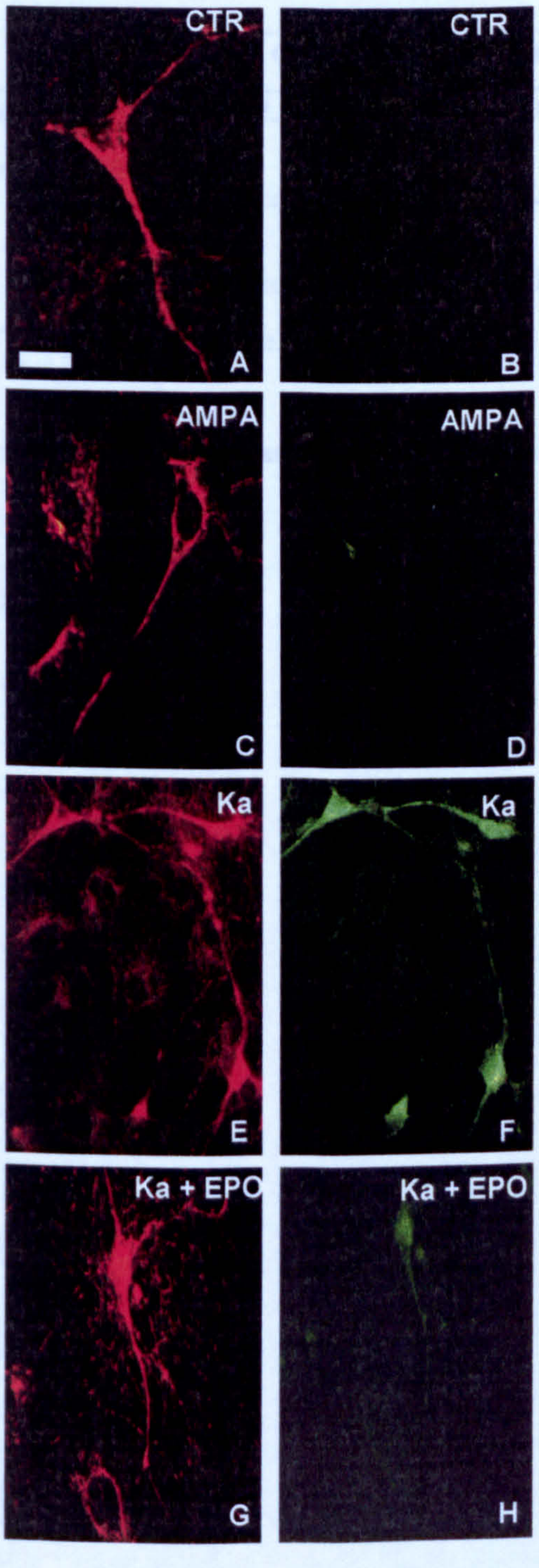

Figure 10.10 Double immunostaining, SMI32 (red A-H, C, E, G) - caspase 3 (green B, D, F, H), in mixed glia/neurons cultures. Scale bar 50 μm. At the basal conditions SMI32 positive neurons (A) resulted almost completely unstained for anti-active caspase 3 antibody (B). AMPA treatment produced a marked alteration of SMI32 positive neurons morphology but did not increase the active caspase 3 immunoreactivity (D). On the other hand kainate produced both a shrinkage of SMI32 positive neurons (E) and a intense activation of active caspase 3 immunostaining (F). EPO treatment partially reverted the effects of kainate (G and H).

The quantification of active caspase 3 positive motor neurons in these different conditions, expressed as percentage of the total number of SMI 32 positive cells, is reported in the table 10.6.

	CTR	CTR+kainate	CTR+AMPA
% (caspase 3 positive cells in SMI32 positive cells/ SMI32 positive cells)	**2.8±0.7**	**8.8±1.6****	**2.3±0.6**

Table 10.6 The percentage of SMI32 positive cells which expressed active caspase 3 in mixed glia/neuron cultures exposed to AMPA or kainate. **$p<0.005$.

Similarly to caspase 3, kainate-treatment increases the number of activated caspase 9 positive motor neurons (Fig 10.11 E, F) over the control condition (Fig. 10.11 A, B), but not in AMPA-treated cells (Fig. 10.11 C, D).

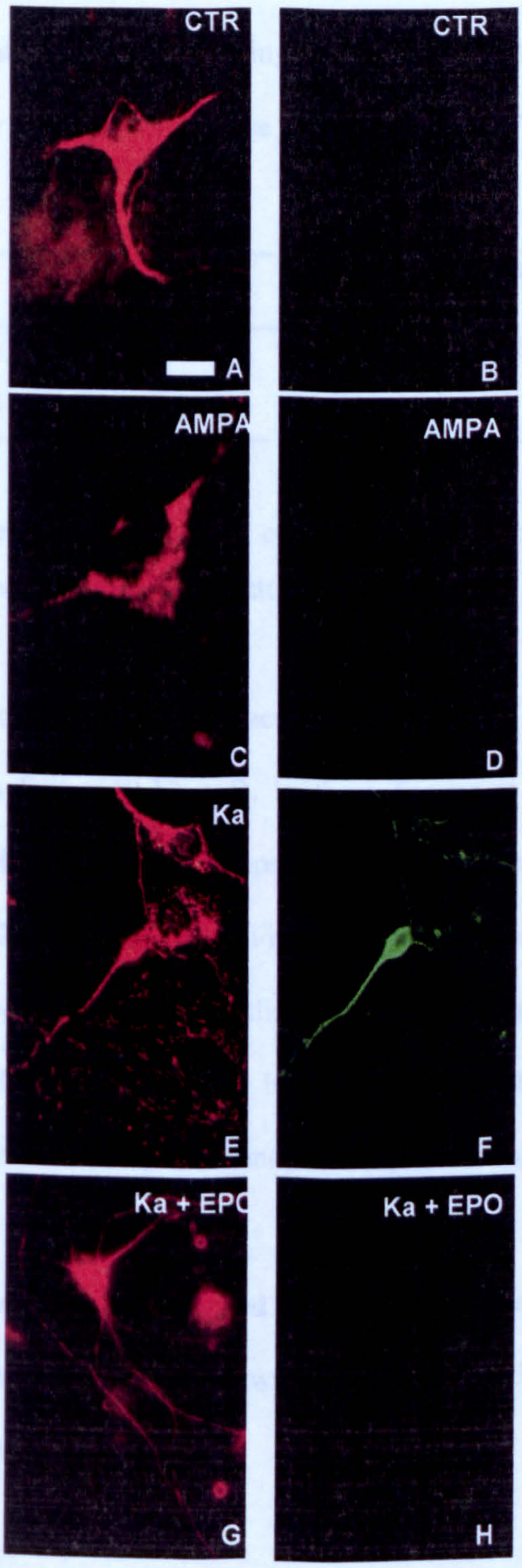

Figure 10.11 Double immunostaining, SMI32 (red A, C, E, G)- caspase 9 (green B, D, F, H), in mixed glia/neurons cultures. Scale bar 50 μm. At the basal conditions SMI32 positive neurons (A) resulted almost completely unstained for anti-active caspase 9 antibody (B). AMPA treatment produced a marked alteration of SMI32 positive neurons morphology but did not increase the active caspase 9 immunoreactivity (D). Kainate produced both a shrinkage of SMI32 positive neurons (E) and a intense activation of active caspase 9 immunostaining (F). EPO treatment completely reverted the effects of kainate (G and H).

The measurement of active caspase 9 positive cells, expressed as percentage of the total number of SMI 32 positive cells, is significantly increased in kainate treated motor neurons compared to the control. AMPA treatment, thus producing a marked decrease in SMI 32 positive cells, did not increase the number of caspase 9 positive cells (see table 10.7).

	CTR	**CTR+kainate**	**CTR+AMPA**
% (caspase 9 positive cells in SMI32 positive cells/ SMI32 positive cells)	**2.3±0.4**	**20.6±1.6*****	**1.9±0.2**

Table 10.7 The percentage of SMI32 positive cells which expressed active caspase 3 in mixed glia/neuron cultures exposed to AMPA or kainate ***p<0.001.

A more detailed pattern of distribution of activated caspases 3 and 9 proteins in SMI-32 positive cells is shown in figure 10.12 A-D. In these figures at higher magnification, it is possible to observe as SMI32 and active caspases 3/9 staining present a different pattern of distribution. While SMI 32 immunostaining (Fig. 10.12 A,C) is clearly detectable both in cell body and in neuronal arborizations and its distribution is homogenous and diffuse, active caspase 3/9 (Fig 10.12 B,D) immunostaining is mainly concentrated on the cytoplasm and is characterized by small areas in which immunopositivity is stronger compared to the rest of cytosol.

The results of the immunostaining for activated caspases 3 and 9 further confirm the hypothesis that, while kainate induces an apoptotic pathway of cell death, AMPA produces a process of death unrelated to apoptosis.

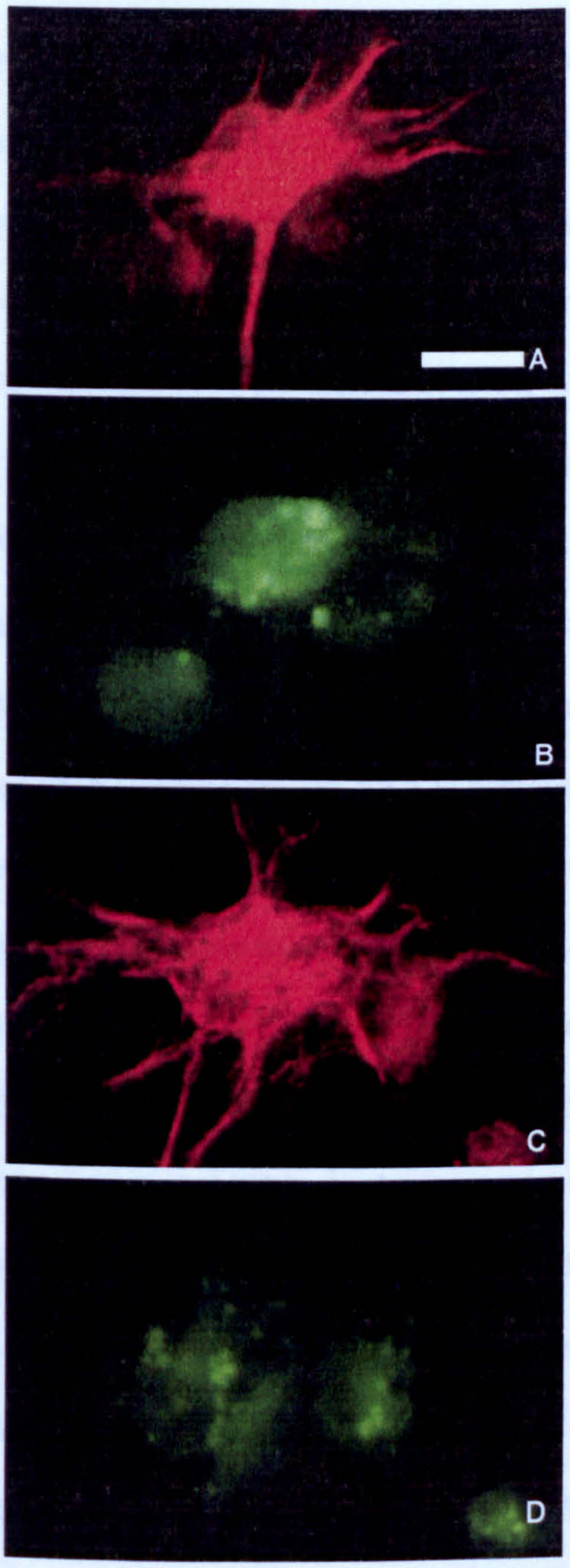

Figura10.12 Double immunostaining, SMI32 (red A, C) - caspase 3 (B) and -9 (D) (green), in mixed glia/neurons cultures. Scale bar, 20 μm. SMI32 antibody clearly shows a pattern of staining in which it is possible to observe the expression of not-phosphorylated neurofilaments both in the cell body and in the peripheral emergences of neuron (A and C). A different pattern of staining can be observed by processing the same cells with active caspase 3 (B) and -9 (D). Both caspases produced an immunoreactivity bordered in the cytoplasmic area. The immunoreactivity for active caspases is characterized by several perinuclear spots having a more intense brightening staining.

10.2.3 Discussion

In this study a model of excitotoxicity, where a comparable toxicity is induced in primary rat spinal motor neuron cultures by low concentrations of kainate or AMPA has been further investigated [Comoletti, 2001].

Before starting the experiments to evaluate the types of cell death associated to AMPA and kainate, the expression of four AMPAr subunits was investigated in purified cultures of motor neurons. The results revealed that, already at the embryonic E-14, rat motor neurons express the four AMPAr subunits [Carriedo, 1995], but the specific localization and distribution varies among each subunit. This result clearly demonstrate that all AMPAr subunits are expressed on motor neurons and also suggests that this receptor can mediate excitotoxic stimuli induced by glutamatergic agonists AMPA and kainate. In addition, electrophysiological recordings and experiments Co^{++} uptake measurements (see section 4.2.2.1) demonstrated that: I) in embryo rat motor neurons, AMPAr are functionally active and; II) motor neurons showing a strong immunopositivity for GluR2 are permeable to Ca^{++}. These results indicated that, despite the abundant expression of GluR2, a subset of AMPAr expressed in the cell surface of embryo rat motor neurons lack of GluR2 that allows the AMPA/kainate mediated Ca^{++} influx.

Time course measurement, performed in this study, suggests that, in this experimental condition, AMPA and kainate possess two different kinetics of death. While kainate produces a slow but long lasting trend of toxicity, AMPA rapidly reduces the motor neuron survival but this effect becomes smaller after 18 hours of treatment. On the basis of previous findings obtained in cerebellar and cortical neurons [Nicotera, 1997;Leist, 1997], in which necrosis was characterized as a fast and acute process while apoptosis requires a lower but more prolonged time of exposure to toxic agents, the different slopes of motor neuron death produced by AMPA and kainate suggested two distinct patterns of death.

The activation of the apoptotic pathway by kainate is clearly demonstrated by DNA fragmentation, nuclear condensation and activation of caspases 3 and 9. On the contrary, AMPA does not activate apoptotic motor neuron death, as indicated by active caspases immunocytochemistry and the double staining experiments using propidium iodide (PI) and

SYTO 59. The lack of DNA fragmentation and caspases activation, together with a marked nuclear swelling and cellular permabilization observed after AMPA treatment, clearly indicate a necrotic-like mechanism of motor neuron death.

In this experimental condition, AMPA and kainate act on the same receptor, as indicated by the fact that NBQX, a selective antagonist of the AMPA subtype of glutamate receptor, inhibits the motor neuron death induced by both AMPA and kainate [Comoletti, 2001]. Thus the differences observed in the cell death processes induced by two agonists are somewhat surprising. An important difference may be due to the different behaviour of AMPA and kainate in stimulating AMPA receptor. In fact, while AMPA (like glutamate) is a strongly desensitizing receptor agonist, kainate is a weakly desensitizing AMPA receptor agonist [Vandenberghe, 2000]. According to this electrophysiological evidence it is possible to hypothesize an intense, but short-lasting Ca^{++} entry after AMPA treatment, capable of triggering necrotic motor neurons death, and a longer-lasting influx of Ca^{++}, under kainate stimulation, that may induce apoptosis.

10.3 EPO selectively protects primary cultures of motor neurons from apoptotis

10.3.1 Introduction

In addition to promoting hematopoiesis [Semenza, 1991], EPO has protective effects in different *in vitro* and *in vivo* models of neurodegeneration. Although the molecular mechanisms involved in EPO activity are still not fully understood, several studies have shown that EPO acts by protecting neurons that are committed to die by apoptosis [Semenza, 1991]. In this study it has been already demonstrated that primary cultures of spinal motor neurons undergo apoptotic death if deprived for 48 hours of serum and BDNF (see section 10.1). The selective induction of apoptosis produced by serum/BDNF deprivation is therefore a valid tool to evaluate the possible protective and anti-apoptotic role of EPO in primary motor neurons. Purified cultures were used to assess the effectiveness of EPO.

Excitotoxicity has been shown to play an important role in neurodegenerative diseases comprising ALS [Rothstein, 1995;Mennini, 2004], mainly through activation of the AMPA/kainate receptors [Van Den Bosch, 2000]. In the section 10.2 it has been shown that, after exposure of motor neuron cultures for 48 h to equipotent concentration of glutamate agonists inducing about 50% cell death, Kainate induced apoptosis while AMPA reduced the viability via a non-apoptotic mechanism. The different processes of death elicited by the two excitotoxins not only allows to further verify the role of EPO as anti-apoptotic agent on motor neurons but also to evaluate if its protective effect could be observed also in other types of neuronal death.

10.3.2 Results

10.3.2.1 EPO receptor is expressed in embryo rat spinal cord motor neurons

Immunocytochemical experiments, performed both in purified and in mixed glia/neurons motor neurons showed a high immunopositivity for EPOr (Fig. 10.13 A). The staining was present on cell bodies and arborizations, and seems to be located both in the membrane and in the cytosol (Fig. 10.13 B). To assess if a repeated EPO treatment modifies the expression or the distribution of EPOr on motor neurons, purified cultures were treated with EPO (2.5 pmol/ml) for 5 days. The staining revealed no difference in the intensity and distribution of EPO receptors in EPO-treated cells compared to vehicle-treated cells (not shown). These results indicate that EPO treatment, under these experimental conditions, did not induce down- or up-regulation of its receptor. To evaluate the specificity of this antibody, the same immunocytochemical staining was repeated in cultures that had been pre-treated with an excess (20x) of the specific blocking peptide. As shown in figure 10.13 C, this procedure almost completely eliminated the EPOr immunostaining, thus confirming the selectivity of this antibody directed against EPOr.

This result first demonstrates that E-14 embryo rat motor neurons already express the EPOr in their cell surface.

10.3.2.2 Serum/BDNF deprivation and EPO

As shown in section 10.1.3, 48 hours of serum/BDNF deprivation, significantly reduced motor neuron viability. In motor neurons deprived of serum/BDNF, EPO (2.5 pmol/ml), pre-incubated for 72h and then added again during serum/BDNF withdrawal, completely reversed this toxicity (see table 10.8).

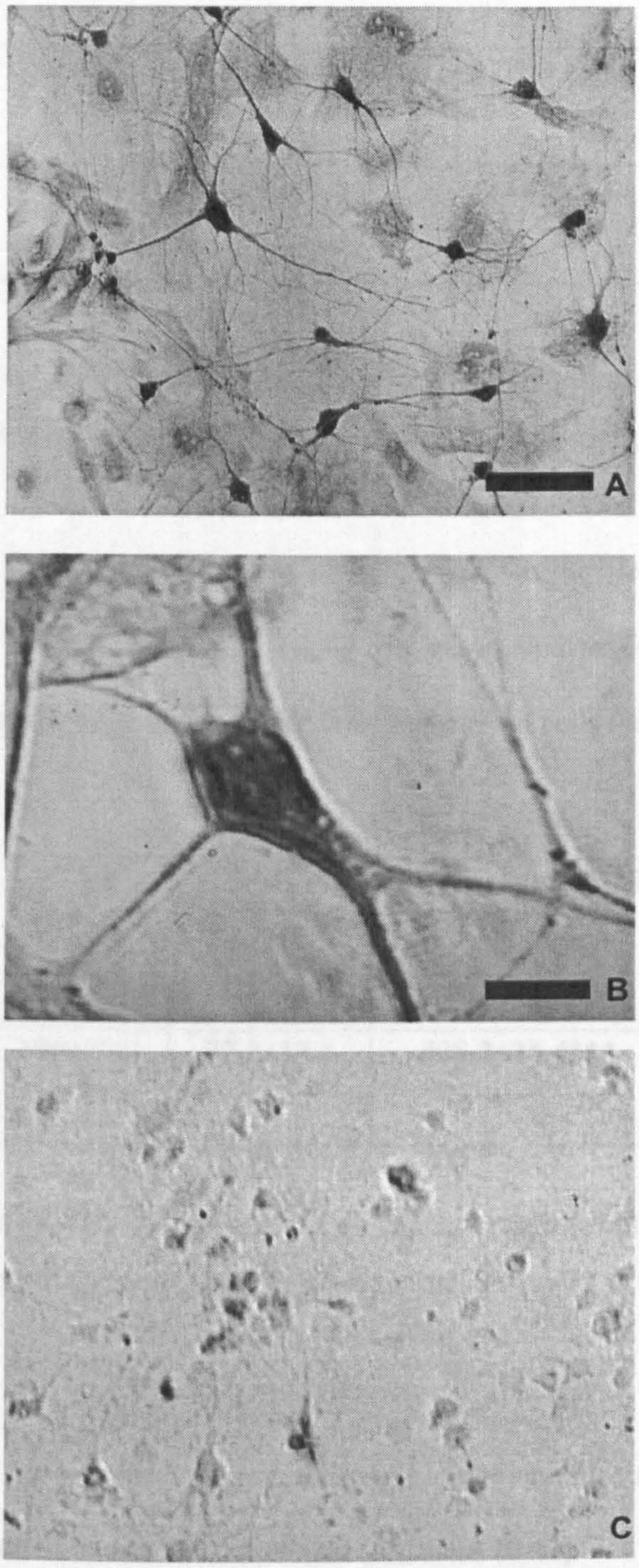

Figure 10.13 EPOr immunostaining : A mixed glia/neurons cultures; B purified cultures of motor neurons; C mixed glia/neurons cultures after incubation with a selective blocking agent of the antibody anti EPOr together with primary antibody. Scale bar, A,C 200 μm. B, 40 μm. As clearly shown in figure A EPOr is already expressed at the embryo stage and its distribution is not only confined into the cell bodies but it is also localized in their arborizations. The highest magnification (B) reveals the immunoreactivity of the perikaryon and in cell membrane. The specificity of antibody is confirmed by the lack of staining obtained by adding a blocking peptide together with the antibody (C).

	CTR	CTR-serum/BDNF	CTR+EPO	CTR-serum/BDNF+EPO
Motor neurons % SMI32 positive cells	**100±6.2**	**68.6±5.5****	**121.3±9.8**	**107.2±4.9**

Table 10.8 Protective effect of EPO treatment on percentage of motor neurons survival in purified cultures after deprivation of serum and BDNF; normalized to controls. ** $p < 0.005$

As shown in section 10.1.3 the percentage of apoptotic nuclei in purified motor neurons 18 hours after serum/BDNF deprivation significantly increased compared to controls. EPO reduced the percentage of apoptotic nuclei in serum/BDNF-deprived cells (see table 10.9).

	CTR	CTR+EPO	CTR- serum/BDNF	CTR-serum/BDNF+EPO
Fragmented nuclei % (Hoechst)	**100±19.3**	**77.3±12.1**	**338.2±26.4*****	**86.2±8.0**

Table 10.9 Protective effect of EPO in reducing the percentage of fragmented nuclei in purified motor neurons after 18 hours of serum/BDNF deprivation; normalized to controls. *** $p < 0.001$

In addition, the increase in the number of active caspase 3 positive motor neurons (see section 10.1.3), was completely reverted by the EPO treatment (see table 10.10).

	CTR	CTR+EPO	CTR- serum/BDNF	CTR- serum/BDNF+EPO
Caspase 3 positive motor neurons (%)	**100±9.6**	**82.9±10.9**	**277±22.3*****	**126±14.9**

Table 10.10 Protective effect of EPO in reducing the percentage of active caspase 3 positive motor neurons in purified cultures after six hours of serum and BDNF deprivation; normalized to controls. ** $p < 0.005$

Representative microphotographs showing the effect of EPO, both alone and following serum/BDNF deprivation, in reducing nuclear fragmentation and caspase 3 activation are shown in fig 10.2 E, F and G, H and in fig 10.3 C, D respectively.

It is important to note that, in purified motor neuron cultures, 5 days treatment with EPO produced a clear neurotrophic effect, increasing the neurite outgrowth and the number (not shown) and differentiation of motor neurons (Fig 10.14 A) compared to control motor neurons (Fig. 10.14 B). It is likely that a similar effect is related to a decrease in spontaneous apoptosis. The reduction below control values of the percentage of apoptotic nuclei and of the number of active caspase 3 positive motor neurons further support this concept.

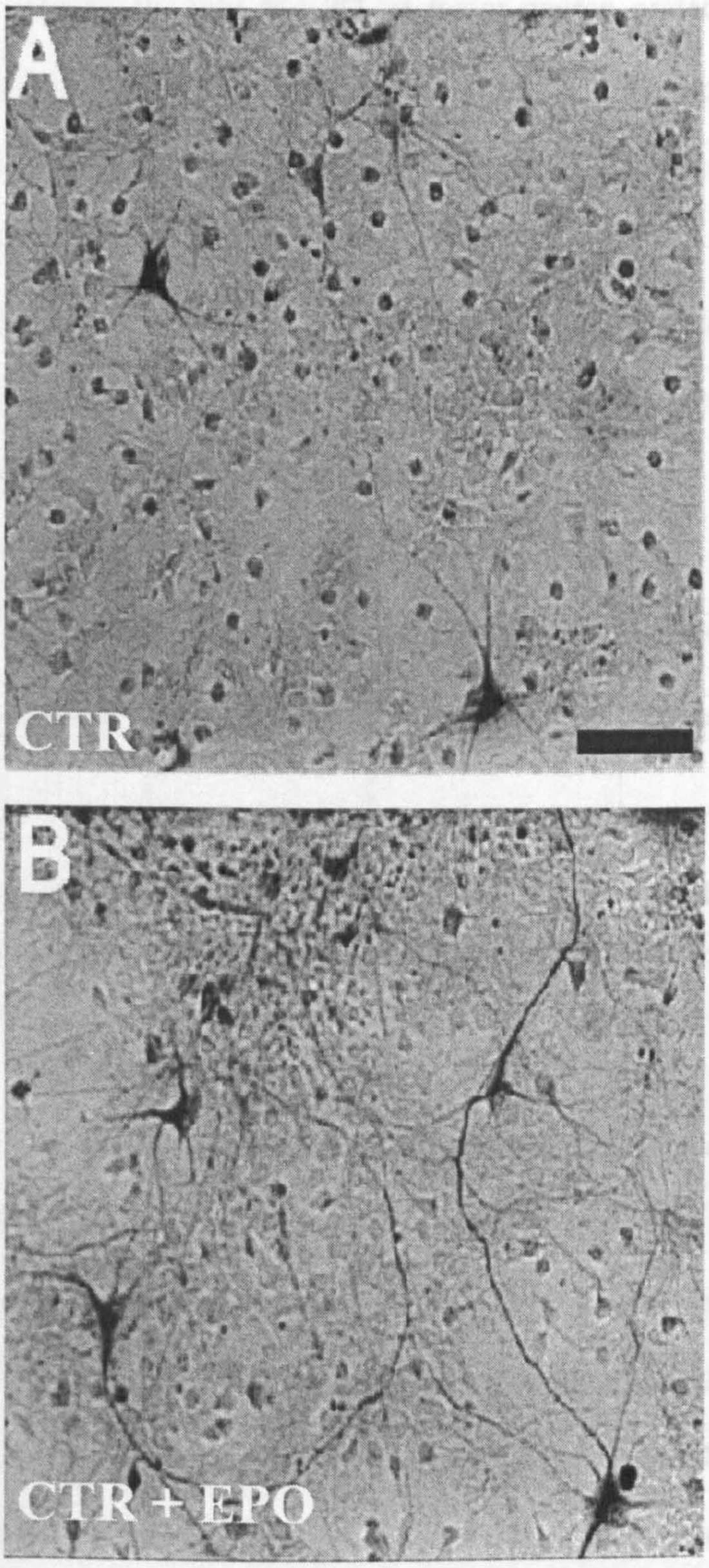

Figure 10.14 SMI32 immunostaining in mixed glia/neurons cultures. Scale bar, 100 µm.

Healthy motorneurons are shown in figure A. They have a high immunoreactivity for SMI32 in the cell body and also presented a weaker immunostaining in their small peripheral processes (axon and dendrites). EPOr treatment (5 days) clearly induced a growing of neuronal arborizations and developing of neuronal network. On the other hand, the size of the cell body does not seem increased in EPO-treated cultures.

10.3.2.3 EPO protects motor neurons exposed to kainate but not to AMPA

In order to evaluate whether the role of EPO on motor neuron protection was exclusively related to its anti-apoptotic component or may be also extended to other processes of death, the effect of EPO in preventing motor neuron loss in glia/neurons cultures exposed to AMPA or kainate was compared.

EPO significantly reduced the mortality of SMI32-positive neurons in mixed glia/neuron cultures following 48 hours to 5 μM Kainate exposure but did not rescue motor neurons upon 1 μM of AMPA exposure (see table 10.11).

	CTR	CTR+kainate	CTR+kainate +EPO	CTR+AMPA	CTR+AMPA +EPO
% of SMI32 positive cells	100±8.1	43.5±.3***	82.4±8.7	39.4±5.2***	43.1±10.2***

Table 10.11 Effect of EPO on SMI32 positive cell survival in mixed glia/neuron cultures exposed for 48 hours to kainate or AMPA. The values are expressed as percentage of mean number of cells measured in control wells (normalized to 100). ***$p<0.001$; *$p<0.05$

EPO alone significantly increased cell viability (128 ± 38% $p<0.02$). The effect of EPO in basal condition further confirms the neurotrophic properties of this compound.

The same EPO concentration protected motor neurons from kainate toxicity even if added simultaneously with kainate (without preincubation) or only during the 72 h pre-treatment (cell viability in control cells 100.0 ± 7.1% ; in kainate treated cells 54.2±8.7% $p<0.01$; in kainate treated cells +EPO 86.9±12.2 % n.s.). However, the maximum protective effect was obtained when EPO was present both in pre-treatment and during kainate exposure.

In order to exclude a potential, glia-mediated effect of EPO in motor neuron protection (either by activating glial factors or by reducing the toxicity of glial cells following exposure to excitotoxins) the action of EPO was also tested on purified motor neurons exposed for 48 hours to kainate 50 μm. A similar protection in purified cultures was found, indicating a direct action

of EPO on motor neurons (cell viability in control cells 100.0± 5.1%; in kainate treated cells 43.5±4.3% $p<0.01$; in kainate treated cells+EPO 74.6±2.7%).

In order to discriminate the molecular mechanism(s) underlying the protection of EPO on motor neurons exposed to kainate, the anti-apoptotic effect of EPO was then examined in detail by evaluating it at different points of apoptotic cascade.

10.3.2.4 EPO reduces nuclear fragmentation in kainate treated motor neurons

The anti-apoptotic effect of EPO against SMI32 positive cells in mixed glia/neurons cultures exposed to kainate for 18 hours was first evaluated by measuring the number of fragmented nuclei by Hoechst 33258 staining. The quantification of the mean number of fragmented nuclei, in EPO treated cultures exposed to AMPA or kainate and expressed as percentage of the ratio between fragmented nuclei in SMI32 positive cells and the total number of SMI32 positive cells, is shown in table 10.12.

	CTR	CTR+ kainate	CTR+kainate +EPO	CTR+ AMPA	CTR+AMPA +EPO
% (fragm. nuclei in SMI32 + cells/ SMI32 + cells)	3.3±0.9	76.2±8.9***	4.4±1.1	3.9±0.6	2.3±0.3

Table 10.12 Effect of EPO on DNA fragmentation in SMI32 positive cells. The experiments were carried out in mixed glia/neurons cultures exposed to AMPA or kainate. The values are expressed as the percentage of the ratio between the number of SMI 32 positive cells showing nuclear fragmentation and the total number of SMI 32 positive cells.

As expected, EPO did not influence the percentage of fragmented nuclei in motor neurons exposed to AMPA, further confirming that apoptosis is not involved in motor neuron death process induced by AMPA.

In figure 10.9 G, H it is possible to observe that, after kainate exposure, EPO treatment maintains the nuclear morphology, and the pattern of syto 59 staining resulted similar to control cells. In contrast to kainate, EPO did not modify the morphology of motor neurons exposed to AMPA (not shown).

10.3.2.5 EPO inhibits caspases 3 and 9 activation in kainate treated motor neurons

The selective protection exerted by EPO in cultures of motor neurons by inhibiting the kainate-induced apoptosis was further confirmed by detecting steps earlier than DNA fragmentation.

EPO treatment completely reverted the effects produced by kainate exposure (6 hours) by reducing the number of active caspase 3 positive cells and increasing the number of SMI 32 positive cells. In addition, EPO showed its anti-apoptotic effect also by reducing the natural cell death occurring in our culture condition, i.e. by reducing the number of caspase 3 SMI-32 positive cells compared to control. On the other hand, EPO did not modify the effect produced by AMPA (see table 10.13).

	CTR	CTR+ kainate	CTR+kainate +EPO	CTR+ AMPA	CTR+AMPA +EPO
% (caspase 3 positive cells in SMI32 positive cells/ SMI32 positive cells)	2.7±0.3	10.9±0.5***	2.9±0.4	2.5±0.3	2.9±1.3

Table 10.13 Effect of EPO in reducing the percentage of active caspase 3 SMI32 positive cells in mixed glia/neurons cultures exposed to kainate. The values as expressed as percentage of the ratio between active caspase 3 positive cells found in SMI32 positive cells and the total number of SMI32 positive cells (SMI32 cells showing caspase 3 positivity/SMI32) in mixed glia/neurons cultures exposed to AMPA or kainate. ***$p<0.001$

Representative microphotographs showing the effect of EPO in counteracting the activation of caspases 3 immunostaing in SMI32 positive cells are reported in figure 10.10 G,H.

Similarly, EPO treatment significantly decreased the number of activated caspase 9 SMI-32 positive cells after 6 hours of exposure to kainate motor neurons and EPO alone reduced this number under control conditions (see table 10.14).

	CTR	CTR+ kainate	CTR+kainate +EPO	CTR+ AMPA	CTR+AMPA +EPO
% (caspase 9 positive cells in SMI32 positive cells/ SMI32 positive cells)	**3.5±0.7**	**20.5±3.5*****	**4.7±1.2**	**1.5±0.7**	**2.7±0.6**

Table 10.14 Effect of EPO in reducing the percentage of active caspase 9 SMI32 positive cells in mixed glia/neurons cultures exposed to kainate. The values as expressed as percentage of the ratio between active caspase 9 positive cells found in SMI32 positive cells and the total number of SMI32 positive cells (SMI32 cells showing caspase 9 positivity/SMI32) in mixed glia/neurons cultures exposed to AMPA or kainate. ***p<0.001

Representative microphotographs showing the effect of EPO in counteracting the increase of immunopositivity in SMI32 positive cells is reported in figure 10.11 G, H.

10.3.3 Discussion

The present study demonstrates for the first time that, in the primary cultures of motor neurons, EPO counteracts the apoptotic cell death induced by kainate or serum/BDNF deprivation, but is inactive on non-apoptotic cell death induced by exposure to AMPA under the same experimental conditions.

In addition, EPO exerts its neuroprotective effect both when motor neurons are purified or maintained in mixed glia/neurons cultures, suggesting a direct effect of EPO on motor neurons rather than a modulator effect exerted via the glial cells.

Furthermore, immunoreactive EPOr were detected in purified cultures of motor neurons, and did not show any down- or up- regulation after 5 days exposure to EPO treatment or following AMPA or kainate treatment. These findings are in agreement with previous studies reporting the presence of EPOr in human and rabbit spinal cord motor neurons. and offers the possibility to perform treatment with EPO also for chronic neurodegenerative diseases of the spinal cord, like ALS.

Moreover, it is important to note the highest neuroprotective effect after kainate exposure was obtained after 72 hours pre-treatment + 48 hours treatment by EPO. However, partial protection is still obtained when EPO is present only during pre-treatment, or when EPO was added only during kainate exposure without pre-treatment. These data suggest that, while activation of survival kinases by EPO in hippocampal neurons is a rapid process [Siren, 2001] the neuroprotective effect in motor neurons takes longer time, possibly requiring induction of gene transcription.

The effects of EPO in *in vitro* cellular models of excitotoxicity is somewhat controversial: protection is reported in cultured hippocampal and cortical neurons against glutamate exposure [Bernaudin, 1999] and in cortical neurons exposed to

NMDA [Bernaudin, 1999]. However, another paper reports that EPO protects cortical neurons against AMPA-, but not glutamate- or NMDA-induced toxicity [Sinor, 2000]. The present data indicates that EPO protects against kainate but not AMPA in cultures of motor neurons. These discrepancies might be related to the type of death induced by: i) the different excitotoxins that

were utilized, ii) their concentration iii) the different time exposure and, iv) the different cell models used.

The EPO concentration (2.5 pmol/ml) I used in this study is relatively high compared to those reported to be effective in other *in vitro* studies on primary neurons (0.3-1 pmol/ml). However, the concentrations of glutamate agonists required for motor neuron death are higher compared to other neuronal cultures [Siren, 2001].

The lack of caspase 3 and 9 activation in motor neurons exposed to kainate are treated with EPO, further confirms previous findings obtained in cortical neurons [Ruscher, 2002], and also indicates that EPO is capable of counteracting motor neuron apoptosis by inhibiting a step before caspases cascade cell signalling. For this reason, the upstream events of the intrinsic apoptotic pathway, i.e. the release of cytochrome-c, the mitochondrial membrane potential and the role of PTP, were then investigated.

10.4 EPO exerts its anti-apoptotic effect on primary cultures of motor neurons by inhibiting the mitochondrial depolarization produced by kainate treatment

10.4.1 Introduction

Both in death receptor- (extrinsic) or mitochondrion-dependent (intrinsic) apoptosis the recruitment and activation of adapter molecules is a key event to activate caspases and to propagate the apoptotic signalling pathways (see sections 2.2.1 and 2.2.2). In death receptor-mediated apoptosis, engagement of death receptors leads to the formation of the DISC containing death receptors, adaptor proteins, caspase 8 and 10. In mitochondrion-dependent apoptosis, the release of cytochrome-c into the cytosol results in the formation of apoptosome containing cytochrome-c, Apaf-1 and caspase 9.

Because neurotrophic withdrawal and glutamate-induced excitotoxicity appear more related to this latter process, and in view of the marked increase of caspase 9 positive cells that in kainate treated motor neurons (see section 10.2.2.4), the role of EPO in preserving mitochondrial activity was studied in purified cultures of motor neurons exposed to kainate or AMPA.

All experiments were performed following the procedures described in chapter 8.

10.4.2 Results

10.4.2.1 Cytochrome-c release

In purified cultured motor neurons, cytochrome-c release was detected by performing a double staining experiment with a mitochondrial dye (Mito Tracker) and an antibody directed against cytochrome-c.

Cultures of purified motorneurons were treated with 50 μM kainate for 4 hours; this concentration was utilized since it has an equipotent effect in inducing motor neuron death as kainate 5 μm in mixed glia/neurons cultures after 48 hours of treatment [Comoletti, 2001].

In contrast to AMPA treated motor neurons, in which a loss of mitochondrial integrity and a consequent loss of cytochrome-c immunoreactivity is already detectable after 4 hours of treatment (Fig 10.15 C, D), both in control and in kainate treated cells mitochondrial integrity was seen (Fig 10.15 A,E). However, in a large percentage (quantification not done) of kainate treated motor neurons, cytochrome-c staining did not overlap with mitochondria, but homogenously diffused throughout the whole cytoplasm (Fig 10.15 B.D). EPO treatment markedly reduced the spreading of cytochrome-c staining, in almost all motor neurons exposed to kainate and treated with EPO (Fig 10.15 G, H).

This evidence supports the hypothesis that kainate produces apoptosis by modifying mitochondrial activity and thus allowing the caspase-cascade activation by cytochrome-c release and consequent apotosome formation.

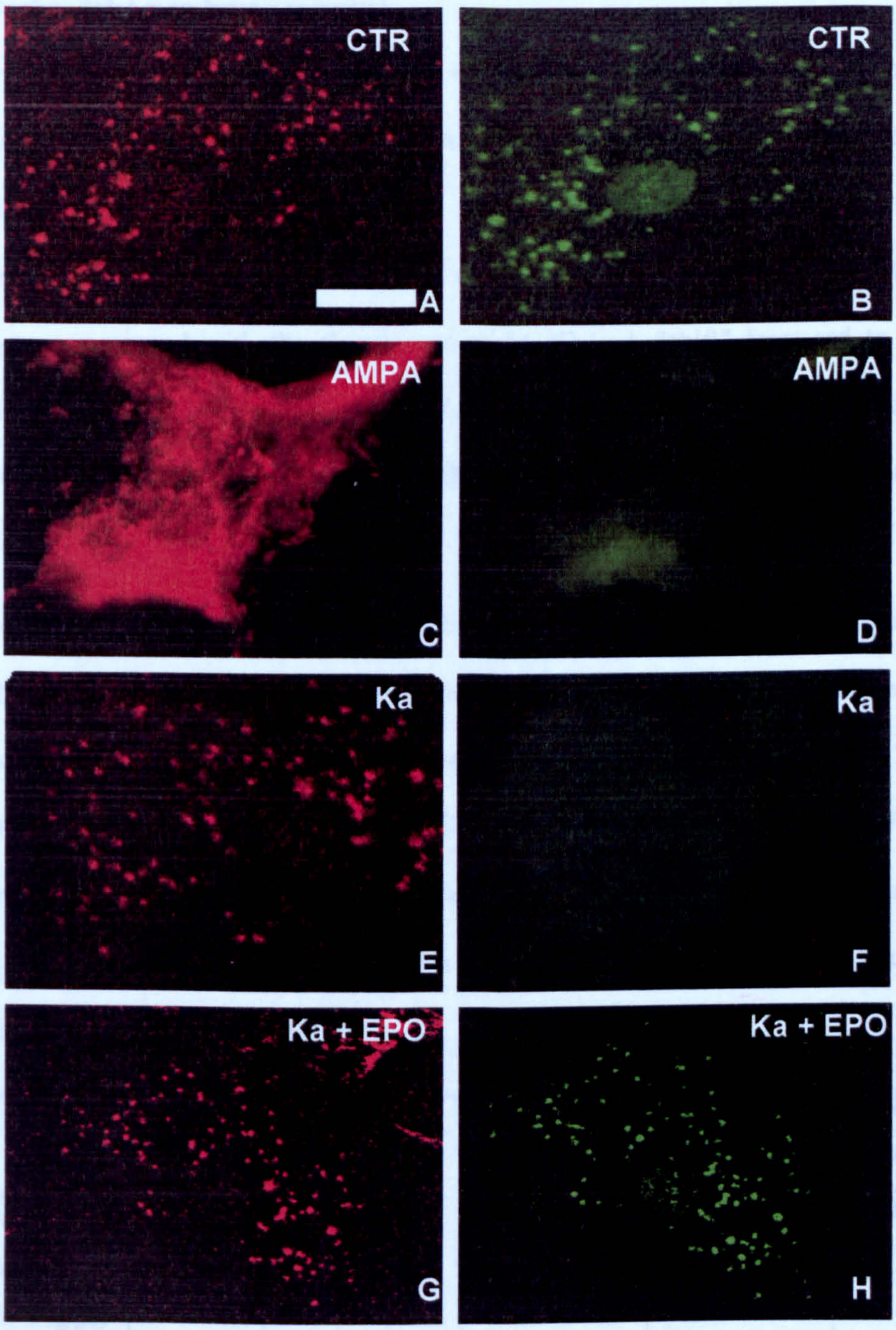

Figure 10.15 Double staining, Mito tracker (red A, C, E, G) and cytochrome-c antibody (green B, D, F, H), in purified cultures of motor neurons. Scale bar, 15 μm. A representative pattern of intra-mitochondrial localization of cytochrome-c in motorneurons exposed to the basal conditions is shown in figure A and B. In control cells it is in fact possible to observe a clear overlapping between red –mitochondrial- staining (A) and green –cytochrome c- immunostaining (B).In contrast, AMPA treated motorneurons showed a collapse of mitochondria (C) with a dispersion of cytochrome-c (D). Kainate treated motorneurons, thus conserving mitochondrial integrity (E) induced the release of cytochrome-c in the cytoplasm (F). EPO treatment markedly counteracted the effects produced by kainate (G and H).

10.4.2.2 Mitochondrial membrane potential

In order to verify if EPO counteracted the decay of mitochondrial activity caused during cell death, the functional expression of this organelle was analyzed by evaluating its state of energy and, indirectly, its $\Delta\Psi_M$.

Purified cultures of motor neurons were incubated with kainate (50 μM) or AMPA (10 μM) for 18 h. $\Delta\Psi_M$ was measured with the fluorescent probe JC-1. A "shift" from red to green fluorescence was observed upon depolarisation of mitochondria (see section 8.6). Red staining is associated to energised mitochondria while green staining represents depolarized mitochondria.

The quantitative measurement of $\Delta\Psi_M$ in control, kainate and AMPA treated motor neurons, with or without EPO, is expressed as degree of mitochondrial energisation (ratio between red fluorescence intensity, FI_{red} at 590 nm, and green fluorescence intensity, FI_{green} at 527 nm). Compared to control cells, kainate exposure significantly reduced the $\Delta\Psi_M$ while AMPA did not. EPO treatment reversed the depolarizing effect produced by kainate but did not increase the $\Delta\Psi_M$ in AMPA treated motor neurons. The levels of mitochondrial energisation in control and in treated cells are reported in table 10.15

	CTR	CTR+kainate	CTR+kainate +EPO	CTR+AMPA	CTR+AMPA +EPO
% of mitochondrial energisation (FI_{red}/ FI_{red} + FI_{green})	**48.8±4.3**	**33.4±0.5****	**45.5±3.2**	**45.0±1.0**	**48.2±7.0**

Table 10.15 Effect of EPO on mitochondrial energistaion levels, expressed as % FI_{red}/ FI_{red} + FI_{green}, in purified cultures of motor neurons exposed to kainate or AMPA.** $p<0.01$

In figure 10.16 representative laser scanning confocal images of cells loaded with JC1 (3 μM) and Hoechst 33258 (1 μM) are shown. A high percentage of red stained mitochondria were found in control condition (Fig 10.16 A) while kainate treatment drastically reduced the number of red stained mitochondria and consequently increased the green component (Fig 10.16 E). Motor neurons exposed to kainate and treated with EPO maintained a high rate of energized (red) mitochondria thus suggesting that mitochondrial depolarization and mitochondrial PTP opening are both prevented by EPO administration (Fig 10.16 G). AMPA treatment, while significantly reducing the total number of cells, did not cause an evident decrease in the ratio between red stained and green stained mitochondria (Fig 10.16 C). Microphotographs of these cells at higher magnification are presented in figure 10.16 B, D, F, H.

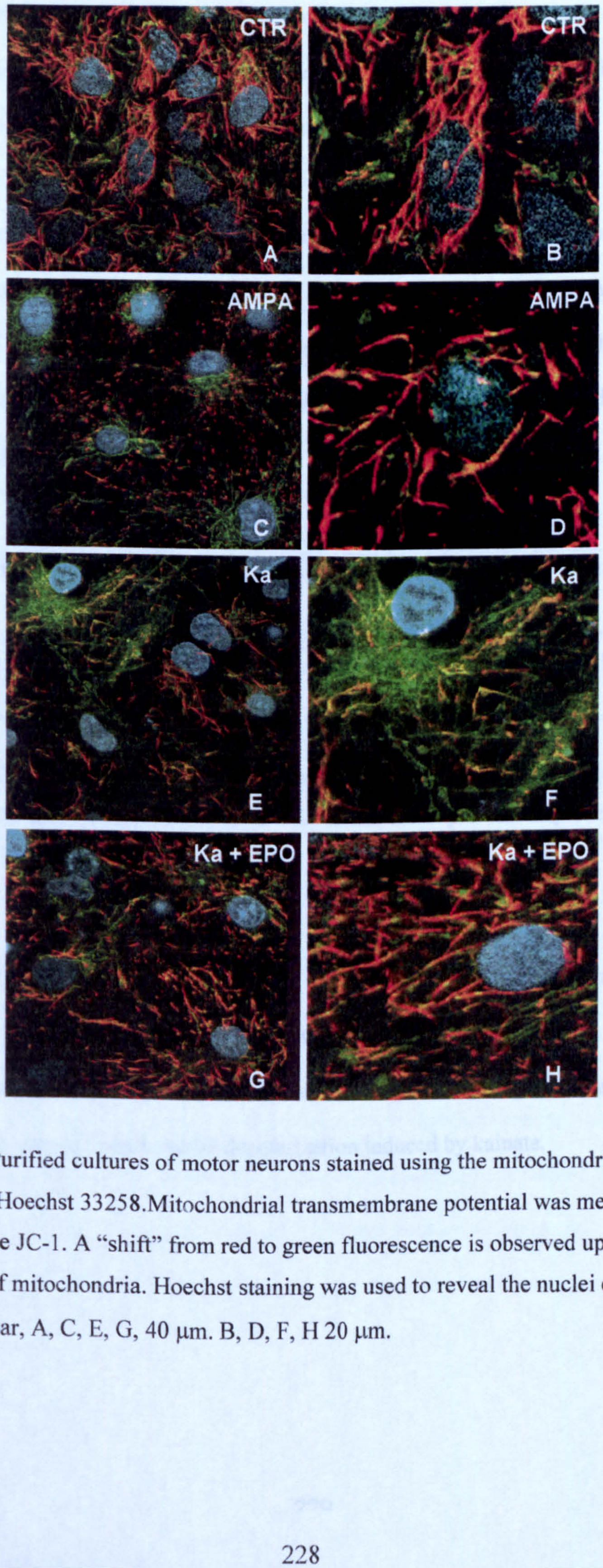

Figure 10.16 Purified cultures of motor neurons stained using the mitochondrial dye JC-1 and the nuclear dye Hoechst 33258.Mitochondrial transmembrane potential was measured with the fluorescent probe JC-1. A "shift" from red to green fluorescence is observed upon depolarization of mitochondria. Hoechst staining was used to reveal the nuclei of motor neurons. Scale bar, A, C, E, G, 40 μm. B, D, F, H 20 μm.

10.4.2.3 AMPA, kainate and the mitochondrial PTP

To better clarify the possible involvement of mitochondrial PTP in kainate-induced apoptotic pathway, the effect of cyclosporin A_2, an anti-apoptotic agent that binds to the PTP and maintains it in a closed position, was measured on SMI-32 cell viability in mixed neuron/cultures exposed to AMPA 1μm or kainate 5μm.

Treatment with cyclosporin A_2 (2 μM, added simultaneously with either one of the glutamate agonists), prevented the decrease of SMI32 positive cell viability induced by kainate, but not by AMPA. Cyclosporin A_2 alone showed a clear Neuroprotective action by reducing the natural death occurring under basal conditions. The number of SMI 32 positive cells in cultures not exposed to excitotoxins and treated with cyclosporin was significantly higher compared to untreated cultures (see table 10.18).

	CTR	CTR+ cyclosporin	CTR+kainate	CTR+kainate +cyclosporin	CTR+AMPA	CTR+AMPA +cyclosporin
% of SMI32 positive cells	100±16.1	137.1±12.6°°	43.5±.3***	97.6±19.2	53.6±13.3***	63.4±7.2***

Table 10.17 Effect of cyclosporin A_2 (on motor neurons survival in mixed glia/neuron cultures exposed for 48 hours to kainate or AMPA. The values are expressed of percentage of controls and normalized to 100.°°$p<0.05$ ***$p<0.001$

It is of interest to note that cyclosporin A_2 slightly hyperpolarises the mitochondrial inner membrane (not shown). The selective protection of cyclosporin A_2 against kainate, but not against AMPA implies that this effect is related not only to the increased number of cells but also to prevention the of mitochondrial depolarization induced by kainate.

10.4.3 Discussion

EPO significantly antagonizes the kainate-induced apoptosis, by decreasing both the release of cytochrome-c and mitochondrial depolarization. It is worth mentioning that a slight, but significant, reduction in mitochondrial depolarization was also observed

after AMPA treatment. In this condition, however, EPO did not prevent the decay of mitochondrial $\Delta\Psi_M$.

To investigate whether the selective effect of EPO, after kainate exposure, was related to an anti-apoptotic mechanism passing through the inhibition of the PTP opening, the effect of a treatment with a well documented inhibitor, like cyclosporin A_2 was tested [Chang, 2002], against the chronic exposure to AMPA or kainate. Like EPO, cyclosporin A_2 protected motor neurons against kainate treatment but not against AMPA. The selective protection of cyclosporin A_2 after kainate treatment suggests that kainate generates a cascade of events that have as a target the mitochondrial transition pore, while AMPA affects a different pathway in which the inhibition of the mitochondrial PTP does not seem to play a relevant role.

Unfortunately, the relative low amount of protein that can be obtained from purified cultures of motor neurons did not allow me performing a quantitative measurement by western blot analyses.

Specific inhibitors of MAPK and PI_3K largely abolish the EPO-induced protection against hypoxia-induced cell death in rat hippocampal neurons [Siren, 2001]. Since PI_3K phosphorylation produces its anti-apoptotic effect by phosporylating and inactivating BAD and consequently reducing the mitochondrial PTP opening, and EPO has been reported to induce a mechanism that increase the phosphorylation of BAD [Siren, 2001], it has been hypothesized that this mechanism may be involved in the selective anti-apoptotic neuroprotection exerted by EPO. Unfortunately, it was impossible to verify the mechanism of action of EPO upstream the mitochondrial PTP regulation because of the high motor neurons toxicity of the PI_3K (LY984002) and MAP-K (PD98059) inhibitors over the period of time required for my studies (5 days of treatment).

Notwithstanding this experimental limitation, this study demonstrates that: I) motor neurons undergoing to apoptosis, induced both by kainate exposure and/or serum/BDNF deprivation, are protected by EPO and; II) this protective mechanism is selectively active in counteracting a mechanism of death associated to the mitochondrion-dependent apoptosis.

A schematic representation of the motor neuron death pathways elicited by both AMPA 5 μm and kainate 1 μm in mixed glia/neurons cultures is reported in figure 10.17.

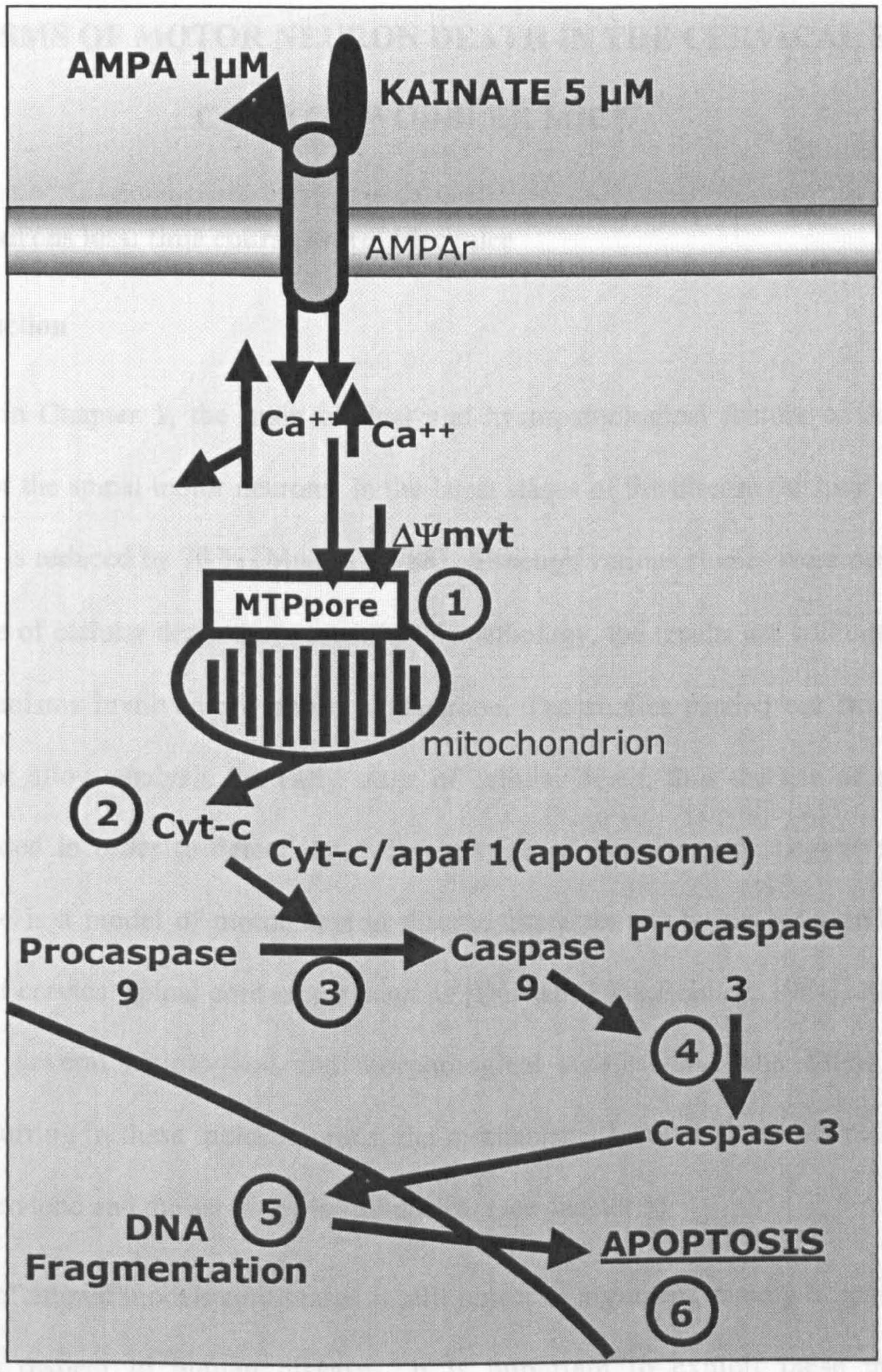

Figure 10.17 Motor neuron pathways activated following chronic exposure (48 hours) with kainate 5 µm and AMPA 1 µm, in mixed glia/neurons cultures. While AMPA induces a fast pattern of death unrelated to apoptosis, kainate activated an intrinsic pattern of death passing through mitochondria 1) and leading to the release of cytochrome-c 2), caspases activation 3-4), DNA fragmentation of 5) and apoptotic death 6).

CHAPTER 11

MECHANISMS OF MOTOR NEURON DEATH IN THE CERVICAL SPINAL CORD OF WOBBLER MICE

11.1 Motor neurons loss: time course in wobbler mice

11.1.1 Introduction

As described in Chapter 1, the main clinical and hystopathological feature of ALS is the degeneration of the spinal motor neurons: in the latest stages of the disease the total amount of motor neurons is reduced by 70 % [Munsat, 1988]. Although various studies were performed to clarify the type of cellular death that occurs in this pathology, the results are still controversial and the mechanisms involved are poorly understood. The studies carried out from autopsy samples do not allow analysis the early stage of cellular death, thus the use of alternative models is needed in order to detect the different steps of motor neuron degeneration. The wobbler mouse is a model of motor neuron disease characterized by an early and selective vulnerability of cervical spinal cord motor neurons [Duchen, 1968;Bradley, 1984]. Although in wobbler mice several histological and morphological studies have elucidated the main alterations occurring in these motor neurons, the mechanisms involved in motor neuron death are poorly understood and the aetiology is still unclear (see chapter 5).

Since the use of animal models of diseases is still object of argument, mainly because of their dissimilarities respect to human diseases, it is important to exploit these models by investigating the features of the diseases that cannot be evaluated in human samples for ethical reasons and to allows studying the early pathological events.

This chapter describes studies aimed at understanding **why** and **how**, in the wobbler mouse, cervical motor neurons motor die.

For this reason the possible involvement of two aetiological factors suggested in ALS, glial-induced neuroinflammation and glutamate induced-excitotoxicity were investigated as possible contributors to the motor neuron degeneration occurring in wobbler mice.

This study was achieved: 1) by investigating the presence of main markers related to these detrimental processes; 2) by evaluating if the propagation of these stimuli could generate apoptotic cell death.

11.1.2 Experimental design

To characterize the rate of motor neurons death from presymptomatic to late symptomatic phase, cell counting was performed before starting the investigation of the different cell death pathways. This measurement was made at three different ages: 3rd week of age, corresponding to the presymptomatic phase (P19-P21), 5th week of age, corresponding to early symptomatic phase (P30-P34), and 12th week of age, corresponding to late symptomatic phase (P60-P66). In each experimental group the mean number of motor neurons measured in wobbler mice was compared to the number found in healthy littermates.

The measurement was done in the region of spinal cord selectively affected, the cervical region. The number of motor neurons for each single animal was calculated by measuring the total number of motor neurons obtained by analysing 100 sections (30 μm of thickness).

For each experimental group, the values of motor neurons were reported as mean of cells counted for each animal, the mean values of motor neurons in wobbler mice was expressed as percentage of the mean values obtained in healthy littermates and normalized to 100.

The number of animals was five for early symptomatic and late symptomatic groups, and three for presymptomatic group.

All experiments were done following the procedures described in the chapter 9.

11.1.3 Results

11.1.3.1 Genotyping

In mice with genetic background as NFR/wr a polymorphism on the Cct4 gene generates a new restriction site on the DNA sequence (intrastrain Restriction Fragment Length Polymorphism, RFLP) that is recognized and cleaved by the restriction enzyme *AluI*. It is known that this mutation is closely related to the mutation on the locus *wr* that generates mutant alleles on the chromosome 11 [Rathke-Hartlieb, 1999]. The identification of mice genotype is based on the presence of this linkage.

The fragment of DNA that is amplified by PCR from the Cct4 gene has a length of 394 bp. Homozygous healthy mice (+/+) displayed only a single DNA band of this length. Heterozygous healthy mice (wr/+) show one band of 394 bp, corresponding to the wild type allele of Cct4, and two bands respectively of 209 and 165 bp, produced by restriction of the mutated Cct4 allele. Homozygous wobbler mice (wr/wr) showed only the two bands at 209 and 165 bp, since both alleles are mutated and no wild type alleles are present.

Figure 11.1 Polymorphism at the Cct4 locus as detected by PCR. Cct4 based diagnosis of the allelic status at the wr locus applied to a litter wr/+ X wr/+. Alu1 (see section 5.1) digested PCR products. Lanes 3, 5, 6, 7 correspond to homozigous healthy mice (+/+). Lanes 1, 2, 4, 8 correspond to heterozygous healthy mice (wr/+). Lane 4 corresponds to homozygous wobbler mouse (wr/wr).

11.1.3.2 Motor neurons counting

The rate of motor neuron loss in the cervical spinal cord of wobbler mice can be estimated by using different criteria. Original studies, performed both by counting the number of motor neurons by Nissl staining [Duchen, 1968;Bradley, 1984;Mitsumoto, 1985] or by utilizing a more advanced technique in which a retrograde tracer fluorogold system for labelling a subpopulation of motor neurons [Haenggeli, 2002], produced similar results. All these measurements were done using a non stereological approach. After genotyping, the number of cervical motor neurons, measured in the most rostral tract, C2-C3 to C5-C7, was performed. Abnormalities in cervical motor neurons of wobbler mice were already reported at the presymptomatic stage [Blondet, 2002;Mitsumoto, 1982], however no significant difference was found by counting the cells both using Nissl staining (% of healthy motor neurons in control mice 100.0 ± 3.5; in wobbler mice 96,5 ± 6,3 n.s) and ChAT immunostaining (% of healthy motor neurons in control mice 100.0 ± 9.7; in wobbler mice 92,5 ± 11.4).

Two weeks later, at 5th week of age, both Nissl and ChAT staining confirmed the previous evidence of a marked decrease in the cervical motor neurons number occurring in wobbler mice. Moreover, Nissl and ChAT methods reproduced the same rate of death, thus confirming the reliability of both techniques. The values found are the following: Nissl staining (% of healthy motor neurons in control mice 100.0 ± 2.7; in wobbler mice 61.4 ± 8.2 $p<0.001$), ChAT immunostaining (% of healthy motor neurons in control mice 100.0 ± 11.7; in wobbler mice 58.3 ± 13.3 $p<0.001$).

During the progression of symptoms a further decrease in motor neurons was found. At the 12th week of age, the cervical number of motor neurons calculated by Nissl staining was significantly lower (% of healthy motor neurons in control mice 100.0 ± 2.1; in wobbler mice 37.6 ± 12.5 $p<0,001$). Interestingly, at this stage of the disease ChAT immunostaining revealed a more marked decrease of cervical motor neuron number, compared to the same group analyzed using Nissl staining, (% of healthy motor neurons in control mice 100.0 ± 12.6; in wobbler mice 26.9 ± 13.0 $p<0,001$), although the two means were not statistically different.

Representative microphotographs of the pattern of staining observed by Nissl and ChAT experiments in sections of cervical spinal cord are shown in figures 11.2 and 11.3 respectively.

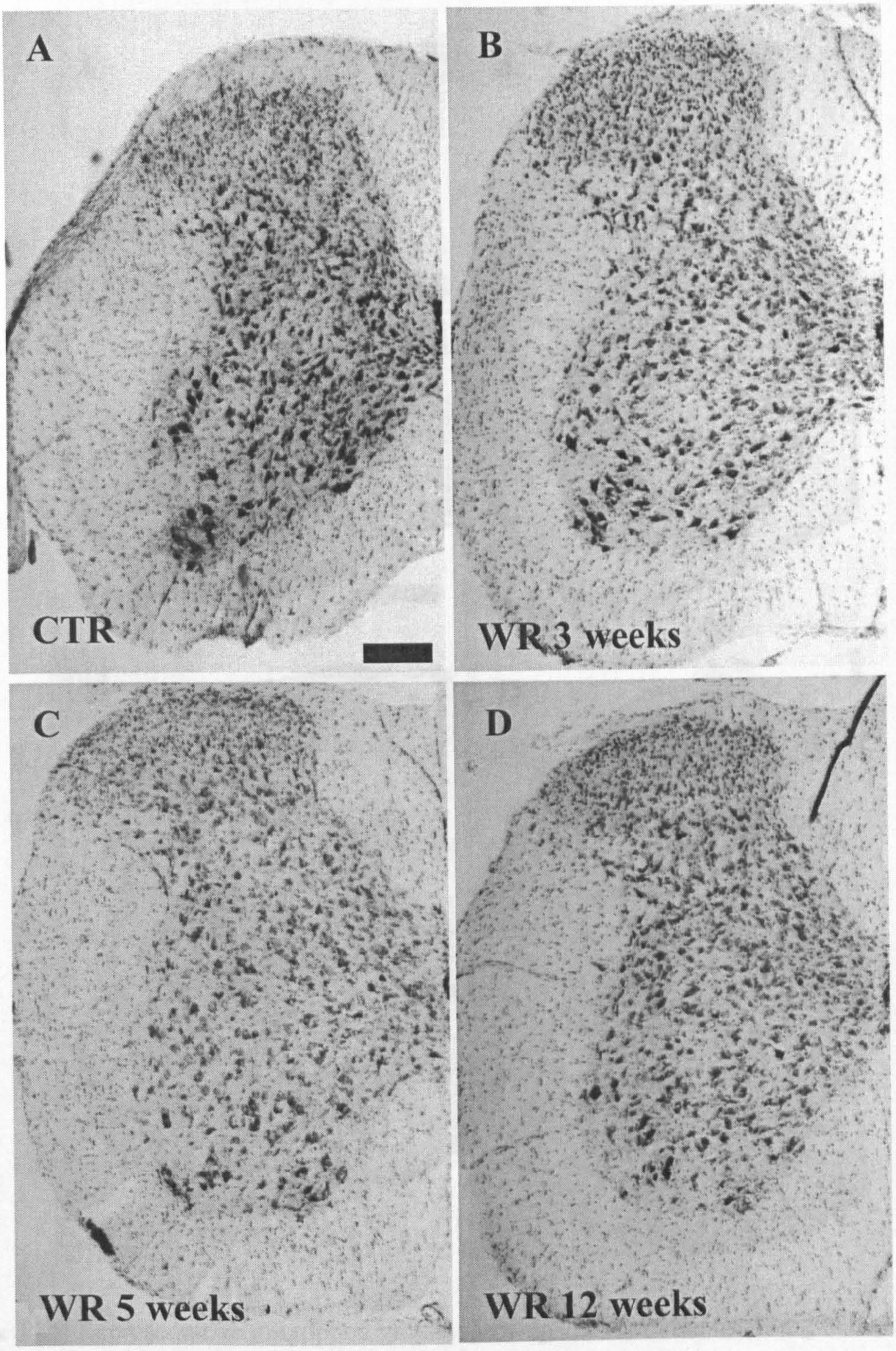

Figure 11.2 Representative microphotographs showing the pattern of Nissl staining in cervical spinal cord sections of healthy mice and affected wobbler mice, at three different stages of the disease. In the anterior horn (lamina IX) motorneurons are easily detectable as they have intense positivity for cresyl violet. They are motor neurons. During clinical progression (B-D) motor neurons number decreases and the strength of staining is markedly reduced. Scale bar 200 μm

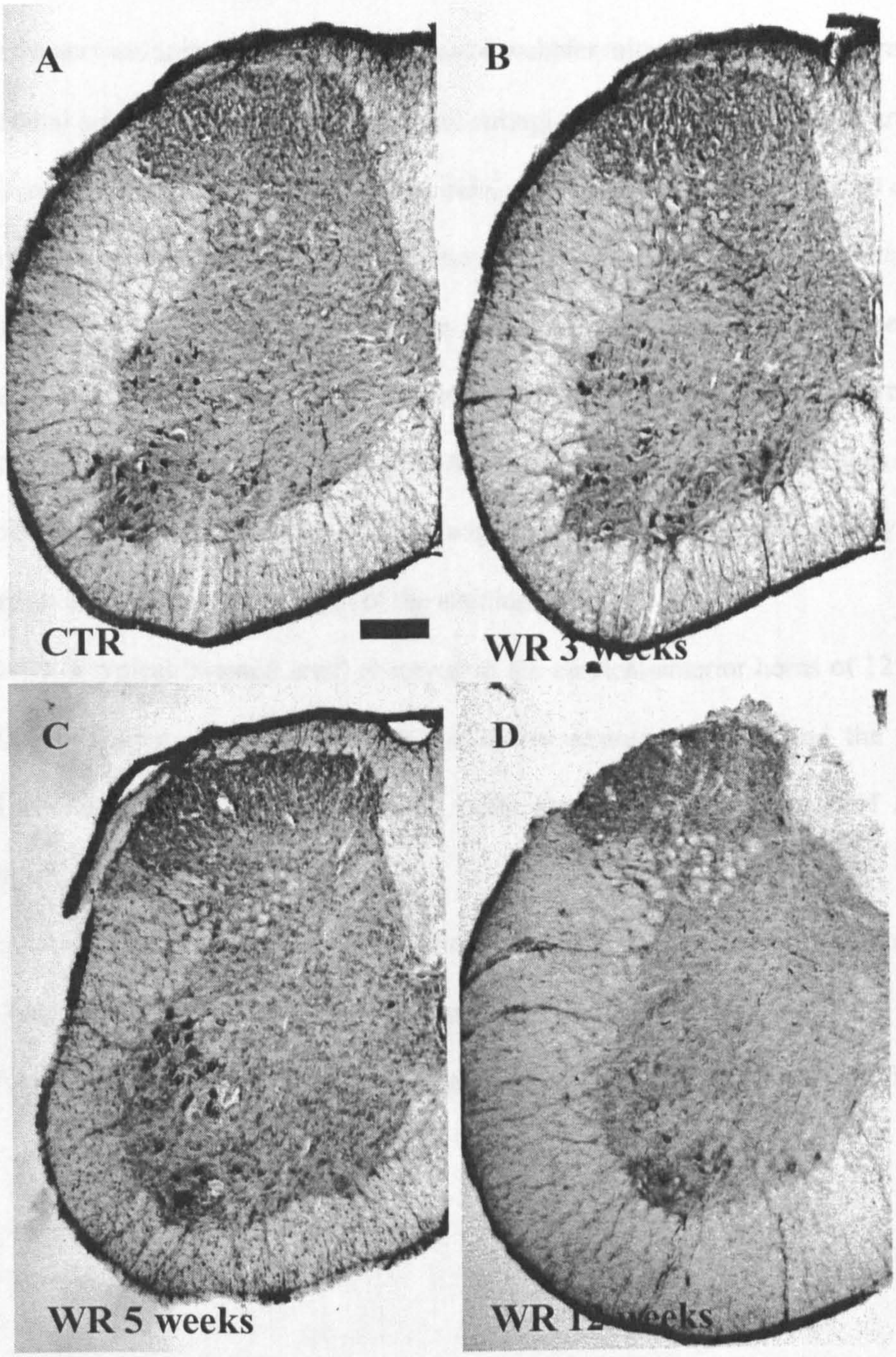

Figure 11.3 Representative microphotographs showing ChAT immunostaining in the cervical spinal cord sections of healthy mice and affected wobbler mice, at three different stages of the disease. In the anterior horn (lamina IX), ChAT staining is observed in healthy mice (A) and presymptomatic wobbler mice (B). During symptom progression the number of ChAT positive cells is progressively diminished (C-D). Interestingly, in figure C, it is possible to observe a marked alteration in ChAT positive cells morphology (such as the loss of typical shape, the lack of immunopositivity in arborizations and a reduced intensity of staining) rather than a relevant number loss. These features of motor neurons alterations at the early symptomatic phase will be more evident in figure 11.5. Scale bar 200 μm

Higher magnification microphotographs clearly showed the progressive neuronal degeneration occurring in the cervical spinal cord motor neurons of wobbler mice. In the anterior horn (lamina IX lateral column) large neurons which are strongly labelled for cresyl violet are easily detectable as motor neurons. Few motor neurons obtained from the cervical spinal cord of wobbler mice are shown in figure (11.4 A). In these cells it is possible to note an intense positivity for the cresyl violet both in the cell body and in their arborizations. During the presymptomatic stage Nissl stained motor neurons did not show relevant signs of abnormality, compared to control motor neurons (Fig 11.4 B). At 5th week of age, marked alterations of motor neurons were easily detected (Fig 11.4 C), with a decreased motor neuron density and a strong reduction in the shape and strength of the staining.

In figure 11.4D, a typical "wasted area" observed in the cervical anterior horns of 12 week-old wobbler mice is shown. Both the decrease in motor neurons number and the profound cytological alterations in the few remaining cells clearly indicate a stage of advanced degeneration.

Four microphotographs showing the ChAT immunostaining in lamina IX of cervical motor neurons in healthy mice and in wobbler mice at the three stages of the disease are shown in figure 11.5 A-D. Similar differences can be noted regarding the pattern of staining from Nissl and ChAT.

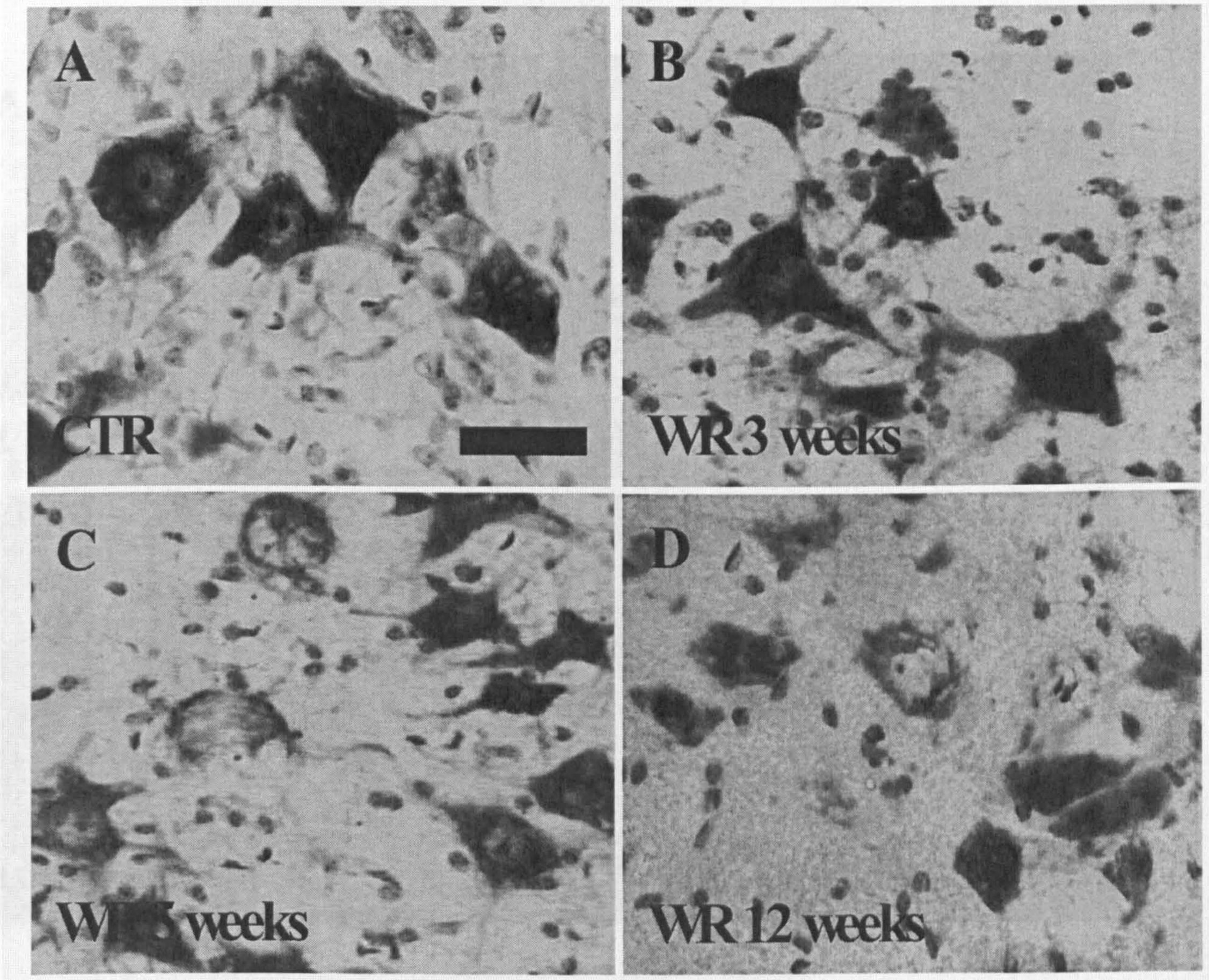

Figure 11.4 Representative microphotographs showing cervical motor neurons stained by Nissl method. In presymptomatic wobbler mouse (B), motor neurons do not differ from unaffected mice (A) either as morphology or as Nissl staining distribution. In early symptomatic mice (C) a marked alteration of motor neurons is clearly detectable. In this phase of the disease, dying motor neurons show morphological alterations and present a reduced intensity of staining, likely due to vacuolization processes. At the end stage of the disease the few motor neurons remaining have completely lost their identity (D). Nissl staining clearly reveals the entity of damage in this late phase of the disease. Scale bar 50 μm.

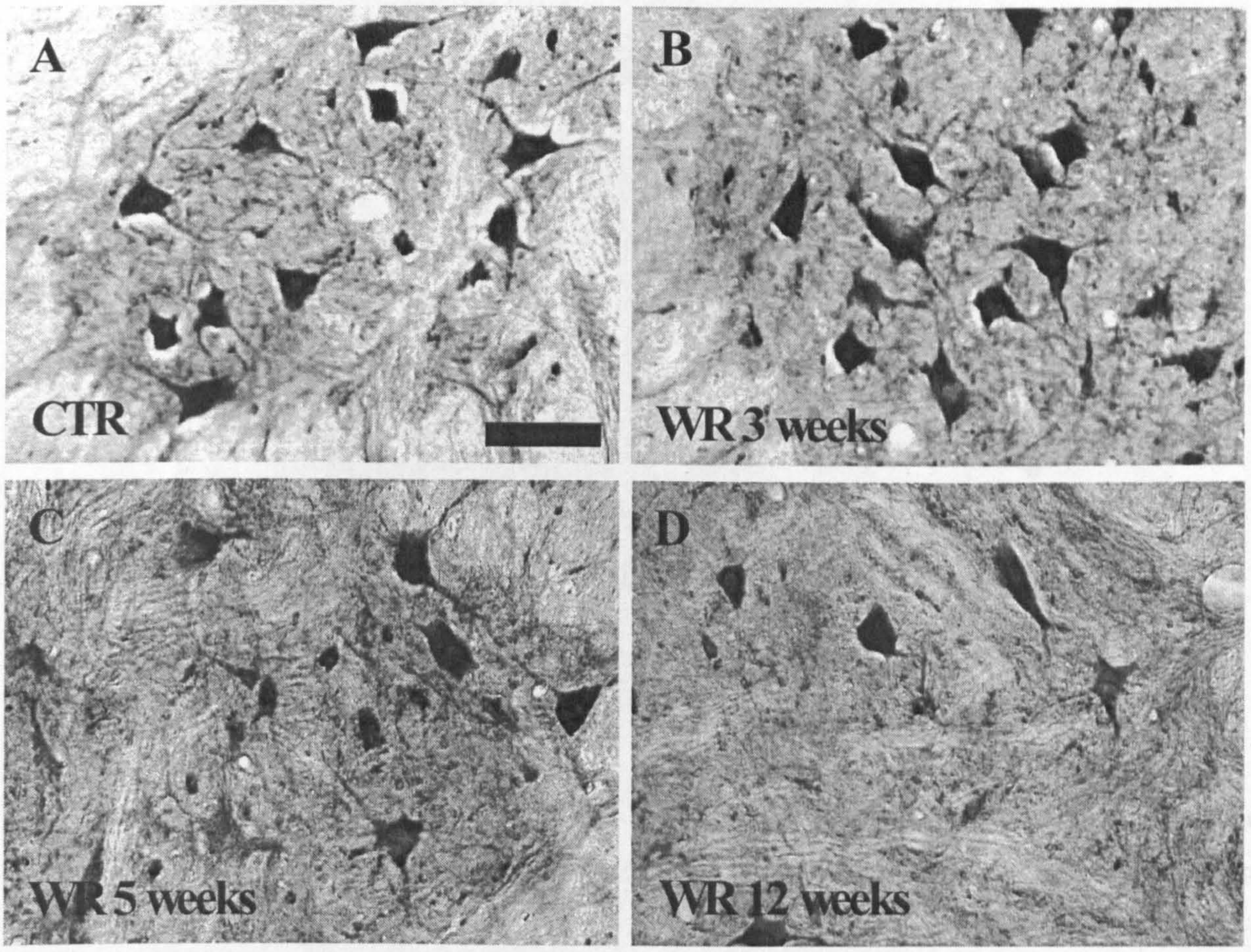

Figure 11.5 Representative microphotographs showing ChAT positive cells in the anterior horn of the cervical spinal cord, lamina IX, in healthy and affected wobbler mice, at three different stages of the disease. In the presymptomatic wobbler mouse (B) ChAT positive cells are similar (as number, shape, size and staining intensity) to healthy mice (A). In 5 week-old wobbler mice (C), lamina IX presents ChAT positive neurons with reduced staining on their arborizations and an altered morphology. Moreover, a significant reduction in ChAT positive cell number is already detectable at this phase of the disease. At the 12th week of age, ChAT positive cells in the cervical spinal cord of wobbler mice are almost completely disappeared (D). Scale bar 60 μm.

Motor neuron death progression in wobbler mice is reported in figure 11.6.

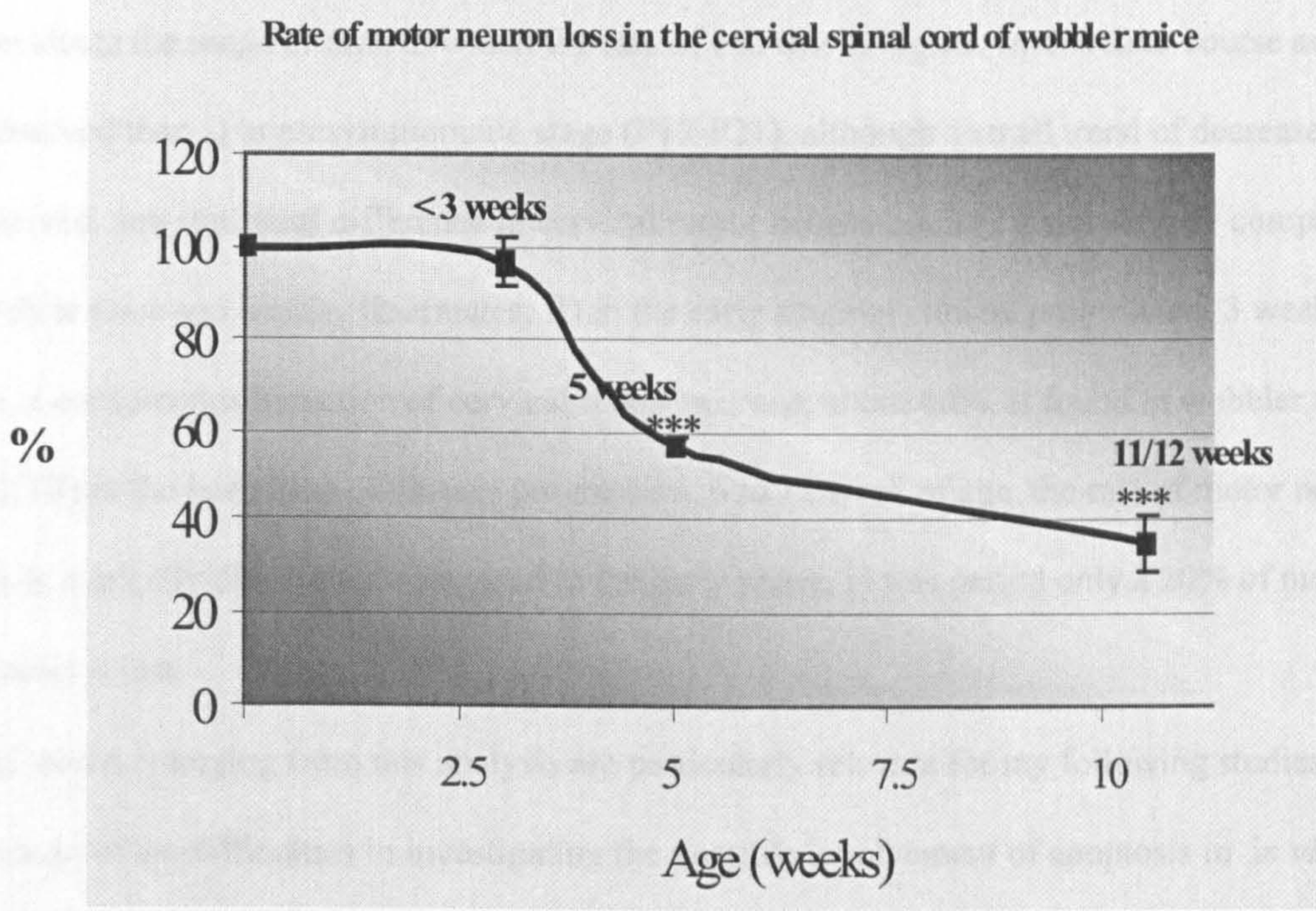

Figure 11.6 Percentage of motor neurons loss in the cervical region (C2-C7) of wobbler mice after 3, 5, 11-12 weeks of life. The mean number of motor neurons measured in control conditions are normalized to 100.The rate of viability is expressed as percentage compared to controls. ***p<0.0001 (Student's t test).

11.1.4 Discussion

This first series of study was planned to confirm the progression of motor neuron loss observed in the cervical spinal cord of wobbler mice from the $3^{rd}/4^{th}$ to the $10^{th}/12^{th}$ week of life and also to evaluate the range of time in which the rate of cell loss is higher. In this time-course analysis I observed that: I) in presymptomatic stage (P18-P21), although a small trend of decrease is observed, any statistical difference in cervical motor neuron number is not seen by comparing wobbler mice and healthy littermates; II) in the early stage of clinical progression, 3 weeks of age, a conspicuous reduction of cervical motor neurons, about 40%, is found in wobbler mice and; III) in the late phase of disease progression, 6 to 12 week of age, the rate of motor neuron loss

11.1.4 Discussion

This first series of study was planned to confirm the progression of motor neuron loss observed in the cervical spinal cord of wobbler mice from the $3^{rd}/4^{th}$ to the $10^{th}/12^{th}$ week of life and also to evaluate the range of time in which the rate of cell loss is higher. In this time-course analysis I observed that: I) in presymptomatic stage (P18-P21), although a small trend of decrease is observed, any statistical difference in cervical motor neuron number is not seen by comparing wobbler mice and healthy littermates; II) in the early stage of clinical progression, 3 weeks of age, a conspicuous reduction of cervical motor neurons, about 40%, is found in wobbler mice and; III) in the late phase of disease progression, 6 to 12 week of age, the rate of motor neuron loss is markedly diminished compared to the early phase, in this period only a 20% of motor neurons is lost.

The results emerging from this analysis are particularly relevant for my following studies. Because of the difficulties in investigating the possible involvement of apoptosis in *in vivo* models of chronic neurodegenerative diseases (see section 2.3), a clear indication of the peak of motor neuron loss in this model is required. My observation clearly indicates that, the narrow range of time from the 4^{th} to the 5^{th} week of age is the most reliable period to investigate about the cell death mechanisms in cervical motor neurons of wobbler mice.

In several neurological human disorders, including ALS, is postulated that the clinical onset is detectable after a large percentage of neurons have already disappeared. Genotyping experiments allowed me to test whether a few days before clinical onset characterization of motor neuron symptoms in wobbler mice, a reduction in motor neurons was already in progress. Since in *mnd* mice a loss of ChAT immunoreactivity has been reported without any apparent loss of motor neurons and a loss in ChAT activity has been repeatedly reported in the cervical region of wobbler mice [Mennini, 2004;Bigini, 2001], I performed my cell counting both by measuring the total number of cholinergic neurons in cervical sections of spinal cord (ChAT immunostaining) and by using Nissl staining. No differences were seen between Nissl staining and ChAT immunostaining, both in total number of motor neurons and in the rate of motor neuron death. Thus, the results obtained by Nissl and ChAT staining, demonstrated the

reliability of both procedures to perform motor neurons counting in the cervical region of wobbler mice.

11.2 Neuroinflammation and apoptosis

11.2.1 Introduction

Although glial-induced neuroinflammation has been postulated as an pathological mechanism in wobbler mice (see section 5), the actual correlation between neuroinflammation and motor neuron disease is not yet fully established, reporting an increased expression of two metalloproteinases that seem to be enhanced by increasing TNF-α levels, are available [Schlomann, 2000;Rathke-Hartlieb, 2000].

Immunohystochemical experiments, therefore, were performed to ascertain if microglia, TNF-α and TNFR1 proteins are over expressed in the cervical spinal cord of 4 week old wobbler mice compared to their respective healthy littermates. In addition, since the coupling to TNF-α/TNFR1 often leads to the activation of an extrinsic apoptotic cell death pathway (see section 2.2.1.1), the possible activation of caspase 8 was evaluated.

11.2.2 Experimental design

The time-course of motor neuron loss, allowed me to determine the time at which the motor neuron death peaked, i.e. from the 3rd to the 5th week of age, with about 50% motor neurons death. For this reason the age of animals utilized in the following experiments ranged from P24 to P28.

PAGE NUMBERING AS ORIGINAL

11.2.3 Results

11.2.3.1 Microglial staining

CD11b immunohystochemistry revealed a marked increase in microglial cells in the wobbler mice compared to healthy littermates. In 4 week-old wobbler mice the pattern of expression of CD11b in the cervical spinal cord was markedly increased in the whole grey matter without immunoreactivity in the white matter (Fig 11.7 A). Unaffected littermates showed a very weak CD11b immunoreactivity (Fig 11.7 B). In the cervical anterior horn of wobbler mice is interesting to note that activated microglial cells, which are easily detectable for their loss of arborizations and their rounded shape, are mainly concentrated in lamina IX in the proximity of the lateral and central column motor neurons. In that zone they cluster and seem to cover dying motor neurons (Fig 11.7C B).

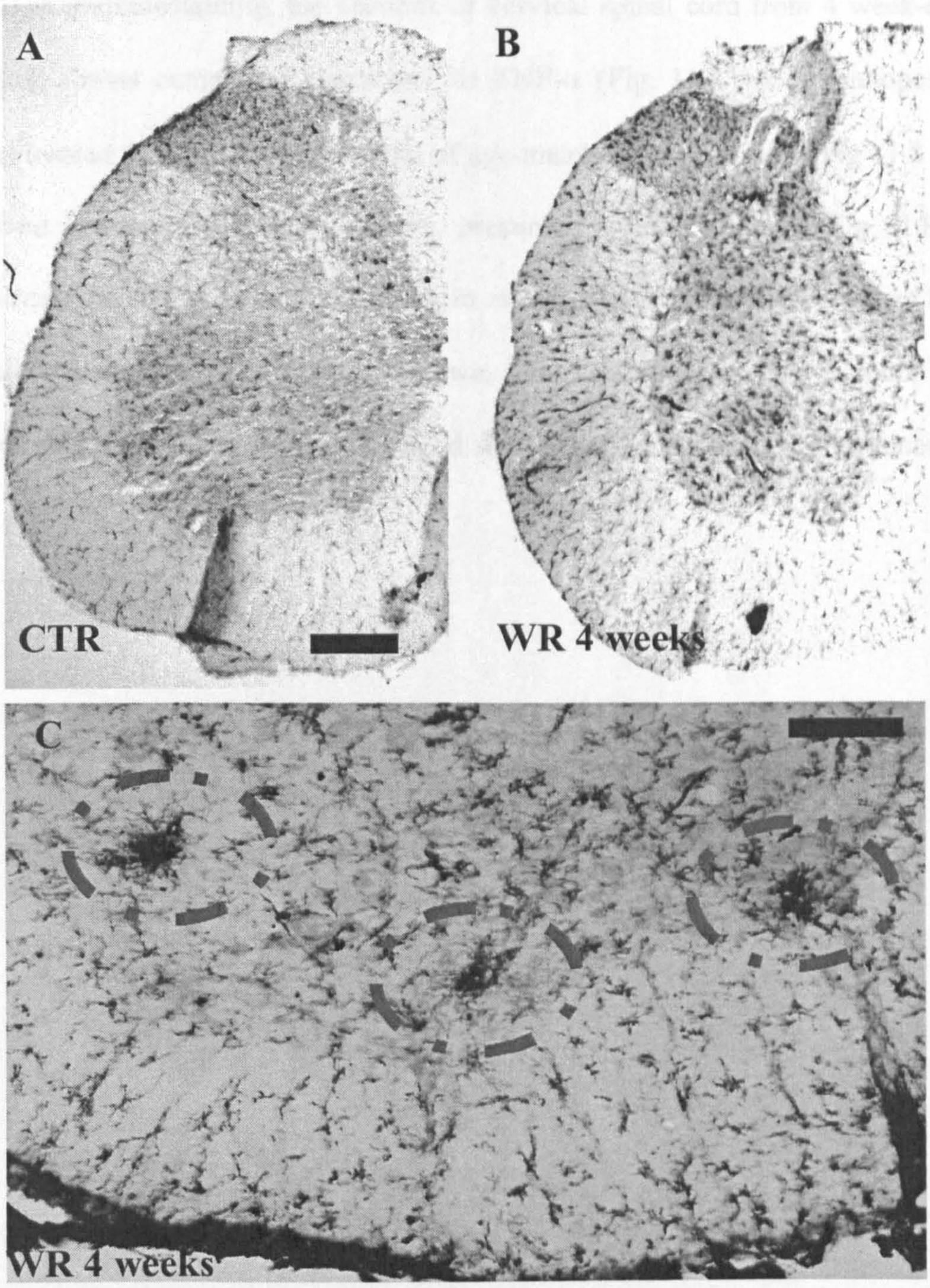

Figure 11.7 Representative microphotographs showing activated microglia staining in the cervical region of early symptomatic wobbler mice (B) and healthy littermates (A), revealed by an anti CD11b antibody. In affected mice a marked increase of CD11b immunopositivity is detectable in the whole gray matter. However, mainly in anterior horns, in correspondence to lateral and central columns of motor neurons, a strong immunopositivity of activated microglia cells is exclusively detectable in affected mice (C). In the latter case microglial cells, completely lose their ramified morphology and acquire a globular shape. More likely they cover and wrap dying motor neurons that have released chemoattractant factors. Scale bar, A-B 200 μm. C 60 μm.

11.2.3.2 TNF-α immunostaining

As for CD11b immunostaining, the sections of cervical spinal cord from 4 week-old control mice resulted almost completely unstained for TNF-α (Fig. 11.8 A). Immunopositivity for TNF-α was instead found in the grey matter of age-matched wobbler mice (Fig 11.8 B), mainly in large sized neurons of the anterior horn, presumably motor neurons (Fig 11.8 C). Such marked increase of TNF-α immunoreactivity in motor neurons might be explained by the fact that an active phenomenon of TNF-α uptake was induced in injured cells or, more likely, that activated microglial cells, wrapping damaged motor neurons, release a high amount of this cytokine.

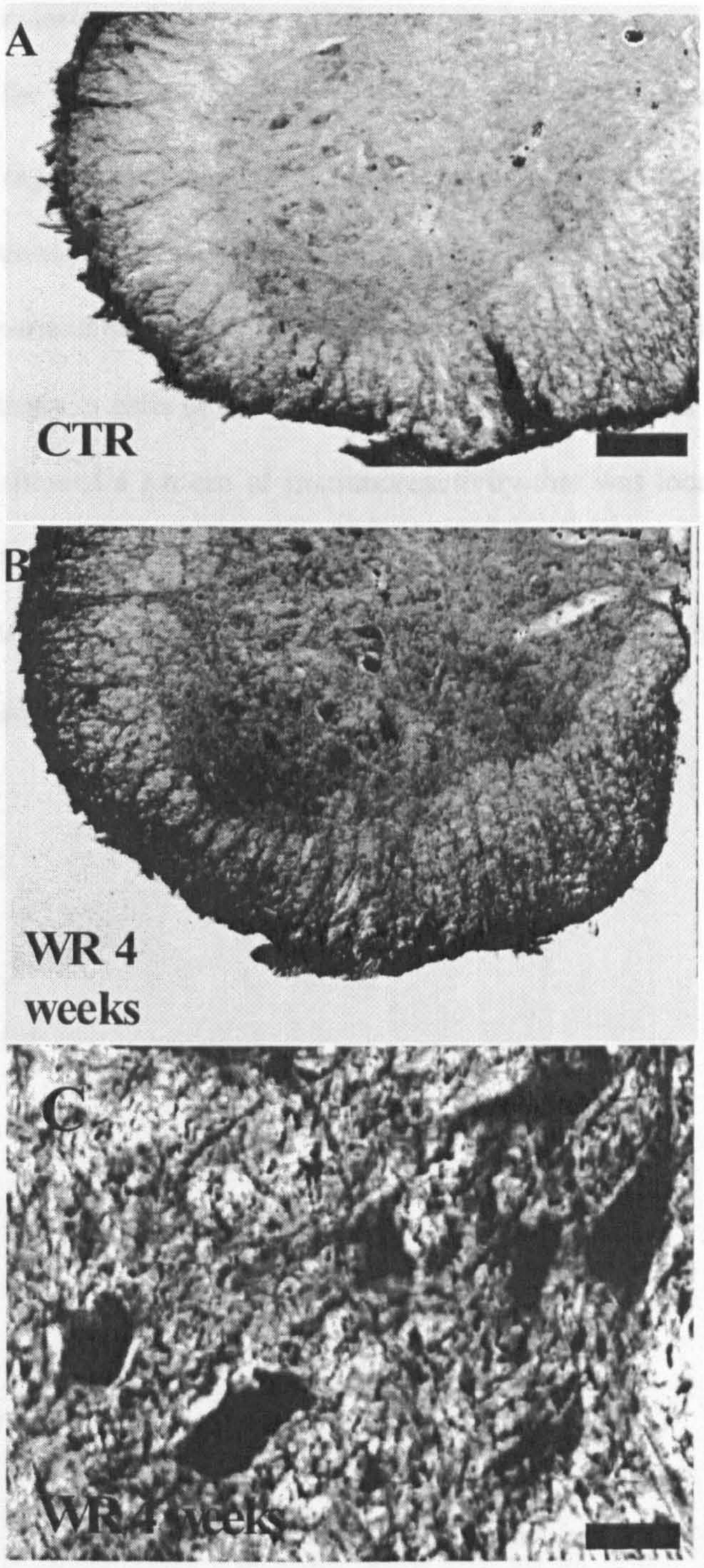

Figure 11.8 Representative microphotographs showing the pattern of staining for TNF-α in the anterior region of cervical spinal cord of control mice and early symptomatic wobbler mice. While the staining for TNF-α in the cervical region from healthy mice was almost completely absent (A), the sections obtained from wobbler mice showed a marked immunoreactivity for TNF-α, mainly in the proximity of lamina IX (B). A clear immunopositivity for TNF-α is detectable also in efferent fibers in the white matter (B). In that region neuronal staining (motor neurons) is clearly evident, but an intense positivity around neurons seems to suggest that other cells, likely astrocytes and microglia, are positive for TNF- a (C). Scale bar A-B 175 μm, C 50 μm.

11.2.3.3 TNF receptors immunohystochemistry

No immunoreactivity for TNFR-I in the cervical sections of healthy mice at 4 weeks of age was detected in the dorsal region, whereas an extremely weak and homogeneously scattered staining was observed in the ventral horn and exclusively in the grey matter (Fig. 11.9 A). In the ventral horn sections of age-matched wobbler mice, a small, but increased immunoreactivity for TNFR1 was found, mainly in cells in the ventral columns (lamina IX). At higher magnification, ventral horn neurons showed a pattern of immunoreactivity that was localized mainly, though not exclusively, in motor neurons (Fig. 11.9 C).

Immunohystochemistry for TNFR2 was also performed. However, in both experimental groups, the staining resulted almost undetectable (not shown).

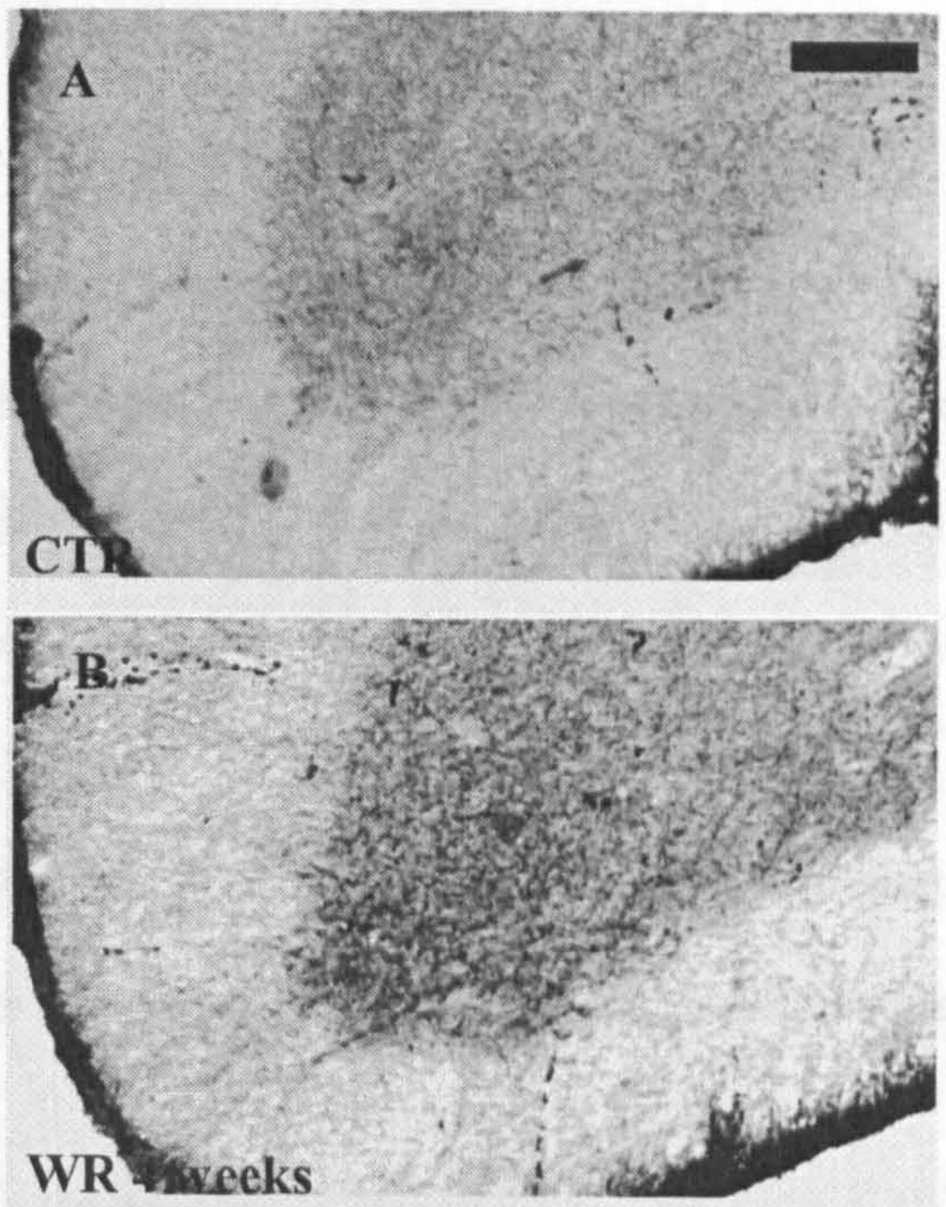

Figure 11.9 Representative microphotographs showing the pattern of staining for TNFR1 in the anterior region of cervical spinal cord of control mice and early symptomatic wobbler mice. In the cervical spinal cord of healthy mice the TNFR1 immunoreactivity was very low and no difference was observed from the anterior horn and the other regions of the gray matter (A). Early symptomatic wobbler mice showed a marked immunopositivity for TNFR1 in the anterior horn of the cervical spinal cord, this staining was particularly intense in the most anterior region of gray mater, in proximity of lamina IX (C). At higher magnification it is possible to note as, in the wobbler mice exclusively, TNFR1 produces a diffuse staining, maybe related to glial cells, and a more intense positivity in the external surface of large sized body cells neurons (motor neurons), suggesting that only cell surface is positive for TNFR1 staining. Scale bar, A-B magnification 175 μm. C 50 μm.

11.2.3.4 Active caspase 8 immunohystochemistry

For these experiments, 50 sections for each animal, and 5 animals for each experimental group were processed by performing immunostaining experiments. Since co localization experiments by using secondary antibodies associated to fluororchrome gave a strong non-specific staining, 100 serial sections were alternatively processed using an antibody directed against the active form of caspase 8 and against the antibody anti-ChAT (previously described, see sections 9.6.1 and 1.1.3.2).

Although a clear activation over expression of TNF-α and its cognate death receptor TNFR1 has been shown in the cervical region of wobbler mice, no indication of caspase 8 activation was seen in either group.

These results indicate that, in the cervical spinal cord of wobbler mice, the percentage of caspase positive motor neurons, expressed as ratio between caspase 8 positive neurons/ ChAT positive neurons, was extremely low and lower than those of healthy littermates. Moreover it is important to note that only 3 wobbler mice showed positive caspase 8 immunostaining and caspase 8 immunopositive motor neurons were also found in 2 healthy animals.

The quantification of active caspase 8 motor neurons is reported in table 11.1.

Animals (C2-C7)	Ctr 1	Ctr 2	Ctr 3	Ctr 4	Ctr 5	Wr 1	Wr 2	Wr 3	Wr 4	Wr 5
N° ChAT positive cells (50 sections)	1565	1622	1529	1662	1494	1102	998	1076	1029	992
N° caspase 8 positive cells (50 sections)	3	0	0	4	0	1	0	2	1	0

Table 11.1 ChAT and caspase 8 positive cells in the cervical spinal cord region of 4 week-old wobbler mice and healthy littermates

A microphotograph of a representative section of a wobbler mouse spinal cord processed for caspase 8 is shown in figure 11.10 A, and a higher magnification microphotograph representing a "rare" motor neuron positive for the active form of caspase 8 is shown in figure 11.10 B.

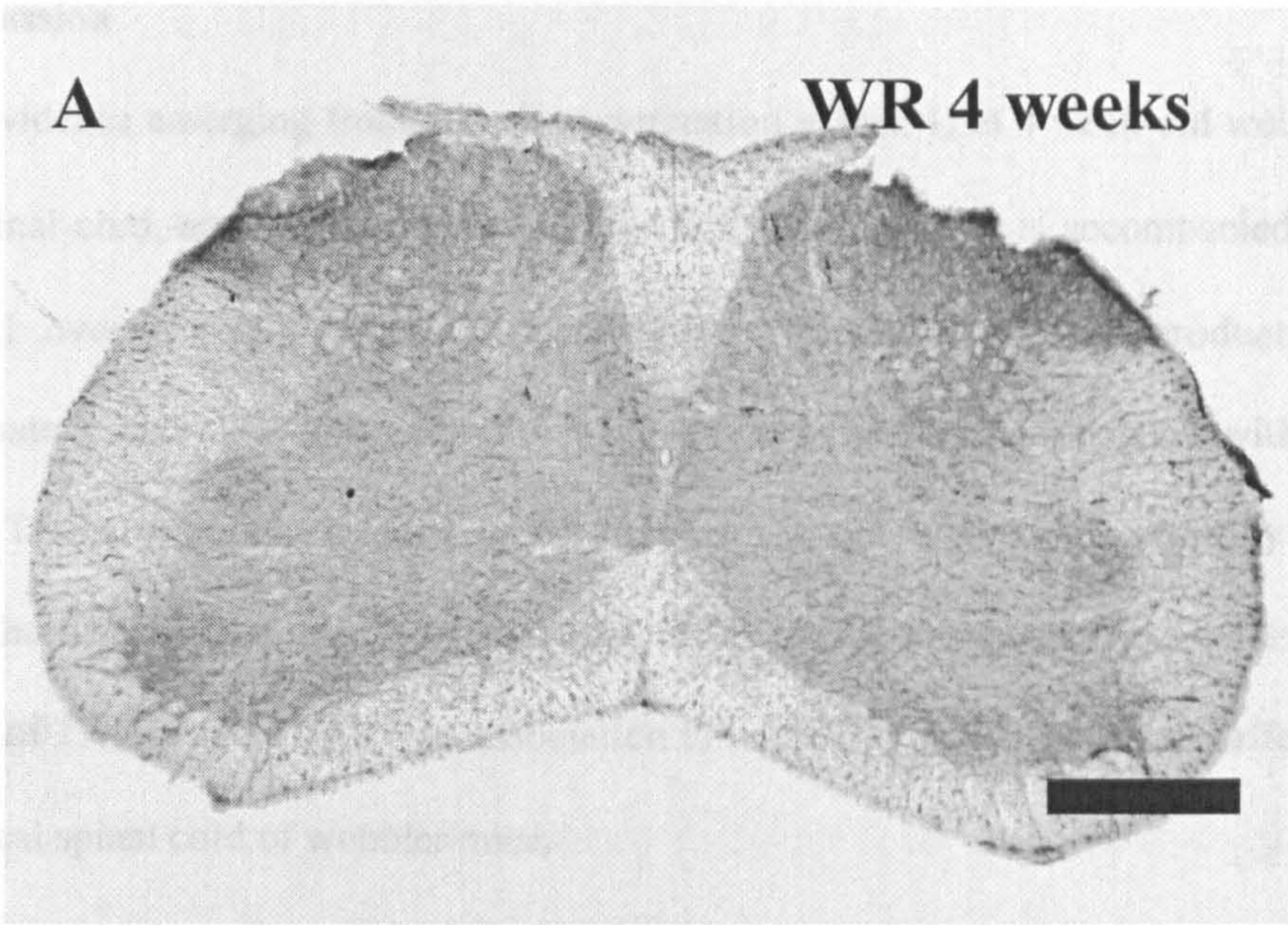

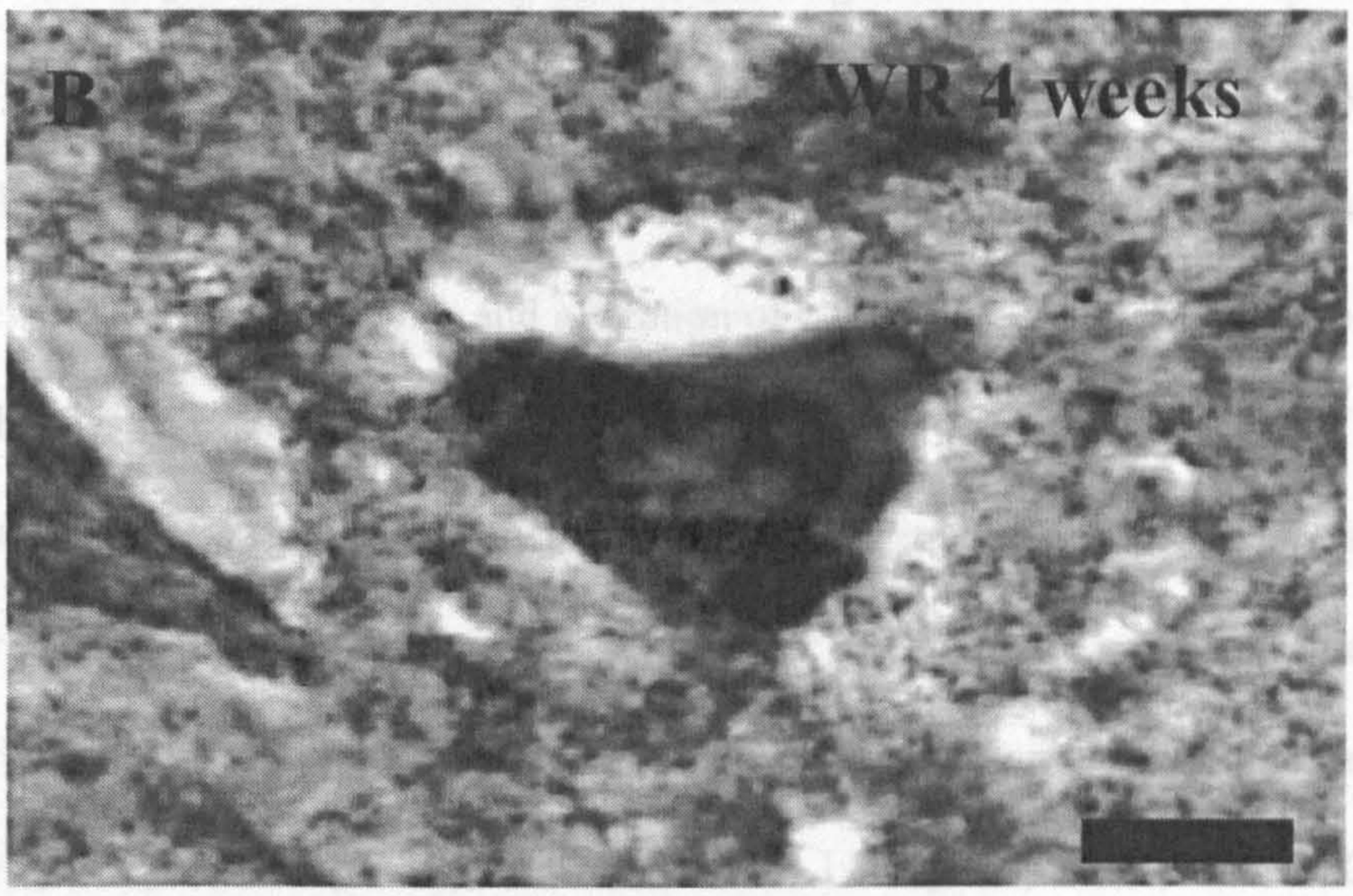

Figure 11.10 A representative pattern of active caspase 8 immunostaining in the cervical spinal cord in early symptomatic wobbler mice is shown in the microphotograph (A). Although a weak and homogeneously diffused staining is detectable in the whole the gray matter, this represents a background due to a not specific reaction of the system of signal enhancing (ABC cholorimetric detection). One of the very rare motor neurons that are clearly found positive for caspase 8 in these sections is shown in B. In this case the staining observed into the motor neuron is markedly higher than the background. The pattern of distribution of staining, more intense on the periphery and weaker on the middle suggests that the immunopositivity for caspase 8 in this cell is bordered to the cytoplasm and excludes a nuclear staining. Scale bar, A 400 μm. B 50 μm.

11.2.4 Discussion

The main evidence emerging from this characterization is that: I) in 4 week-old wobbler mouse cervical spinal cord, and mainly in the anterior horn, microgliosis is accompanied by TNF-α and TNFR1 overexpression and; II) the reactive gliosis and the overproduction of this proinflammatory cytokine does not trigger an apoptotic pathway associated with caspase 8 activation. These results further confirm the involvement of reactive gliosis already at the early phases of the disease [Boillee, 2001;Blondet, 1992] and represent the first evidence for the appearance of TNF-α and TNFR1, in association to microglial activation, in the affected region of the cervical spinal cord of wobbler mice.

TNF-α is not merely a factor which is involved in regulation of immune response or which inhibits the tumour proliferation, but has been also correlated to various diseases of CNS. Elevated TNF-α levels were found in animal models of motor neuron diseases [Ghezzi, 1998;Hensley, 2002;Hensley, 2003], and alteration of circulating levels of TNF-α has been also reported in the plasma of ALS patients [Poloni, 2000].

In vitro studies have strongly demonstrated that LPS-stimulated microglia is able to over express TNF-α, thus inducing apoptosis [Cheng, 2002;Nichols, 1998] and it has been reported that TNF-α has a detrimental action in the NSC-34 cell line co-cultured with an immortalized mouse microglial cell line (BV-2) stimulated with LPS [Hou, 2003;Woo, 2003]. On the contrary, in the absence of the stimulation with LPS, the dose of TNF-α required to produce the same effect is twenty fold higher. These data indicate that activated microglia secrete factor(s) that facilitate TNF-α mediated neuron death *in vitro* and it has been observed that LPS induced TNF-α acts through TNFR1 to modulate the expression of apoptotic genes and activate caspases-3 and -8 [He, 2002]. In addition, subcutaneous inoculation of LPS in TNFR1, TNFR2, and TNFR1+TNFR2 knockout mice have shown that TNFR1, but not TNFR 2 lead to an apoptotic neuronal death accompanied by a significant increase of caspase-8 and caspase-3 activation [Pelagi, 2000;Heneka, 1998;De Simone, 2003].

In vivo, the survival of injured motor neurons after axotomy has been examined in a line of transgenic mice that over express the soluble form of TNFR1 [Terrado, 2000]. The results indicate that the neutralization of endogenous TNF-α by means of over expression of the soluble receptor can decrease cell death of injured motor neurons, suggesting that this cytokine may play an important role in neuronal degeneration in the CNS following a lesion.

Different hypotheses have been put forward suggesting both a beneficial or detrimental role of reactive astrocytosis and reactive microglia in the CNS [Eddleston, 1993]. It is well-known that once activated, astrocytes and microglia increase the expression of a large number of molecules that may have toxic effect (i.e. nitric oxide) or may directly support neuronal survival (some cytokines, neurotrophic factors).

However, TNF also induces IL-6 [Benigni, 1996] and LIF [Ding, 1995], two cytokines that have neurotrophic activities, already demonstrated to be protective to reduce the clinical progression in the wobbler mouse, and whose receptors use the gp130 signal transducer [Mitsumoto, 1994].

In order to better investigate whether TNF-α/TNFR1 might induce motor neurodegeneration in wobbler mice, treatments with agents able to block this detrimental pathway (such as anti-TNF-α monoclonal antibodies, soluble TNFRs, TNFR1 receptor antagonist), are required.

Although anti-TNF-α will reveal a link between the over expression of this cytokine and the death of motor neurons, a further treatment by using a caspase 8 inhibitor should be performed to clarify the possible involvement of this type of apoptotic pathway in the cervical motor neuron death.

11.3 Excitotoxicity and wobbler mouse motor neuron disease

11.3.1 Introduction

The role of glutamate-induced excitotoxicity in ALS and in different animal models of motor neuron degeneration has been previously reported in sections 1.3.2, 4.2.2 and 5.4.1. Moreover, the mechanism of death induced by AMPA/Kainate overstimulation in primary neuron cultures (using Ca^{++} influx, proteases activation, mitochondrial damage, and, depending on the intensity of stimulus, caspases activation dependent- or energetic catastrophe dependent-cell death) has been widely described in the sections 2.2.2.3.

It has been already reported that the exposure to glutamate in neuronal cultures induces a rapid and massive pattern of death in a non-apoptotic manner, while more prolonged exposure to lowere concentration of glutamate generates apoptosis in neurons [Leist, 1997;Nicotera, 1997].

Although the possible involvement of glutamate-induced excitotoxicity in motor neuron degeneration was extensively investigated both in ALS patients and in almost all animal models of ALS, few and controversial results about excitotoxic involvement have been reported in the wobbler mouse [Ait-Ikhlef, 2000;Krieger, 1991;Tomiyama, 1994].

11.3.2 Experimental design

To better evaluate the possible link between excitotoxicity and wobbler mice motor neuron degeneration, different experiments were carried out in this study: I) plasma levels of amino acids; II) glutamate in synaptosomes and glial fraction homogenates from the cervical spinal cord of wobbler mice and age-matched healthy littermates at 4 and 12 weeks of age; III) immunohystochemistry and western blots to determine the levels of AMPA in the early symptomatic wobbler mice.

11.3.3 Results

11.3.3.1 Glutamate determination in plasma

The plasma levels of amino acids in wobbler and control mice at 4 and 12 weeks of ages (five animals for each group) are reported in table 11.2. In the control group, older animals (12 weeks) higher plasma amino acids levels were found compared to younger mice (4 weeks). This increase was not restricted to glutamic acid, but involved all the amino acids (glycine, glutamine, isoleucine) analyzed. Wobbler mice also showed age-related increases of aminoacids levels (data not shown).

Mean glutamic acid concentrations were no different in wobbler and control mice at any age. However, while isoleucine concentrations were similar in wobbler and control mice, concentrations of glutamate, glycine and glutamine tended to be lower in wobbler mice. However, not significant differences were found.

	Glutamic Acid	Glycine	Glutamine	Isoleucine
Ctr 4 weeks	**53.1±40.7**	**372.6±442.0**	**208.5±197.4**	**59.5±58.8**
Wr 4 weeks	**40.3±28.6**	**298.8±227.7**	**146.5±106.6**	**61.9±54.3**

Table 11.2. Amino acids concentrations in the plasma of wobbler mice and age matched healthy littermates. The values are expressed as mean ± S.D.

11.3.3.2 Glutamate transporters

This part of the study was designed to verify the possible role of glutamate transporters in wobbler mice, by comparing the levels of glutamate transporters (GLT-1 and GLAST) in the cervical spinal cord of control and wobbler mice, and their functional expression by glutamate uptake activity.

Representative immunoblot for glutamate transporters in 4 week-old wobbler mice and healthy littermates, are shown in figure 11.11.

Representative immunoblot for glutamate transporters in 4 week-old wobbler mice and healthy littermates, are shown in figure 11.11.

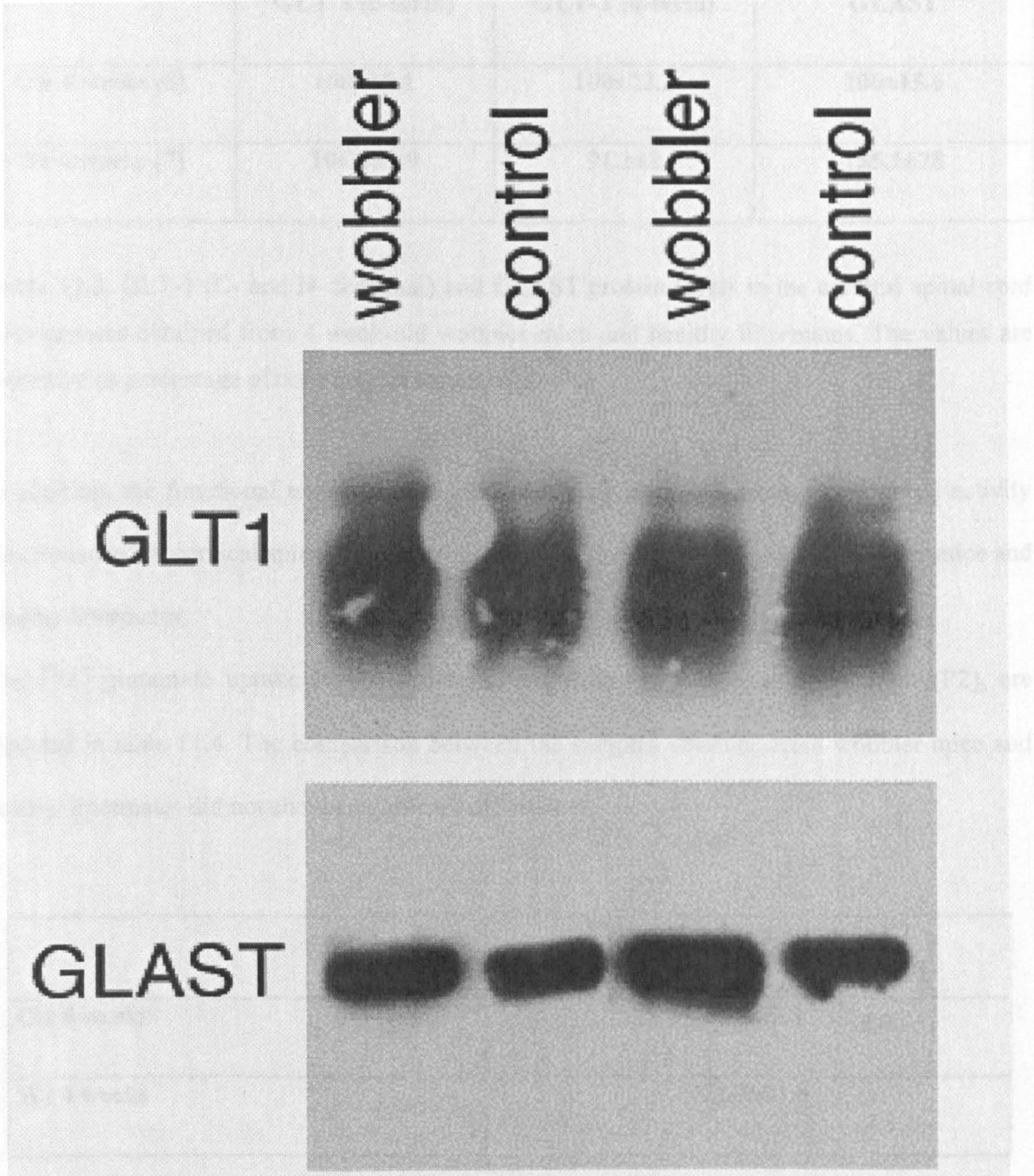

Figure 11.11 Representative immunoblot obtained for C-terminal GLT1 and GLAST from homogenates of the cervical region of spinal cord in wobbler mice and healthy littermates at 4 weeks of age.

No differences in immunoblot density were found for the GLT-1 protein measured with Ab raised against both the N- and the C- terminal; and for the GLAST protein (see table 11.3).

	GLT-1 (c-term)	GLT-1 (n-term)	GLAST
Ctr 4 weeks (8)	**100±18.1**	**100±22.2**	**100±15.6**
Wr 4 weeks (7)	**106.3±9.9**	**91.1±2**	**135.1±78**

Table 11.3. GLT-1 (C- and N- terminal) and GLAST protein levels in the cervical spinal cord homogenates obtained from 4 week-old wobbler mice and healthy littermates. The values are expressed as percentage of controls, (as mean ± S.D.).

In addition, the functional expression of glial and presynaptic glutamate transporters activity was measured in cervical spinal cord homogenates obtained from 4 week-old wobbler mice and healthy littermates.

The [^{3}H] glutamate uptake levels, measured in crude synaptosomal preparation (P2), are reported in table 11.4. The comparison between the samples obtained from wobbler mice and healthy littermates did not shown significant differences.

	[^{3}H] glutamate activity in P2
Ctr 4 weeks	**227.1±9.3**
Wr 4 weeks	**222.7±11.8**

Table 11.4. [^{3}H] glutamate uptake in P2 obtained from 4 weeks aged cervical spinal cord homogenates from wobbler mice and healthy littermates (six animals for each group). (The numbers reported are the mean values expressed as pmol/min/mg protein ± S.D.).

11.3.3.3 AMPAr expression and localization

GluR1

Representative microphotographs showing the immunostaining in the cervical spinal cord of 4 week-old wobbler mice and healthy littermates are shown in figure (11.12 A, B). In both sections it is possible to observe a weak but homogenous staining in the whole the gray matter, whereas the white matter were almost unstained for GluR1. No marked differences were seen between wobbler and healthy mice sections.

Two microphotographs showing the distribution and the localization of GluR1 staining in anterior horn neurons of cervical spinal are shown in figure 11.12.

In order to obtain a semi-quantitative estimation of the GluR1 expression in the anterior horn neurons, indirect measurements of immunostaining were performed by calculating the optical density for each single motor neuron. For this analysis, 20 cervical spinal cord sections (25 μm of thick) for each animal, 5 animals for each experimental group, and four different experimental groups (4 and 12 week-old wobbler mice and healthy littermates) were processed. The following procedure was also adopted to determine the immunostaining density for all the other three subunits.

No significant differences in the mean levels of immunostaining density in wobbler mice, at both ages examed were found. The mean level of GluR1 immunostaining density in cervical motor neurons is expressed as a percentage compared to their respective controls, normalized to 100 (% GluR1 immunostaining density control 4 weeks 100±4.2; wobbler 4 weeks 103±9.9 n.s) (% GluR1 immunostaining density control 12 weeks 100±4.9; wobbler 12 weeks 104±7.7 n.s).

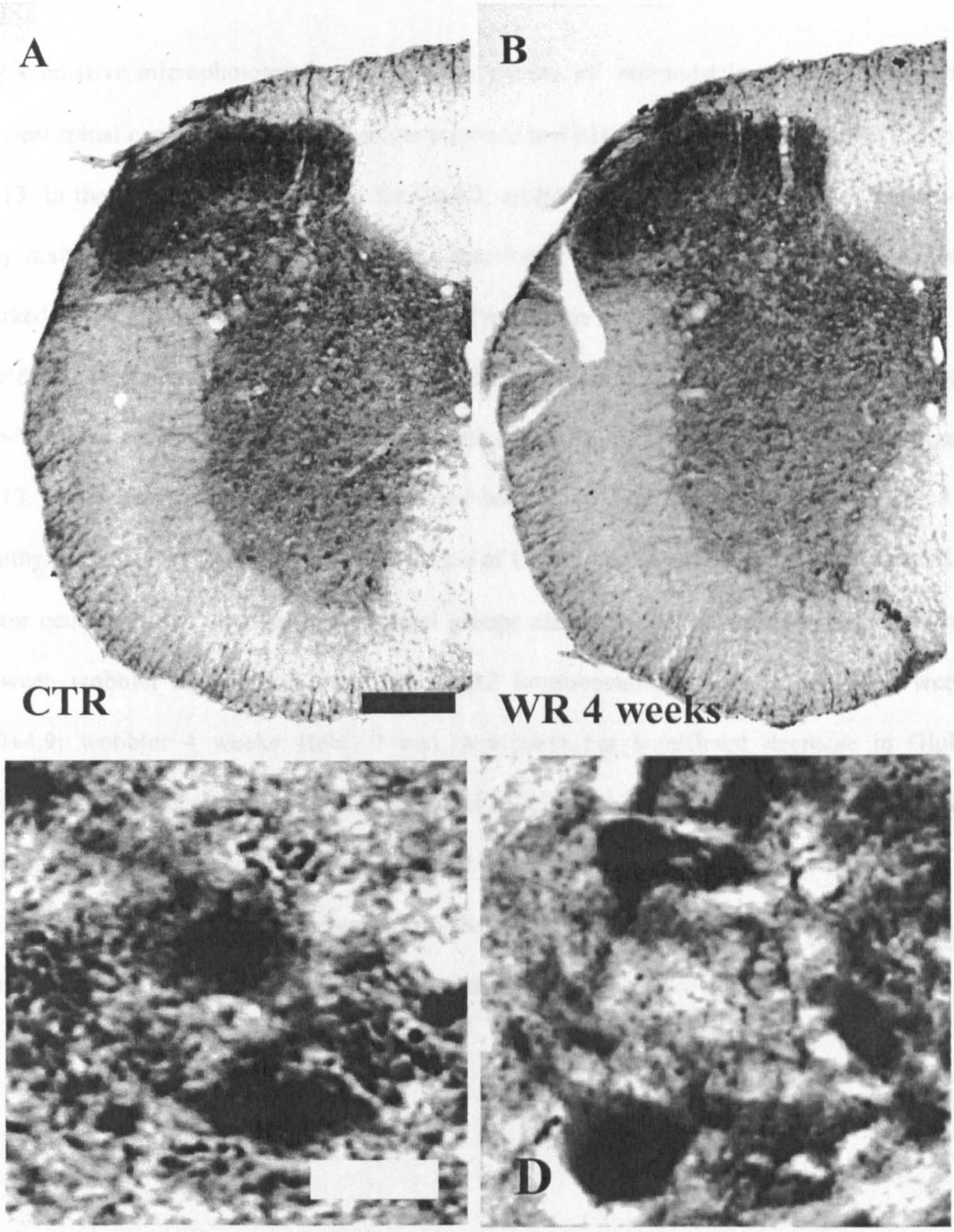

Figure 11.12 Representative microphotographs showing GluR1 immunostaining in the cervical spinal cord region of healthy mice (A) and early symptomatic wobbler mice (B). GluR1 immunostaining localization in motor neurons from the cervical spinal cord sections of healthy mice (C) and early symptomatic wobbler mice (D).
Scale bar, A,B 200 μm. C,D 50 μm.

GluR2

Representative microphotographs showing the pattern of immunostaining for GluR2 in the cervical spinal cord of 4 week-old wobbler mice are and healthy littermates are shown in figure 11.13. In the section immunostained for GluR2, an intense positivity is evident in the whole gray matter, and neurons, above all in the anterior horn, resulted more intensively stained. Marked differences between wobbler and control mice were not seen.

The distribution and the localization of GluR2 immunostaining in anterior horn neurons of the cervical spinal cord in 4 week-old wobbler mice and healthy littermates is shown in figure 11.13. Motor neurons were intensively stained both in wobbler mice (Fig 11.13 B, D) and in healthy littermates (Fig 11.13 A,C). The values of GluR2 immunostaining density measured in motor neurons in the younger experimental groups did not revealed any statistical difference between wobbler and control mice (% GluR2 immunostaining density control 4 weeks 100±4.9; wobbler 4 weeks 109±7.7 n.s), a modest but significant decrease in GluR2 immunostaining density was instead observed in 12 weeks aged wobbler mice (% GluR2 immunostaining density control 12 weeks 100±9.4; wobbler 12 weeks 83.6±3.4 $p<0.05$).

The reason of this decrease is unclear: it may be related to the process of cellular vacuolization that reduce the cellular density in wobbler mice motor neurons.

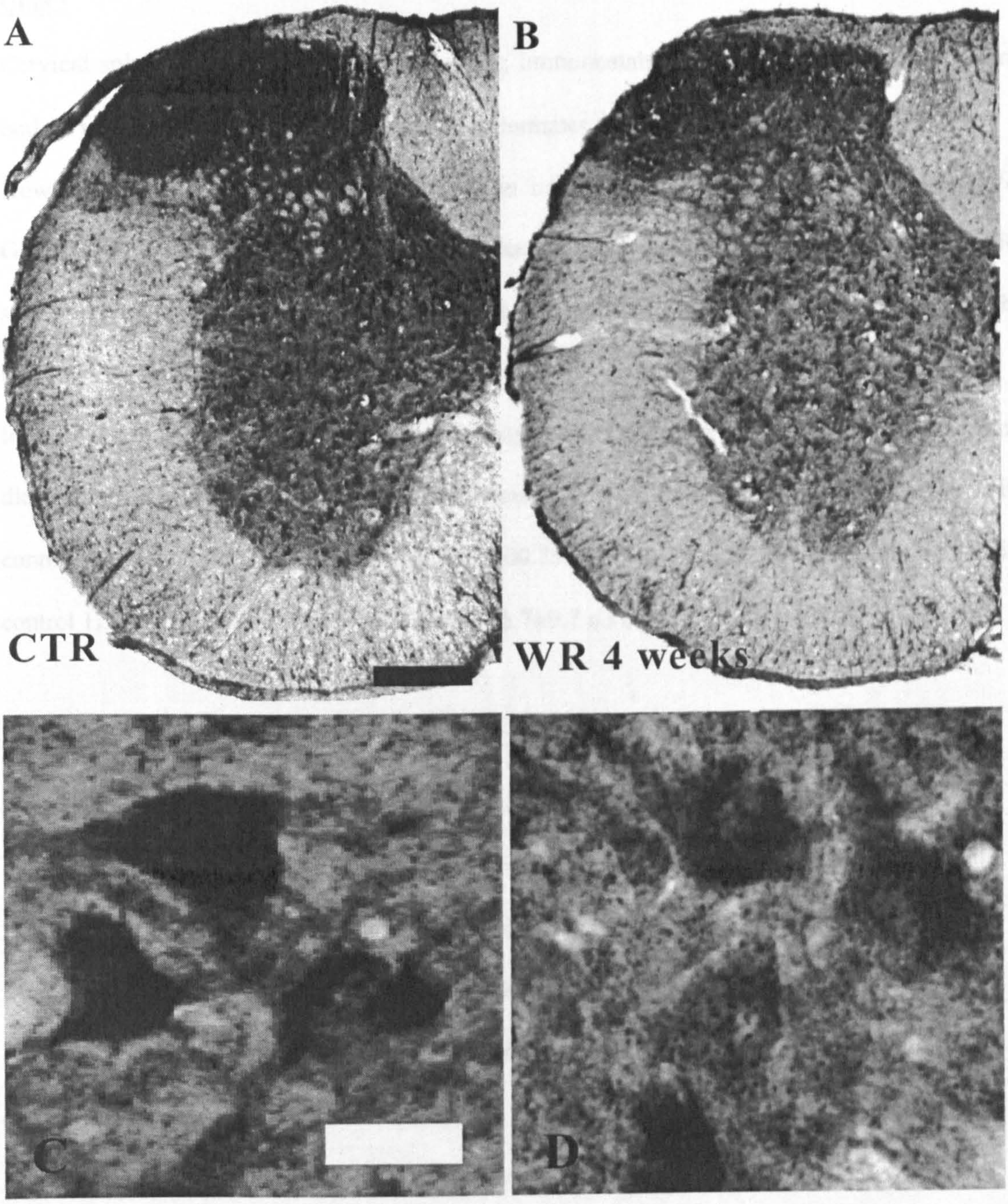

Figure 11.13 Representative microphotographs showing GluR2 immunostaining in the cervical spinal cord region of healthy mice (A) and early symptomatic wobbler mice (B). GluR2 immunostaining localization in motor neurons from the cervical spinal cord sections of healthy mice (C) and early symptomatic wobbler mice (D).

Scale bar, A,B 200 μm. C,D 50 μm.

GluR3

Cervical spinal cord sections showed a strong immunostaining for GluR3 in the dorsal horn, both in wobbler (Fig 11.14 B) and in healthy littermates (Fig 11.14 A).

However, by observing anterior horn at higher magnification, a strong immunopositivity for GluR3 was found. No marked differences in localization, distribution and intensity for GluR3 staining were seen in motor neurons between wobbler mice (Fig 11.14 D) and healthy littermates (Fig 11.14 C).

In both stages of the disease the immunodensity in wobbler mice, measured in motor neurons, did not statistically differ to age-matched healthy mice (% GluR3 immunostaining density control 4 weeks 100.0±7.8; wobbler 4 weeks 100.7±23.7 n.s) (%GluR3 immunostaining density control 12 weeks 100±9.1; wobbler 12 weeks 85.7±9.7 n.s).

GluR4

As for GluR1 and GluR3, staining for GluR4 was mainly localized in the dorsal region. A modest but detectable immunostaining was also observed in the anterior horns, but mainly in fibers rather than in cell bodies (fig 11.15 A, B).

Motor neuron staining revealed a marked nuclear immunopositivity and a weaker signal in the periphery in unaffected (Fig 11.15 C) and diseased mice (Fig 11.15 C). No differences were determined by measuring the immunodensity in healthy and wobbler mice (% GluR4 immunostaining density control 4 weeks 100.0±15.8 wobbler 4 weeks 83.9±11.5 n.s) (%Glur4 immunostaining density control 12 weeks 100.0±1.5; wobbler 12 weeks 99.0±0.9 n.s).

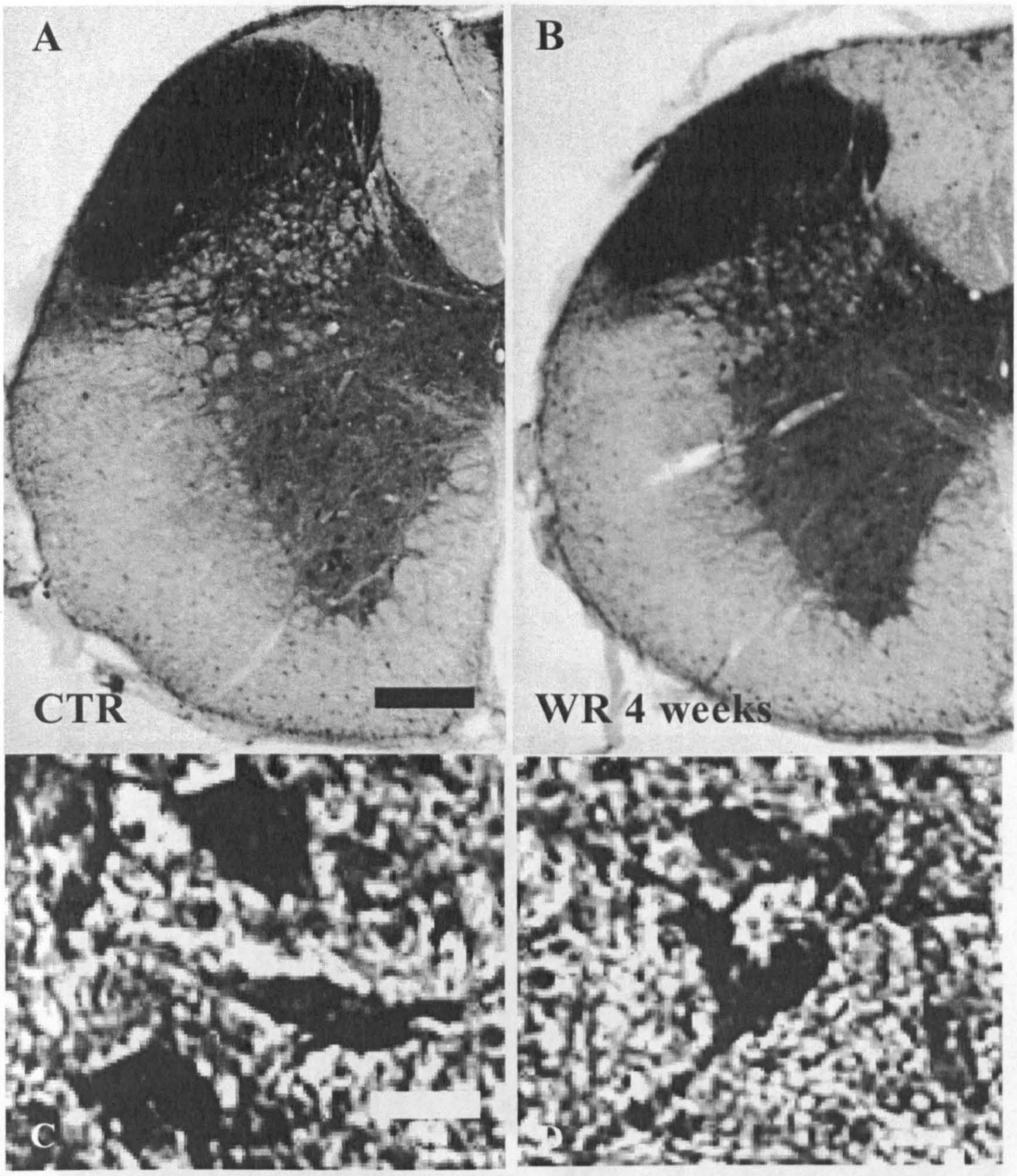

Figure 11.14 Representative microphotographs showing GluR3 immunostaining in the cervical spinal cord region of healthy mice (A) and early symptomatic wobbler mice (B). GluR3 immunostaining localization in motor neurons from the cervical spinal cord sections of healthy mice (C) and early symptomatic wobbler mice (D).
Scale bar, A,B 200 μm. C,D 50 μm.

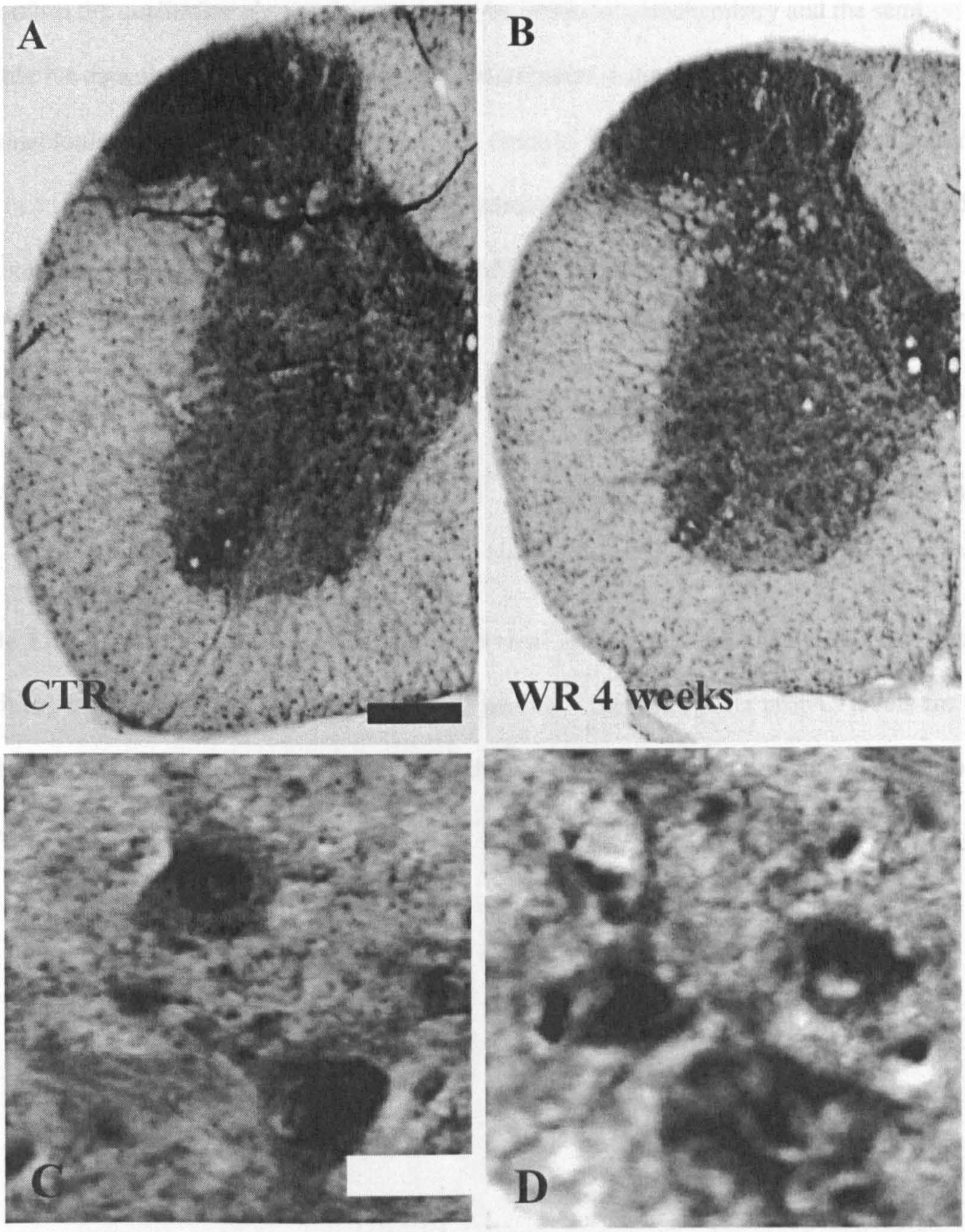

Figure 11.15 Representative microphotographs showing GluR4 immunostaining in the cervical spinal cord region of healthy mice (A) and early symptomatic wobbler mice (B). GluR4 immunostaining localization in motor neurons from the cervical spinal cord sections of healthy mice (C) and early symptomatic wobbler mice (D).
Scale bar, A,B 200 µm. C,D 50 µm.

To confirm the qualitative observations obtained by immunohystochemistry and the semi quantitative data obtained by optical density measurements, a quantification (by immunoblotting experiments) of all proteins was made in the ventral region of cervical spinal cord in 4 weeks wobbler mice and healthy littermates (5 animals for each group were utilized). No significant differences were found for other AMPA subunits (see table

	GluR1	**GluR2**	**GluR3**	**GluR4**
Ctr 4 weeks	**100±20.8**	**100±36.9**	**100±13.8**	**100±30.6**
Wr 4 weeks	**107±0.3**	**89.9±19.5**	**121.1±20**	**111.3±37.4**

Table 11.5. GluR 1-4 protein levels in the cervical spinal cord homogenates (post synaptic densities) from 4 week-old wobbler mice and healthy littermates. The protein levels for each subunit are expressed as percentage compared to their respective controls normalized to 100 and are reported as mean ± S.D.** $p<0.05$

Representative immunoblotting of the GluR 1-4 subunits is shown in figure 11.16.

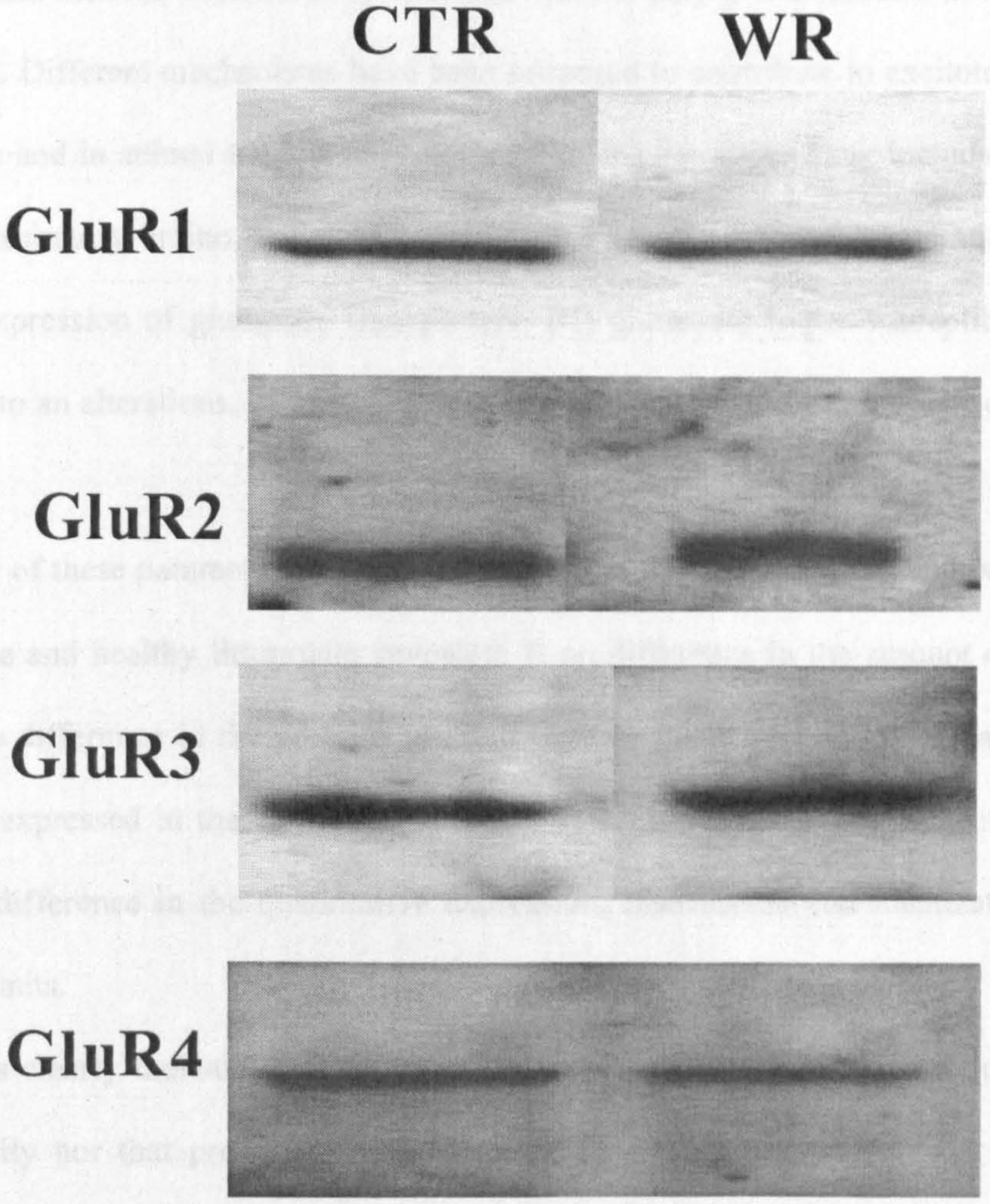

Figure 11.16 Representative immunoblot obtained for AMPA receptor subunits GluR 1-4 from homogenates of the cervical region (post synaptic densities) of spinal cord in wobbler mice and healthy littermates at 4 weeks of age.

11.3.4 Discussion

The main evidence emerging from this investigation is that, in early symptomatic wobbler mice, glutamate-induced excitotoxicity does not seem to play a relevant role in inducing motor neuron death. Different mechanisms have been proposed to contribute to excitotoxic damage in ALS patients and in animal models of motor neuron degeneration. They included: I) increased amount of excitatory amino acids in plasma and CSF, II) reduced levels and/or decreased functional expression of glutamate transporters, III) glutamate hyper susceptibility of motor neurons due to an alterations, in the number or in electrophysilogical properties, of postsynaptic AMPAR.

The majority of these parameters have been analyzed in this study and the comparison between wobbler mice and healthy littermates revealed: I) no difference in the amount of amino acids levels, II) no difference in the proteins level of the two main glial and presynaptic glutamate transporters expressed in the cervical spinal cord (GLT1, GLAST), and in glutamate uptake, and IV) no difference in the quantitative expression, distribution and localization of AMPA receptor subunits.

These results clearly indicate that neither an overstimulation induced by a reduced glutamate uptake activity nor that produced by an increase of AMPA receptors and/or a decrease of GluR2 expression, are involved.

However, it is not yet possible to fully exclude this aetiological hypothesis. In fact, neither the electrophysiological properties of AMPA receptors nor the possible expression of the edited form of GluR2 (the Ca^{++} permeable conformation) were investigated in this study.

Alterations in such parameters may be responsible for making the AMPA receptor more vulnerable to physiological exposure to glutamate and therefore leading to motor neuron death.

For this reason the effects of two pharmacological treatments, with a selective antagonist of AMPA receptors reported to be active in $SOD1^{G93A}$ mice [Canton, 2001], and with riluzole, a non selective antiexcitotoxic agents that is, the only FDA-approved drug for ALS treatment, were tested in early symptomatic wobbler mice and healthy littermates (see chapter 12).

1.4 Mitochondria and apoptosis

11.4.1 Introduction

The mechanisms of motor neuron degeneration in ALS are still unknown and the evidence for an apoptotic-like cell death is controversial (see section 2.3.3). Although animal models of ALS display remarkable differences with respect to human disease, they represent a useful tool to investigate the early processes leading to motor neuron death (see section 5.6). To verify the possible involvement of apoptosis and motor neurons death in the wobbler mouse, the pathway passing through mitochondria and activating caspases cascade cell signaling was investigated in this part of the study.

11.4.2 Experimental design

Before evaluating whether apoptotic markers were induced, a detailed characterization of the mitochondrial activity was carried out. Mitochondrial activity was measured in 4 week-old wobbler mice and healthy littermates by measuring the oxygen consumption rate and the activities of ETC complexes by spectrophotometric analysis, complex I activity was also determined using a quantitative hystochemical assay.

Intrinsic apoptotic pathway mainly involves caspase 9, -3 and, in the CNS, caspase 7 (see section 2.2.5). For this reason immunohystochemical experiments with antibodies directed against the active form of these three caspases were carried out. A further investigation using ISEL staining to determine possible alterations of nuclear integrity was performed. These latter experiments were done by comparing cervical spinal cord of 4 week-old wobbler mice and healthy littermates.

All experiments were done following the procedures described in the chapter 9.

11.4.3 Results

11.4.3.1 Mitochondrial activity

Mitochondria from early symptomatic wobbler mice showed a significant decrease in basal oxygen consumption (% QO_2 control 4 weeks 100.0±2.1; wobbler 4 weeks 79.8±5.2 $p<0.03$) At 4 weeks of age, mitochondrial enzymatic activities seemed to be lower in the cervical region, though a statistical significance was only found for complex I. When the respiratory enzyme activities were expressed as a ratio to citrate synthase (CS) activity, only complex I resulted to be significantly decreased (% activity complex I /CS, control 4 weeks 100.0±1.8; wobbler 4 weeks 86.5±3.5 $p<0.04$). No differences were found in the lumbar spinal cord of the wobbler mice in comparison with controls (see Fig 11.17 A, B).

Histochemical measurement of complex I activity in ventral horn motor neurons showed a significant decrease of staining intensity in the early symptomatic wobbler mice, the values are expressed as percentage respect to the controls (% of complex I, control mice 100±12.7; wobbler mice 65.7 ± 10.8% ($p<0.05$)) .

Representative microphotographs of complex I positive staining in the anterior horn of the cervical spinal cord are shown in Fig 11.18 A, B.

PAGE NUMBERING AS ORIGINAL

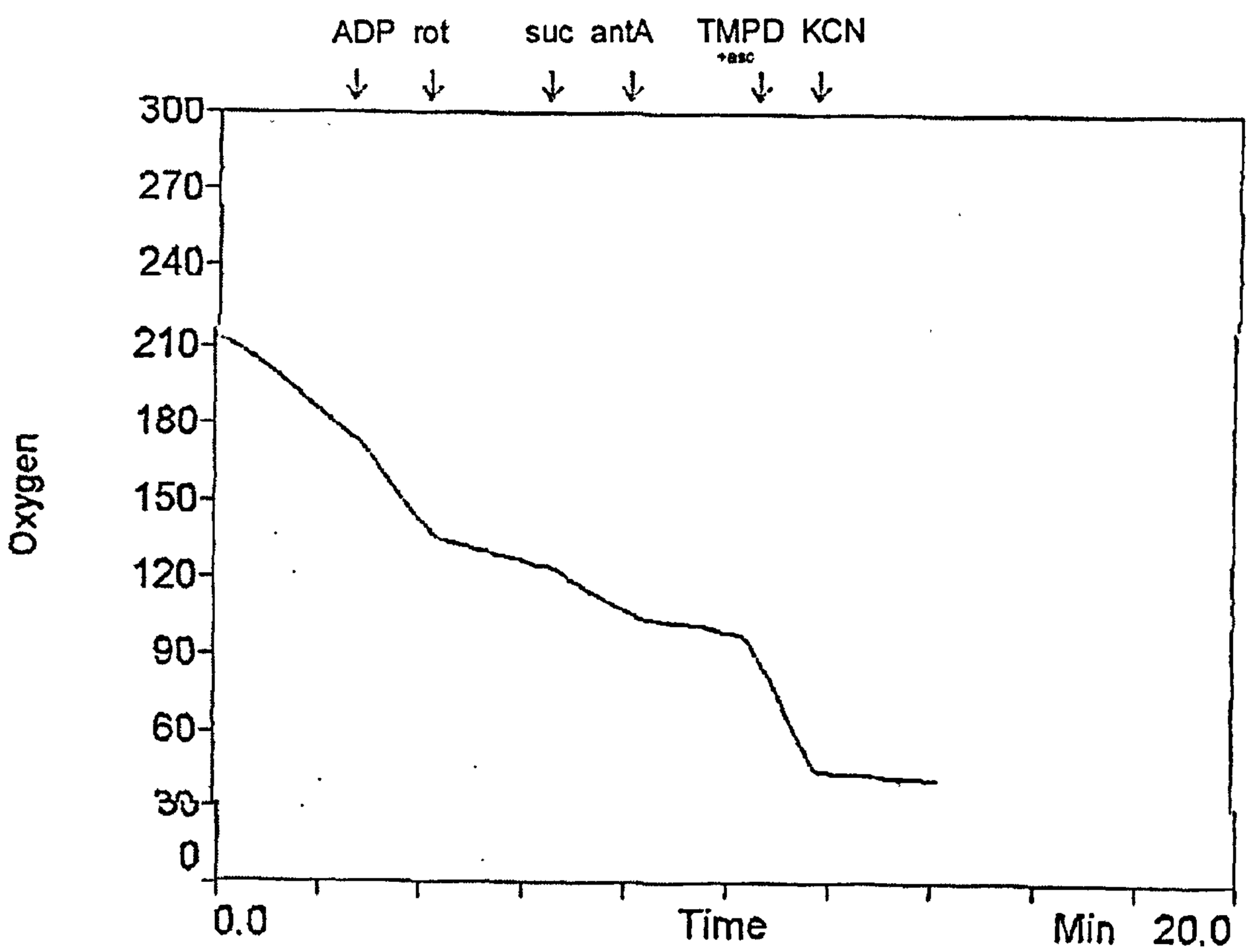

Figure 11.17. A representative diagram showing the oxygen consumption in the cervical spinal cord of control mice is represented in this figure. The different enzymatic activities (complex I-IV) were estimated by adding specific blockers and/or uncouplers during the experiment, following the procedure described in the section (9.11.1). In the cervical spinal cord of wobbler mice the activity recorded by oxygraphy resulted significantly lower compared to control mice.

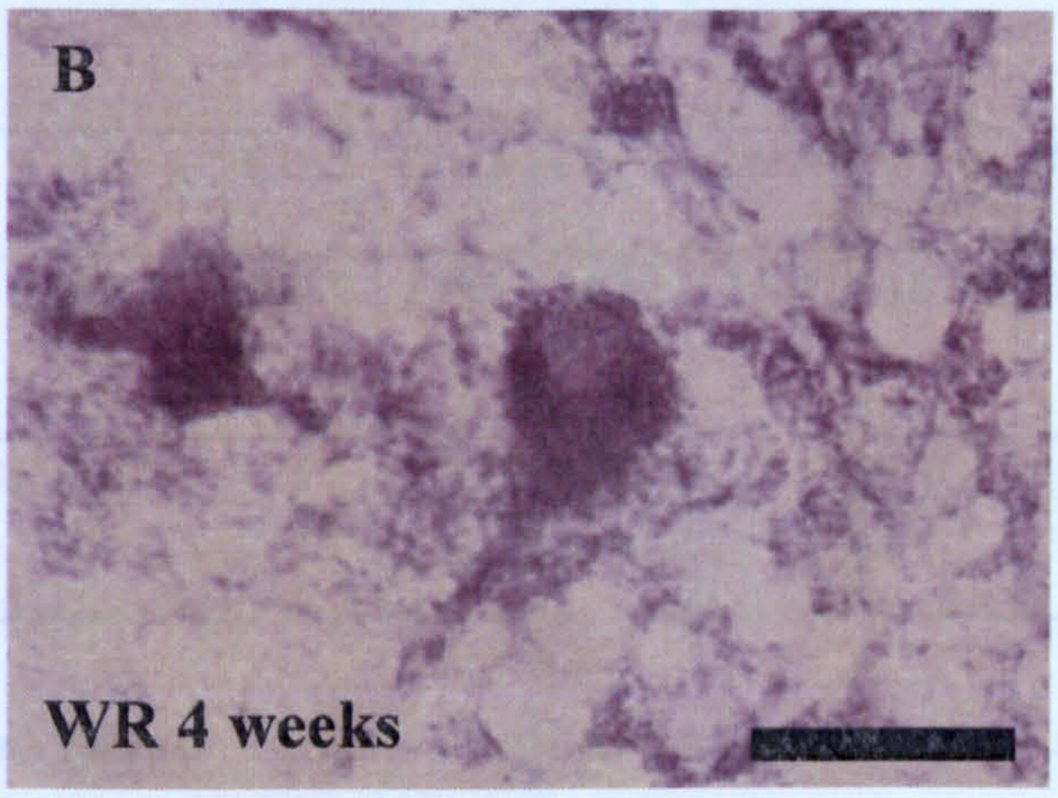

Figure 11.18 Hystochemical determination of complex I activity evaluated in the cervical spinal cord of wobbler mice and healthy littermates. Complex I staining is proportional to the amount of substrate reduced (NADH) by complex I and the consequent activation of a colorimetric reaction following the oxidation of the nitro blue tetrazolium (blue staining). In the upper microphotograph a representative distribution of staining in the cervical spinal cord region is shown (A). It is possible to note as motor neurons appear highly immunopositive for this staining procedure. The cellular localization of complex I staining clearly shows an intense positivity into the cytoplasm with a lack of staining in the nucleus. Scale bar, A 200 μm. B 40 μm.

11.4.3.2 Active caspase 3, -7 and -9 immunohystochemistry

Mitochondria alterations can often generate the release of cytochrome-c and the consequent formation of apoptosome and procaspase 9 cleavage [Ferraro, 2003]. Caspase 9 activation can furthermore propagate this process by recruiting caspases 3 and 7 by hierarchical activation [Slee, 1999].

To evaluate if mitochondrion-dependent apoptotic pathway might be related to motor neurons death in wobbler mice, the activated caspases 3, 7 and 9 were investigated in 4 week-old wobbler mice and healthy littermates.

For activated caspase 9, a very low number of positively stained motor neurons in the anterior horn of cervical spinal cord of early symptomatic wobbler mice were observed, and this value was not significantly higher than in healthy littermates.

Animals (C2-C7)	Ctr 1	Ctr 2	Ctr 3	Ctr 4	Ctr 5	Wr 1	Wr 2	Wr 3	Wr 4	Wr 5
N° ChAT positive cells (50 sections)	1662	1589	1486	1536	1501	1076	834	1145	1201	894
N° caspase 9 positive cells (50 sections)	2	3	1	0	4	0	2	2	3	1

Table 11.6 ChAT and caspase 9 positive cells in the cervical spinal cord region of 4 weeks aged wobbler mice and healthy littermates.

Immunohystochemical experiments in the cervical spinal cord of 4 week-old wobbler mice and healthy littermates for active caspases 7 and -3, revealed an extremely low number of positive cells for both caspases. The values of positive cells for caspase 7 and caspase 3 are reported in tables 11.7 and 11.8.

Animals (C2-C7)	Ctr 1	Ctr 2	Ctr 3	Ctr 4	Ctr 5	Wr 1	Wr 2	Wr 3	Wr 4	Wr 5
N° ChAT positive cells (50 sections)	1539	1492	1631	1597	1533	973	1118	1206	1099	1149
N° caspase 7 positive cells (50 sections)	0	3	0	0	2	2	0	1	0	2

Table 11.7 ChAT and caspase 7 positive cells in the cervical spinal cord region of 4 weeks aged wobbler mice and healthy littermates

Animals (C2-C7)	Ctr 1	Ctr 2	Ctr 3	Ctr 4	Ctr 5	Wr 1	Wr 2	Wr 3	Wr 4	Wr 5
N° ChAT positive cells (50 sections)	1652	1432	1558	1601	1529	896	1024	1202	1155	1204
N° caspase 3 positive cells (50 sections)	2	2	1	0	3	1	0	0	3	4

Table 11.8 ChAT and caspase 3 positive cells in the cervical spinal cord region of 4 weeks aged wobbler mice and healthy littermates.

Representative microphotographs showing sections of wobbler mice processed to caspase 9, 7 and 3 are reported in figure 11.18 (A-C).

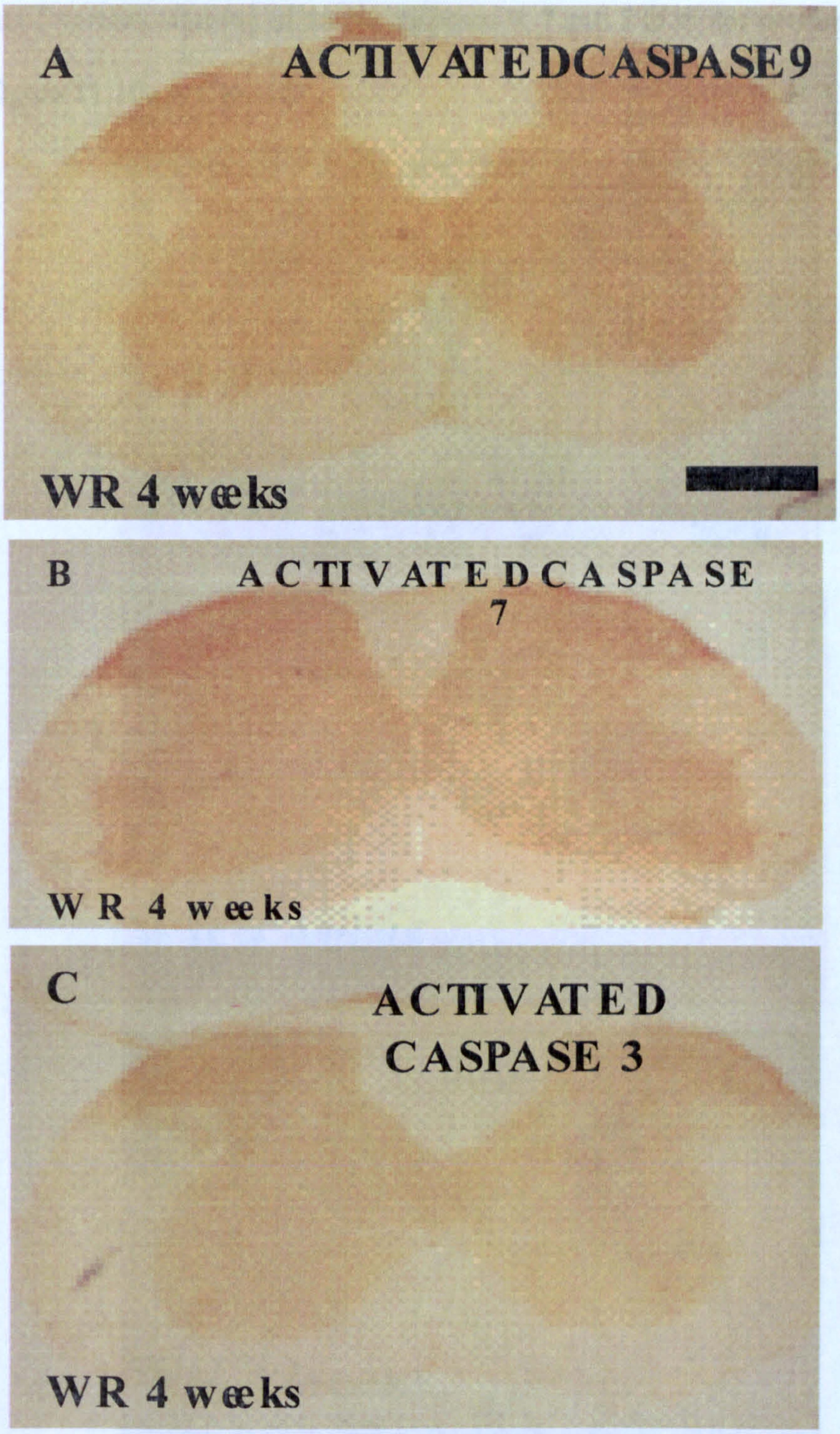

Figure 11.19 Representative section of the cervical spinal cord in early symptomatic wobbler mice immunostained for active caspase 9 (A), active caspase 7 (B) and active caspase 3 (C) are shown here. Although a weak and homogeneously diffused staining is detectable in the whole gray matter in each section, this represents a background due to a not specific reaction of the system of signal enhancing (ABC colorimetric detection). Scale bar, 400 μm.

The pattern of immunostaining of active caspases 9, 7 and 3 in motor neurons are shown in figure 11.19 (A-C).

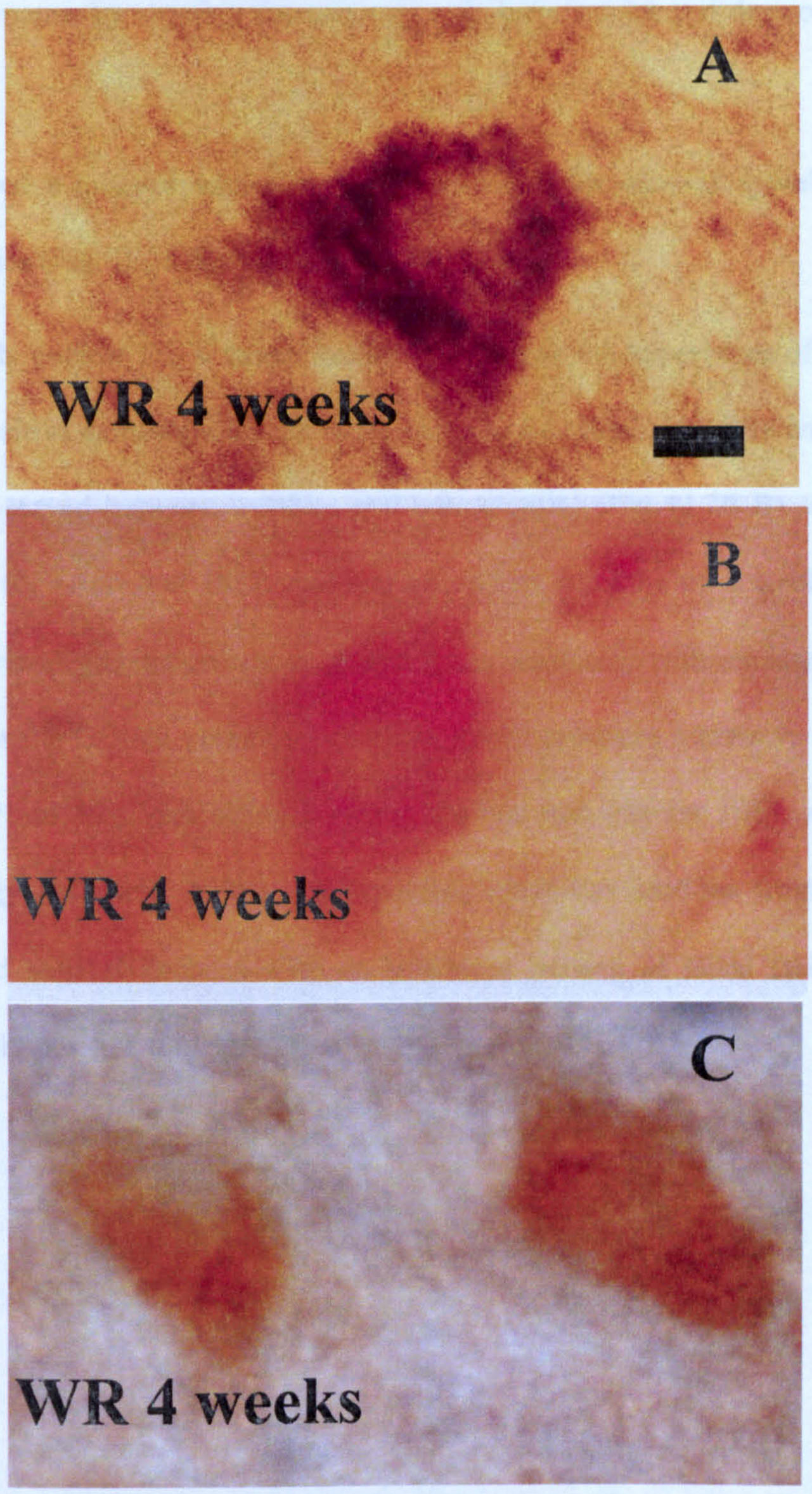

Figure 11.20 Pattern of staining and cellular localization observed for the active caspase 9 (A), capase 7 (B), and caspase 3 (C) in the cervical spinal cord motor neurons in wobbler mice. For each caspases no nuclear immunopositivity was found. Scale bar, 20 μm.

11.4.3.3 ISEL staining

DNA fragmentation was investigated in the cervical spinal cord of 4 week-old wobbler mice, and age healthy littermates, by staining the sections with cresyl violet and then performing an ISEL assay.

Nissl staining revealed a marked vacuolar degeneration in the cervical spinal cord motor neurons in wobbler mice (Fig 11.20 A).

Although ISEL reveals nuclear DNA strand breaks well before the appearance of an apoptotic morphology, ISEL positive cells were absent in all sections examined. No difference in nuclear morphology, were observed between wobbler and control mice (Fig 11.20 B). As a positive control, I processed for Nissl and ISEL staining cerebellar sections of 3 week-old weaver mouse, a model of neurodegeneration whose phenotype is associated with a missense mutation in the gene coding for the GIRK2 potassium channel, which produces a massive and selective loss of CGC form P1 to P21, exhibiting a strong nuclear staining for ISEL and a typical apoptotic morphology [Migheli, 2004]. As expected, cerebellar sections from 3 week-old weaver mice showed several neurons with an unaltered pattern of Nissl staining, purple staining, but intensively positive for ISEL, brown staining. (11.20 C, D).

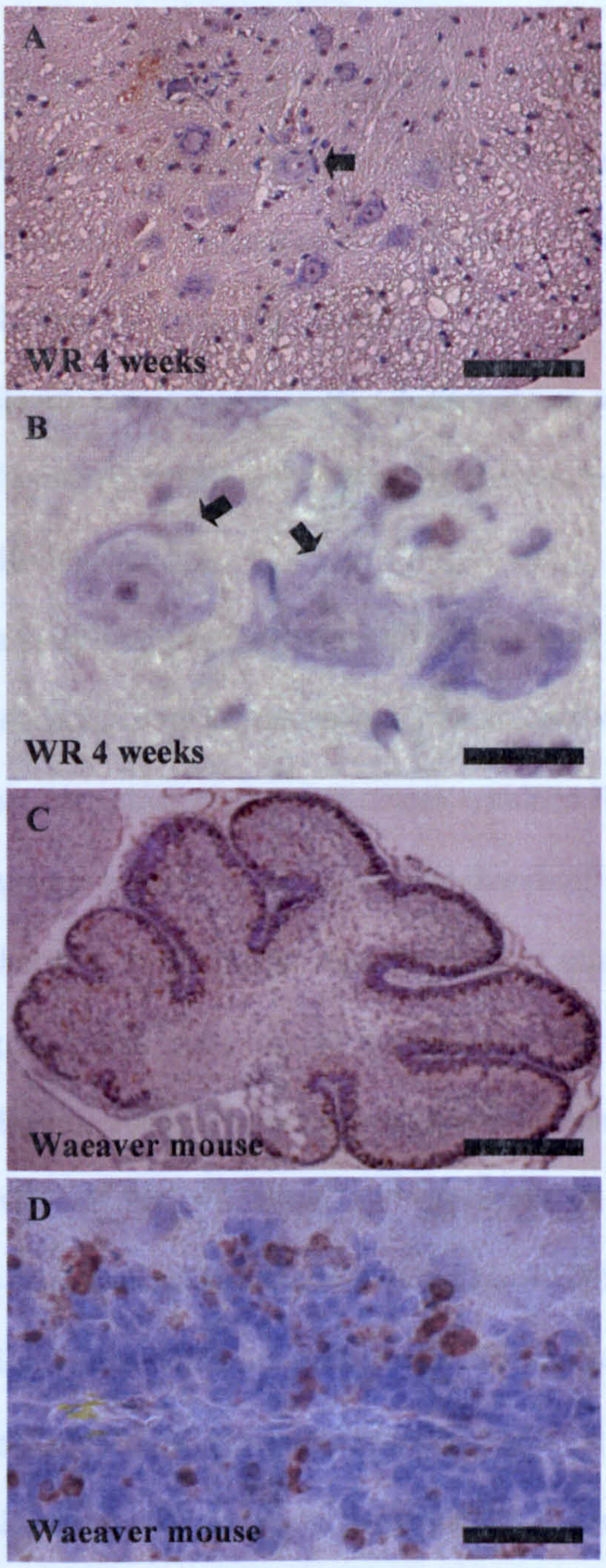

Figure 11.21 Representative microphotograps showing a cervical spinal cord section (early symptomatic wobbler mice), processed for Nissl staining and ISEL staining (A-B). Dying motor neurons (arrows), clearly show morphological alterations but maintain their nuclear integrity and are not positive for ISEL staining. On the other hand, dying cerebellar neurons in 3 week-old weaver mouse (C-D), are found highly positive for ISEL staining. Scale bar, A 100 μm. B, 40 mm. C, 200 μm. D, 50 μm.

11.4.4 Discussion

Many agents can trigger possible mitochondria-dependent apoptotic pathways (see section 2.2.2.1 and 2.2.2.2), and, to make a correlation between environmental alterations and intrinsic apoptosis of cervical motor neurons in wobbler mice, Ca^{++} influx, through AMPAr stimulation, and neurotrophic factor withdrawal, must be considered.

In chapter 10, it has been clearly shown that both BDNF deprivation and stimulation of AMPAr produce typical features of apoptosis and that the apoptotic process, induced by this excitotoxic stimulus, passes through mitochondria.

Here, the mitochondrial activity was first investigated in the spinal cord of wobbler mice at early symptomatic phase. A decrease of the respiratory rate and activities of the mitochondrial enzymes were found in cervical spinal cord homogenates obtained from wobbler mice. Since these techniques for measuring respiratory rate and mitochondrial enzyme activities cannot distinguish between mitochondria deriving from neurons or from glial cells, the results maybe due to the reactive astrogliosis and motor neuron loss observed at this stage of the disease [Hantaz-Ambroise, 1994;Bigini, 2001]. However a decrease of complex I activity was also detectable when the activity of motor neurons was measured by hystochemical staining. Complex I is a critical site of mitochondria oxygen free radical (ROS) production. Even a small degree of enzyme inhibition seems sufficient to enhance ROS generation and chronic, low-grade complex I inhibition, induced by rotenone exposure, has been described to cause slight elevation in basal apoptosis. Complex I seems to participate in the regulation of PTP opening and the following propagation of apoptotic cell signaling [Chauvin, 2001;Fontaine, 1999;Higuchi, 1998] and may therefore provide a link between mitochondria and the downstream pathway for cell death.

In addition, it is important to note that in the lumbar spinal cord homogenates, obtained from the animals tested for cervical spinal cord mitochondria activities, by performing the same types of experiments, no differences were found both in oxygen consumption rate and in ETC complexes efficiency between affected and healthy mice (see appendix "Published papers arising from this thesis").

The activation of caspases and the nuclear fragmentation in cervical spinal cord motor neurons of early symptomatic wobbler mice further investigated these aspects and the presence of signs indicative of apoptosis.

A lowest percentage of motor neurons showed a positive staining for caspases 9, -7 and -3. Moreover, for each capsase, this percentage was not significantly higher than healthy littermates. In agreement with this result, no fragmented nuclei (ISEL positive) were found in the cervical motor neurons of both groups.

The lack of caspases-associated apoptotic pathway, together with a loss of mitochondrial activity can be explained by a different mechanism of death in which mitochondria also play a relevant role. For instance, PTP has a role in regulating the fate of cells and in preventing or promoting apoptosis but also in contributing to enhance a necrotic cell death [Tatton, 1999]. If permeability transition pore can stimulate both primary necrosis and apoptosis, what makes the difference?

It is possible that the bioenergetics and redox catastrophe (which would induce non-apoptotic cell death) and the activation of catabolic enzymes (caspases and nucleases) might compete with each other. Mitochondria are the main target of stress and their alterations could represent a trigger for distinct cell death pathways depending on the type of stress involved. This picture is compatible with the evidence that different agents can induce apoptosis at low doses, when permeability of the transition pore is induced smoothly and cells can activate caspases cascade cell signaling, and induce necrosis at higher doses, when permeability of transition pore is abruptly altered and the cell activate stronger pattern of death before cytochrome-c release-induced caspases cascade [Leist, 1997;Hirsch, 1997].

The concomitant observation of mitochondrial alterations in the absence of a caspases-associated apoptotic pathway could be generated by a methodological problem. Although the antibodies directed against the four different caspases that are utilized in this study have been found to work reliably in other conditions (see chapter 10), it is possible that a so low number of caspases positive cells might be due to the low probability to find a cell undergoing apoptotic process.

For this reason the immunohystochemical experiments a very high number of cells, 100 sections for each animal and 5 animals for each experimental group), and were performed at a time point (from the 4^{th} to 5^{th} week of age) when the more sustained loss of motor neurons was observed.

To further exclude that intrinsic apotosis is involved in wobbler mouse motor neuron death, a pharmacological approach with EPO, a compound that have been shown to posses a selective antiapoptotic activity in primary cultures of motor neurons (see sections 10.3 and 10.4), was performed in early symptomatic wobbler mice. These data are reported in the next chapter.

CHAPTER 12

PHARMACOLOGICAL TREATMENTS

12.1 EPO fails to arrest neuromuscular impairment and motor neurons loss in wobbler mice

12.1.1 Introduction

In order to clarify the role of apoptosis in motor neuron degeneration occurring in the cervical spinal cord of wobbler mice, in addition to hystochemical characterization described in the Chapter 11, I investigated the effects of a chronic treatment with a selective anti-apoptotic compound (EPO) that had already been reported to be active in other forms of neurodegenerative diseases. Since treatments with EPO have demonstrated its protective role in reducing neuronal loss and in preventing the symptomatological worsening both in acute and in chronic neurological disorders (see section 2.4.2) and its selective anti-apoptotic effects in primary cultures of motor neurons exposed to kainate or deprived of serum/BDNF have confirmed this role (see chapter 10), this agent was used in the experiments described in this chapter.

Konishi et al. [Konishi, 1993] first demonstrated that some haematopoietic factors, including EPO, acted as neurotrophic factors on central cholinergic neurons, influencing their differentiation and regeneration. The anti-apoptotic mechanism of EPO that has been described in erythroid precursors was also observed in. Jak2 has been shown to trigger NF-kB, and the anti-apoptotic action of NF-kB in neurons also involves activation of Akt1 and BAD phosphorylation as well as BCL-xL up-regulation [Marti, 2004;Ruscher, 2002].

By characterizing the protective effect of EPO against oxygen/glucose deprivation-induced apoptosis of primary cortical neurons, Ruscher demonstrated that EPO produced its protection by activating a pathway involving Jak2 MAPK and PI_3K. In fact, using specific inhibitors of these kinases, PD98059 and the LY984002, the protective effect of EPO was completely

prevented. These molecular mechanisms also included the activation of STAT5, Akt1, cysteine proteases, protein-tyrosine phosphatases, nuclear factor-KB [Ruscher, 2002].

Since PI_3K activation produces an anti-apoptotic effect through BAD inactivation and the subsequent reduction of the $\Delta\Psi_M$ by inhibition of the mitochondrial PTP opening [237], and EPO has been reported to induce BAD phosphorylation [330], it is possible to argue that EPO exerts its neuroprotective and anti-apoptotic effect by blocking and thus inhibiting the downstream steps (cytochrome-c release, caspases activation, nuclear fragmentation). The data obtained in red blood cells precursors (over expression of BCL-xL, an anti-apoptotic agent that acts blocking the mitochondrial PTP) [315], further confirm this suggestion. Interestingly, I observed the same evidence (i.e. block of $\Delta\Psi_M$, inhibition of cytochrome-c release, and lack of mitochondrion-dependent apoptotic pathway) in primary cultures of motor neurons exposed to an apoptpgenic insult, as described in Chapter 10.

12.1.2 Experimental design

To detect whether EPO could produce a beneficial effect in slowing the neuromuscular deficit in the wobbler mouse, a group of wobbler mice was chronically treated, upon clear diagnosis at 3 weeks of age, with rHuEPO until 12 weeks of age. To test the symptomatological progression, behavioural tests were done during the treatment. Biochemical and hystological experiments were carried in order to evaluate the treatment. All experiments were done according to the protocols reported in the chapter 9.

12.1.3 Results

12.1.3.1 Behavioural scores

Body weight

As previously reported (see Chapter 5), the weight of wobbler mice was markedly lower compared to that asymptomatic littermates and the body weight increase is less marked in wobbler mice. Growth was more pronounced in the first period of treatment (from 3rd to 7th week of age), in the last period of treatment, till 12th week of life, the rate of increase lowered. As shown in figure 12.1 A, EPO treatment did not produce effects on the rate of growth in wobbler mice.

Paw abnormality and walking abnormality

The semi quantitative studies (paw abnormality and walking abnormality) showed a similar trend by comparing EPO- and vehicle-treated wobbler mice (Fig 12.1 B, C). In both groups the scores of paw and walking abnormality showed a rapid worsening in the first period of treatment, markedly increasing from the 3rd to the 7th week of age, at the 12th week of age the values of the degree of paw and walking abnormality was similar. During the treatment, healthy mice treated with EPO did not show any abnormality both in paw and in walking compared to untreated mice.

Text cut off in original

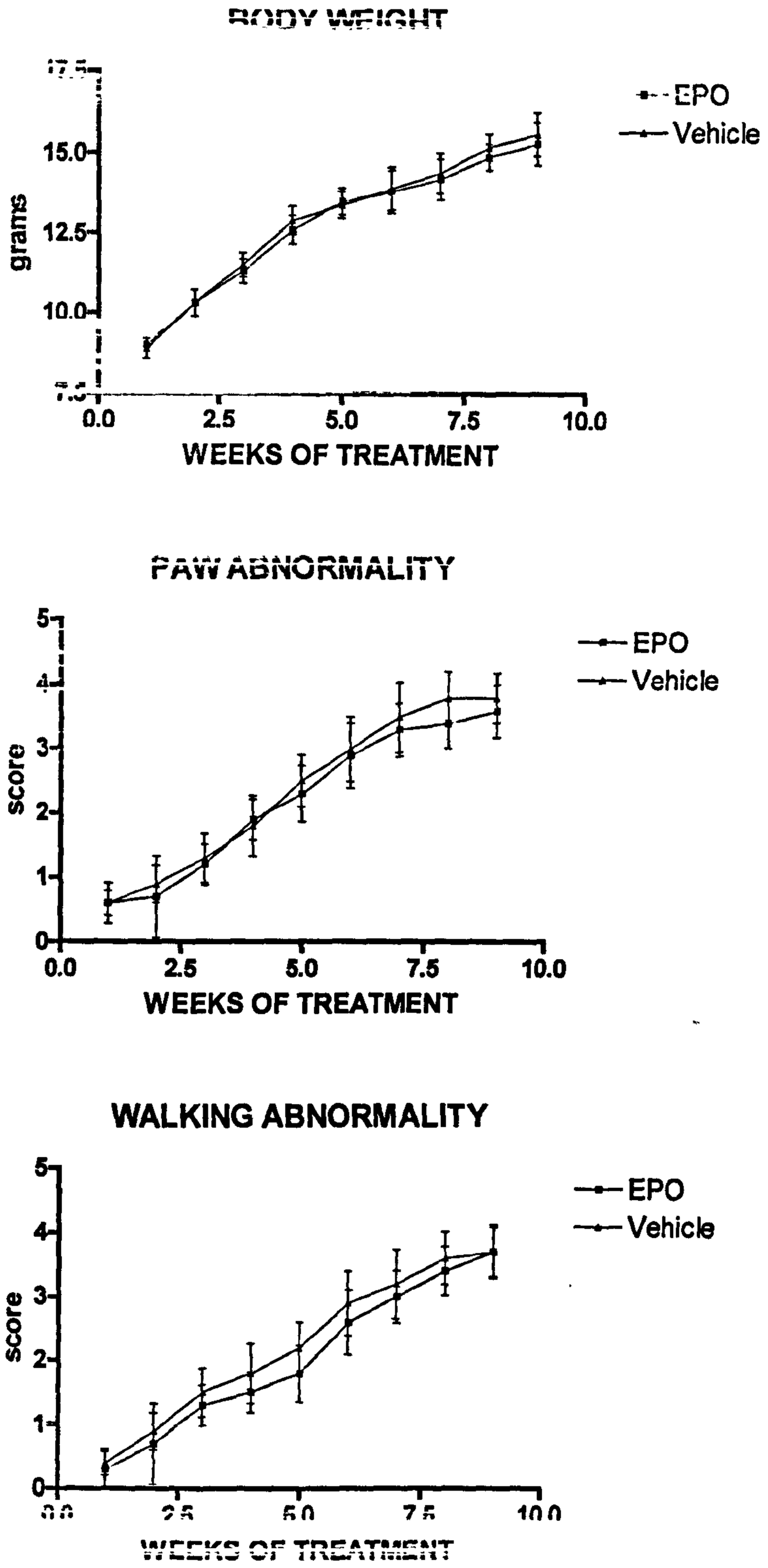

Figure 12.1 Behavioural tests in wobbler mice treated with rHuEPO at the dose of 4000 unit/kg/day, i.p. three times a week from the 4th to the 12th week of age. Panel A: body weight; panel B: paw abnormality; panel C: walking abnormality. In panel A each single point

Grip strength and running time

In both EPO- and vehicle-treated mice, grip strength homogeneously declined during the treatment without any significant difference between the two groups (Fig 12.2 B). In order to avoid any possible interference due to the gain of body weight data of the grip strength were normalized by dividing each measurement by body weight before comparisons were made (data not shown): no difference in the scores and the degree of worsening was found in either normalized or raw data.

The running time trials did not shown any significant difference between EPO- and vehicle-treated wobbler mice (Fig 12.2 A). In both groups a progressive decay was detected from the 3rd to the 12th week of age.

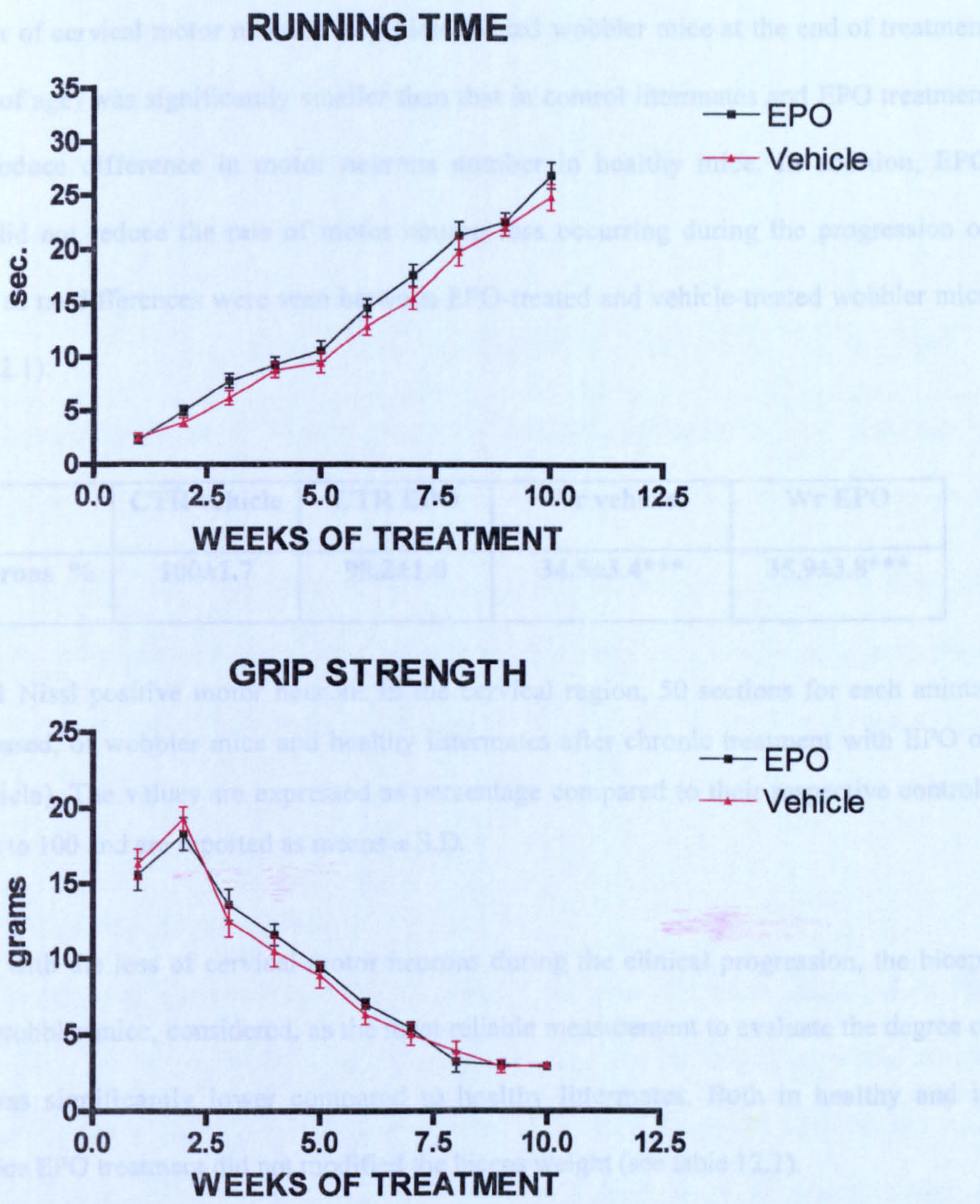

Figure 12.2 Behavioural tests in wobbler mice treated with rHuEPO at the dose of 4000 unit/kg/day, i.p. three times a week from the 4th to the 12th week of age. Panel A: running time; panel B:grip strength. Each point represents the mean ± SD of 10 mice for each experimental group.

12.1.3.2 Neuropathological estimation

Nissl motor neurons counting and biceps weight

The number of cervical motor neurons in vehicle-treated wobbler mice at the end of treatment (12^{th} week of age) was significantly smaller than that in control littermates and EPO treatment did not produce difference in motor neurons number in healthy mice. In addition, EPO treatment did not reduce the rate of motor neuron loss occurring during the progression of symptoms, as no differences were seen between EPO-treated and vehicle-treated wobbler mice (see table 12.1).

	CTR vehicle	CTR EPO	Wr vehicle	Wr EPO
Motor neurons %	**100±1.7**	**98.2±1.0**	**34.5±3.4*** **	**35.9±3.8*** **

Table 12.1 Nissl positive motor neurons in the cervical region, 50 sections for each animal were processed, of wobbler mice and healthy littermates after chronic treatment with EPO or saline (vehicle). The values are expressed as percentage compared to their respective controls normalized to 100 and are reported as means ± S.D.

Consistent with the loss of cervical motor neurons during the clinical progression, the biceps weight of wobbler mice, considered, as the most reliable measurement to evaluate the degree of atrophy, was significantly lower compared to healthy littermates. Both in healthy and in affected mice EPO treatment did not modified the biceps weight (see table 12.2).

	CTR vehicle	CTR EPO	Wr vehicle	Wr EPO
Weight (milligrams)	**32±6.8**	**34.1±8.3**	**9.0±3.1*** **	**7.9±2.6*** **

Table 12.2 Biceps weight of wobbler mice and healthy littermates after chronic treatment with EPO or saline (vehicle). The values are reported as means ± S.D. ***$p<0.001$

ChAT activity

Total ChAT activity was measured in the spinal cord of wobbler mice (EPO and vehicle-treated) and littermates at 12 weeks of age. ChAT activity in the cervical region of wobbler mice was similar between EPO and vehicle-treated wobbler mice, but was significantly reduced compared to control mice, where EPO-treated mice group showed a slight trend of increase respect to vehicle treated healthy littermates (see table 12.3).

	CTR vehicle	CTR EPO	Wr vehicle	Wr EPO
Chat activity (% vehicle control)	**100±10.2**	**113.6±16**	**69.2±13.9***	**70.3±18.5***

Table 12.3 ChAT activity measured in the cervical spinal cord homogenates of EPO and vehicle treated wobbler mice and healthy littermates. The values are expressed as percentage compared to their respective controls normalized to 100 and are reported as means ± S.D. *p<0.01

12.1.3.3 EPOr immunohystochemistry

Representative microphotographs showing the cervical spinal cord immunostaining for EPOr after chronic treatment with EPO are reported in figure 12.3. The staining in the whole cellular body of spinal cord neurons indicates a clear expression of EPOr also in the adult healthy mice (Fig 12.3 A). A comparison between the staining of EPOr in the cervical spinal cord of controls and wobbler mice did not show any difference between the two groups (Fig 12. 3 B). The experiment carried out after chronic treatment did not reveal a loss of immunopositivity in spinal cord sections from EPO chronically treated mice. A higher magnification microphotograph of cervical motor neurons in healthy mice chronically treated with EPO, which had been stained for EPOr antibody, is shown in figure 12.3 C.

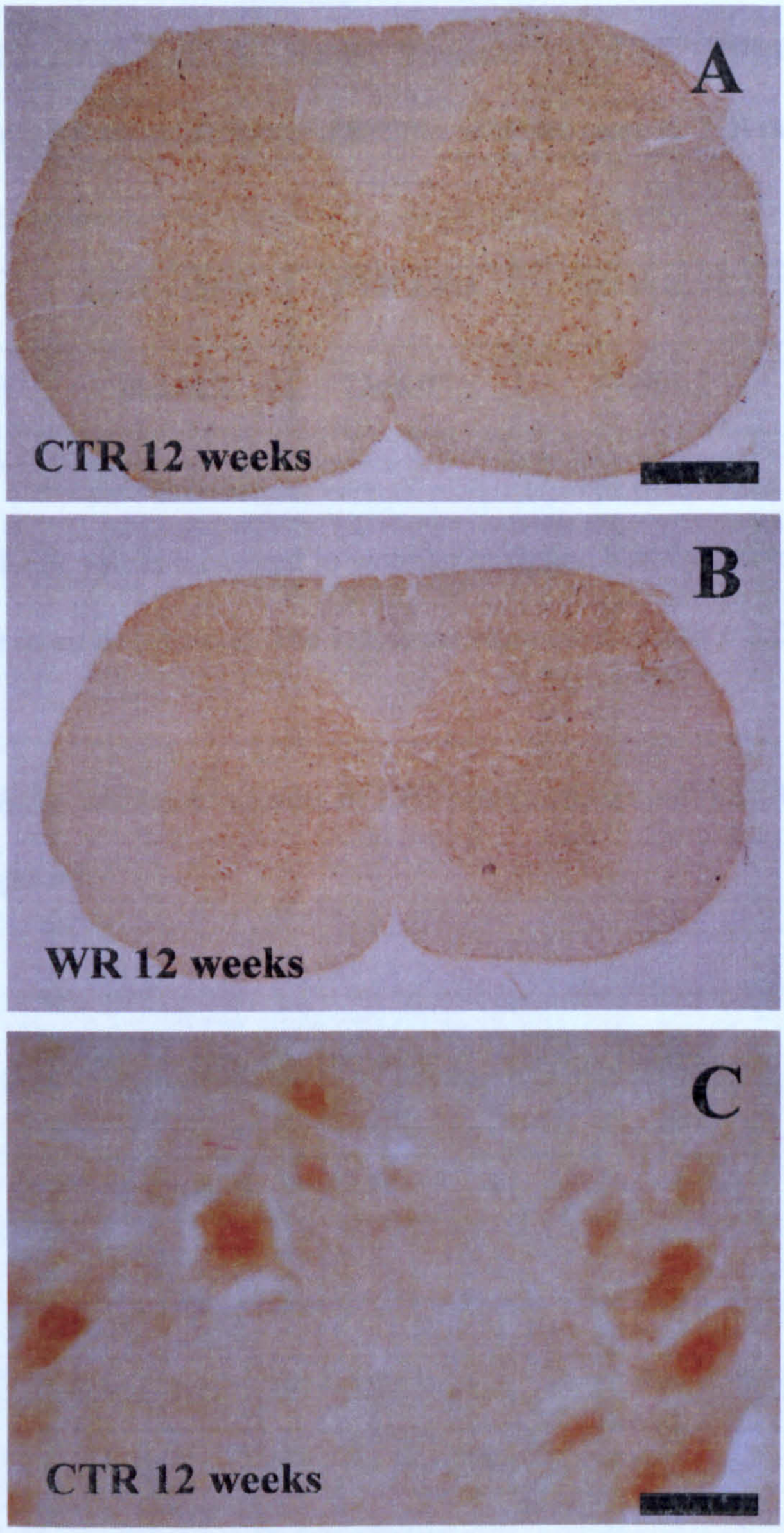

Figure 12.3 Representative microphotographs showing the pattern of staining and the distribution of EPOr antibody in the cervical spinal cord section of chronically treated healthy (A) and wobbler mice (B). After 9 weeks of treatment with rHuEPO EPOr immupositivity was maintained in almost all neurons, not exclusively motor neurons, in the cervical spinal cord and did not seem to be decreased compared to untreated animals (not shown). Interestingly, a marked immunopositivity in correspondence of the nuclear region was found both in EPO treated than in vehicle treated mice (C). Scale bar, A-B 400 μm. C, 50 μm.

12.1.3.4 Haematocrit measurement

Both in healthy and in affected animals chronic treatment with rHuEPO significantly increased the red blood percentage from values lower than 50% to values close to 70% (see table 12. 4).

	CTR vehicle	CTR EPO	Wr vehicle	Wr EPO
Haematocrit (%)	**45.3±4.2**	**73±6.0****	**47.8±1.2**	**63.2±4.9****

Table 12.4 Haematocrit values measured in wobbler mice and healthy littermates after chronic treatment with EPO or saline (vehicle). The values are reported as means ± S.D. **p<0.005

The increased levels of haematocrit levels in EPO treated mice confirmed the haematopoietic activity of this compound.

12.1.4 Discussion

These results indicate that EPO is not effective *in vivo* in reducing motor impairment and motor neuron loss in wobbler mice. Since EPO is reported to be active in different *in vitro* and *in vivo* models of neurodegeneration, and it can be considered a selective anti-apoptotic agent, the lack of efficacy in the wobbler mouse suggest that apoptosis is not involved [Chong, 2002;Martinez-Estrada, 2003;Agnello, 2002;Siren, 2001;Villa, 2003;Digicaylioglu, 2001;Sadamoto, 1998;Bernaudin, Nissenson, 1992;Kawakami, 2001;Sinor, 2000].

However, it is important to consider that EPO has been mainly utilized in acute models of neurodegeneration. Due to its effect of increasing blood red cells percentage chronic treatment with EPO can induce side effects related to cardiovascular alterations. Also in the present study, the mice treated with EPO for 9 weeks had high haematocrit values compared to vehicle treated mice. Thus I cannot exclude that this cardiovascular effect could have masked a beneficial neuroprotective action of EPO [Smith, 1991].

In addition, the receptor by which EPO exerts its neuroprotective effects is not clearly identified. However, very recent studies indicate that the haematopoietic and the neuroprotective effect can be dissociated, since compounds that do not bind to the EPO receptor yet are fully tissue protective. It is hypothesized that EPOr interacts with the common beta receptor (CD131), the signal-transducing subunit shared by GMCSF, IL3 and IL5. Therefore further studies using EPO derivatives lacking the haematopoietic effect are planned in order to verify the possible anti-apoptotic effect in wobbler mice.

12.2 Riluzole, unlike the AMPA antagonist RPR119990, reduces motor impairment and partially prevents motor neurons death in the wobbler mouse

12.2.1 Introduction

Glutamate-induced excitotoxicity is considered to play an important role leading to cell death in several neurodegenerative diseases, such as amyotrophic lateral sclerosis (ALS), Alzheimer's disease, and ischemia (see 1.3.2).

The link between excitotoxic damage and ALS is highlighted in several studies which have shown alterations of glutamatergic transmission. A significant increase of glutamate levels in cerebrospinal fluid, plasma and serum was reported in patients affected by sporadic ALS [Bastone, 1995;Plaitakis, 1987;Rothstein, 1990;Shaw, 1995] and decreased levels of glutamate were found in post-mortem tissues from ALS patients [Perry, 1987]. As reported by Rothstein, the high extracellular levels of glutamate were probably due to a selective loss of the glial glutamate transporters EAAT2 in the motor cortex and spinal cord of ALS patients [Rothstein, 1995;Bristol, 1996]. This decrease of EAAT2 was correlated with a reduced glutamate uptake found in synaptosomes prepared from brain and spinal cord of sporadic ALS patients [Rothstein, 1992].

AMPA-mediated excitotoxicity has been implicated in neuronal loss in ALS, where motor neurons seem to be selectively vulnerable to the Ca^{++}-dependent injury mediated by these receptors [Carriedo, 1996;Carriedo, 2000;Laslo, 2001;Rothstein, 1993;Rothstein, 1996;Takuma, 1999;Vandenberghe, 2000;Williams, 1997]. AMPAr that contain the edited GluR2 subunit show low Ca^{++} permeability, because this subunit carries an arginine residue in a position occupied by glutamine in the other subunits, that are unedited [Burnashev, 1992;Hume, 1991;Pellegrini-Giampietro, 1997;Washburn, 1997]. Recent studies suggest that the same neuron can express different sub-populations of AMPAr with non-fixed stoichiometry of GluR2/non-GluR2 subunits [Petralia, 1997;Vandenberghe, 2001;Wenthold, 1996]. Moreover the ratio of GluR2 to non-GluR2 subunits can vary in different neuronal populations, and may change in pathological conditions [Pellegrini-Giampietro, 1992;Pollard, 1993;Prince, 1995]. Therefore, although the mechanisms are not fully understood, the selective vulnerability of

motor neurons in ALS might result from a predominant expression of highly Ca^{++}-permeable AMPAr or from the lack of the GluR2 subunit in this cell type. The role of glutamate receptors-mediated excitotoxicity has been shown *in vivo* in animal models of motor neuron degeneration. In particular in $SOD1^{G93A}$ transgenic mice and *mnd* mice, it has been demonstrated that treatment with AMPA antagonists can show neuroprotective properties [Canton, 2001;Bendotti, 2002;Mennini, 1999;Van Damme, 2003].

Several clinical trials have been undertaken in ALS using anti-excitotoxic agents [Blin, 1992;Eisen, 1993;Gredal, 1997;Hollander, 1994;Miller, 1996;Tandan, 1996]. However none of these drugs had beneficial effects in prolonging survival or in decreasing the rate of clinical decline in ALS patients. The only pharmacological strategy that provided a modest increase in survival followed was that with riluzole [Bensimon, 1994;Lacomblez, 1996;Miller, 2003]. The mechanism of action of riluzole is complex, since the drug is able to alter glutamatergic transmission both pre- and postsynaptically, to inhibit the activity of protein kinase C and to interact with a variety of ion channels [Doble, 1996;Huang, 1997;Martin, 1993;Noh, 2000;Xu, 2001;Zona, 1998]. Riluzole inhibits responses mediated by NMDA and AMPAr, by an indirect mechanism not fully clarified [Couratier, 1994;Doble, 1996;Kretschmer, 1998]. Experimental evidence suggests that riluzole also inhibits presynaptic glutamate release [Doble, 1992;Martin, 1993] and it has been shown that the mechanism is dependent on the reduction of Ca^{++}-influx mediated by P/Q-type calcium channels, probably through a G-protein signalling pathway [Wang, 2004].

Riluzole was previously tested in $SOD1^{G93A}$ and $SOD1^{G37R}$ transgenic mice, and has also shown neuroprotective properties in these animal models of ALS, both alone and in association with other drugs [Gurney, 1996;Gurney, 1998;Kriz, 2003;Snow, 2003].

12.2.2 Experimental design

To investigate if the efficacy of riluzole is linked to its anti-glutamatergic activity or if different mechanisms could be involved, a chronic treatment with riluzole wobbler mice was performed and compared with that of the selective competitive AMPAr antagonist, RPR119990. Since it was reported that BDNF was increased in motor neurons of wobbler mice [Tsuzaka, 2001] and that riluzole was able to enhance the production of neurotrophins [Mizuta, 2001;Katoh-Semba, 2002], I have also investigated the effect of riluzole treatment on BDNF levels in wobbler mice.

12.2.3 Results

12.2.3.1 Behavioural scores.

Body weight

As previously reported, in wobbler mice the mean body weight is lower compared to that of healthy littermates; this feature is characteristic of the animal model. No significant differences in the growth rate were noted during the treatment with riluzole or with RPR119990 between treated and untreated mice (Fig 12.4 A, B).

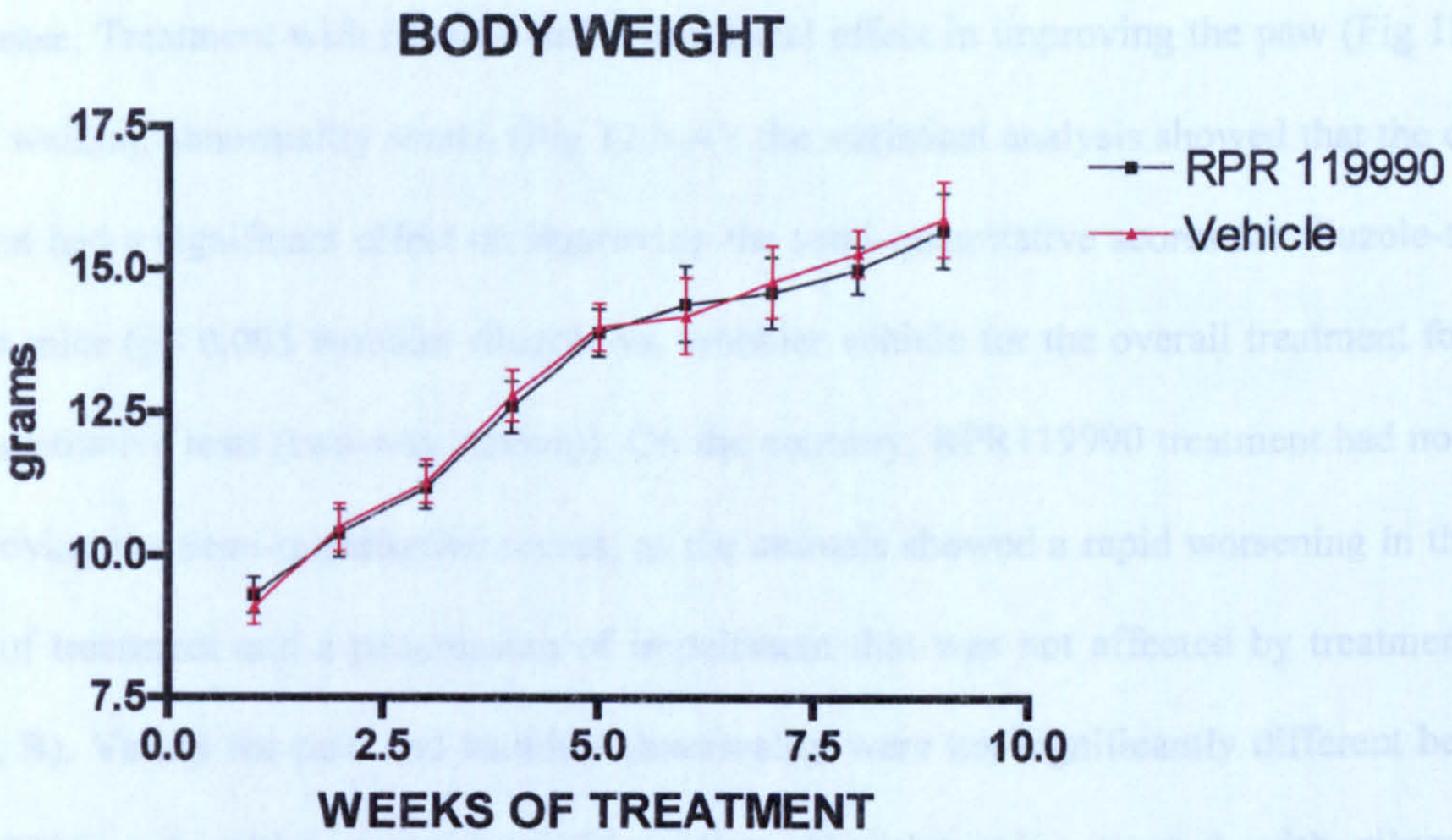

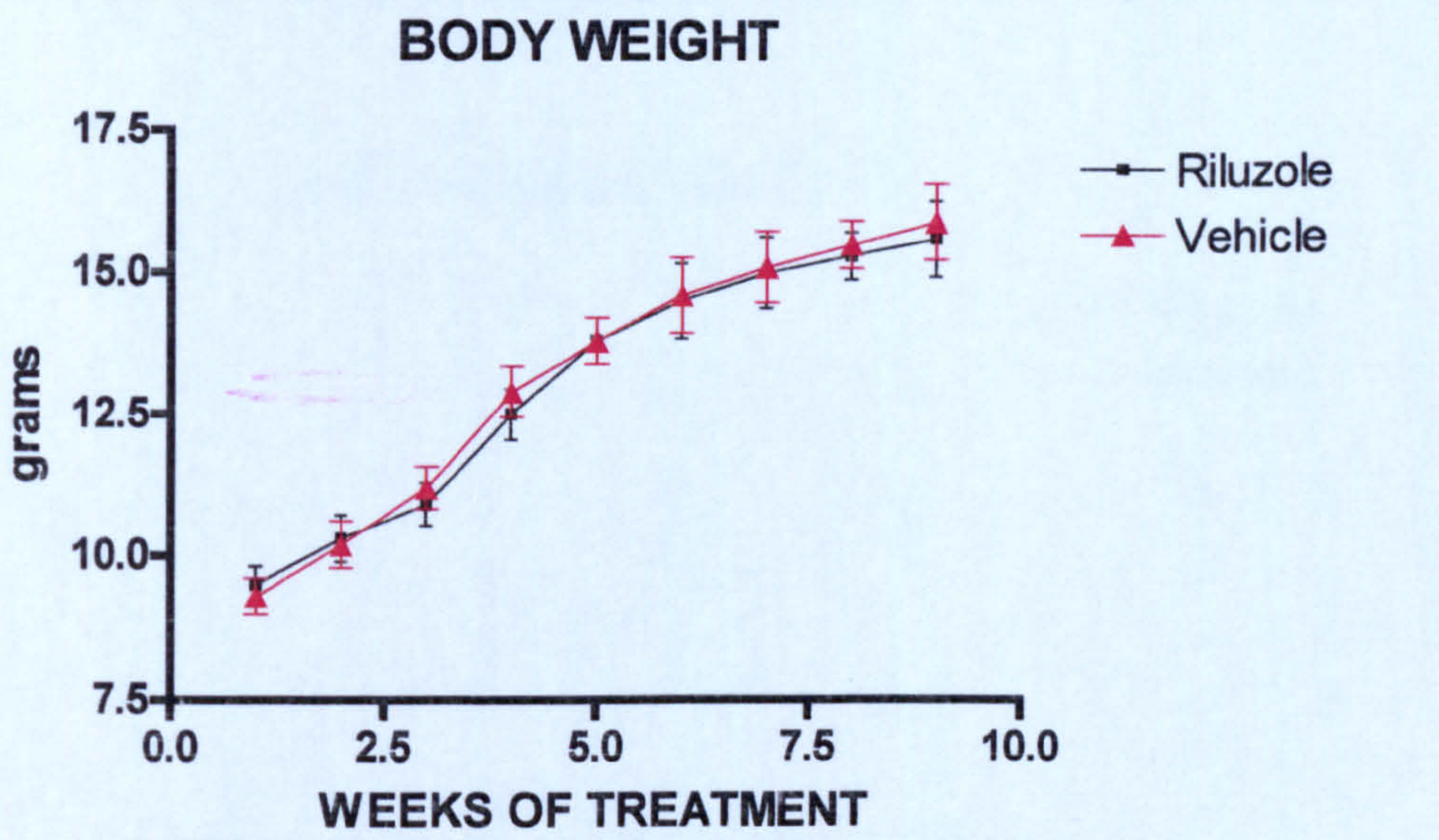

Figure 12.4 Body weight recording in wobbler mice treated with: riluzole (40 mg/kg/day in the drinking water) -panel A- and; RPR 1199900 (3 mg/Kg/day, i.p.) -panel B-.Each point represents the mean of 10 mice for each experimental group.

Paw abnormality and walking abnormality

Vehicle-treated wobbler mice showed a rapid worsening of symptoms, as already described for this disease. Treatment with riluzole had a beneficial effect in improving the paw (Fig 12.5 A) and the walking abnormality scores (Fig 12.6 A); the statistical analysis showed that the overall treatment had a significant effect on improving the semi-quantitative scores for riluzole-treated wobbler mice ($p < 0.005$ wobbler riluzole vs. wobbler vehicle for the overall treatment for both semi-quantitative tests (two-way Anova)). On the contrary, RPR119990 treatment had no effect in improving the semi-quantitative scores, as the animals showed a rapid worsening in the first period of treatment and a progression of impairment that was not affected by treatment (Fig 12.6 A, B). Values for paw and walking abnormality were not significantly different between RPR119990 and vehicle-treated wobbler mice. Healthy mice treated with riluzole or RPR119990 did not show paw or walking abnormalities when compared to vehicle-treated mice.

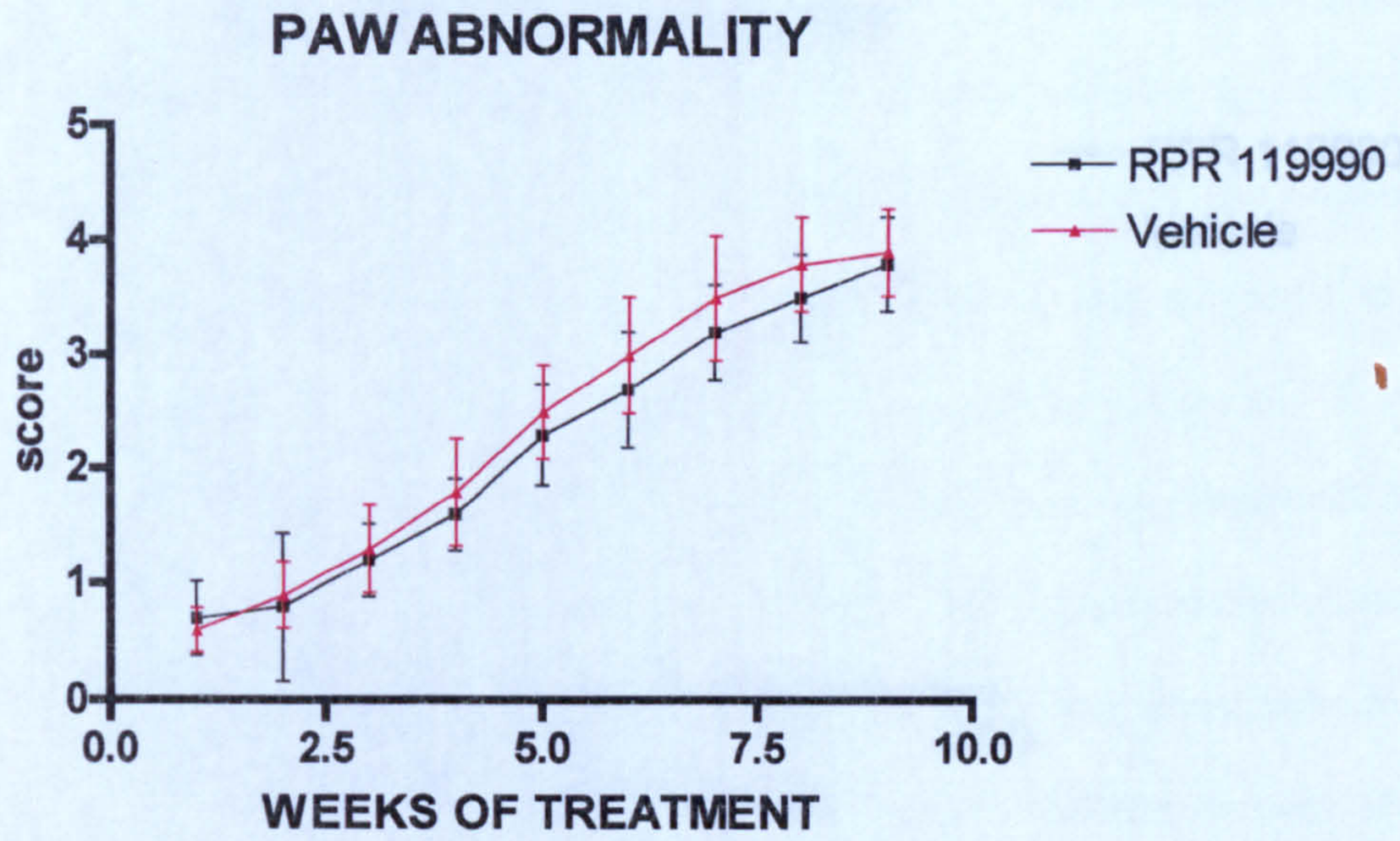

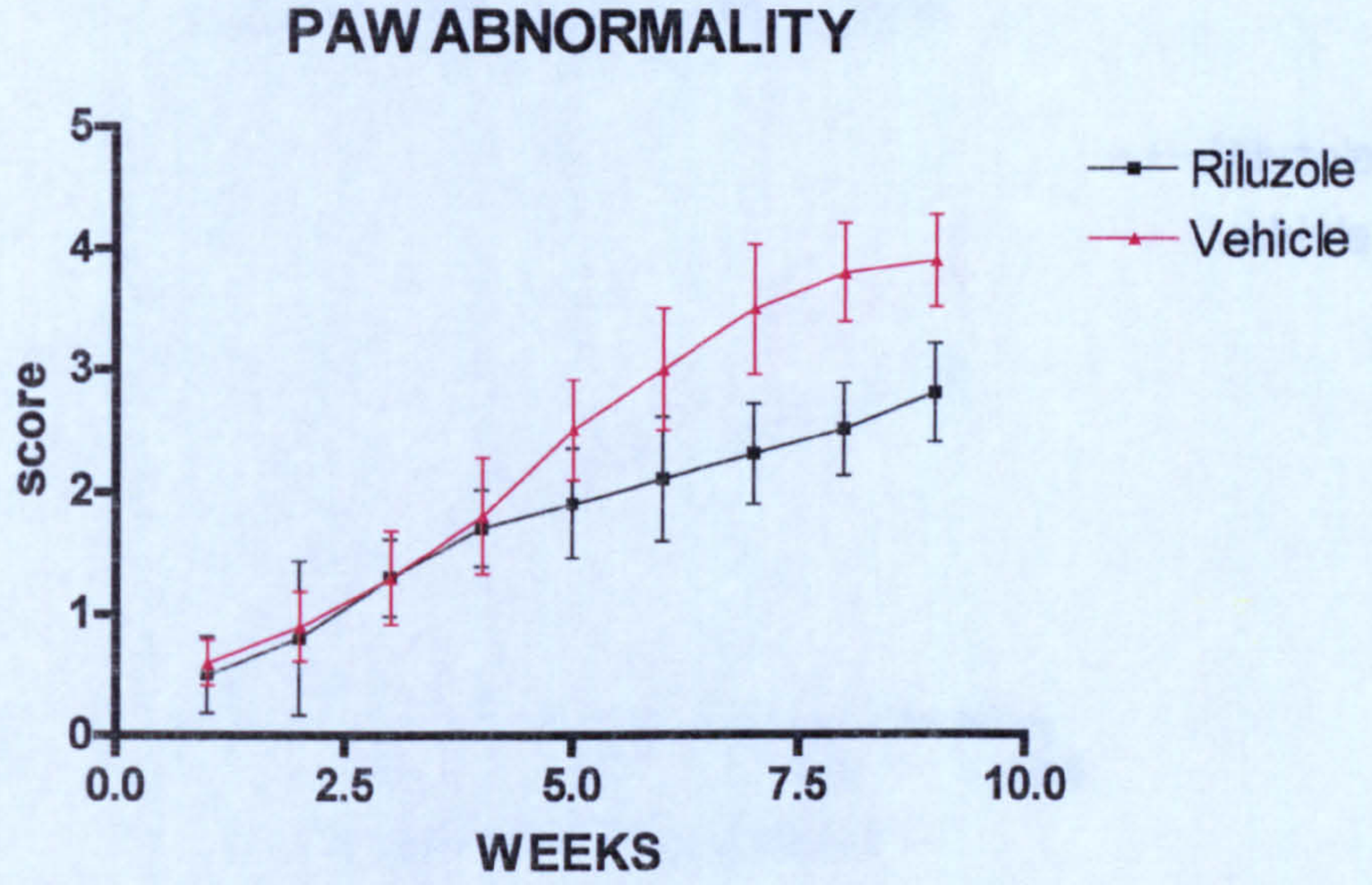

Figure 12.5 Paw abnormality tests performed in wobbler mice treated with: riluzole (40 mg/kg/day in the drinking water) -panel A- and; RPR 1199900 (3 mg/Kg/day, i.p.) -panel B- .Each point represents the mean ± SD of 10 mice for each experimental group. **p<0.05 Vs.wobbler vehicle (two-way anova).

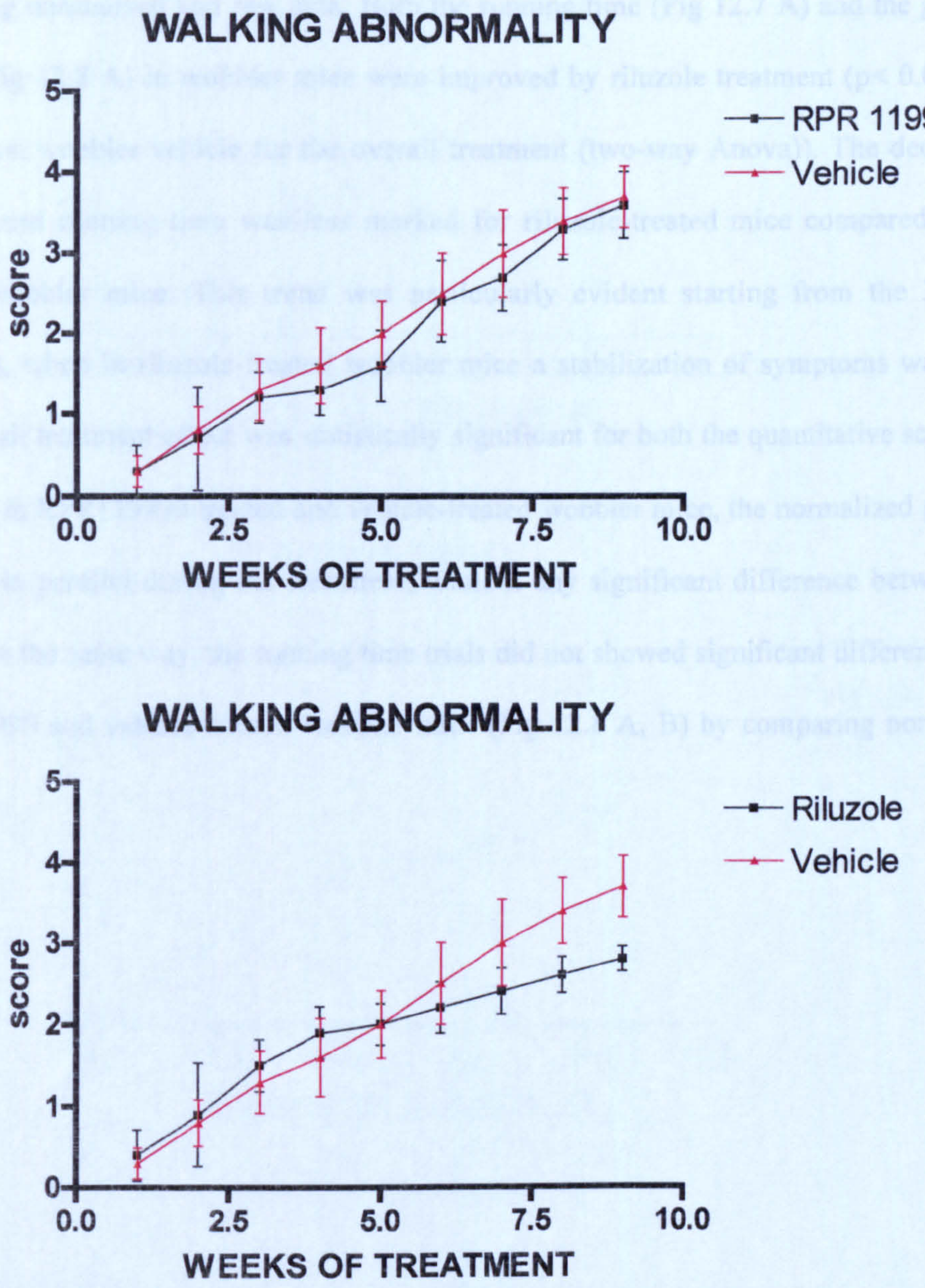

Figure 12.6 Walking abnormality tests performed in wobbler mice treated with: riluzole (40 mg/kg/day in the drinking water) -panel A- and; RPR 1199900 (3 mg/Kg/day, i.p.) -panel B- .Each point represents the mean ± SD of 10 mice for each experimental group. **p<0.05 Vs.wobbler vehicle (two-way anova).

Grip strength and running time.

For the confirmation of grip strength values, data were normalized by dividing the absolute values by body weight before comparisons were made No difference was seen by comparing by comparing normalized and raw data. Both the running time (Fig 12.7 A) and the grip strength scores (Fig 12.8 A) in wobbler mice were improved by riluzole treatment ($p < 0.001$ wobbler riluzole vs. wobbler vehicle for the overall treatment (two-way Anova)). The decline of grip strength and running time was less marked for riluzole-treated mice compared to vehicle-treated wobbler mice. This trend was particularly evident starting from the 3rd week of treatment, when in riluzole-treated wobbler mice a stabilization of symptoms was observed. The overall treatment effect was statistically significant for both the quantitative scores. On the contrary, in RPR119990-treated and vehicle-treated wobbler mice, the normalized grip strength declined in parallel during the treatment, without any significant difference between the two groups. In the same way, the running time trials did not showed significant differences between RPR119990 and vehicle-treated wobbler mice (Fig 12.8 A, B) by comparing normalized and raw data.

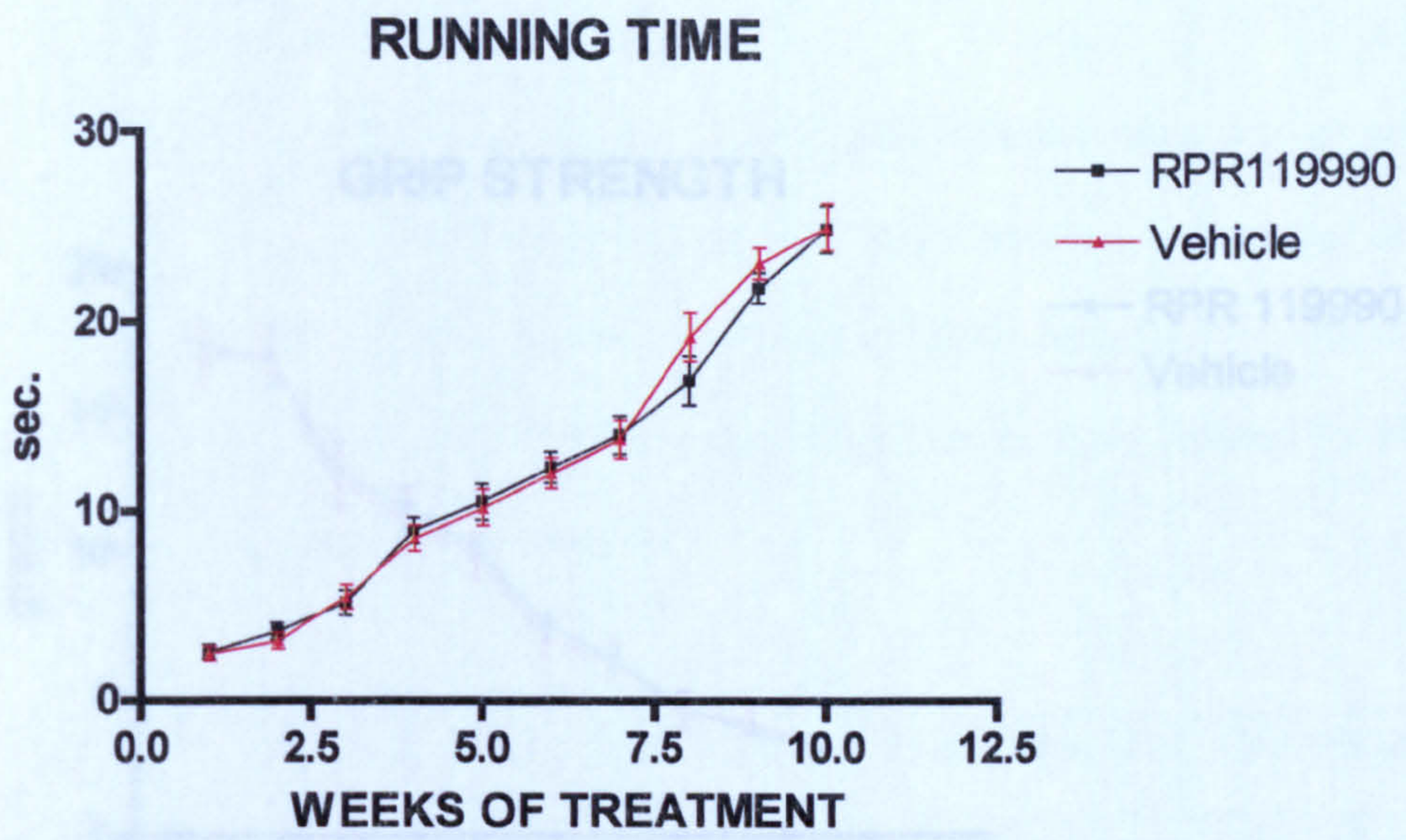

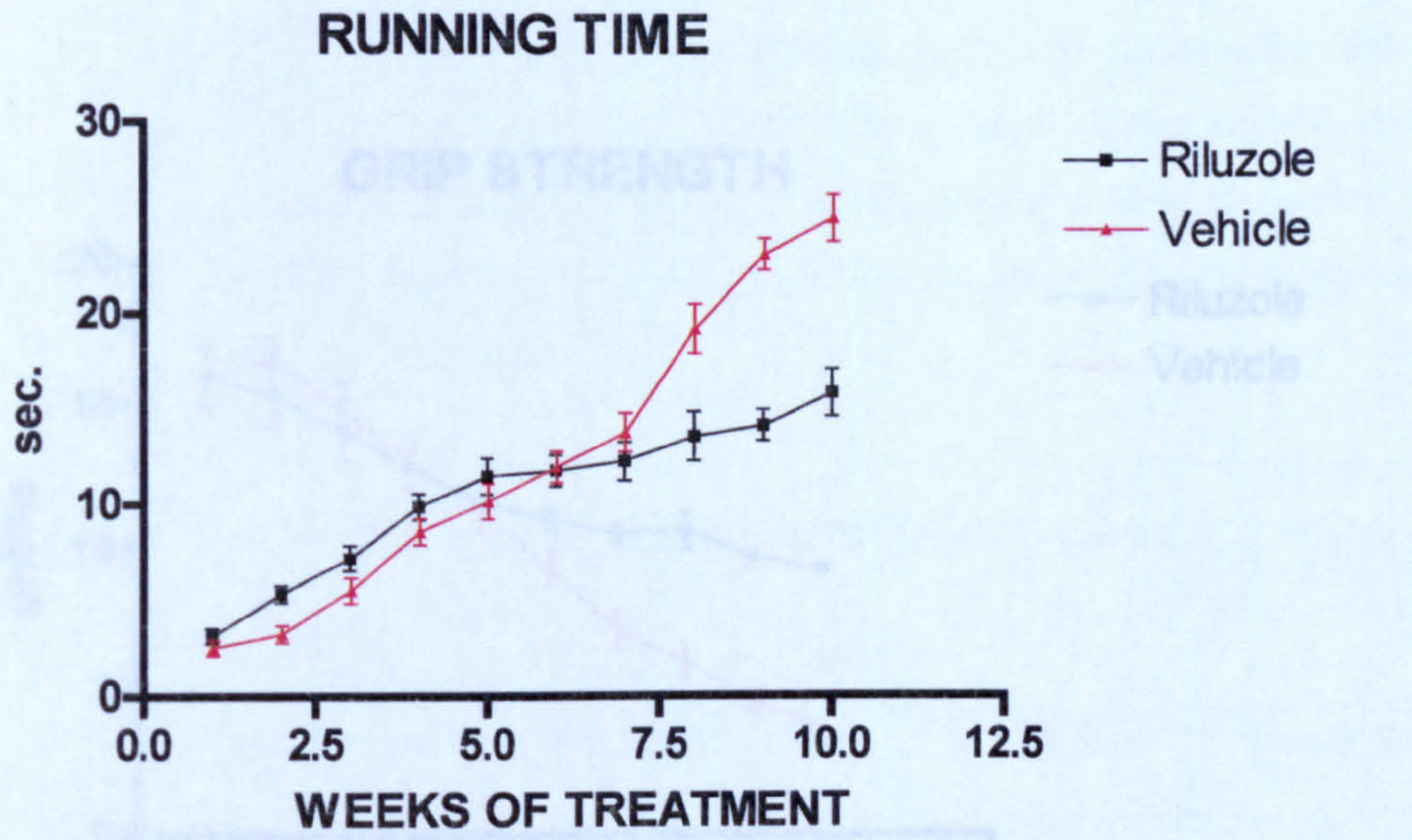

Figure 12.7 Running time measurements performed in wobbler mice treated with: riluzole (40 mg/kg/day in the drinking water) -panel A- and; RPR 1199900 (3 mg/Kg/day, i.p.) -panel B- .Each point represents the mean ± SD of 10 mice for each experimental group. **p<0.05 Vs.wobbler vehicle (two-way anova).

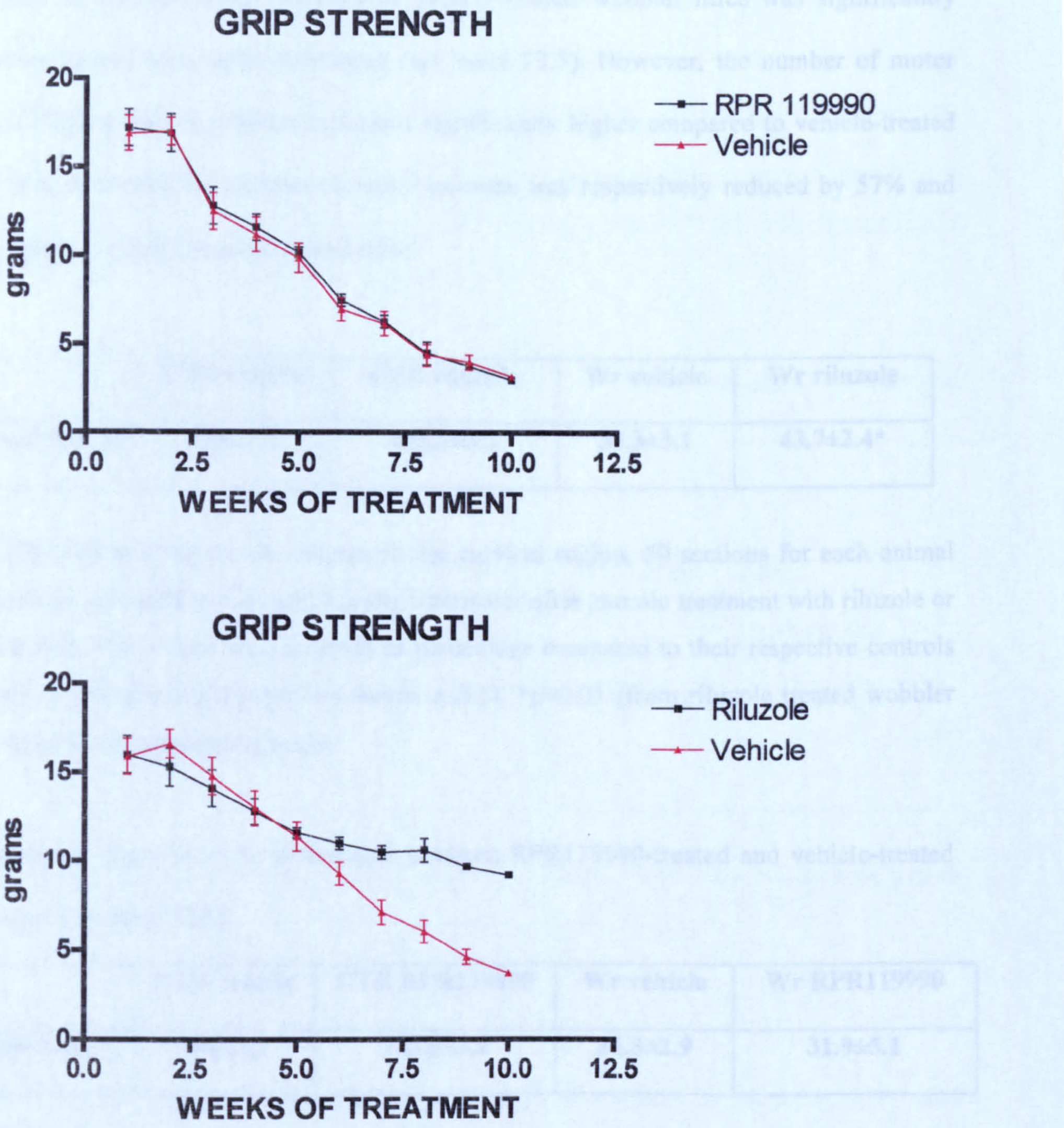

Figure 12.8 Grip strength measurements performed in wobbler mice treated with: riluzole (40 mg/kg/day in the drinking water) -panel A- and; RPR 1199900 (3 mg/Kg/day, i.p.) -panel B- .Each point represents the mean ± SD of 10 mice for each experimental group. **p<0.05 Vs.wobbler vehicle (two-way anova).

12.2.3.3 Neuropathological estimation

Nissl motor neurons counting and biceps weight

The number of cervical motor neurons in vehicle-treated wobbler mice was significantly decreased compared to control littermates (see table 12.5). However, the number of motor neurons in riluzole-treated wobbler mice was significantly higher compared to vehicle-treated wobbler mice ($p<0.05$); the number of motor neurons was respectively reduced by 57% and 70%, compared to vehicle-treated control mice.

	CTR vehicle	CTR riluzole	Wr vehicle	Wr riluzole
Motor neurons %	100±3.2	102.3±3.3	30.3±3.1	43.7±2.4*

Table 12.5 Nissl positive motor neurons in the cervical region, 50 sections for each animal were processed, of wobbler mice and healthy littermates after chronic treatment with riluzole or saline (vehicle). The values are expressed as percentage compared to their respective controls normalized to 100 and are reported as means ± S.D. *$p<0.01$ (from riluzole treated wobbler mice and vehicle treated wobbler mice)

On the contrary, there were no differences between RPR119990-treated and vehicle-treated wobbler mice (see table 12.6).

	CTR vehicle	CTR RPR119990	Wr vehicle	Wr RPR119990
Motor neurons %	100±5.6	103.3±3.4	36.3±2.9	31.9±5.1

Table 12.6 Nissl positive motor neurons in the cervical region, 50 sections for each animal were processed, of wobbler mice and healthy littermates after chronic treatment with RPR119990 or saline (vehicle). The values are expressed as percentage compared to their respective controls normalized to 100 and are reported as means ± S.D.

Consistent with the reduced loss of cervical motor neurons after riluzole treatment, the degree of atrophy, measured by biceps weight, was significantly lower in riluzole-treated wobbler mice compared to vehicle-treated wobbler mice (see table 12.7).

	CTR vehicle	CTR riluzole	Wr vehicle	Wr riluzole
Weight (milligrams)	**36.2±5.0**	**33.5±4.3**	**7.6±0.9**	**13.1±2.6****

Table 12.7 Biceps weight of wobbler mice and healthy littermates after chronic treatment with riluzole or saline (vehicle). The values are reported as means ± S.D. **p<0.005 (from riluzole treated wobbler mice and vehicle treated wobbler mice)

Contrary to riluzole, RPR119990 treatment did not modify the biceps weight in wobbler and healthy mice (see table 12.8).

	CTR vehicle	CTR RPR119990	Wr vehicle	Wr RPR119990
Weight (milligrams)	**28,9±7.2**	**32.8±6.7**	**8.0±1.2**	**7.3±0.7**

Table 12.8 Biceps weight of wobbler mice and healthy littermates after chronic treatment with RPR119990 or saline (vehicle). The values are reported as means ± S.D.

ChAT activity

ChAT activity in the cervical spinal cord of wobbler mice was reduced by about 35% compared to control mice. However, in wobbler mice riluzole treatment significantly increased ChAT activity by about 70% compared to vehicle-treated wobbler mice ($p<0.001$).

12.2.3.3 BDNF immunostaining

BDNF immunoreactivity in wobbler mice (Fig 12. 9 B) was higher than in control mice (Fig 12.9 A); riluzole treatment further increased BNDF immunostaining in motor neurons of the ventral horn in wobbler mice (Fig 12. 9 D), as it did in healthy controls (Fig 12.9 C).

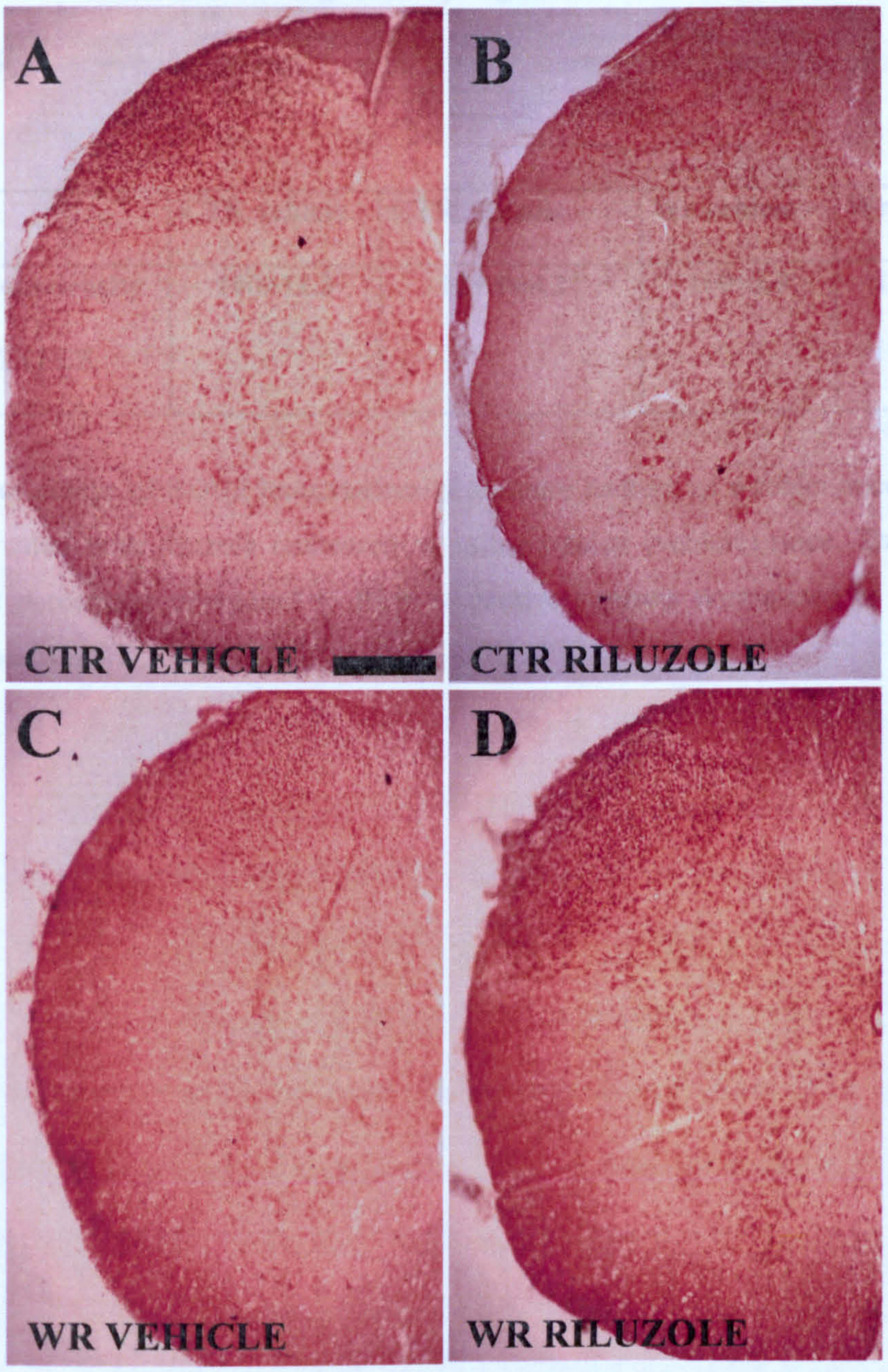

Figure 12.9 Representative microphotographs showing the pattern of BDNF immunostaining (distribution, localization and intensity of signal) in the cervical spinal cord of healthy mice treated with vehicle (A), healthy mice treated with riluzole (B), wobbler mice treated with vehicle(C), wobbler mice treated with riluzole (D). It is easily detectable as riluzole treatment increased the BDNF immunoreactivity both in healthy and in diseased mice. Moreover, it is also interesting to note that only wobbler mice (both groups) showed an intense immunopositivity in the most anterior part of the white matter, likely corresponding to efferent fibers (axons).Scale bar, 200 μm.

Statistical analysis of the densitometric values confirmed that BDNF immunodensity in riluzole-treated wobbler mice was significantly higher than in vehicle-treated wobbler mice (see table 12.9).

	CTR vehicle	CTR riluzole	Wr vehicle	Wr riluzole
BDNF immunodensity RODxPIXELS	**100±11.3**	**129.0±8.2***	**100±3.9**	**118.9±3.1***

Table 12.9 Percentage of BDNF immunodensity in motor neurons of wobbler mice and healthy littermates treated with riluzole compared to saline treated (vehicle) mice. The values are expressed as percentage compared to their respective controls normalized to 100 and are reported as means ± S.D. *$p<0.05$

12.2.4 Discussion

The most relevant information emerging from this study is that chronic treatment with riluzole, started from the 4th week of age, is effective in improving the motor impairment in wobbler mice. All behavioural scores used to describe the clinical worsening of the disease; paw and walking abnormality, running time and grip strength are significantly improved by treatment with riluzole. Ex vivo analyses showed that riluzole significantly decreases the loss of motor neurons that occurs in the cervical spinal cord of wobbler mice. Moreover riluzole partially reduced the muscular atrophy in the forelegs, which is a typical feature of the wobbler disease: weight of biceps muscles was significantly higher in riluzole-treated compared to vehicle-treated wobbler mice.

Riluzole has previously been tested in transgenic SOD1^{G93A} and SOD1^{G37R} mice. In these animal models of ALS, chronic treatment with riluzole, started before the onset of evident symptoms, was also effective in preserving the motor function [Gurney, 1996]; moreover, treatment with riluzole alone or in combination with other drugs delayed the onset of symptoms, with different effects on animal survival [Gurney, 1998;Kriz, 2003;Snow, 2003].

Although the mechanism of action was not investigated, the efficacy of riluzole in transgenic SOD1^{G93A} mice seems to be due to its anti-glutamatergic activity. In fact it was reported that SOD1^{G93A} mice show a significant impairment in the glutamate uptake activity, linked to selective loss or inactivation of the main glutamate transporter GLT1 [Bendotti, 2001;Bruijn, 1997;Dunlop, 2003]. In particular, the glutamate uptake in synaptosomes prepared from spinal cord of transgenic SOD1^{G93A} rats was significantly enhanced after riluzole treatment, compared to untreated animals.

It has been previously shown that in wobbler mice there are no changes in the levels of the glutamate transporters GLT1 and GLAST in the cervical spinal cord, nor in uptake and in plasma levels of glutamate [Bigini, 2001]. These data suggest that removal of the released glutamate through glutamate transporters occurs normally in the wobbler mice; thus it is unlikely that the effects of riluzole observed here are related to its interaction with the processes involved in glutamate removal.

Together with a mechanism linked to the interaction with glutamate transporters, which might reduce excitotoxicity by lowering the extracellular glutamate concentration, riluzole might also interact indirectly with postsynaptic receptors that are known to trigger neurodegeneration following overstimulation.

Treatments with several AMPAr antagonists clearly demonstrated the involvement of glutamate receptor-mediated excitotoxicity in animal models of neurodegeneration. It has been previously reported as the treatment with NBQX significantly improved muscle strength performances and delayed the onset of clinical symptoms in the *mnd* mouse, an animal model characterized by progressive motor neuron dysfunction and functional impairment [Mennini, 1999]. Significant delay in mortality was observed in transgenic $SOD1^{G93A}$ transgenic mice after NBQX treatment [Van Damme, 2003]. The non-competitive AMPAr antagonist ZK187638 significantly decreased the symptoms of neuromuscular deficit and improved the motor behavioural impairment in both $SOD1^{G93A}$ and *mnd* mice, and extended the survival of $SOD1^{G93A}$ transgenic mice [Bendotti, 2002]. In $SOD1^{G93A}$, the competitive AMPA antagonist RPR119990 was found to significantly improve muscle strength and to prolong survival of treated mice; it was also reported that the marked decrease of glutamate uptake observed in synaptosomes prepared from spinal cord of untreated $SOD1^{G93A}$ transgenic mice was significantly prevented by treatment with RPR119990 [Canton, 2001]. Taken together, these data confirm the neuroprotective role for AMPA antagonist drugs in these animal models of neurodegeneration.

Little evidence is available about the involvement of glutamate receptors-mediated injury in motor neuronal loss in wobbler mice. It is unlikely that neurodegeneration of motor neurons is linked to NMDA receptor activation, since treatment of wobbler mice with the non-competitive NMDA receptor antagonist MK801 was completely ineffective in delaying the progression of the disease [Krieger, 1992].

My results clearly indicate that treatment of wobbler mice with the competitive AMPA antagonist RPR11990 has no effect on the onset and the progression of the disease. Both semi-quantitative and quantitative behavioural trials show no difference between treated and

untreated wobbler mice. Moreover, the motor neuronal loss is not reduced by treatment with RPR119990. In the same way, the muscular atrophy of the forelegs is not reduced by the treatment, since no differences are seen in the weight of biceps muscles between treated and untreated wobbler mice. It is possible to conclude that RPR119990 is unable to improve the progression of symptoms in wobbler disease. These data, together with our previous findings, strongly support the conclusion that there is no involvement of glutamate receptor-mediated excitotoxicity in the motor neuronal death observed in the wobbler mouse and that the glutamatergic transmission is probably not altered in this animal model of neurodegeneration. Thus the wobbler mouse can be considered to be a useful animal model of neurodegeneration to investigate other processes leading to motor neuronal death in the absence of glutamate-mediated excitotoxicity.

These conclusions also imply that riluzole, which is effective in improving the motor impairment and in partially preventing motor neuronal loss in the wobbler disease, probably acts via a different mechanism that does not involve glutamatergic transmission. In some experimental models it was demonstrated that riluzole increases the expression of neurotrophic factors. Cultured mouse brain astrocytes showed enhanced levels of BDNF, GDNF and NGF after treatment with riluzole [Mizuta, 2001]; moreover it was reported that repeated injections with riluzole in rats produced persistent increases of BDNF levels in hippocampus, enthorinal cortex and hypothalamus [Katoh-Semba, 2002]. These evidence indicate that riluzole could exert a neuroprotective action by increasing the production of neurotrophic factor, since it has been shown that neurotrophins, in particular BDNF, prevent cell death in several experimental models, including the wobbler mouse [Henderson, 1993;Mitsumoto, 1999;Yan, 1992;Peluffo, 1997]. Ikeda et al. reported that treatment with BDNF significantly slowed the neuronal degeneration and the impairment of the motor function in wobbler mice [Ikeda, 1995]. It was also shown that BDNF expression was significantly increased in the ventral spinal cord of wobbler mice, both at early and advanced stages of the disease [Tsuzaka, 2001]. Probably, the increased expression of BDNF can be considered as a compensatory mechanism activated to counteract cell processes that are involved in the motor neurons neurodegeneration.

This study confirmed a significant increase in the BDNF immunoreactivity in motor neurons of wobbler mice; moreover, it has been shown that riluzole treatment produced a further increase in BDNF levels in degenerating cells, associated with a significant decrease in the number of motor neurons lost in treated wobbler mice. The mechanism underlying this up-regulation of BDNF is not fully clear; recently it was suggested that the blockade of sodium channels mediated by riluzole can stimulate BDNF synthesis, due to low levels of ecto-adenosine [Katoh-Semba, 2002].

The protective role of riluzole is further confirmed by ChAT activity measurement. In the cervical spinal cord of riluzole-treated wobbler mice I observed a significant increase in the ChAT activity compared to vehicle-treated wobbler mice. This result not only supports the evidence that in riluzole-treated mice a higher number of motor neurons are spared but also indicates that the cholinergic activity is preserved compared to vehicle-treated wobbler mice.

In conclusion, this study clearly shown that riluzole has a neuroprotective effect on motor neuron degeneration in wobbler mice, by improving motor behaviour of treated mice and partially reducing the muscular atrophy in the forelegs. This neuroprotective effect seems to be mediated by a mechanism of action not involving anti-glutamatergic activity suggested for riluzole in ALS patients and in other animal models of neurodegeneration, but that is likely to be linked to the increase in the synthesis of the neurotrophic factor BDNF.

Whether this effect of riluzole also contributes to its protective effect in ALS patients clearly deserves further investigation.

GENERAL DISCUSSION

CHAPTER 13

APOPTOSIS AND MOTOR NEURON DISEASE: A LESSON FROM CELLULAR AND ANIMAL MODELS OF ALS

The aim of my thesis was to evaluate possible apoptotic processes induced by aetiopathological factors that are relevant to ALS, such as neurotrophic factors starvation, glutamate-induced excitotoxicity and glial-induced neuroinflammation, and to confirm the presence of these mechanisms in an animal model of ALS, the wobbler mouse.

Some of the aetiopathological factors that are associated with ALS and are able to trigger apoptosis include (see Chapters 1 and 2): I) deficit of trophic factors which maintain the neuronal integrity by inhibiting the induction of the mitochondria-dependent apoptotic pathway, passing through cytochrome-c release, apoptosome formation and induction of caspases cascade cell signalling leading to DNA fragmentation [Swerdlow, 1998; Swerdlow, 2000;Borthwick, 1999;Green, 1998;Luo, 1998; Wadia, 1998;Mignotte, 1998;Gorman, 2000;Guegan, 2001;Mitsumoto, 1994;Mitsumoto, 1999];

II) glutamate-induced excitotoxicity, that generates a modest but prolonged overstimulation of postsynaptic glutamate receptors, lower motor neurons in this case, accompanied by an increased Ca^{++} influx [Shaw, 1997;Rothstein, 1994;Nicotera 1997;Ankarcrona, 1995;Mitchell, 1994;Hassinger 1995;Steinonen, 1999;Rothstein, 1990;Petralia 1997] ; III) mechanisms of neuroinflammation with an overproduction of proinflammatory cytokines, in particular TNF-α, that are expressed by activated microglial cells. These, once released, can interact with death receptors (or TNF-family receptors) that are expressed on the motor neuron surface and can trigger an apoptotic pathway involving an even larger number of adapter molecules, leading to procaspase 8 cleavage and caspase 3 activation [Raivich, 1999;Turner, 2004;Streit, 1989;Duchen,

1968; Cheng, 2002;De Simone, 2003]. Data suggesting a possible involvement of these factors in the wobbler mouse motor neurons death and in other animal models of ALS were summarized in Chapters 3 and 5 [Streit, 1988;Zona, 1998;Riviere, 1998; Mennini, 2002;Vance, 1997;Bertamini, 2002;Wong, 1995;Howland, 2002;Tsuzaka, 2001;Xu, 2001;Dave, 2003;Hantaz-Hambroise, 1994;Gonzalez Deniselle, 1999; Laage, 1988;Bigini, 2001;Mitsumoto, 1994; Mennini, 1999; Krieger, 1992; Pasinelli, 2004; Mitsumoto, 1994;Hensley, 2002; Tomiyama, 1994;Bendotti, 2001].

13.1 Neurotrophic factors starvation and apoptosis

As far as the role of neurotrophic factors, and their involvement in the wobbler mouse motor neuron disease, are concerned, it has been shown that, although a significant increase of BDNF levels occurs in the affected region of the wobbler spinal cord, treatments with BDNF, and others neurotrophins, protect motor neurons and delay the progression of symptoms [Mitsumoto, 1994]. The increased expression of basal BDNF might thus be considered as a compensatory effect, and exogenous neurotrophins could play a relevant role in the survival of cervical motor neurons in treated mice [Tsuzaka, 2001]. Unfortunately, treatments of ALS patients with neurotrophins are ineffective, possibly because in contrast to animal models they are initiated when a clear pathology is already present [ALS CNTF GROUP, 1999].

While apoptosis is easily detectable in *in vitro* condition, *in vivo* the cells undergoing apoptosis are rapidly removed and the time window to observe apoptotic markers is very narrow. In addition, it is difficult to study the role of apoptosis in chronic diseases, because the mechanism of cell death is in operation over several weeks. For this reason, this process was studied in the time window in which the greatest percentage of motor neurons are dying, (i.e. in wobbler mice from the 4^{th} to the 5^{th} week of life).

Before characterizing these mechanisms in the wobbler mouse, however, the action of BDNF withdrawal at the single cell level was evaluated in a cellular model, the primary cultures of rat embryo motor neurons. As expected [Henderson, 1993], toxic effects were observed following a chronic (48 hours) deprivation of serum+BDNF in these primary cultures. Furthermore, by comparing the toxicity produced by BDNF deprivation in mixed glia/neurons and in purified cultures a significant higher resistance to trophic factors withdrawal (60% vs. 40% of viability) in mixed cultures was detected. This can be due to the fact that the astrocytes can supply trophic factors, as GDNF, which can partially counteract the detrimental effects caused by the lack of BDNF [Mitsumoto, 1999].

The cell death induced by BDNF deprivation in purified cultures was associated with a higher percentage of fragmented nuclei and a marked activation of the activated form of caspase 3. In addition, EPO treatment significantly increased cell viability in BDNF-deprived motor neurons and, at the same time, markedly decreased the percentage of cells with nuclear fragmentation and the number of active caspase 3 positive cells.

BDNF is known to produce its anti-apoptotic effect by inhibiting the activation and the translocation from the cytosol to the mitochondrion, of different pro-apoptotic agents, such as BID, BAK, BAX, that mainly act by opening PTP [Yuan, 1995;Whitfield, 2001;Sanchez, 2001;Sartorius, 2001]. The PTP opening induces mitochondrial depolarization and thus produces decay in mitochondrial efficiency [Tatton, 1999]. A reduced mitochondrial activity has been described, but these measurements had been obtained in brain regions that are not strictly associated to the affected areas of the wobbler motor neuron disease, such as the cerebral cortex and the whole spinal cord [Xu, 2001]. In addition, only few and controversial data are available on the activity of the ETC enzymatic complexes [Dave, 2003], which have been documented to be particularly vulnerable to mitochondrial depolarization [Chauvin, 2001;Fontaine, 1999;Higuchi, 1998]. I was able to show that both oxygen consumption and enzymatic activities were significantly lower in the cervical region of early symptomatic wobbler mice. On the other hand, no difference was found by comparing the same parameters of mitochondrial activity in the lumbar tract of wobbler mice and healthy littermates.

A detailed morphological characterization may be more reliable to elucidate the degree of mitochondrial alteration occurring in cervical motor neurons of wobbler mice. In a recent ultrastructural study [Gonzalez Deniselle, 2004] a massive vacuolization of mitochondria with the rupture of inner/outer mitochondrial membranes and the disruption of cristae has been reported in 10 week-old wobbler mice. However, as clearly demonstrated in a series of study in $SOD1^{G93A}$ mice, morphological abnormalities in mitochondria occur earlier than symptoms onset [Bendotti, 2001], and a morphological

analysis at a time when 70% of the cells have already died and the remaining ones are highly vacuolized and altered, is somewhat questionable.

The first steps in mitochondrion-dependent apoptosis are the release of cytochrome-c into the cytosol and the apoptosome formation. In the lumbar motor neurons of early symptomatic $SOD1^{G93A}$ mice a homogeneously diffused staining for cytochrome-c and a clear activation of caspase 9 has been reported. The presence of immunopositivity for both markers may indicate a clear link between cytochrome-c release and caspase 9 activation in this process of motor neuron degeneration. Cytochrome-c immunostaining, however, cannot be taken as strong evidence of an active release of cytochrome-c from intact mitochondria if it is not supported by an ultrastructural investigation of immunogold staining (cyotochrome-c antibody) or double staining co localization with a marker that detects mitochondria integrity, as reported in my in vitro experiment with Mito Tracker (Chapter 10). For this reason, the caspases cascade cell signalling was directly evaluated by performing immunohystochemical experiments with antibodies against the activated form of caspases 3, -7 and -9, and a hystochemical assay (ISEL) was used to determine nuclear fragmentation. To decrease any bias due to the low probability of finding apoptotic motor neurons, a large number of cells were evaluated (about 1500 motor neurons for each animal in healthy tissues and 1150 in affected regions) and at least 5 animals for each antibody were used. An extremely small number (<0.1%) of motor neurons were positively stained for the three caspases and no ISEL positive nuclei was detected. In addition, no differences were seen by comparing the percentage of active caspases 3, -7 and -9 in the cervical motor neurons of wobbler mice and healthy littermates. It is difficult to explain why a similar number of active caspases positive motor neurons in both experimental groups were observed, and a significant decrease was observed in older healthy mice when comparing the percentage of active caspases-positive motor neurons at 4 and 12 weeks of age (data not shown). It might be that the few caspases-positive motor neurons observed at the 5^{th} week of life are undergoing a physiological apoptosis, possibly as the latest effect of the developmental

reduction of neuron number, rather than a pathological process associated to the disease. However, although the sensitivity and the specificity of antibodies was already tested both on primary cultures and in other in vitro models of apoptosis, it is not possible to exclude a false negative result, particularly as we are dealing with a process of chronic neurodegeneration.

To further exclude the possibility that motor neurons death in wobbler mice occurs by apoptosis , the effects of a chronic treatment with EPO, an anti-apoptotic agent that I have previously shown to inhibit mitochondrion dependent apoptosis by blocking cytochrome-c release and mitochondrial PTP opening (see section 10.4), was studied in early symptomatic wobbler mice. EPO treatment failed to delay the progression of the symptoms and did not reduce the rate of motor neurons loss and the biceps atrophy. This finding further support the notion that in the wobbler mouse motor neuron disease the mitochondrion-dependent apoptotic pathway is not involved in the process of motor neuron death.

13.2 Glutamate-induced excitotoxicity and apoptosis

Another aetiological mechanism that has been suggested to play a relevant role in motor neurons death in ALS patients is glutamate-induced excitotoxicity [Shaw, 1997;Kato, 2000;Hentati, 1994;Hadano, 2001;Kanekura, 2004;Choi, 1987;Rothstein, 1993;Rothstein, 1994]. In the last decade, many experimental results obtained from autoptic samples have shown a reduced level and a decreased efficiency of glutamate transporters (that could decrease glutamate clearance in the synaptic cleft) [Rothstein, 1994; Rothstein, 1995], a post translational mutation of GluR2 AMPAr subunit (that would render the AMPA receptors more permeable to Ca^{++}) [Takuma, 1999;Pellegrini-Giampietro, 1997;Laslo, 2001] and increased levels of excitatory aminoacids in the plasma and liquor of ALS patients [Haenggeli, 2002]. These findings support the hypothesis that alterations in the glutamatergic system might be the primary source of motor neuron damage in ALS patients. In addition, similar changes in the glutamate system have been reported in different animal models of motor neuron degeneration [Casciola-Rosen, 1994;Mennini, 1999].

In contrast to acute processes of excitotoxicity, such as ischemia/riperfusion, in which a rapid and strong glutamatergic overstimulation is often associated to a massive Ca^{++} influx [Howland, 2002;Gredal, 1997], in a chronic process of neurodegeneration, such as ALS, glutamatergic overstimulation is associated with a mild but prolonged glutamatergic overstimulation [Pellegrini-Giampietro, 1992]. Indeed, in cerebellar granule cells cultures exposed to glutamate, the mechanisms of cell death depends on the intensity of stimulation, with high doses of glutamate inducing a fast process of necrotic death, and a lower but more prolonged application of this neurotransmitter producing a slower death with the typical features of apoptosis [Nicotera, 1997]. Since the latter mechanism of death seems to be more correlated to the process that could occur in ALS, the effects of chronic AMPAr stimulation in primary cultures of motor neurons was studied using AMPA and kainite, as they are known to induce two different mechanisms

of death. While AMPA treatment induced a rapid decay of motor neurons survival and a plateau phase in the second part of the treatment and did not show apoptotic features, kainate produced a clear apoptotic pattern, with a slower kinetic of death and a marked increase of nuclear fragmentation and caspases 3 and -9 activation.

Whether such mechanism of death involved the mitochondrion-dependent cell death was further evaluated by measuring the release of cytochrome-c, the mitochondrial depolarization, and the protective effect of a pharmacological agent that inhibits the PTP opening, cyclosporin A_2. The results of the chronic treatment with kainate confirm the hypothesis that mitochondrion plays a key role in this mechanism of apoptosis. Moreover, the different mechanism of death produced by AMPA and kainate exposure on primary cultures of motor neurons allowed evaluating if EPO treatment is selective active against apoptosis or showed a broader spectrum of action. EPO was found to selectively rescue motor neurons exposed to kainate and was ineffective on AMPA-treated motor neurons. This evidence further confirms the anti-apoptotic effects exerted by EPO, and is also supported by the ability of EPO to inhibit caspases 3/9 activation, cytochrome-c release and mitochondrial depolarization in motor neurons chronically exposed to kainate.

The lack of any difference in the EAA plasma levels, the expression and activity of glutamate transporters, and the expression and the localization of AMPAr subunits (GluR 1-4) between early symptomatic wobbler mice and healthy littermates does not completely rule out an involvement of glutamate overstimulation in the wobbler mouse motor neurons disease, since an increased Ca^{++} permeability, due to modifications of GluR2 subunit, was not investigated in this work. In order to clarify the role of AMPAr in motor neuron death occurring in wobbler mice a chronic treatment with a selective AMPA antagonist (RPR 119990) was performed. However, no beneficial effect in the motor performance, as well as in the survival rate and atrophy of motor neurons, was seen in early symptomatic wobbler mice after 9 weeks of treatment with RPR 119990, a compound that has been shown to be active in $SOD1^{G93A}$ mice. All together, therefore,

these behavioural, biochemical and hystochemical findings suggest that glutamate-induced excitotoxicity is not involved in the pathogenesis occurring in cervical motor neurons of wobbler mice.

Together with an altered glutamate metabolism in CNS samples obtained from ALS patients, the link between ALS and excitotoxicity is supported by the evidence that riluzole, a non selective anti-excitotoxic compound, slightly but significantly reduces the clinical progression in ALS patients, such that clinical trials which do not include riluzole treatment in the "placebo group" are considered unethical and deleterious. Indeed, in contrast to the lack of action of RPR119990, riluzole significantly reduced motor impairment, with a stabilization of symptoms in the second half of the treatment, and a marked decrease of motor neurons loss and biceps atrophy in wobbler mice. This finding opens a new perspective about the mechanism of riluzole protection in motor neuron disease, like scavenger effects, increase in trophic factors and/or stimulation of neurogenesis. In view of these results, therefore, the wobbler mouse should be considered as a useful tool to investigate the mechanism(s) of motor neuron death that are unrelated to excitotoxicity but sensitive to the reference drug riluzole.

13.3 Glial-induced neuroinflammation and apoptosis

A marked increase of activated microglial cells, particularly close to degenerating areas, and a clear expression of TNF-α and its cognate receptor for the induction of apoptosis (TNFR1) were observed in the cervical region of early symptomatic wobbler mice. However, an extremely low number of active caspase 8 and -3 positive motor neurons were found in these tissues. These data suggest that TNF-α can contribute to motor neuron death by activating alternative mechanisms of damage. Regarding the involvement of TNF-α and TNFR1 and in motor neuron disorders, it is important to note that an even larger expression of TNF-α and TNFR1 has been recently reported in the anterior horn, and that this expression parallels the symptoms progression in the *mnd* mouse, a model of motor impairment in which motor neuron death is lacking [Mennini, 2004,Ghezzi, 1998]. Further experiments to clarify the possible role of TNF-α and its receptors in wobbler mice motor neurons death should include treatments with agents able to block this detrimental pathway (such as anti-TNF-α monoclonal antibodies, soluble TNF-α receptor, TNFR1 receptor antagonist). These experiments alone, however, will not elucidate the possible link between microglial and TNF-α activation and extrinsic apoptotic pathway induction, because detrimental action of TNF-α might be dissociated to apoptosis. Thus, treatment with specific caspase 8 inhibitors would be required.

In summary, this study suggests that apoptosis is not involved in the process of death leading to the loss of about the 70% of motor neurons in the cervical spinal cord region of the wobbler mouse. Future studies, aimed at investigating alternative pathways of death, such as autophagic cell death, will be fundamental to answer this important question which is of great relevance for finding new therapeutic strategies for ALS patients.

REFERENCES

References

- **Brooks,**

- ***A controlled trial of recombinant methionyl human BDNF in ALS: The BDNF Study Group (Phase III).*** **Neurology, 1999. 52(7): p. 1427-33.**
- ***A double-blind placebo-controlled clinical trial of subcutaneous recombinant human ciliary neurotrophic factor (rHCNTF) in amyotrophic lateral sclerosis. ALS CNTF Treatment Study Group.*** **Neurology, 1996. 46(5): p. 1244-9.**
- **Abarbanel, J.M., Y. Herishanu, and S. Frisher, *Motor neuron disease in textile factory workers.* Isr J Med Sci, 1985. 21(11): p. 924-5.**
- **Abe, K., *Clinical and molecular analysis of neurodegenerative diseases.* Tohoku J Exp Med, 1997. 181(4): p. 389-409.**
- **Ackerley, S., et al., *Glutamate slows axonal transport of neurofilaments in transfected neurons.* J Cell Biol, 2000. 150(1): p. 165-76.**
- **Adams, J.M. and S. Cory, *The Bcl-2 protein family: arbiters of cell survival.* Science, 1998. 281(5381): p. 1322-6.**
- **Agnello, D., et al., *Erythropoietin exerts an anti-inflammatory effect on the CNS in a model of experimental autoimmune encephalomyelitis.* Brain Res, 2002. 952(1): p. 128-34.**
- **Ait-Ikhlef, A., et al., *Influence of factors secreted by wobbler astrocytes on neuronal and motoneuronal survival.* J Neurosci Res, 2000. 59(1): p. 100-6.**
- **Al-Abdulla, N.A. and L.J. Martin, *Apoptosis of retrogradely degenerating neurons occurs in association with the accumulation of perikaryal mitochondria and oxidative damage to the nucleus.* Am J Pathol, 1998. 153(2): p. 447-56.**
- **Albrecht, P.J., et al., *Ciliary neurotrophic factor activates spinal cord astrocytes, stimulating their production and release of fibroblast growth factor-2, to increase motor neuron survival.* Exp Neurol, 2002. 173(1): p. 46-62.**
- **Al-Chalabi, A. and C.C. Miller, *Neurofilaments and neurological disease.* Bioessays, 2003. 25(4): p. 346-55.**
- **Andersen, P.M., et al., *Phenotypic heterogeneity in motor neuron disease patients with CuZn-superoxide dismutase mutations in Scandinavia.* Brain, 1997. 120 (Pt 10): p. 1723-37.**
- **Anderson, A.J., J.H. Su, and C.W. Cotman, *DNA damage and apoptosis in Alzheimer's disease: colocalization with c-Jun immunoreactivity, relationship to brain area, and effect of postmortem delay.* J Neurosci, 1996. 16(5): p. 1710-9.**
- **Andrews, J.M. and M.B. Gardner, *Lower motor neuron degeneration associated with type C RNA virus infection in mice: neuropathological features.* J Neuropathol Exp Neurol, 1974. 33(2): p. 285-307.**
- **Angelov, D.N., et al., *Nimodipine accelerates axonal sprouting after surgical repair of rat facial nerve.* J Neurosci, 1996. 16(3): p. 1041-8.**

- **Ankarcrona, M., et al., *Glutamate-induced neuronal death: a succession of necrosis or apoptosis depending on mitochondrial function.* Neuron, 1995. 15(4): p. 961-73.**
- **Aquilonius, S.M., et al., *Increased binding of 3H-L-deprenyl in spinal cords from patients with amyotrophic lateral sclerosis as demonstrated by autoradiography.* J Neural Transm Gen Sect, 1992. 89(1-2): p. 111-22.**
- **Arvidson, B., *Inorganic mercury is transported from muscular nerve terminals to spinal and brainstem motoneurons.* Muscle Nerve, 1992. 15(10): p. 1089-94.**
- **Asahara, H., et al., *Glutamate enhances phosphorylation of neurofilaments in cerebellar granule cell culture.* J Neurol Sci, 1999. 171(2): p. 84-7.**
- **Ashkenazi, A. and V.M. Dixit, *Death receptors: signaling and modulation.* Science, 1998. 281(5381): p. 1305-8.**
- **Askmark, H., et al., *A pilot trial of dextromethorphan in amyotrophic lateral sclerosis.* J Neurol Neurosurg Psychiatry, 1993. 56(2): p. 197-200.**
- **Augustin, M., et al., *Spinal muscular atrophy gene wobbler of the mouse: evidence from chimeric spinal cord and testis for cell-autonomous function.* Dev Dyn, 1997. 209(3): p. 286-95.**
- **Bastone, A., et al., *The imbalance of brain large-chain aminoacid availability in amyotrophic lateral sclerosis patients treated with high doses of branched-chain aminoacids.* Neurochem Int, 1995. 27(6): p. 467-72.**
- **Battaglioli, G., et al., *Synaptosomal glutamate uptake declines progressively in the spinal cord of a mutant mouse with motor neuron disease.* J Neurochem, 1993. 60(4): p. 1567-9.**
- **Bauer, J., et al., *The role of macrophages, perivascular cells, and microglial cells in the pathogenesis of experimental autoimmune encephalomyelitis.* Glia, 1995. 15(4): p. 437-46.**
- **Beal, M.F., *Mitochondria and the pathogenesis of ALS.* Brain, 2000. 123 (Pt 7): p. 1291-2.**
- **Beal, M.F., *Mitochondria, oxidative damage, and inflammation in Parkinson's disease.* Ann N Y Acad Sci, 2003. 991: p. 120-31.**
- **Beaulaton, J. and R.A. Lockshin, *The relation of programmed cell death to development and reproduction: comparative studies and an attempt at classification.* Int Rev Cytol, 1982. 79: p. 215-35.**
- **Beckman, J.S., et al., *The interactions of nitric oxide with oxygen radicals and scavengers in cerebral ischemic injury.* Adv Neurol, 1996. 71: p. 339-50; discussion 350-4.**
- **Beckman, J.S., et al., *ALS, SOD and peroxynitrite.* Nature, 1993. 364(6438): p. 584.**

- **Beghi, E., et al., *A randomized controlled trial of recombinant interferon beta-1a in ALS. Italian Amyotrophic Lateral Sclerosis Study Group.* Neurology, 2000. 54(2): p. 469-74.**
- **Bellairs, R., *The structure of the yolk of the hen's egg as studied by electron microscopy. I. The yolk of the unincubated egg.* J Biophys Biochem Cytol, 1961. 11: p. 207-25.**
- **Bendotti, C., et al., *Early vacuolization and mitochondrial damage in motor neurons of FALS mice are not associated with apoptosis or with changes in cytochrome oxidase histochemical reactivity.* J Neurol Sci, 2001. 191(1-2): p. 25-33.**
- **Bendotti, C., et al., *Late therapy with AMPA receptor antagonist ZK187638 improves the neuromuscular impairment and the survival in experimental models of motor neuron disorders.* Amyotroph Lateral Scler Other Motor Neuron Disord, 2002. 3(Suppl 2): p. 77.**
- **Bendotti, C., et al., *Transgenic SOD1 G93A mice develop reduced GLT-1 in spinal cord without alterations in cerebrospinal fluid glutamate levels.* J Neurochem, 2001. 79(4): p. 737-46.**
- **Benigni, F., et al., *TNF receptor p55 plays a major role in centrally mediated increases of serum IL-6 and corticosterone after intracerebroventricular injection of TNF.* J Immunol, 1996. 157(12): p. 5563-8.**
- **Bennet, M.R., W.G. Gibson, and G. Lemon, *Neuronal cell death, nerve growth factor and neurotrophic models: 50 years on.* Auton Neurosci, 2002. 95(1-2): p. 1-23.**
- **Benoit, E. and D. Escande, *Riluzole specifically blocks inactivated Na channels in myelinated nerve fibre.* Pflugers Arch, 1991. 419(6): p. 603-9.**
- **Bensimon, G., L. Lacomblez, and V. Meininger, *A controlled trial of riluzole in amyotrophic lateral sclerosis. ALS/Riluzole Study Group.* N Engl J Med, 1994. 330(9): p. 585-91.**
- **Beretta, S., et al., *The sinister side of Italian soccer.* Lancet Neurol, 2003. 2(11): p. 656-7.**
- **Bernardi, P. and V. Petronilli, *The permeability transition pore as a mitochondrial calcium release channel: a critical appraisal.* J Bioenerg Biomembr, 1996. 28(2): p. 131-8.**
- **Bernardi, P., *The permeability transition pore. Control points of a cyclosporin A-sensitive mitochondrial channel involved in cell death.* Biochim Biophys Acta, 1996. 1275(1-2): p. 5-9.**
- **Bernaudin, M., et al., *A potential role for erythropoietin in focal permanent cerebral ischemia in mice.* J Cereb Blood Flow Metab, 1999. 19(6): p. 643-51.**
- **Bertamini, M., et al., *Mitochondrial oxidative metabolism in motor neuron degeneration (mnd) mouse central nervous system.* Eur J Neurosci, 2002. 16(12): p. 2291-6.**

- **Bertoni-Freddari, C., et al., *Cytochrome oxidase activity in hippocampal synaptic mitochondria during aging: a quantitative cytochemical investigation.* Ann N Y Acad Sci, 2004. 1019: p. 33-6.**
- **Bezzi, P., et al., *Prostaglandins stimulate calcium-dependent glutamate release in astrocytes.* Nature, 1998. 391(6664): p. 281-5.**
- **Bigini, P., A. Bastone, and T. Mennini, *Glutamate transporters in the spinal cord of the wobbler mouse.* Neuroreport, 2001. 12(9): p. 1815-20.**
- **Bigini, P., et al., *Acetyl-L-carnitine shows neuroprotective and neurotrophic activity in primary culture of rat embryo motoneurons.* Neurosci Lett, 2002. 329(3): p. 334-8.**
- **Bignami, A., et al., *Localization of the glial fibrillary acidic protein in astrocytes by immunofluorescence.* Brain Res, 1972. 43(2): p. 429-35.**
- **Biscoe, T.J. and S.J. Lewkowicz, *Quantitative light and electron microscopic studies on the ventral roots of the wobbler mutant mouse.* Q J Exp Physiol, 1982. 67(4): p. 543-55.**
- **Blatt, N.B. and G.D. Glick, *Signaling pathways and effector mechanisms pre-programmed cell death.* Bioorg Med Chem, 2001. 9(6): p. 1371-84.**
- **Blin, O., et al., *A double-blind placebo-controlled trial of L-threonine in amyotrophic lateral sclerosis.* J Neurol, 1992. 239(2): p. 79-81.**
- **Blondet, B., et al., *Motoneuron morphological alterations before and after the onset of the disease in the wobbler mouse.* Brain Res, 2002. 930(1-2): p. 53-7.**
- **Blondet, B., et al., *Plasminogen activators in the neuromuscular system of the wobbler mutant mouse.* Brain Res, 1992. 580(1-2): p. 303-10.**
- **Bloom, G.S. and L.S. Goldstein, *Cruising along microtubule highways: how membranes move through the secretory pathway.* J Cell Biol, 1998. 140(6): p. 1277-80.**
- **Boillee, S., et al., *Differential microglial response to progressive neurodegeneration in murine mutant wobbler*. Glia, 2001. 33(4): p. 277-87.**
- **Boldin, M.P., et al., *A novel protein that interacts with the death domain of Fas/APO1 contains a sequence motif related to the death domain.* J Biol Chem, 1995. 270(14): p. 7795-8.**
- **Boldin, M.P., et al., *Involvement of MACH, a novel MORT1/FADD-interacting protease, in Fas/APO-1- and TNF receptor-induced cell death.* Cell, 1996. 85(6): p. 803-15.**
- **Bomont, P., et al., *Homozygosity mapping of spinocerebellar ataxia with cerebellar atrophy and peripheral neuropathy to 9q33-34, and with hearing impairment and optic atrophy to 6p21-23.* Eur J Hum Genet, 2000. 8(12): p. 986-90.**
- **Bonfoco, E., et al., *Apoptosis and necrosis: two distinct events induced, respectively, by mild and intense insults with N-methyl-D-aspartate or nitric oxide/superoxide in cortical cell cultures.* Proc Natl Acad Sci U S A, 1995. 92(16): p. 7162-6.**

- **Borasio, G.D. and R. Voltz, *Palliative care in amyotrophic lateral sclerosis.* J Neurol, 1997. 244 Suppl 4: p. S11-7.**
- **Borasio, G.D., et al., *A placebo-controlled trial of insulin-like growth factor-I in amyotrophic lateral sclerosis. European ALS/IGF-I Study Group.* Neurology, 1998. 51(2): p. 583-6.**
- **Borthwick, G.M., et al., *Mitochondrial enzyme activity in amyotrophic lateral sclerosis: implications for the role of mitochondria in neuronal cell death.* Ann Neurol, 1999. 46(5): p. 787-90.**
- **Bose, P. and L.L. Vacca-Galloway, *Increase in fiber density for immunoreactive serotonin, substance P, enkephalin and thyrotropin-releasing hormone occurs during the early presymptomatic period of motoneuron disease in Wobbler mouse spinal cord ventral horn.* Neurosci Lett, 1999. 260(3): p. 196-200.**
- **Bose, P., et al., *A novel behavioral method to detect motoneuron disease in Wobbler mice aged three to seven days old.* Brain Res, 1998. 813(2): p. 334-42.**
- **Bowling, A.C., et al., *Superoxide dismutase activity, oxidative damage, and mitochondrial energy metabolism in familial and sporadic amyotrophic lateral sclerosis.* J Neurochem, 1993. 61(6): p. 2322-5.**
- **Braak, H., et al., *Vulnerability of select neuronal types to Alzheimer's disease.* Ann N Y Acad Sci, 2000. 924: p. 53-61.**
- **Bracco, P. and G.F. Solinas, *[Use and control of the "functional bite plate" in the early treatment of crossbite].* Mondo Ortod, 1979. 4(4): p. 7-17.**
- **Bradley, W.G. and F. Krasin, *A new hypothesis of the etiology of amyotrophic lateral sclerosis. The DNA hypothesis.* Arch Neurol, 1982. 39(11): p. 677-80.**
- **Bradley, W.G., *Double-blind controlled trial of purified brain gangliosides in amyotrophic lateral sclerosis and experience with peripheral neuropathies.* Adv Exp Med Biol, 1984. 174: p. 565-73.**
- **Bratton, S.B., et al., *Protein complexes activate distinct caspase cascades in death receptor and stress-induced apoptosis.* Exp Cell Res, 2000. 256(1): p. 27-33.**
- **Brines, M.L., et al., *Erythropoietin crosses the blood-brain barrier to protect against experimental brain injury.* Proc Natl Acad Sci U S A, 2000. 97(19): p. 10526-31.**
- **Bristol, L.A. and J.D. Rothstein, *Glutamate transporter gene expression in amyotrophic lateral sclerosis motor cortex.* Ann Neurol, 1996. 39(5): p. 676-9.**
- **Bronson, R.T., et al., *Motor neuron degeneration of mice is a model of neuronal ceroid lipofuscinosis (Batten's disease).* Ann Neurol, 1993. 33(4): p. 381-5.**
- **Brooke, M.H., *Thyrotropin-releasing hormone in ALS. Are the results of clinical studies inconsistent?* Ann N Y Acad Sci, 1989. 553: p. 422-30.**

- **Brooks, B.R., et al., *Intravenous thyrotropin-releasing hormone in patients with amyotrophic lateral sclerosis. Dose-response and randomized concurrent placebo-controlled pilot studies.* Neurol Clin, 1987. 5(1): p. 143-58.**
- **Brooks, B.R., *El Escorial World Federation of Neurology criteria for the diagnosis of amyotrophic lateral sclerosis. Subcommittee on Motor Neuron Diseases/Amyotrophic Lateral Sclerosis of the World Federation of Neurology Research Group on Neuromuscular Diseases and the El Escorial "Clinical limits of amyotrophic lateral sclerosis" workshop contributors.* J Neurol Sci, 1994. 124 Suppl: p. 96-107.**
- **Brown, R.H., Jr., et al., *Failure of immunosuppression with a ten- to 14-day course of high-dose intravenous cyclophosphamide to alter the progression of amyotrophic lateral sclerosis.* Arch Neurol, 1986. 43(4): p. 383-4.**
- **Browne, S.E., et al., *Metabolic dysfunction in familial, but not sporadic, amyotrophic lateral sclerosis.* J Neurochem, 1998. 71(1): p. 281-7.**
- **Bruijn, L.I., et al., *ALS-linked SOD1 mutant G85R mediates damage to astrocytes and promotes rapidly progressive disease with SOD1-containing inclusions.* Neuron, 1997. 18(2): p. 327-38.**
- **Brunialti, A.L., et al., *The mouse mutation progressive motor neuronopathy (pmn) maps to chromosome 13.* Genomics, 1995. 29(1): p. 131-5.**
- **Burnashev, N., et al., *Calcium-permeable AMPA-kainate receptors in fusiform cerebellar glial cells.* Science, 1992. 256(5063): p. 1566-70.**
- **Burnashev, N., et al., *Divalent ion permeability of AMPA receptor channels is dominated by the edited form of a single subunit.* Neuron, 1992. 8(1): p. 189-98.**
- **Caelles, C., A. Helmberg, and M. Karin, *p53-dependent apoptosis in the absence of transcriptional activation of p53-target genes.* Nature, 1994. 370(6486): p. 220-3.**
- **Callahan, L.M., et al., *Neurofilament distribution is altered in the Mnd (motor neuron degeneration) mouse.* J Neuropathol Exp Neurol, 1991. 50(4): p. 491-504.**
- **Camu, W., et al., *Genetics of familial ALS and consequences for diagnosis. French ALS Research Group.* J Neurol Sci, 1999. 165 Suppl 1: p. S21-6.**
- **Canton, T., et al., *RPR 119990, a novel alpha-amino-3-hydroxy-5-methyl-4-isoxazolepropionic acid antagonist: synthesis, pharmacological properties, and activity in an animal model of amyotrophic lateral sclerosis.* J Pharmacol Exp Ther, 2001. 299(1): p. 314-22.**
- **Canu, N. and P. Calissano, *In vitro cultured neurons for molecular studies correlating apoptosis with events related to Alzheimer disease.* Cerebellum, 2003. 2(4): p. 270-8.**
- **Carpenter, S., *Proximal axonal enlargement in motor neuron disease.* Neurology, 1968. 18(9): p. 841-51.**
- **Carriedo, S.G., et al., *AMPA exposures induce mitochondrial Ca(2+) overload and ROS generation in spinal motor neurons in vitro.* J Neurosci, 2000. 20(1): p. 240-50.**

- **Carriedo, S.G., et al., *In vitro kainate injury to large, SMI-32(+) spinal neurons is Ca2+ dependent.* Neuroreport, 1995. 6(6): p. 945-8.**
- **Carriedo, S.G., H.Z. Yin, and J.H. Weiss, *Motor neurons are selectively vulnerable to AMPA/kainate receptor-mediated injury in vitro.* J Neurosci, 1996. 16(13): p. 4069-79.**
- **Casciola-Rosen, L.A., et al., *Specific cleavage of the 70-kDa protein component of the U1 small nuclear ribonucleoprotein is a characteristic biochemical feature of apoptotic cell death.* J Biol Chem, 1994. 269(49): p. 30757-60.**
- **Cashman, N.R., et al., *Neuroblastoma x spinal cord (NSC) hybrid cell lines resemble developing motor neurons.* Dev Dyn, 1992. 194(3): p. 209-21.**
- **Cassarino, D.S. and J.P. Bennett, Jr., *An evaluation of the role of mitochondria in neurodegenerative diseases: mitochondrial mutations and oxidative pathology, protective nuclear responses, and cell death in neurodegeneration.* Brain Res Brain Res Rev, 1999. 29(1): p. 1-25.**
- **Cassina, P., et al., *Peroxynitrite triggers a phenotypic transformation in spinal cord astrocytes that induces motor neuron apoptosis.* J Neurosci Res, 2002. 67(1): p. 21-9.**
- **Cattaneo, E., et al., *Loss of normal huntingtin function: new developments in Huntington's disease research.* Trends Neurosci, 2001. 24(3): p. 182-8.**
- **Chambers, D.M., J. Peters, and C.M. Abbott, *The lethal mutation of the mouse wasted (wst) is a deletion that abolishes expression of a tissue-specific isoform of translation elongation factor 1alpha, encoded by the Eef1a2 gene.* Proc Natl Acad Sci U S A, 1998. 95(8): p. 4463-8.**
- **Chan, K.F., M.R. Siegel, and J.M. Lenardo, *Signaling by the TNF receptor superfamily and T cell homeostasis.* Immunity, 2000. 13(4): p. 419-22.**
- **Chang, H.Y. and X. Yang, *Proteases for cell suicide: functions and regulation of caspases.* Microbiol Mol Biol Rev, 2000. 64(4): p. 821-46.**
- **Chang, L.K., et al., *Mitochondrial involvement in the point of no return in neuronal apoptosis.* Biochimie, 2002. 84(2-3): p. 223-31.**
- **Chao, D.T. and S.J. Korsmeyer, *BCL-2 family: regulators of cell death.* Annu Rev Immunol, 1998. 16: p. 395-419.**
- **Chaudhary, P.M., et al., *Death receptor 5, a new member of the TNFR family, and DR4 induce FADD-dependent apoptosis and activate the NF-kappaB pathway.* Immunity, 1997. 7(6): p. 821-30.**
- **Chauvin, C., et al., *Rotenone inhibits the mitochondrial permeability transition-induced cell death in U937 and KB cells.* J Biol Chem, 2001. 276(44): p. 41394-8.**
- **Cheng, Y.J., et al., *Enhancement of TNF-alpha expression does not trigger apoptosis upon exposure of glial cells to lead and lipopolysaccharide.* Toxicology, 2002. 178(3): p. 183-91.**

- **Cheramy, A., et al., *Riluzole inhibits the release of glutamate in the caudate nucleus of the cat in vivo.* Neurosci Lett, 1992. 147(2): p. 209-12.**
- **Chiesa, R. and D.A. Harris, *Nerve growth factor-induced differentiation does not alter the biochemical properties of a mutant prion protein expressed in PC12 cells.* J Neurochem, 2000. 75(1): p. 72-80.**
- **Choi, D.W., *Calcium: still center-stage in hypoxic-ischemic neuronal death.* Trends Neurosci, 1995. 18(2): p. 58-60.**
- **Choi, D.W., M. Maulucci-Gedde, and A.R. Kriegstein, *Glutamate neurotoxicity in cortical cell culture.* J Neurosci, 1987. 7(2): p. 357-68.**
- **Chong, Z.Z., J.Q. Kang, and K. Maiese, *Erythropoietin is a novel vascular protectant through activation of Akt1 and mitochondrial modulation of cysteine proteases.* Circulation, 2002. 106(23): p. 2973-9.**
- **Chou, S.M., *Immunohistochemical and ultrastructural classification of peripheral neuropathies with onion-bulbs.* Clin Neuropathol, 1992. 11(3): p. 109-14.**
- **Chung, M.J. and Y.L. Suh, *Ultrastructural changes of mitochondria in the skeletal muscle of patients with amyotrophic lateral sclerosis.* Ultrastruct Pathol, 2002. 26(1): p. 3-7.**
- **Clarke, P.G., *Developmental cell death: morphological diversity and multiple mechanisms.* Anat Embryol (Berl), 1990. 181(3): p. 195-213.**
- **Clarke, P.G., *Proceedings: Neuronal death as an error-correcting mechanism in the development of the chick's isthmo-optic nucleus.* J Physiol, 1976. 256(1): p. 44P-45P.**
- **Cleveland, D.W. and J.D. Rothstein, *From Charcot to Lou Gehrig: deciphering selective motor neuron death in ALS.* Nat Rev Neurosci, 2001. 2(11): p. 806-19.**
- **Clowry, G.J. and S. McHanwell, *Expression of nitric oxide synthase by motor neurones in the spinal cord of the mutant mouse wobbler.* Neurosci Lett, 1996. 215(3): p. 177-80.**
- **Clowry, G.J., *Axotomy induces NADPH diaphorase activity in neonatal but not adult motoneurones.* Neuroreport, 1993. 5(3): p. 361-4.**
- **Collier, T.J., et al., *Cellular models to study dopaminergic injury responses.* Ann N Y Acad Sci, 2003. 991: p. 140-51.**
- **Comoletti, D., et al., *Nitric oxide produced by non-motoneuron cells enhances rat embryonic motoneuron sensitivity to excitotoxins: comparison in mixed neuron/glia or purified cultures.* J Neurol Sci, 2001. 192(1-2): p. 61-9.**
- **Compston, A., et al., *Glial lineages and myelination in the central nervous system.* J Anat, 1997. 190 (Pt 2): p. 161-200.**
- **Corbo, M. and A.P. Hays, *Peripherin and neurofilament protein coexist in spinal spheroids of motor neuron disease.* J Neuropathol Exp Neurol, 1992. 51(5): p. 531-7.**

- Corvino, V., et al., *S100B protein and 4-hydroxynonenal in the spinal cord of wobbler mice.* Neurochem Res, 2003. 28(2): p. 341-5.
- Cote, F., J.F. Collard, and J.P. Julien, *Progressive neuronopathy in transgenic mice expressing the human neurofilament heavy gene: a mouse model of amyotrophic lateral sclerosis.* Cell, 1993. 73(1): p. 35-46.
- Cotman, C.W., et al., *Possible role of apoptosis in Alzheimer's disease.* Ann N Y Acad Sci, 1994. 747: p. 36-49.
- Cotter, T.G., *Induction of apoptosis in cells of the immune system by cytotoxic stimuli.* Semin Immunol, 1992. 4(6): p. 399-405.
- Coulpier, M., et al., *Bcl-2 sensitivity differentiates two pathways for motoneuronal death in the wobbler mutant mouse.* J Neurosci, 1996. 16(19): p. 5897-904.
- Couratier, P., et al., *Cell culture evidence for neuronal degeneration in amyotrophic lateral sclerosis being linked to glutamate AMPA/kainate receptors.* Lancet, 1993. 341(8840): p. 265-8.
- Couratier, P., et al., *Neuroprotective effects of riluzole in ALS CSF toxicity.* Neuroreport, 1994. 5(8): p. 1012-4.
- Cudkowicz, M.E., et al., *Epidemiology of mutations in superoxide dismutase in amyotrophic lateral sclerosis.* Ann Neurol, 1997. 41(2): p. 210-21.
- Curti, D., et al., *Amyotrophic lateral sclerosis: oxidative energy metabolism and calcium homeostasis in peripheral blood lymphocytes.* Neurology, 1996. 47(4): p. 1060-4.
- Curtis, D.R. and R. Malik, *The differential effects of baclofen on segmental and descending excitation of spinal interneurones in the cat.* Exp Brain Res, 1985. 58(2): p. 333-7.
- Danbolt, N.C., *Glutamate uptake.* Prog Neurobiol, 2001. 65(1): p. 1-105.
- Daube, J.R., *Electrodiagnostic studies in amyotrophic lateral sclerosis and other motor neuron disorders.* Muscle Nerve, 2000. 23(10): p. 1488-502.
- Daughaday, W.H., et al., *Somatomedin: proposed designation for sulphation factor.* Nature, 1972. 235(5333): p. 107.
- Dave, K.R., W.G. Bradley, and M.A. Perez-Pinzon, *Early mitochondrial dysfunction occurs in motor cortex and spinal cord at the onset of disease in the Wobbler mouse.* Exp Neurol, 2003. 182(2): p. 412-20.
- de Carvalho, M., A. Turkman, and M. Swash, *Motor responses evoked by transcranial magnetic stimulation and peripheral nerve stimulation in the ulnar innervation in amyotrophic lateral sclerosis: the effect of upper and lower motor neuron lesion.* J Neurol Sci, 2003. 210(1-2): p. 83-90.
- de Carvalho, M., et al., *Clinical and neurophysiological evaluation of progression in amyotrophic lateral sclerosis.* Muscle Nerve, 2003. 28(5): p. 630-3.

- **De Simone, R., et al., *Apoptotic PC12 cells exposing phosphatidylserine promote the production of anti-inflammatory and neuroprotective molecules by microglial cells.* J Neuropathol Exp Neurol, 2003. 62(2): p. 208-16.**
- **De Yebenes, J.G., M. Sanchez, and M.A. Mena, *Neurotrophic factors for the investigation and treatment of movement disorders.* Neurotox Res, 2003. 5(1-2): p. 119-38.**
- **Deas, O., et al., *Caspase-independent cell death induced by anti-CD2 or staurosporine in activated human peripheral T lymphocytes.* J Immunol, 1998. 161(7): p. 3375-83.**
- **Declercq, W., P. Vandenabeele, and W. Fiers, *Dimerization of chimeric erythropoietin/75 kDa tumour necrosis factor (TNF) receptors transduces TNF signals: necessity for the 75 kDa-TNF receptor transmembrane domain.* Cytokine, 1995. 7(7): p. 701-9.**
- **Desnuelle, C., et al., *A double-blind, placebo-controlled randomized clinical trial of alpha-tocopherol (vitamin E) in the treatment of amyotrophic lateral sclerosis. ALS riluzole-tocopherol Study Group.* Amyotroph Lateral Scler Other Motor Neuron Disord, 2001. 2(1): p. 9-18.**
- **Digicaylioglu, M. and S.A. Lipton, *Erythropoietin-mediated neuroprotection involves cross-talk between Jak2 and NF-kappaB signalling cascades.* Nature, 2001. 412(6847): p. 641-7.**
- **Ding, M., R.P. Hart, and G.M. Jonakait, *Tumor necrosis factor-alpha induces substance P in sympathetic ganglia through sequential induction of interleukin-1 and leukemia inhibitory factor.* J Neurobiol, 1995. 28(4): p. 445-54.**
- **Dipasquale, B., A.M. Marini, and R.J. Youle, *Apoptosis and DNA degradation induced by 1-methyl-4-phenylpyridinium in neurons.* Biochem Biophys Res Commun, 1991. 181(3): p. 1442-8.**
- **Doble, A., J.P. Hubert, and J.C. Blanchard, *Pertussis toxin pretreatment abolishes the inhibitory effect of riluzole and carbachol on D-[3H]aspartate release from cultured cerebellar granule cells.* Neurosci Lett, 1992. 140(2): p. 251-4.**
- **Doble, A., *The pharmacology and mechanism of action of riluzole.* Neurology, 1996. 47(6 Suppl 4): p. S233-41.**
- **Dockery, P., et al., *Neuron volume in the ventral horn in Wobbler mouse motoneuron disease: a light microscope stereological study.* J Anat, 1997. 191 (Pt 1): p. 89-98.**
- **Dolcet, X., et al., *Activation of phosphatidylinositol 3-kinase, but not extracellular-regulated kinases, is necessary to mediate brain-derived neurotrophic factor-induced motoneuron survival.* J Neurochem, 1999. 73(2): p. 521-31.**
- **Dragunow, M., et al., *In situ evidence for DNA fragmentation in Huntington's disease striatum and Alzheimer's disease temporal lobes.* Neuroreport, 1995. 6(7): p. 1053-7.**

- **Duchen, L.W. and S.J. Strich, *An hereditary motor neurone disease with progressive denervation of muscle in the mouse: the mutant 'wobbler'.* J Neurol Neurosurg Psychiatry, 1968. 31(6): p. 535-42.**
- **Dunlop, J., et al., *Impaired spinal cord glutamate transport capacity and reduced sensitivity to riluzole in a transgenic superoxide dismutase mutant rat model of amyotrophic lateral sclerosis.* J Neurosci, 2003. 23(5): p. 1688-96.**
- **Eddleston, M., et al., *Astrocytes are the primary source of tissue factor in the murine central nervous system. A role for astrocytes in cerebral hemostasis.* J Clin Invest, 1993. 92(1): p. 349-58.**
- **Eglitis, M.A., et al., *Gene therapy: efforts at developing large animal models for autologous bone marrow transplant and gene transfer with retroviral vectors.* Ciba Found Symp, 1987. 130: p. 229-46.**
- **Eisen, A., et al., *Anti-glutamate therapy in amyotrophic lateral sclerosis: a trial using lamotrigine.* Can J Neurol Sci, 1993. 20(4): p. 297-301.**
- **Eisen, A., et al., *Duration of amyotrophic lateral sclerosis is age dependent.* Muscle Nerve, 1993. 16(1): p. 27-32.**
- **Ekegren, T., et al., *Upregulation of Bax protein and increased DNA degradation in ALS spinal cord motor neurons.* Acta Neurol Scand, 1999. 100(5): p. 317-21.**
- **Erkman, L., et al., *Characterization of dissociated monolayer cultures of human spinal cord.* Brain Res Bull, 1989. 22(1): p. 57-65.**
- **Escurat, M., et al., *Differential expression of two neuronal intermediate-filament proteins, peripherin and the low-molecular-mass neurofilament protein (NF-L), during the development of the rat.* J Neurosci, 1990. 10(3): p. 764-84.**
- **Faust, J.R., et al., *Two related proteolipids and dolichol-linked oligosaccharides accumulate in motor neuron degeneration mice (mnd/mnd), a model for neuronal ceroid lipofuscinosis.* J Biol Chem, 1994. 269(13): p. 10150-5.**
- **Fisher, J.W., et al., *Extrarenal erythropoietin production.* Isr J Med Sci, 1971. 7(7): p. 991-2.**
- **Fonnum, F., *A rapid radiochemical method for the determination of choline acetyltransferase.* J Neurochem, 1975. 24(2): p. 407-9.**
- **Fontaine, E. and P. Bernardi, *Progress on the mitochondrial permeability transition pore: regulation by complex I and ubiquinone analogs.* J Bioenerg Biomembr, 1999. 31(4): p. 335-45.**
- **Ford, M. and C. Leperlier, *Any placebo controlled trial of riluzole would surely be unethical now.* Bmj, 2001. 323(7312): p. 573-4.**
- **Forloni, G., et al., *Apoptosis-mediated neurotoxicity induced by beta-amyloid and PrP fragments.* Mol Chem Neuropathol, 1996. 28(1-3): p. 163-71.**

- **Fraser, A. and G. Evan, *A license to kill.* Cell, 1996. 85(6): p. 781-4.**
- **Fuchs, S., et al., *Comparative transcription map of the wobbler critical region on mouse chromosome 11 and the homologous region on human chromosome 2p13-14.* BMC Genet, 2002. 3(1): p. 14.**
- **Gambetti, P., et al., *Neurofibrillary changes in human brain. An immunocytochemical study with a neurofilament antiserum.* J Neuropathol Exp Neurol, 1983. 42(1): p. 69-79.**
- **Garrido, C., et al., *HSP27 inhibits cytochrome c-dependent activation of procaspase-9.* Faseb J, 1999. 13(14): p. 2061-70.**
- **Gatzinsky, K.P., et al., *Early onset of degenerative changes at nodes of Ranvier in alpha-motor axons of Cntf null (-/-) mutant mice.* Glia, 2003. 42(4): p. 340-9.**
- **Gelanis, D.F., *Respiratory Failure or Impairment in Amyotrophic Lateral Sclerosis.* 2001. 3(2): p. 133-138.**
- **Ghezzi, P., et al., *Tumor necrosis factor is increased in the spinal cord of an animal model of motor neuron degeneration.* Eur Cytokine Netw, 1998. 9(2): p. 139-44.**
- **Gilden, D.H., et al., *Human brain in tissue culture. I. Acquisition, initial processing, and establishment of brain cell cultures.* J Comp Neurol, 1975. 161(3): p. 295-306.**
- **Ginty, D.D., A. Bonni, and M.E. Greenberg, *Nerve growth factor activates a Ras-dependent protein kinase that stimulates c-fos transcription via phosphorylation of CREB.* Cell, 1994. 77(5): p. 713-25.**
- **Giovannini, M.G., et al., *Effect of thyrotropin releasing hormone (TRH) on acetylcholine release from different brain areas investigated by microdialysis.* Br J Pharmacol, 1991. 102(2): p. 363-8.**
- **Glucksmann, A., *Local factors in the histogenesis of hypertrophic scars.* Br J Plast Surg, 1951. 4(2): p. 88-103.**
- **Goldstein, J.C., et al., *The coordinate release of cytochrome c during apoptosis is rapid, complete and kinetically invariant.* Nat Cell Biol, 2000. 2(3): p. 156-62.**
- **Gonzalez Deniselle, M.C., et al., *Basis of progesterone protection in spinal cord neurodegeneration.* J Steroid Biochem Mol Biol, 2002. 83(1-5): p. 199-209.**
- **Gonzalez Deniselle, M.C., et al., *Evidence for down-regulation of GAP-43 mRNA in Wobbler mouse spinal motoneurons by corticosterone and a 21-aminosteroid.* Brain Res, 1999. 841(1-2): p. 78-84.**
- **Gonzalez Deniselle, M.C., et al., *Glucocorticoid receptors and actions in the spinal cord of the Wobbler mouse, a model for neurodegenerative diseases.* J Steroid Biochem Mol Biol, 1997. 60(3-4): p. 205-13.**
- **Gonzalez Deniselle, M.C., et al., *Progesterone neuroprotection in the Wobbler mouse, a genetic model of spinal cord motor neuron disease.* Neurobiol Dis, 2002. 11(3): p. 457-68.**

- **Gonzalez Deniselle, M.C., et al., *Progesterone treatment reduces NADPH-diaphorase/nitric oxide synthase in Wobbler mouse motoneuron disease.* Brain Res, 2004. 1014(1-2): p. 71-9.**
- **Gonzalez Deniselle, M.C., et al., *The 21-aminosteroid U-74389F attenuates hyperexpression of GAP-43 and NADPH-diaphorase in the spinal cord of wobbler mouse, a model for amyotrophic lateral sclerosis.* Neurochem Res, 1999. 24(1): p. 1-8.**
- **Gorio, A., et al., *Co-administration of IGF-I and glycosaminoglycans greatly delays motor neurone disease and affects IGF-I expression in the wobbler mouse: a long-term study.* J Neurochem, 2002. 81(1): p. 194-202.**
- **Gorio, A., et al., *Neuroprotection, neuroregeneration, and interaction with insulin-like growth factor-I: novel non-anticoagulant action of glycosaminoglycans.* J Neurosci Res, 1998. 51(5): p. 559-62.**
- **Gorman, A.M., S. Ceccatelli, and S. Orrenius, *Role of mitochondria in neuronal apoptosis.* Dev Neurosci, 2000. 22(5-6): p. 348-58.**
- **Gourie-Devi, M., A. Nalini, and D.K. Subbakrishna, *Temporary amelioration of symptoms with intravenous cyclophosphamide in amyotrophic lateral sclerosis.* J Neurol Sci, 1997. 150(2): p. 167-72.**
- **Gredal, O., et al., *A clinical trial of dextromethorphan in amyotrophic lateral sclerosis.* Acta Neurol Scand, 1997. 96(1): p. 8-13.**
- **Green, D.R. and J.C. Reed, *Mitochondria and apoptosis.* Science, 1998. 281(5381): p. 1309-12.**
- **Griffith, T.S., et al., *Intracellular regulation of TRAIL-induced apoptosis in human melanoma cells.* J Immunol, 1998. 161(6): p. 2833-40.**
- **Guegan, C., et al., *Recruitment of the mitochondrial-dependent apoptotic pathway in amyotrophic lateral sclerosis.* J Neurosci, 2001. 21(17): p. 6569-76.**
- **Gurney, M.E., et al., *Benefit of vitamin E, riluzole, and gabapentin in a transgenic model of familial amyotrophic lateral sclerosis.* Ann Neurol, 1996. 39(2): p. 147-57.**
- **Gurney, M.E., et al., *Motor neuron degeneration in mice that express a human Cu,Zn superoxide dismutase mutation.* Science, 1994. 264(5166): p. 1772-5.**
- **Gurney, M.E., et al., *Riluzole preserves motor function in a transgenic model of familial amyotrophic lateral sclerosis.* Neurology, 1998. 50(1): p. 62-6.**
- **Gurney, M.E., *Transgenic-mouse model of amyotrophic lateral sclerosis.* N Engl J Med, 1994. 331(25): p. 1721-2.**
- **Haase, G., et al., *Adenovirus-mediated transfer of the neurotrophin-3 gene into skeletal muscle of pmn mice: therapeutic effects and mechanisms of action.* J Neurol Sci, 1998. 160 Suppl 1: p. S97-105.**

- **Hadano, S., et al., *A gene encoding a putative GTPase regulator is mutated in familial amyotrophic lateral sclerosis 2.* Nat Genet, 2001. 29(2): p. 166-73.**
- **Haenggeli, C. and A.C. Kato, *Differential vulnerability of cranial motoneurons in mouse models with motor neuron degeneration.* Neurosci Lett, 2002. 335(1): p. 39-43.**
- **Haenggeli, C. and A.C. Kato, *Rapid and reproducible methods using fluorogold for labelling a subpopulation of cervical motoneurons: application in the wobbler mouse.* J Neurosci Methods, 2002. 116(2): p. 119-24.**
- **Hantaz-Ambroise, D., et al., *Abnormal astrocyte differentiation and defective cellular interactions in wobbler mouse spinal cord.* J Neurocytol, 1994. 23(3): p. 179-92.**
- **Hartley, A., et al., *Complex I inhibitors induce dose-dependent apoptosis in PC12 cells: relevance to Parkinson's disease.* J Neurochem, 1994. 63(5): p. 1987-90.**
- **Hartmann, A., et al., *Caspase-8 is an effector in apoptotic death of dopaminergic neurons in Parkinson's disease, but pathway inhibition results in neuronal necrosis.* J Neurosci, 2001. 21(7): p. 2247-55.**
- **Hassinger, T.D., et al., *Evidence for glutamate-mediated activation of hippocampal neurons by glial calcium waves.* J Neurobiol, 1995. 28(2): p. 159-70.**
- **Haupt, Y. and M. Oren, *p53-mediated apoptosis: mechanisms and regulation.* Behring Inst Mitt, 1996(97): p. 32-59.**
- **Haverkamp, L.J., R.G. Smith, and S.H. Appel, *Trial of immunosuppression in amyotrophic lateral sclerosis using total lymphoid irradiation.* Ann Neurol, 1994. 36(2): p. 253-4.**
- **Hayes, S.A. and J.F. Dice, *Roles of molecular chaperones in protein degradation.* J Cell Biol, 1996. 132(3): p. 255-8.**
- **He, B.P., W. Wen, and M.J. Strong, *Activated microglia (BV-2) facilitation of TNF-alpha-mediated motor neuron death in vitro.* J Neuroimmunol, 2002. 128(1-2): p. 31-8.**
- **Heimann, P., S. Laage, and H. Jockusch, *Defect of sperm assembly in a neurological mutant of the mouse, wobbler (WR).* Differentiation, 1991. 47(2): p. 77-83.**
- **Heimer, L. and R. Kalil, *Rapid transneuronal degeneration and death of cortical neurons following removal of the olfactory bulb in adult rats.* J Comp Neurol, 1978. 178(3): p. 559-609.**
- **Henderson, C.E., et al., *Neurotrophins promote motor neuron survival and are present in embryonic limb bud.* Nature, 1993. 363(6426): p. 266-70.**
- **Heneka, M.T., et al., *Induction of nitric oxide synthase and nitric oxide-mediated apoptosis in neuronal PC12 cells after stimulation with tumor necrosis factor-alpha/lipopolysaccharide.* J Neurochem, 1998. 71(1): p. 88-94.**
- **Hengartner, M.O. and H.R. Horvitz, *The ins and outs of programmed cell death during C. elegans development.* Philos Trans R Soc Lond B Biol Sci, 1994. 345(1313): p. 243-6.**

- **Hengartner, M.O., *Apoptosis and the shape of death.* Dev Genet, 1997. 21(4): p. 245-8.**
- **Hengartner, M.O., *Apoptosis. DNA destroyers.* Nature, 2001. 412(6842): p. 27, 29.**
- **Hensley, K., et al., *Message and protein-level elevation of tumor necrosis factor alpha (TNF alpha) and TNF alpha-modulating cytokines in spinal cords of the G93A-SOD1 mouse model for amyotrophic lateral sclerosis.* Neurobiol Dis, 2003. 14(1): p. 74-80.**
- **Hensley, K., et al., *Temporal patterns of cytokine and apoptosis-related gene expression in spinal cords of the G93A-SOD1 mouse model of amyotrophic lateral sclerosis.* J Neurochem, 2002. 82(2): p. 365-74.**
- **Hentati, A., et al., *Linkage of a locus for autosomal dominant familial spastic paraplegia to chromosome 2p markers.* Hum Mol Genet, 1994. 3(10): p. 1867-71.**
- **Higuchi, M., et al., *Regulation of reactive oxygen species-induced apoptosis and necrosis by caspase 3-like proteases.* Oncogene, 1998. 17(21): p. 2753-60.**
- **Hirano, A., et al., *Fine structural study of neurofibrillary changes in a family with amyotrophic lateral sclerosis.* J Neuropathol Exp Neurol, 1984. 43(5): p. 471-80.**
- **Hirsch, T., et al., *The apoptosis-necrosis paradox. Apoptogenic proteases activated after mitochondrial permeability transition determine the mode of cell death.* Oncogene, 1997. 15(13): p. 1573-81.**
- **Hoglinger, G.U., et al., *Dopamine depletion impairs precursor cell proliferation in Parkinson disease.* Nat Neurosci, 2004. 7(7): p. 726-35.**
- **Hollander, D., et al., *High-dose dextromethorphan in amyotrophic lateral sclerosis: phase I safety and pharmacokinetic studies.* Ann Neurol, 1994. 36(6): p. 920-4.**
- **Hou, R.C., et al., *Effect of sesame antioxidants on LPS-induced NO production by BV2 microglial cells.* Neuroreport, 2003. 14(14): p. 1815-9.**
- **Howland, D.S., et al., *Focal loss of the glutamate transporter EAAT2 in a transgenic rat model of SOD1 mutant-mediated amyotrophic lateral sclerosis (ALS).* Proc Natl Acad Sci U S A, 2002. 99(3): p. 1604-9.**
- **Hsu, C.K., et al., *Bcl-X(L) expression and its downregulation by a novel retinoid in breast carcinoma cells.* Exp Cell Res, 1997. 232(1): p. 17-24.**
- **Hu, Y.L., et al., *Sustained JNK activation induces endothelial apoptosis: studies with colchicine and shear stress.* Am J Physiol, 1999. 277(4 Pt 2): p. H1593-9.**
- **Huang, C.S., et al., *Effects of the neuroprotective agent riluzole on the high voltage-activated calcium channels of rat dorsal root ganglion neurons.* J Pharmacol Exp Ther, 1997. 282(3): p. 1280-90.**
- **Hugon, J., J.M. Vallat, and M. Dumas, *[Role of glutamate and excitotoxicity in neurologic diseases].* Rev Neurol (Paris), 1996. 152(4): p. 239-48.**

- **Hume, R.I., R. Dingledine, and S.F. Heinemann, *Identification of a site in glutamate receptor subunits that controls calcium permeability.* Science, 1991. 253(5023): p. 1028-31.**
- **Ikeda, J., T. Kohriyama, and S. Nakamura, *Elevation of serum soluble E-selectin and antisulfoglucuronyl paragloboside antibodies in amyotrophic lateral sclerosis.* Eur J Neurol, 2000. 7(5): p. 541-7.**
- **Ikeda, K., et al., *Effects of brain-derived neurotrophic factor on motor dysfunction in wobbler mouse motor neuron disease.* Ann Neurol, 1995. 37(4): p. 505-11.**
- **Ikeda, K., et al., *Lecithinized superoxide dismutase retards wobbler mouse motoneuron disease.* Neuromuscul Disord, 1995. 5(5): p. 383-90.**
- **Ikeda, K., Y. Iwasaki, and M. Kinoshita, *JTP-2942, a novel thyrotropin-releasing hormone analogue, protects against spinal motor neuron degeneration in the wobbler mouse.* Neurosci Lett, 1998. 250(1): p. 9-12.**
- **Ince, P.G., J. Lowe, and P.J. Shaw, *Amyotrophic lateral sclerosis: current issues in classification, pathogenesis and molecular pathology.* Neuropathol Appl Neurobiol, 1998. 24(2): p. 104-17.**
- **Ishiyama, T., et al., *Methionine-free brain-derived neurotrophic factor in wobbler mouse motor neuron disease: dose-related effects and comparison with the methionyl form.* Brain Res, 2002. 944(1-2): p. 195-9.**
- **Iwasaki, Y., et al., *Trophic effect of various neuropeptides on the cultured ventral spinal cord of rat embryo.* Neurosci Lett, 1989. 101(3): p. 316-20.**
- **Jaarsma, D., et al., *Human Cu/Zn superoxide dismutase (SOD1) overexpression in mice causes mitochondrial vacuolization, axonal degeneration, and premature motoneuron death and accelerates motoneuron disease in mice expressing a familial amyotrophic lateral sclerosis mutant SOD1.* Neurobiol Dis, 2000. 7(6 Pt B): p. 623-43.**
- **Jablecki, C.K., C. Berry, and J. Leach, *Survival prediction in amyotrophic lateral sclerosis.* Muscle Nerve, 1989. 12(10): p. 833-41.**
- **Jacobson, L.O. and E. Goldwasser, *The dynamic equilibrium of erythropoiesis.* Brookhaven Symp Biol, 1957. 30(10): p. 110-31.**
- **Johnson, J.W. and P. Ascher, *Glycine potentiates the NMDA response in cultured mouse brain neurons.* Nature, 1987. 325(6104): p. 529-31.**
- **Jonas, P. and N. Burnashev, *Molecular mechanisms controlling calcium entry through AMPA-type glutamate receptor channels.* Neuron, 1995. 15(5): p. 987-90.**
- **Jordan, J., M.F. Galindo, and R.J. Miller, *Role of calpain- and interleukin-1 beta converting enzyme-like proteases in the beta-amyloid-induced death of rat hippocampal neurons in culture.* J Neurochem, 1997. 68(4): p. 1612-21.**

- **Julien, J.P. and J.M. Beaulieu, *Cytoskeletal abnormalities in amyotrophic lateral sclerosis: beneficial or detrimental effects?* J Neurol Sci, 2000. 180(1-2): p. 7-14.**
- **Jung, C., C.M. Higgins, and Z. Xu, *A quantitative histochemical assay for activities of mitochondrial electron transport chain complexes in mouse spinal cord sections.* J Neurosci Methods, 2002. 114(2): p. 165-72.**
- **Junier, M.P., et al., *Transforming growth factor alpha (TGF alpha) expression in degenerating motoneurons of the murine mutant wobbler: a neuronal signal for astrogliosis?* J Neurosci, 1994. 14(7): p. 4206-16.**
- **Jurand, A. and C. Pavan, *Ultrastructural aspects of histolytic processes in the salivary gland cells during metamorphic stages in Rhynchosciara hollaenderi (Diptera, Sciaridae).* Cell Differ, 1975. 4(4): p. 219-36.**
- **Kaal, E.C., E.A. Joosten, and P.R. Bar, *Prevention of apoptotic motoneuron death in vitro by neurotrophins and muscle extract.* Neurochem Int, 1997. 31(2): p. 193-201.**
- **Kaal, E.C., et al., *Cobalt prevents nitric oxide-induced apoptotic motoneuron death in vitro.* Neuroreport, 1999. 10(11): p. 2335-9.**
- **Kaiserlian, D., et al., *The wasted mutant mouse. II. Immunological abnormalities in a mouse described as a model of ataxia-telangiectasia.* Clin Exp Immunol, 1986. 63(3): p. 562-9.**
- **Kalra, S., D.L. Arnold, and N.R. Cashman, *Biological markers in the diagnosis and treatment of ALS.* J Neurol Sci, 1999. 165 Suppl 1: p. S27-32.**
- **Kanekura, K., et al., *Alsin, the product of ALS2 gene, suppresses SOD1 mutant neurotoxicity through RhoGEF domain by interacting with SOD1 mutants.* J Biol Chem, 2004. 279(18): p. 19247-56.**
- **Kapaki, E., et al., *Essential trace element alterations in amyotrophic lateral sclerosis.* J Neurol Sci, 1997. 147(2): p. 171-5.**
- **Kaspar, B.K., et al., *Retrograde viral delivery of IGF-1 prolongs survival in a mouse ALS model.* Science, 2003. 301(5634): p. 839-42.**
- **Kato, S., et al., *New consensus research on neuropathological aspects of familial amyotrophic lateral sclerosis with superoxide dismutase 1 (SOD1) gene mutations: inclusions containing SOD1 in neurons and astrocytes.* Amyotroph Lateral Scler Other Motor Neuron Disord, 2000. 1(3): p. 163-84.**
- **Katoh-Semba, R., et al., *Riluzole enhances expression of brain-derived neurotrophic factor with consequent proliferation of granule precursor cells in the rat hippocampus.* Faseb J, 2002. 16(10): p. 1328-30.**
- **Kaupmann, K., et al., *Wobbler, a mutation affecting motoneuron survival and gonadal functions in the mouse, maps to proximal chromosome 11.* Genomics, 1992. 13(1): p. 39-43.**

- **Kawakami, M., et al., *Erythropoietin receptor-mediated inhibition of exocytotic glutamate release confers neuroprotection during chemical ischemia.* J Biol Chem, 2001. 276(42): p. 39469-75.**
- **Kennel, P.F., et al., *Neuromuscular function impairment is not caused by motor neurone loss in FALS mice: an electromyographic study.* Neuroreport, 1996. 7(8): p. 1427-31.**
- **Kerr, I.M., E.A. Pratt, and I.R. Lehman, *Exonucleolytic degradation of high-molecular-weight DNA and RNA to nucleoside 3'-phosphates by a nuclease from B. subtilis.* Biochem Biophys Res Commun, 1965. 20(2): p. 154-62.**
- **Kerr, J.B., et al., *Ultrastructural analysis of the effect of ethane dimethanesulphonate on the testis of the rat, guinea pig, hamster and mouse.* Cell Tissue Res, 1987. 249(2): p. 451-7.**
- **Kerr, J.F., A.H. Wyllie, and A.R. Currie, *Apoptosis: a basic biological phenomenon with wide-ranging implications in tissue kinetics.* Br J Cancer, 1972. 26(4): p. 239-57.**
- **Kerr, J.F., B. Harmon, and J. Searle, *An electron-microscope study of cell deletion in the anuran tadpole tail during spontaneous metamorphosis with special reference to apoptosis of striated muscle fibers.* J Cell Sci, 1974. 14(3): p. 571-85.**
- **Kerr, J.F., *Shrinkage necrosis: a distinct mode of cellular death.* J Pathol, 1971. 105(1): p. 13-20.**
- **Kiernan, J.A. and A.J. Hudson, *Changes in sizes of cortical and lower motor neurons in amyotrophic lateral sclerosis.* Brain, 1991. 114 (Pt 2): p. 843-53.**
- **Kikuchi, S., et al., *Effect of geranylgeranylaceton on cellular damage induced by proteasome inhibition in cultured spinal neurons.* J Neurosci Res, 2002. 69(3): p. 373-81.**
- **Kim, S.U., *Neurobiology of human oligodendrocytes in culture.* J Neurosci Res, 1990. 27(4): p. 712-28.**
- **Kischkel, F.C., et al., *Cytotoxicity-dependent APO-1 (Fas/CD95)-associated proteins form a death-inducing signaling complex (DISC) with the receptor.* Embo J, 1995. 14(22): p. 5579-88.**
- **Klivenyi, P., et al., *Neuroprotective effects of creatine in a transgenic animal model of amyotrophic lateral sclerosis.* Nat Med, 1999. 5(3): p. 347-50.**
- **Kluck, R.M., et al., *The release of cytochrome c from mitochondria: a primary site for Bcl-2 regulation of apoptosis.* Science, 1997. 275(5303): p. 1132-6.**
- **Konishi, Y., et al., *Trophic effect of erythropoietin and other hematopoietic factors on central cholinergic neurons in vitro and in vivo.* Brain Res, 1993. 609(1-2): p. 29-35.**
- **Korthaus, D., et al., *The gene for cytoplasmatic malate dehydrogenase, Mor2, is closely linked to the wobbler spinal muscular atrophy gene (wr).* Mamm Genome, 1996. 7(3): p. 250.**

- **Kozachuk, W.E., et al., *Thyrotropin-releasing hormone (TRH) in murine motor neuron disease (the wobbler mouse).* J Neurol Sci, 1987. 78(3): p. 253-60.**
- **Kretschmer, B.D., U. Kratzer, and W.J. Schmidt, *Riluzole, a glutamate release inhibitor, and motor behavior.* Naunyn Schmiedebergs Arch Pharmacol, 1998. 358(2): p. 181-90.**
- **Krieger, C., et al., *Excitatory amino acid receptor antagonist in murine motoneuron disease (the wobbler mouse).* Can J Neurol Sci, 1992. 19(4): p. 462-5.**
- **Krieger, C., et al., *The wobbler mouse: amino acid contents in brain and spinal cord.* Brain Res, 1991. 551(1-2): p. 142-4.**
- **Kriz, J., G. Gowing, and J.P. Julien, *Efficient three-drug cocktail for disease induced by mutant superoxide dismutase.* Ann Neurol, 2003. 53(4): p. 429-36.**
- **Kurek, J.B., et al., *LIF (AM424), a promising growth factor for the treatment of ALS.* J Neurol Sci, 1998. 160 Suppl 1: p. S106-13.**
- **Kurosumi, K., U. Kurosumi, and K. Inoue, *Morphological and morphometric studies with the electron microscope on the Merkel cells and associated nerve terminals of normal and denervated skin.* Arch Histol JP, 1979. 42(3): p. 243-61.**
- **Laage, S., G. Zobel, and H. Jockusch, *Astrocyte overgrowth in the brain stem and spinal cord of mice affected by spinal atrophy, wobbler.* Dev Neurosci, 1988. 10(3): p. 190-8.**
- **Lacomblez, L., et al., *A double-blind, placebo-controlled trial of high doses of gangliosides in amyotrophic lateral sclerosis.* Neurology, 1989. 39(12): p. 1635-7.**
- **Lacomblez, L., et al., *Dose-ranging study of riluzole in amyotrophic lateral sclerosis. Amyotrophic Lateral Sclerosis/Riluzole Study Group II.* Lancet, 1996. 347(9013): p. 1425-31.**
- **Lai, E.C., et al., *Effect of recombinant human insulin-like growth factor-I on progression of ALS. A placebo-controlled study. The North America ALS/IGF-I Study Group.* Neurology, 1997. 49(6): p. 1621-30.**
- **Lange, D.J., et al., *Selegiline is ineffective in a collaborative double-blind, placebo-controlled trial for treatment of amyotrophic lateral sclerosis.* Arch Neurol, 1998. 55(1): p. 93-6.**
- **Langston, C.E., N.J. Reine, and D. Kittrell, *The use of erythropoietin.* Vet Clin North Am Small Anim Pract, 2003. 33(6): p. 1245-60.**
- **Lansbury, P.T., Jr. and K.S. Kosik, *Neurodegeneration: new clues on inclusions.* Chem Biol, 2000. 7(1): p. R9-R12.**
- **Laslo, P., et al., *GluR2 AMPA receptor subunit expression in motoneurons at low and high risk for degeneration in amyotrophic lateral sclerosis.* Exp Neurol, 2001. 169(2): p. 461-71.**

- **LaVail, J.H., E.H. Koo, and N.P. Dekker, *Motoneuron loss in the abducens nucleus of wobbler mice.* Brain Res, 1987. 404(1-2): p. 127-32.**
- **Lazebnik, Y.A., et al., *Cleavage of poly(ADP-ribose) polymerase by a proteinase with properties like ICE.* Nature, 1994. 371(6495): p. 346-7.**
- **Leigh, P.N., et al., *New aspects of the pathology of neurodegenerative disorders as revealed by ubiquitin antibodies.* Acta Neuropathol (Berl), 1989. 79(1): p. 61-72.**
- **Leigh, P.N., et al., *Ubiquitin-immunoreactive intraneuronal inclusions in amyotrophic lateral sclerosis. Morphology, distribution, and specificity.* Brain, 1991. 114 (Pt 2): p. 775-88.**
- **Leist, M., et al., *Caspase-mediated apoptosis in neuronal excitotoxicity triggered by nitric oxide.* Mol Med, 1997. 3(11): p. 750-64.**
- **Levi-Montalcini, R., *The nerve growth factor 35 years later.* Science, 1987. 237(4819): p. 1154-62.**
- **Lewkowicz, S.J., *The relationship of Schwann cell migration in vitro to injury, using normal, Wobbler, and dystrophic mice.* Brain Res, 1979. 169(3): p. 443-54.**
- **Li, A.H., et al., *Amyotrophic lateral sclerosis with a 'pseudo-infarction' pattern on the electrocardiograph. A case report.* Cardiology, 2000. 93(1-2): p. 133-6.**
- **Li, H., et al., *Activation of caspase-2 in apoptosis.* J Biol Chem, 1997. 272(34): p. 21010-7.**
- **Li, X.Y., et al., *Aqueous humor-borne factor upregulates Bcl-2 expression in corneal endothelial cells.* Curr Eye Res, 1998. 17(10): p. 970-8.**
- **Libertin, C.R., et al., *Subnormal albumin gene expression is associated with weight loss in immunodeficient/DNA-repair-impaired wasted mice.* J Am Coll Nutr, 1994. 13(2): p. 149-53.**
- **Lin, C.L., et al., *Improved anemia and reduced erythropoietin need by medical or surgical intervention of secondary hyperparathyroidism in hemodialysis patients.* Ren Fail, 2004. 26(3): p. 289-95.**
- **Lisovoski, F., et al., *Transforming growth factor alpha expression as a response of murine motor neurons to axonal injury and mutation-induced degeneration.* J Neuropathol Exp Neurol, 1997. 56(5): p. 459-71.**
- **Liu, Q.A. and M.O. Hengartner, *The molecular mechanism of programmed cell death in C. elegans.* Ann N Y Acad Sci, 1999. 887: p. 92-104.**
- **Liu, X., et al., *Extracellular matrix of retinal pigment epithelium regulates choriocapillaris endothelial survival in vitro.* Exp Eye Res, 1997. 65(1): p. 117-26.**
- **Liu, X., et al., *Induction of apoptotic program in cell-free extracts: requirement for dATP and cytochrome c.* Cell, 1996. 86(1): p. 147-57.**

- **Louwerse, E.S., et al., *Randomized, double-blind, controlled trial of acetylcysteine in amyotrophic lateral sclerosis.* Arch Neurol, 1995. 52(6): p. 559-64.**
- **Lucas, R.L. and A.K. Salm, *Astroglia proliferate in response to oxytocin and vasopressin.* Brain Res, 1995. 681(1-2): p. 218-22.**
- **Lukes, A., et al., *Extracellular matrix degradation by metalloproteinases and central nervous system diseases.* Mol Neurobiol, 1999. 19(3): p. 267-84.**
- **Lund, P.K., et al., *Somatomedin-C/insulin-like growth factor-I and insulin-like growth factor-II mRNAs in rat fetal and adult tissues.* J Biol Chem, 1986. 261(31): p. 14539-**

  Bothwell, M., *Insulin and somatemedin MSA promote nerve growth factor-independent neurite formation by cultured chick dorsal root ganglionic sensory neurons.* J Neurosci Res, 1982. 8(2-3): p. 225-31.
- **Luo, X., et al., *Bid, a Bcl2 interacting protein, mediates cytochrome c release from mitochondria in response to activation of cell surface death receptors.* Cell, 1998. 94(4): p. 481-90.**
- **Lutsep, H.L. and M. Rodriguez, *Ultrastructural, morphometric, and immunocytochemical study of anterior horn cells in mice with "wasted" mutation.* J Neuropathol Exp Neurol, 1989. 48(5): p. 519-33.**
- **MacFarlane, M., et al., *Active caspases and cleaved cytokeratins are sequestered into cytoplasmic inclusions in TRAIL-induced apoptosis.* J Cell Biol, 2000. 148(6): p. 1239-**

  54.
- **MacGibbon, G.A., et al., *Bax expression in mammalian neurons undergoing apoptosis, and in Alzheimer's disease hippocampus.* Brain Res, 1997. 750(1-2): p. 223-34.**
- **Magal, E., P. Burnham, and S. Varon, *Effects of ciliary neuronotrophic factor on rat spinal cord neurons in vitro: survival and expression of choline acetyltransferase and low-affinity nerve growth factor receptors.* Brain Res Dev Brain Res, 1991. 63(1-2): p. 141-50.**
- **Maher, T.J. and R.J. Wurtman, *L-Threonine administration increases glycine concentrations in the rat central nervous system.* Life Sci, 1980. 26(16): p. 1283-6.**
- **Manetto, V., et al., *Phosphorylation of neurofilaments is altered in amyotrophic lateral sclerosis.* J Neuropathol Exp Neurol, 1988. 47(6): p. 642-53.**
- **Marti, H.H., *Erythropoietin and the hypoxic brain.* J Exp Biol, 2004. 207(Pt 18): p. 3233-42.**
- **Martin, D., M.A. Thompson, and J.V. Nadler, *The neuroprotective agent riluzole inhibits release of glutamate and aspartate from slices of hippocampal area CA1.* Eur J Pharmacol, 1993. 250(3): p. 473-6.**

- **Martin, L.J., *Neuronal death in amyotrophic lateral sclerosis is apoptosis: possible contribution of a programmed cell death mechanism.* J Neuropathol Exp Neurol, 1999. 58(5): p. 459-71.**
- **Martin, S.J., et al., *Phosphatidylserine externalization during CD95-induced apoptosis of cells and cytoplasts requires ICE/CED-3 protease activity.* J Biol Chem, 1996. 271(46): p. 28753-6.**
- **Martinez-Estrada, O.M., et al., *Erythropoietin protects the in vitro blood-brain barrier against VEGF-induced permeability.* Eur J Neurosci, 2003. 18(9): p. 2538-44.**
- **Mazurkiewicz, J.E., *Ubiquitin deposits are present in spinal motor neurons in all stages of the disease in the motor neuron degeneration (Mnd) mutant of the mouse.* Neurosci Lett, 1991. 128(2): p. 182-6.**
- **Meier, P. and G. Evan, *Dying like flies.* Cell, 1998. 95(3): p. 295-8.**
- **Mendell, J.R., T.N. Chase, and W.K. Engel, *Amyotrophic lateral sclerosis. A study of central monoamine metabolism and therapeutic trial of levodopa.* Arch Neurol, 1971. 25(4): p. 320-5.**
- **Mennini, T., et al., *Biochemical and pharmacological evidence of a functional role of AMPA receptors in motor neuron dysfunction in mnd mice.* Eur J Neurosci, 1999. 11(5): p. 1705-10.**
- **Mennini, T., et al., *Expression of glutamate receptor subtypes in the spinal cord of control and mnd mice, a model of motor neuron disorder.* J Neurosci Res, 2002. 70(4): p. 553-60.**
- **Mennini, T., et al., *Glial activation and TNFR-I upregulation precedes motor dysfunction in the spinal cord of mnd mice.* Cytokine, 2004. 25(3): p. 127-35.**
- **Messer, A. and J. Plummer, *Accumulating autofluorescent material as a marker for early changes in the spinal cord of the Mnd mouse.* Neuromuscul Disord, 1993. 3(2): p. 129-34.**
- **Messer, A., et al., *Mapping of the motor neuron degeneration (Mnd) gene, a mouse model of amyotrophic lateral sclerosis (ALS).* Genomics, 1992. 13(3): p. 797-802.**
- **Messer, A., *Mutant mouse models of ALS.* Neurobiol Aging, 1994. 15(2): p. 247-8.**
- **Meucci, N., E. Nobile-Orazio, and G. Scarlato, *Intravenous immunoglobulin therapy in amyotrophic lateral sclerosis.* J Neurol, 1996. 243(2): p. 117-20.**
- **Migheli, A., et al., *A study of apoptosis in normal and pathologic nervous tissue after in situ end-labeling of DNA strand breaks.* J Neuropathol Exp Neurol, 1994. 53(6): p. 606-16.**
- **Migheli, A., et al., *Lack of apoptosis in mice with ALS.* Nat Med, 1999. 5(9): p. 966-7.**
- **Migheli, A., et al., *Peripherin immunoreactive structures in amyotrophic lateral sclerosis.* Lab Invest, 1993. 68(2): p. 185-91.**

- **Migheli, A., et al., *S-100beta protein is upregulated in astrocytes and motor neurons in the spinal cord of patients with amyotrophic lateral sclerosis.* Neurosci Lett, 1999. 261(1-2): p. 25-8.**
- **Mignotte, B. and J.L. Vayssiere, *Mitochondria and apoptosis.* Eur J Biochem, 1998. 252(1): p. 1-15.**
- **Miller, R.G., et al., *Consensus guidelines for the design and implementation of clinical trials in ALS. World Federation of Neurology committee on Research.* J Neurol Sci, 1999. 169(1-2): p. 2-12.**
- **Miller, R.G., et al., *Placebo-controlled trial of gabapentin in patients with amyotrophic lateral sclerosis. WALS Study Group. Western Amyotrophic Lateral Sclerosis Study Group.* Neurology, 1996. 47(6): p. 1383-8.**
- **Miller, R.G., et al., *Riluzole for amyotrophic lateral sclerosis (ALS)/motor neuron disease (MND).* Amyotroph Lateral Scler Other Motor Neuron Disord, 2003. 4(3): p. 191-206.**
- **Miller, R.G., J.D. Mitchell, and D.H. Moore, *Riluzole for amyotrophic lateral sclerosis (ALS)/motor neuron disease (MND).* Cochrane Database Syst Rev, 2001(4): p. CD001447.**
- **Mitchell, I.J., et al., *Glutamate-induced apoptosis results in a loss of striatal neurons in the parkinsonian rat.* Neuroscience, 1994. 63(1): p. 1-5.**
- **Mitsumoto, H. and K. Tsuzaka, *Neurotrophic factors and neuro-muscular disease: II. GDNF, other neurotrophic factors, and future directions.* Muscle Nerve, 1999. 22(8): p. 1000-21.**
- **Mitsumoto, H. and R.K. Olney, *Drug combination treatment in patients with ALS: current status and future directions.* Neurology, 1996. 47(4 Suppl 2): p. S103-7.**
- **Mitsumoto, H. and W.G. Bradley, *Murine motor neuron disease (the wobbler mouse): degeneration and regeneration of the lower motor neuron.* Brain, 1982. 105 (Pt 4): p. 811-34.**
- **Mitsumoto, H., et al., *Arrest of motor neuron disease in wobbler mice cotreated with CNTF and BDNF.* Science, 1994. 265(5175): p. 1107-10.**
- **Mitsumoto, H., et al., *Effects of cardiotrophin-1 (CT-1) in a mouse motor neuron disease.* Muscle Nerve, 2001. 24(6): p. 769-77.**
- **Mitsumoto, H., et al., *Histometric characteristics and regenerative capacity in wobbler mouse motor neuron disease.* Brain, 1990. 113 (Pt 2): p. 497-507.**
- **Mitsumoto, H., et al., *Motor neuron disease and adult hexosaminidase A deficiency in two families: evidence for multisystem degeneration.* Ann Neurol, 1985. 17(4): p. 378-85.**
- **Mitsumoto, H., et al., *The effects of ciliary neurotrophic factor on motor dysfunction in wobbler mouse motor neuron disease.* Ann Neurol, 1994. 36(2): p. 142-8.**

- Mizuta, I., et al., *Riluzole stimulates nerve growth factor, brain-derived neurotrophic factor and glial cell line-derived neurotrophic factor synthesis in cultured mouse astrocytes.* Neurosci Lett, 2001. 310(2-3): p. 117-20.
- Mochizuki, H., et al., *Histochemical detection of apoptosis in Parkinson's disease.* J Neurol Sci, 1996. 137(2): p. 120-3.
- Mochizuki, H., et al., *Iron accumulation in the substantia nigra of 1-methyl-4-phenyl-1,2,3,6-tetrahydropyridine (MPTP)-induced hemiparkinsonian monkeys.* Neurosci Lett, 1994. 168(1-2): p. 251-3.
- Mora, J.S., et al., *Intrathecal administration of natural human interferon alpha in amyotrophic lateral sclerosis.* Neurology, 1986. 36(8): p. 1137-40.
- Morris, H.R., et al., *A clinical and pathological study of motor neurone disease on Guam.* Brain, 2001. 124(Pt 11): p. 2215-22.
- Mottet, N.K. and S.P. Hammar, *Ribosome crystals in necrotizing cells from the posterior necrotic zone of the developing chick limb.* J Cell Sci, 1972. 11(2): p. 403-14.
- Mu, X., et al., *Altered expression of bcl-2 and bax mRNA in amyotrophic lateral sclerosis spinal cord motor neurons.* Ann Neurol, 1996. 40(3): p. 379-86.
- Mulder, D.W., et al., *Motor neuron disease (ALS): evaluation of detection thresholds of cutaneous sensation.* Neurology, 1983. 33(12): p. 1625-7.
- Muller, W.E., et al., *gp120 of HIV-1 induces apoptosis in rat cortical cell cultures: prevention by memantine.* Eur J Pharmacol, 1992. 226(3): p. 209-14.
- Munsat, T.L., et al., *Intrathecal thyrotropin-releasing hormone does not alter the progressive course of ALS: experience with an intrathecal drug delivery system.* Neurology, 1992. 42(5): p. 1049-53.
- Munsat, T.L., et al., *The natural history of motoneuron loss in amyotrophic lateral sclerosis.* Neurology, 1988. 38(3): p. 409-13.
- Murakami, T., *Motor neuron disease: quantitative morphological and microdensitophotometric studies of neurons of anterior horn and ventral root of cervical spinal cord with special reference to the pathogenesis.* J Neurol Sci, 1990. 99(1): p. 101-15.
- Mutoh, T., et al., *Decreased phosphorylation levels of TrkB neurotrophin receptor in the spinal cords from patients with amyotrophic lateral sclerosis.* Neurochem Res, 2000. 25(2): p. 239-45.
- Nath, K.A., et al., *Renal oxidant injury and oxidant response induced by mercury.* Kidney Int, 1996. 50(3): p. 1032-43.
- Neame, S.J., L.L. Rubin, and K.L. Philpott, *Blocking cytochrome c activity within intact neurons inhibits apoptosis.* J Cell Biol, 1998. 142(6): p. 1583-93.

- **Newmeyer, D.D., D.M. Farschon, and J.C. Reed, *Cell-free apoptosis in Xenopus egg extracts: inhibition by Bcl-2 and requirement for an organelle fraction enriched in mitochondria.* Cell, 1994. 79(2): p. 353-64.**
- **Newton, K. and A. Strasser, *The Bcl-2 family and cell death regulation.* Curr Opin Genet Dev, 1998. 8(1): p. 68-75.**
- **Nichols, A., et al., *The p75 neurotrophin receptor: effects on neuron survival in vitro and interaction with death domain-containing adaptor proteins.* Apoptosis, 1998. 3(4): p. 289-94.**
- **Nicholson, D.W., et al., *Identification and inhibition of the ICE/CED-3 protease necessary for mammalian apoptosis.* Nature, 1995. 376(6535): p. 37-43.**
- **Nicotera, P., et al., *Neuronal necrosis and apoptosis: two distinct events induced by exposure to glutamate or oxidative stress.* Adv Neurol, 1997. 72: p. 95-101.**
- **Nissenson, A.R., *Epoetin and cognitive function.* Am J Kidney Dis, 1992. 20(1 Suppl 1): p. 21-4.**
- **Noda, K., et al., *Decrease of neurons in the medullary arcuate nucleus of multiple system atrophy: quantitative comparison with Parkinson's disease and amyotrophic lateral sclerosis.* J Neurol Sci, 1997. 151(1): p. 89-91.**
- **Noh, K.M., et al., *A novel neuroprotective mechanism of riluzole: direct inhibition of protein kinase C.* Neurobiol Dis, 2000. 7(4): p. 375-83.**
- **Norris, F.H., et al., *Trial of oral physostigmine in amyotrophic lateral sclerosis.* Clin Pharmacol Ther, 1993. 54(6): p. 680-2.**
- **Nowicki, M., *Erythropoietin and hypertension.* J Hum Hypertens, 1995. 9(2): p. 81-8.**
- **O'Connor, T.M. and C.R. Wyttenbach, *Cell death in the embryonic chick spinal cord.* J Cell Biol, 1974. 60(2): p. 448-59.**
- **Okamoto, K., et al., *New ubiquitin-positive intraneuronal inclusions in the extra-motor cortices in patients with amyotrophic lateral sclerosis.* Neurosci Lett, 1991. 129(2): p. 233-6.**
- **Olson, W.H., J.A. Simons, and G.W. Halaas, *Therapeutic trial of tilorone in ALS: lack of benefit in a double-blind, placebo-controlled study.* Neurology, 1978. 28(12): p. 1293-5.**
- **Ono, S., et al., *Decrease in the ciliary neurotrophic factor of the spinal cord in amyotrophic lateral sclerosis.* Eur Neurol, 1999. 42(3): p. 163-8.**
- **Oppenheim, R.W., I.W. Chu-Wang, and R.F. Foelix, *Some aspects of synaptogenesis in the spinal cord of the chick embryo: a quantitative electron microscopic study.* J Comp Neurol, 1975. 161(3): p. 383-418.**
- **Orrenius, S. and P. Nicotera, *The calcium ion and cell death.* J Neural Transm Suppl, 1994. 43: p. 1-11.**

- **Oteiza, P.I., et al., *Evaluation of antioxidants, protein, and lipid oxidation products in blood from sporadic amyotrophic lateral sclerosis patients.* Neurochem Res, 1997. 22(4): p. 535-9.**
- **Pan, G., E.W. Humke, and V.M. Dixit, *Activation of caspases triggered by cytochrome c in vitro.* FEBS Lett, 1998. 426(1): p. 151-4.**
- **Pardo, C.A., et al., *Accumulation of the adenosine triphosphate synthase subunit C in the mnd mutant mouse. A model for neuronal ceroid lipofuscinosis.* Am J Pathol, 1994. 144(4): p. 829-35.**
- **Parpura, V., et al., *Glutamate-mediated astrocyte-neuron signalling.* Nature, 1994. 369(6483): p. 744-7.**
- **Pasinelli, P., et al., *Amyotrophic lateral sclerosis-associated SOD1 mutant proteins bind and aggregate with Bcl-2 in spinal cord mitochondria.* Neuron, 2004. 43(1): p. 19-30.**
- **Pasti, L., et al., *Intracellular calcium oscillations in astrocytes: a highly plastic, bidirectional form of communication between neurons and astrocytes in situ.* J Neurosci, 1997. 17(20): p. 7817-30.**
- **Pelagi, M., et al., *Caspase inhibition reveals functional cooperation between p55- and p75-TNF receptors in cell necrosis.* Eur Cytokine Netw, 2000. 11(4): p. 580-8.**
- **Pellegrini-Giampietro, D.E., et al., *Switch in glutamate receptor subunit gene expression in CA1 subfield of hippocampus following global ischemia in rats.* Proc Natl Acad Sci U S A, 1992. 89(21): p. 10499-503.**
- **Pellegrini-Giampietro, D.E., et al., *The GluR2 (GluR-B) hypothesis: Ca(2+)-permeable AMPA receptors in neurological disorders.* Trends Neurosci, 1997. 20(10): p. 464-70.**
- **Peluffo, H., et al., *Riluzole promotes survival of rat motoneurons in vitro by stimulating trophic activity produced by spinal astrocyte monolayers.* Neurosci Lett, 1997. 228(3): p. 207-11.**
- **Penn, R.D., et al., *Intrathecal ciliary neurotrophic factor delivery for treatment of amyotrophic lateral sclerosis (phase I trial).* Neurosurgery, 1997. 40(1): p. 94-9; discussion 99-100.**
- **Pernas-Alonso, R., et al., *Early upregulation of medium neurofilament gene expression in developing spinal cord of the wobbler mouse mutant.* Brain Res Mol Brain Res, 1996. 38(2): p. 267-75.**
- **Perry, T.L., S. Hansen, and K. Jones, *Brain glutamate deficiency in amyotrophic lateral sclerosis.* Neurology, 1987. 37(12): p. 1845-8.**
- **Peterson, G.L., *A simplification of the protein assay method of Lowry et al. which is more generally applicable.* Anal Biochem, 1977. 83(2): p. 346-56.**

- **Petralia, R.S., et al., *Glutamate receptor subunit 2-selective antibody shows a differential distribution of calcium-impermeable AMPA receptors among populations of neurons.* J Comp Neurol, 1997. 385(3): p. 456-76.**
- **Pilar, G. and L. Landmesser, *Ultrastructural differences during embryonic cell death in normal and peripherally deprived ciliary ganglia.* J Cell Biol, 1976. 68(2): p. 339-56.**
- **Pioro, E.P. and H. Mitsumoto, *Animal models of ALS.* Clin Neurosci, 1995. 3(6): p. 375-85.**
- **Pioro, E.P., et al., *Neuronal pathology in the wobbler mouse brain revealed by in vivo proton magnetic resonance spectroscopy and immunocytochemistry.* Neuroreport, 1998. 9(13): p. 3041-6.**
- **Plaitakis, A. and J.T. Caroscio, *Abnormal glutamate metabolism in amyotrophic lateral sclerosis.* Ann Neurol, 1987. 22(5): p. 575-9.**
- **Pollard, H., et al., *Alterations of the GluR-B AMPA receptor subunit flip/flop expression in kainate-induced epilepsy and ischemia.* Neuroscience, 1993. 57(3): p. 545-54.**
- **Pollin, M.M., S. McHanwell, and C.R. Slater, *Loss of motor neurons from the median nerve motor nucleus of the mutant mouse 'wobbler'.* J Neurocytol, 1990. 19(1): p. 29-38.**
- **Poloni, M., et al., *Circulating levels of tumour necrosis factor-alpha and its soluble receptors are increased in the blood of patients with amyotrophic lateral sclerosis.* Neurosci Lett, 2000. 287(3): p. 211-4.**
- **Popper, P., et al., *TRPM-2 expression and tunel staining in neurodegenerative diseases: studies in wobbler and rd mice.* Exp Neurol, 1997. 143(2): p. 246-54.**
- **Porter, R.H., R.S. Briggs, and P.J. Roberts, *L-aspartate-beta-hydroxamate exhibits mixed agonist/antagonist activity at the glutamate metabotropic receptor in rat neonatal cerebrocortial slices.* Neurosci Lett, 1992. 144(1-2): p. 87-9.**
- **Portera-Cailliau, C., D.L. Price, and L.J. Martin, *N-methyl-D-aspartate receptor proteins NR2A and NR2B are differentially distributed in the developing rat central nervous system as revealed by subunit-specific antibodies.* J Neurochem, 1996. 66(2): p. 692-700.**
- **Pratt, J., et al., *Neuroprotective actions of riluzole in rodent models of global and focal cerebral ischaemia.* Neurosci Lett, 1992. 140(2): p. 225-30.**
- **Price, D.L. and S.S. Sisodia, *Cellular and molecular biology of Alzheimer's disease and animal models.* Annu Rev Med, 1994. 45: p. 435-46.**
- **Prince, H.K., et al., *Down-regulation of AMPA receptor subunit GluR2 in amygdaloid kindling.* J Neurochem, 1995. 64(1): p. 462-5.**
- **Provinciali, L. and A.R. Giovagnoli, *Antecedent events in amyotrophic lateral sclerosis: do they influence clinical onset and progression?* Neuroepidemiology, 1990. 9(5): p. 255-62.**

- **Pruss, R.M., et al., *Agonist-activated cobalt uptake identifies divalent cation-permeable kainate receptors on neurons and glial cells.* Neuron, 1991. 7(3): p. 509-18.**
- **Putcha, G.V. and E.M. Johnson, Jr., *Men are but worms: neuronal cell death in C elegans and vertebrates.* Cell Death Differ, 2004. 11(1): p. 38-48.**
- **Rabizadeh, S., et al., *Mutations associated with amyotrophic lateral sclerosis convert superoxide dismutase from an antiapoptotic gene to a proapoptotic gene: studies in yeast and neural cells.* Proc Natl Acad Sci U S A, 1995. 92(7): p. 3024-8.**
- **Raivich, G., et al., *Neuroglial activation repertoire in the injured brain: graded response, molecular mechanisms and cues to physiological function.* Brain Res Brain Res Rev, 1999. 30(1): p. 77-105.**
- **Raman, I.M., S. Zhang, and L.O. Trussell, *Pathway-specific variants of AMPA receptors and their contribution to neuronal signaling.* J Neurosci, 1994. 14(8): p. 4998-5010.**
- **Raoul, C., et al., *Motoneuron death triggered by a specific pathway downstream of Fas. potentiation by ALS-linked SOD1 mutations.* Neuron, 2002. 35(6): p. 1067-83.**
- **Rathke-Hartlieb, S., et al., *Elevated expression of membrane type 1 metalloproteinase (MT1-MMP) in reactive astrocytes following neurodegeneration in mouse central nervous system.* FEBS Lett, 2000. 481(3): p. 227-34.**
- **Rathke-Hartlieb, S., et al., *Spatiotemporal progression of neurodegeneration and glia activation in the wobbler neuropathy of the mouse.* Neuroreport, 1999. 10(16): p. 3411-6.**
- **Ratovitski, E.A., et al., *Midkine induces tumor cell proliferation and binds to a high affinity signaling receptor associated with JAK tyrosine kinases.* J Biol Chem, 1998. 273(6): p. 3654-60.**
- **Recio-Pinto, E., M.M. Rechler, and D.N. Ishii, *Effects of insulin, insulin-like growth factor-II, and nerve growth factor on neurite formation and survival in cultured sympathetic and sensory neurons.* J Neurosci, 1986. 6(5): p. 1211-9.**
- **Reed, J.C., *Mechanisms of apoptosis.* Am J Pathol, 2000. 157(5): p. 1415-30.**
- **Resch, K., et al., *Homology between human chromosome 2p13.3 and the wobbler critical region on mouse chromosome 11: comparative high-resolution mapping of STS and EST loci on YAC/BAC contigs.* Mamm Genome, 1998. 9(11): p. 893-8.**
- **Ripps, M.E., et al., *Transgenic mice expressing an altered murine superoxide dismutase gene provide an animal model of amyotrophic lateral sclerosis.* Proc Natl Acad Sci U S A, 1995. 92(3): p. 689-93.**
- **Rivera, V.M., et al., *Modified snake venom in amyotrophic lateral sclerosis. Lack of clinical effectiveness.* Arch Neurol, 1980. 37(4): p. 201-3.**

- **Riviere, M., et al., *An analysis of extended survival in patients with amyotrophic lateral sclerosis treated with riluzole.* Arch Neurol, 1998. 55(4): p. 526-8.**
- **Rosen, D.R., et al., *Mutations in Cu/Zn superoxide dismutase gene are associated with familial amyotrophic lateral sclerosis.* Nature, 1993. 362(6415): p. 59-62.**
- **Ross, C.A. and M.A. Poirier, *Protein aggregation and neurodegenerative disease.* Nat Med, 2004. 10 Suppl: p. S10-7.**
- **Roth, K.A. and C. D'Sa, *Apoptosis and brain development.* Ment Retard Dev Disabil Res Rev, 2001. 7(4): p. 261-6.**
- **Rothstein, J.D., et al., *Abnormal excitatory amino acid metabolism in amyotrophic lateral sclerosis.* Ann Neurol, 1990. 28(1): p. 18-25.**
- **Rothstein, J.D., et al., *Chronic inhibition of glutamate uptake produces a model of slow neurotoxicity.* Proc Natl Acad Sci U S A, 1993. 90(14): p. 6591-5.**
- **Rothstein, J.D., et al., *Localization of neuronal and glial glutamate transporters.* Neuron, 1994. 13(3): p. 713-25.**
- **Rothstein, J.D., et al., *Selective loss of glial glutamate transporter GLT-1 in amyotrophic lateral sclerosis.* Ann Neurol, 1995. 38(1): p. 73-84.**
- **Rothstein, J.D., *Excitotoxicity hypothesis.* Neurology, 1996. 47(4 Suppl 2): p. S19-25.**
- **Rothstein, J.D., L.J. Martin, and R.W. Kuncl, *Decreased glutamate transport by the brain and spinal cord in amyotrophic lateral sclerosis.* N Engl J Med, 1992. 326(22): p. 1464-8.**
- **Rouleau, G.A., et al., *SOD1 mutation is associated with accumulation of neurofilaments in amyotrophic lateral sclerosis.* Ann Neurol, 1996. 39(1): p. 128-31.**
- **Rowland, L.P., *Diagnosis of amyotrophic lateral sclerosis.* J Neurol Sci, 1998. 160 Suppl 1: p. S6-24.**
- **Rowland, L.P., *Ten central themes in a decade of ALS research.* Adv Neurol, 1991. 56: p. 3-23.**
- **Ruscher, K., et al., *Erythropoietin is a paracrine mediator of ischemic tolerance in the brain: evidence from an in vitro model.* J Neurosci, 2002. 22(23): p. 10291-301.**
- **Sadamoto, Y., et al., *Erythropoietin prevents place navigation disability and cortical infarction in rats with permanent occlusion of the middle cerebral artery.* Biochem Biophys Res Commun, 1998. 253(1): p. 26-32.**
- **Sagot, Y., et al., *Polymer encapsulated cell lines genetically engineered to release ciliary neurotrophic factor can slow down progressive motor neuronopathy in the mouse.* Eur J Neurosci, 1995. 7(6): p. 1313-22.**
- **Sahara, S., Y. Eguchi, and Y. Tsujimoto, *[Apoptotic signal transduction from cytosol to nucleus].* Tanpakushitsu Kakusan Koso, 1999. 44(12 Suppl): p. 1907-13.**

- **Sakahira, H., M. Enari, and S. Nagata, *Cleavage of CAD inhibitor in CAD activation and DNA degradation during apoptosis.* Nature, 1998. 391(6662): p. 96-9.**
- **Salcedo, R.M., B.W. Festoff, and B.A. Citron, *Quantitative reverse transcriptase PCR to gauge increased protease-activated receptor 1 (PAR-1) mRNA copy numbers in the Wobbler mutant mouse.* J Mol Neurosci, 1998. 10(2): p. 113-9.**
- **Sanchez, I. and J. Yuan, *A convoluted way to die.* Neuron, 2001. 29(3): p. 563-6.**
- **Sanchez-Alcazar, J.A., A. Khodjakov, and E. Schneider, *Anticancer drugs induce increased mitochondrial cytochrome c expression that precedes cell death.* Cancer Res, 2001. 61(3): p. 1038-44.**
- **Sartorius, U., I. Schmitz, and P.H. Krammer, *Molecular mechanisms of death-receptor-mediated apoptosis.* Chembiochem, 2001. 2(1): p. 20-9.**
- **Sasaki, C., et al., *Temporal profile of cytochrome c and caspase-3 immunoreactivities and TUNEL staining after permanent middle cerebral artery occlusion in rats.* Neurol Res, 2000. 22(2): p. 223-8.**
- **Sasaki, S., et al., *iNOS and nitrotyrosine immunoreactivity in amyotrophic lateral sclerosis.* Neurosci Lett, 2000. 291(1): p. 44-8.**
- **Sastry, P.S. and K.S. Rao, *Apoptosis and the nervous system.* J Neurochem, 2000. 74(1): p. 1-20.**
- **Saunders, J.W., Jr., *Death in embryonic systems.* Science, 1966. 154(749): p. 604-12.**
- **Schlomann, U., et al., *Tumor necrosis factor alpha induces a metalloprotease-disintegrin, ADAM8 (CD 156): implications for neuron-glia interactions during neurodegeneration.* J Neurosci, 2000. 20(21): p. 7964-71.**
- **Schmalbruch, H., W.S. al-Amood, and D.M. Lewis, *Morphology of long-term denervated rat soleus muscle and the effect of chronic electrical stimulation.* J Physiol, 1991. 441: p. 233-41.**
- **Schnaar, R.I. and A.E. Schaffner, *Separation of cell types from embryonic chicken and rat spinal cord: characterization of motoneuron-enriched fractions.* J Neurosci, 1981. 1(2): p. 204-17.**
- **Schumacher, M., et al., *Local synthesis and dual actions of progesterone in the nervous system: neuroprotection and myelination.* Growth Horm IGF Res, 2004. 14 Suppl A: p. S18-33.**
- **Schweichel, J.U. and H.J. Merker, *The morphology of various types of cell death in prenatal tissues.* Teratology, 1973. 7(3): p. 253-66.**
- **Schweichel, J.U., *[Electron microscopic studies on the degradation of the apical ridge during the development of limbs in rat embryos].* Z Anat Entwicklungsgesch, 1972. 136(2): p. 192-203.**

- **Semenza, G.L., et al., *Cell-type-specific and hypoxia-inducible expression of the human erythropoietin gene in transgenic mice.* Proc Natl Acad Sci U S A, 1991. 88(19): p. 8725-9.**
- **Shaw, P.J. and P.G. Ince, *Glutamate, excitotoxicity and amyotrophic lateral sclerosis.* J Neurol, 1997. 244 Suppl 2: p. S3-14.**
- **Shaw, P.J., et al., *CSF and plasma amino acid levels in motor neuron disease: elevation of CSF glutamate in a subset of patients.* Neurodegeneration, 1995. 4(2): p. 209-16.**
- **Shea, T.B., C. Jung, and H.C. Pant, *Does neurofilament phosphorylation regulate axonal transport?* Trends Neurosci, 2003. 26(8): p. 397-400.**
- **Shi, L., et al., *Premature p34cdc2 activation required for apoptosis.* Science, 1994. 263(5150): p. 1143-5.**
- **Siddique, T., et al., *A molecular genetic approach to amyotrophic lateral sclerosis.* Int J Neurol, 1991. 25-26: p. 60-9.**
- **Siegel, R.M., et al., *Fas preassociation required for apoptosis signaling and dominant inhibition by pathogenic mutations.* Science, 2000. 288(5475): p. 2354-7.**
- **Silva, M., et al., *Erythropoietin can promote erythroid progenitor survival by repressing apoptosis through Bcl-XL and Bcl-2.* Blood, 1996. 88(5): p. 1576-82.**
- **Sinor, A.D. and D.A. Greenberg, *Erythropoietin protects cultured cortical neurons, but not astroglia, from hypoxia and AMPA toxicity.* Neurosci Lett, 2000. 290(3): p. 213-5.**
- **Siren, A.L., et al., *Erythropoietin prevents neuronal apoptosis after cerebral ischemia and metabolic stress.* Proc Natl Acad Sci U S A, 2001. 98(7): p. 4044-9.**
- **Slee, E.A., et al., *Ordering the cytochrome c-initiated caspase cascade: hierarchical activation of caspases-2, -3, -6, -7, -8, and -10 in a caspase-9-dependent manner.* J Cell Biol, 1999. 144(2): p. 281-92.**
- **Sloviter, R.S., *Apoptosis: a guide for the perplexed.* Trends Pharmacol Sci, 2002. 23(1): p. 19-24.**
- **Smith, J.P., et al., *Quantitative measurement of muscle strength in the mouse.* J Neurosci Methods, 1995. 62(1-2): p. 15-9.**
- **Smith, K.J., et al., *The cardiovascular effects of erythropoietin.* Cardiovasc Res, 2003. 59(3): p. 538-48.**
- **Snow, R.J., et al., *Creatine supplementation and riluzole treatment provide similar beneficial effects in copper, zinc superoxide dismutase (G93A) transgenic mice.* Neuroscience, 2003. 119(3): p. 661-7.**
- **Sommer, B., et al., *RNA editing in brain controls a determinant of ion flow in glutamate-gated channels.* Cell, 1991. 67(1): p. 11-9.**
- **Stadelman, C., et al., *Expression of cell death-associated proteins in neuronal apoptosis associated with pontosubicular neuron necrosis.* Brain Pathol, 2001. 11(3): p. 273-81.**

- Stanger, B.Z., et al., *RIP: a novel protein containing a death domain that interacts with Fas/APO-1 (CD95) in yeast and causes cell death.* Cell, 1995. 81(4): p. 513-23.
- Steinberg, G.K., et al., *Dextromethorphan alters cerebral blood flow and protects against cerebral injury following focal ischemia.* Neurosci Lett, 1991. 133(2): p. 225-8.
- Stenoien, D.L., et al., *Polyglutamine-expanded androgen receptors form aggregates that sequester heat shock proteins, proteasome components and SRC-1, and are suppressed by the HDJ-2 chaperone.* Hum Mol Genet, 1999. 8(5): p. 731-41.
- Sterneck, E., D.R. Kaplan, and P.F. Johnson, *Interleukin-6 induces expression of peripherin and cooperates with Trk receptor signaling to promote neuronal differentiation in PC12 cells.* J Neurochem, 1996. 67(4): p. 1365-74.
- Streit, W.J. and G.W. Kreutzberg, *Response of endogenous glial cells to motor neuron degeneration induced by toxic ricin.* J Comp Neurol, 1988. 268(2): p. 248-63.
- Streit, W.J., M.B. Graeber, and G.W. Kreutzberg, *Expression of Ia antigen on perivascular and microglial cells after sublethal and lethal motor neuron injury.* Exp Neurol, 1989. 105(2): p. 115-26.
- Strickland, D., et al., *Amyotrophic lateral sclerosis and occupational history. A pilot case-control study.* Arch Neurol, 1996. 53(8): p. 730-3.
- Stroh, C. and K. Schulze-Osthoff, *Death by a thousand cuts: an ever increasing list of caspase substrates.* Cell Death Differ, 1998. 5(12): p. 997-1000.
- Strong, M.J. and G.L. Pattee, *Creatine and coenzyme Q10 in the treatment of ALS.* Amyotroph Lateral Scler Other Motor Neuron Disord, 2000. 1 Suppl 4: p. 17-20.
- Strong, M.J., A.J. Hudson, and W.G. Alvord, *Familial amyotrophic lateral sclerosis, 1850-1989: a statistical analysis of the world literature.* Can J Neurol Sci, 1991. 18(1): p. 45-58.
- Su, J.H., et al., *Activated caspase-3 expression in Alzheimer's and aged control brain: correlation with Alzheimer pathology.* Brain Res, 2001. 898(2): p. 350-7.
- Swash, M. and J. Desai, *Motor neuron disease: classification and nomenclature.* Amyotroph Lateral Scler Other Motor Neuron Disord, 2000. 1(2): p. 105-12.
- Swerdlow, R.H., et al., *Mitochondria in sporadic amyotrophic lateral sclerosis.* Exp Neurol, 1998. 153(1): p. 135-42.
- Swerdlow, R.H., et al., *Role of mitochondria in amyotrophic lateral sclerosis.* Amyotroph Lateral Scler Other Motor Neuron Disord, 2000. 1(3): p. 185-90.
- Tager, J.M., et al., *Control of mitochondrial respiration.* FEBS Lett, 1983. 151(1): p. 1-9.
- Takuma, H., et al., *Reduction of GluR2 RNA editing, a molecular change that increases calcium influx through AMPA receptors, selective in the spinal ventral gray of patients with amyotrophic lateral sclerosis.* Ann Neurol, 1999. 46(6): p. 806-15.

- **Tandan, R., et al., *A controlled trial of amino acid therapy in amyotrophic lateral sclerosis: I. Clinical, functional, and maximum isometric torque data.* Neurology, 1996. 47(5): p. 1220-6.**
- **Tatton, W.G., *Apoptotic mechanisms in neurodegeneration: possible relevance to glaucoma.* Eur J Ophthalmol, 1999. 9 Suppl 1: p. S22-9.**
- **Tatton, W.G., et al., *Apoptosis in neurodegenerative disorders: potential for therapy by modifying gene transcription.* J Neural Transm Suppl, 1997. 49: p. 245-68.**
- **Taylor, A.L., G.W. Cottrell, and W.B. Kristan, Jr., *Analysis of oscillations in a reciprocally inhibitory network with synaptic depression.* Neural Comput, 2002. 14(3): p. 561-81.**
- **Terrado, J., et al., *Soluble TNF receptors partially protect injured motoneurons in the postnatal CNS.* Eur J Neurosci, 2000. 12(9): p. 3443-7.**
- **Tetzlaff, W., et al., *Increased glial fibrillary acidic protein synthesis in astrocytes during retrograde reaction of the rat facial nucleus.* Glia, 1988. 1(1): p. 90-5.**
- **Tewari, M., et al., *Yama/CPP32 beta, a mammalian homolog of CED-3, is a CrmA-inhibitable protease that cleaves the death substrate poly(ADP-ribose) polymerase.* Cell, 1995. 81(5): p. 801-9.**
- **Tews, D.S., H.H. Goebel, and H.M. Meinck, *DNA-fragmentation and apoptosis-related proteins of muscle cells in motor neuron disorders.* Acta Neurol Scand, 1997. 96(6): p. 380-6.**
- **Thomas, L., *Responding to Alzheimer's.* Elder Care, 1995. 7(4): p. 3.**
- **Ting, A.T., F.X. Pimentel-Muinos, and B. Seed, *RIP mediates tumor necrosis factor receptor 1 activation of NF-kappaB but not Fas/APO-1-initiated apoptosis.* Embo J, 1996. 15(22): p. 6189-96.**
- **Tomiyama, M., et al., *Quantitative autoradiographic distribution of glutamate receptors in the cervical segment of the spinal cord of the wobbler mouse.* Brain Res, 1994. 650(2): p. 353-7.**
- **Tortarolo, M., et al., *Persistent activation of p38 mitogen-activated protein kinase in a mouse model of familial amyotrophic lateral sclerosis correlates with disease progression.* Mol Cell Neurosci, 2003. 23(2): p. 180-92.**
- **Trotti, D., et al., *SOD1 mutants linked to amyotrophic lateral sclerosis selectively inactivate a glial glutamate transporter.* Nat Neurosci, 1999. 2(9): p. 848.**
- **Troy, C.M., et al., *Regulation of peripherin and neurofilament expression in regenerating rat motor neurons.* Brain Res, 1990. 529(1-2): p. 232-8.**
- **Tsang, Y.M., et al., *Motor neurons are rich in non-phosphorylated neurofilaments: cross-species comparison and alterations in ALS.* Brain Res, 2000. 861(1): p. 45-58.**

- Tsutsumi, M., et al., *Increased susceptibility of poly(ADP-ribose) polymerase-1 knockout mice to nitrosamine carcinogenicity.* Carcinogenesis, 2001. 22(1): p. 1-3.
- Tsuzaka, K., et al., *Role of brain-derived neurotrophic factor in wobbler mouse motor neuron disease.* Muscle Nerve, 2001. 24(4): p. 474-80.
- Turner, M.R., et al., *Evidence of widespread cerebral microglial activation in amyotrophic lateral sclerosis: an [11C](R)-PK11195 positron emission tomography study.* Neurobiol Dis, 2004. 15(3): p. 601-9.
- Valentine, J.S. and P.J. Hart, *Misfolded CuZnSOD and amyotrophic lateral sclerosis.* Proc Natl Acad Sci U S A, 2003. 100(7): p. 3617-22.
- Van Damme, P., et al., *The AMPA receptor antagonist NBQX prolongs survival in a transgenic mouse model of amyotrophic lateral sclerosis.* Neurosci Lett, 2003. 343(2): p. 81-4.
- Van Den Bosch, L. and W. Robberecht, *Different receptors mediate motor neuron death induced by short and long exposures to excitotoxicity.* Brain Res Bull, 2000. 53(4): p. 383-8.
- Van Den Bosch, L., et al., *Ca(2+)-permeable AMPA receptors and selective vulnerability of motor neurons.* J Neurol Sci, 2000. 180(1-2): p. 29-34.
- Vance, J.E., S.J. Stone, and J.R. Faust, *Abnormalities in mitochondria-associated membranes and phospholipid biosynthetic enzymes in the mnd/mnd mouse model of neuronal ceroid lipofuscinosis.* Biochim Biophys Acta, 1997. 1344(3): p. 286-99.
- Vandenberghe, W., et al., *AMPA receptor current density, not desensitization, predicts selective motoneuron vulnerability.* J Neurosci, 2000. 20(19): p. 7158-66.
- Vandenberghe, W., et al., *Subcellular localization of calcium-permeable AMPA receptors in spinal motoneurons.* Eur J Neurosci, 2001. 14(2): p. 305-14.
- Vandenberghe, W., W. Robberecht, and J.R. Brorson, *AMPA receptor calcium permeability, GluR2 expression, and selective motoneuron vulnerability.* J Neurosci, 2000. 20(1): p. 123-32.
- Vaught, J.L., et al., *Potential utility of rhIGF-1 in neuromuscular and/or degenerative disease.* Ciba Found Symp, 1996. 196: p. 18-27; discussion 27-38.
- Vaziri, N.D. and K. Liang, *Down-regulation of VLDL receptor expression in chronic experimental renal failure.* Kidney Int, 1997. 51(3): p. 913-9.
- Vergani, L., et al., *Glycosaminoglycans boost insulin-like growth factor-I-promoted neuroprotection: blockade of motor neuron death in the wobbler mouse.* Neuroscience, 1999. 93(2): p. 565-72.
- Verhagen, A.M., et al., *Identification of DIABLO, a mammalian protein that promotes apoptosis by binding to and antagonizing IAP proteins.* Cell, 2000. 102(1): p. 43-53.

- Villa, P., et al., *Erythropoietin selectively attenuates cytokine production and inflammation in cerebral ischemia by targeting neuronal apoptosis.* J Exp Med, 2003. 198(6): p. 971-5.
- Viviani, B., et al., *Dying neural cells activate glia through the release of a protease product.* Glia, 2000. 32(1): p. 84-90.
- Volbracht, C., M. Leist, and P. Nicotera, *ATP controls neuronal apoptosis triggered by microtubule breakdown or potassium deprivation.* Mol Med, 1999. 5(7): p. 477-89.
- Vyas, S., et al., *Expression of Bcl-2 in adult human brain regions with special reference to neurodegenerative disorders.* J Neurochem, 1997. 69(1): p. 223-31.
- Wadia, J.S., et al., *Mitochondrial membrane potential and nuclear changes in apoptosis caused by serum and nerve growth factor withdrawal: time course and modification by (-)-deprenyl.* J Neurosci, 1998. 18(3): p. 932-47.
- Wagner, A.J., J.M. Kokontis, and N. Hay, *Myc-mediated apoptosis requires wild-type p53 in a manner independent of cell cycle arrest and the ability of p53 to induce p21waf1/cip1.* Genes Dev, 1994. 8(23): p. 2817-30.
- Walkinshaw, G. and C.M. Waters, *Induction of apoptosis in catecholaminergic PC12 cells by L-DOPA. Implications for the treatment of Parkinson's disease.* J Clin Invest, 1995. 95(6): p. 2458-64.
- Wang, S.J., K.Y. Wang, and W.C. Wang, *Mechanisms underlying the riluzole inhibition of glutamate release from rat cerebral cortex nerve terminals (synaptosomes).* Neuroscience, 2004. 125(1): p. 191-201.
- Washburn, M.S., et al., *Differential dependence on GluR2 expression of three characteristic features of AMPA receptors.* J Neurosci, 1997. 17(24): p. 9393-406.
- Wedemeyer, N., et al., *YAC contigs of the Rab1 and wobbler (wr) spinal muscular atrophy gene region on proximal mouse chromosome 11 and of the homologous region on human chromosome 2p.* Genomics, 1996. 32(3): p. 447-54.
- Weiss, J.H. and D.W. Choi, *Slow non-NMDA receptor mediated neurotoxicity and amyotrophic lateral sclerosis.* Adv Neurol, 1991. 56: p. 311-8.
- Wenthold, R.J., et al., *Evidence for multiple AMPA receptor complexes in hippocampal CA1/CA2 neurons.* J Neurosci, 1996. 16(6): p. 1982-9.
- Whitfield, J., et al., *Dominant-negative c-Jun promotes neuronal survival by reducing BIM expression and inhibiting mitochondrial cytochrome c release.* Neuron, 2001. 29(3): p. 629-43.
- Wiley, S.R., et al., *Identification and characterization of a new member of the TNF family that induces apoptosis.* Immunity, 1995. 3(6): p. 673-82.

- Williams, T.L., et al., *Calcium-permeable alpha-amino-3-hydroxy-5-methyl-4-isoxazole propionic acid receptors: a molecular determinant of selective vulnerability in amyotrophic lateral sclerosis.* Ann Neurol, 1997. 42(2): p. 200-7.
- Wilson, C.M., et al., *Cognitive impairment in sporadic ALS: a pathologic continuum underlying a multisystem disorder.* Neurology, 2001. 57(4): p. 651-7.
- Wolozin, B.L., et al., *Differential regulation of APP secretion by apolipoprotein E3 and E4.* Ann N Y Acad Sci, 1996. 777: p. 322-6.
- Wong, J.T., et al., *Immunogenic epitopes of the p55 chain of the IL-2 receptor. Relationships to high-affinity IL-2 binding and modulation of the p55 chain.* Transplantation, 1990. 49(3): p. 587-96.
- Wong, P.C., et al., *An adverse property of a familial ALS-linked SOD1 mutation causes motor neuron disease characterized by vacuolar degeneration of mitochondria.* Neuron, 1995. 14(6): p. 1105-16.
- Woo, M.S., et al., *Selective modulation of lipopolysaccharide-stimulated cytokine expression and mitogen-activated protein kinase pathways by dibutyryl-cAMP in BV2 microglial cells.* Brain Res Mol Brain Res, 2003. 113(1-2): p. 86-96.
- Wu, H., et al., *Interaction of the erythropoietin and stem-cell-factor receptors.* Nature, 1995. 377(6546): p. 242-6.
- Wyllie, A.H., et al., *Chromatin cleavage in apoptosis: association with condensed chromatin morphology and dependence on macromolecular synthesis.* J Pathol, 1984. 142(1): p. 67-77.
- Wyllie, A.H., G.J. Beattie, and A.D. Hargreaves, *Chromatin changes in apoptosis.* Histochem J, 1981. 13(4): p. 681-92.
- Wyllie, A.H., J.F. Kerr, and A.R. Currie, *Cell death in the normal neonatal rat adrenal cortex.* J Pathol, 1973. 111(4): p. 255-61.
- Xu, G.P., et al., *Dysfunctional mitochondrial respiration in the wobbler mouse brain.* Neurosci Lett, 2001. 300(3): p. 141-4.
- Xu, L., J.A. Enyeart, and J.J. Enyeart, *Neuroprotective agent riluzole dramatically slows inactivation of Kv1.4 potassium channels by a voltage-dependent oxidative mechanism.* J Pharmacol Exp Ther, 2001. 299(1): p. 227-37.
- Xu, Z., et al., *Involvement of neurofilaments in motor neuron disease.* J Cell Sci Suppl, 1993. 17: p. 101-8.
- Yan, Q., J. Elliott, and W.D. Snider, *Brain-derived neurotrophic factor rescues spinal motor neurons from axotomy-induced cell death.* Nature, 1992. 360(6406): p. 753-5.
- Yuan, J., *Molecular control of life and death.* Curr Opin Cell Biol, 1995. 7(2): p. 211-4.
- Yung, K.K., F. Tang, and L.L. Vacca-Galloway, *Alterations in acetylcholinesterase and choline acetyltransferase activities and neuropeptide levels in the ventral spinal cord of*

the W'obbler mouse during inherited motoneuron disease. Brain Res, 1994. 638(1-2): p. 337-42.

- Zanjani, E.D., et al., *Liver as the primary site of erythropoietin formation in the fetus.* J Lab Clin Med, 1977. 89(3): p. 640-4.
- Zha, H., et al., *Proapoptotic protein Bax heterodimerizes with Bcl-2 and homodimerizes with Bax via a novel domain (BH3) distinct from BH1 and BH2.* J Biol Chem, 1996. 271(13): p. 7440-4.
- Zhang, G., et al., *Caspase inhibition prevents staurosporine-induced apoptosis in CHO-K1 cells.* Apoptosis, 1998. 3(1): p. 27-33.
- Zhao, C., et al., *Charcot-Marie-Tooth disease type 2A caused by mutation in a microtubule motor KIF1Bbeta.* Cell, 2001. 105(5): p. 587-97.
- Zimmermann, K.C. and D.R. Green, *How cells die: apoptosis pathways.* J Allergy Clin Immunol, 2001. 108(4 Suppl): p. S99-103.
- Ziv, I., et al., *Can nimodipine affect progression of motor neuron disease? A double-blind pilot study.* Clin Neuropharmacol, 1994. 17(5): p. 423-8.
- Zona, C., et al., *Kainate-induced currents in rat cortical neurons in culture are modulated by riluzole.* Synapse, 2002. 43(4): p. 244-51.
- Zona, C., et al., *Riluzole interacts with voltage-activated sodium and potassium currents in cultured rat cortical neurons.* Neuroscience, 1998. 85(3): p. 931-8.
- Zoratti, M. and I. Szabo, *The mitochondrial permeability transition.* Biochim Biophys Acta, 1995. 1241(2): p. 139-76.
- Zou, H., et al., *An APAF-1.cytochrome c multimeric complex is a functional apoptosome that activates procaspase-9.* J Biol Chem, 1999. 274(17): p. 11549-56.

• PUBLISHED PAPERS ARISING FROM THIS THESIS